Einstein-Yang-Mills black holes in anti de-Sitter space

Benjamin Lee Shepherd

Submitted for the degree of PhD

School of Mathematics and Statistics

To be submitted March 2012

Supervisor: Prof. Elizabeth Winstanley

University of Sheffield

Abstract

In this thesis we consider Einstein-Yang-Mills black holes in asymptotically anti-de Sitter space, in the presence of an $\mathfrak{su}(N)$ gauge field. For a purely magnetic gauge field we define a set of charges, namely the mass and $N-1$ gauge invariant magnetic charges, and show that they characterize stable black holes.

We then go on to consider dyonic black holes which carry both electric and magnetic charge. We investigate spherically symmetric black holes and solitons, and find equations of motion for solutions with $\mathfrak{su}(N)$ gauge fields. These equations are solved numerically to find black hole and soliton solutions with $\mathfrak{su}(2)$ and $\mathfrak{su}(3)$ gauge groups.

We then turn to dyonic black holes with planar event horizons and investigate their suitability as gravitational analogues to high temperature superconductors under the AdS/CFT correspondence. We generalise a previously known ansatz for $\mathfrak{su}(2)$ gauge groups to $\mathfrak{su}(N)$, and show that there is a critical temperature above which non-abelian solutions do not exist. Below this critical temperature, we show that they are thermodynamically favoured over equivalent Reissner-Nordström solutions, and have infinite D.C. conductivity.

Contents

List of Figures

Preface

Throughout this thesis, the metric signature is $(-,+,+,+)$, and unless otherwise stated we take $4\pi G/g^2 = 1$, where G is the four dimensional Newton's gravitational constant and g is the gauge coupling constant. Greek indices are used to denote space-time dimensions, which take the values $0, 1, 2, 3$. Roman letters are used for Lie algebra indices, which take integer values greater than zero, the largest of which depends on the gauge group. Repeated indices are summed over in both cases.

Much of chapter 2 reviews research already undertaken, although expressions for the charges (section 2.5.2) are an original contribution by the author, as is the distinguishabillity of solitons from black holes (section 2.6.2) [69]. Numerical results were produced by the author using code in C++ developed by M. Helbling [8, 9].

Chapter 3 reproduces and extends known results for the $\mathfrak{su}(2)$ gauge groups [18, 19]. All work for $\mathfrak{su}(N)$ gauge groups with general N, as well as numerical results and soliton boundary conditions for $\mathfrak{su}(3)$ are original contributions [70].

The ansatze in chapter 4 are known for $\mathfrak{su}(2)$ [37, 38, 62], but generalised to $\mathfrak{su}(N)$ by the author. While some of the results for $\mathfrak{su}(2)$ are known, the $\mathfrak{su}(2)$ conductivity as well as all results for $\mathfrak{su}(3)$ or $\mathfrak{su}(N)$ with general N are original contributions [71].

The author would like to acknowledge the help and support of his supervisor, Prof. E. Winstanley, as well as the financial support of the EPSRC.

Chapter 1

Introduction

In this thesis we consider black holes in the presence of $\mathfrak{su}(N)$ Yang-Mills fields, known as Einstein-Yang-Mills (EYM) black holes, in asymptotically anti-de Sitter (AdS) space. Yang-Mills fields are of interest in particle physics, as the strong and weak nuclear forces are $\mathfrak{su}(3)$ and $\mathfrak{su}(2)$ Yang-Mills fields respectively. While we will try to use a generalised $\mathfrak{su}(N)$ field as much as possible, it will be necessary to specify a value of N in order to generate numerical solutions to the field equations. When this happens, we consider the $\mathfrak{su}(2)$ and $\mathfrak{su}(3)$ cases.

Anti-de Sitter (AdS) space is a space with a negative (attractive) cosmological constant. While observations suggest that this does not reflect the universe in which we live, there is still considerable interest in AdS. We will consider two reasons for this. Firstly, we investigate an extension to the black hole uniqueness theorem known as the "no-hair" conjecture, and secondly we examine the possibility of an application to condensed matter physics through a correspondence between gravitational systems in AdS, and conformal field theories (CFTs) known as the AdS/CFT correspondence [60].

The black hole uniqueness theorem [25, 26, 44] states that stationary, four dimensional, asymptotically flat black hole solutions of the Einstein equations in a vacuum or in the presence of an electromagnetic field are characterized uniquely by their mass, angular momentum and electric or magnetic charge. The geometry exterior to the event horizon is then a member of the Kerr-Newman family and is determined entirely by these three global quantities which can, at least in principle, be measured at infinity. When applied to other matter models this statement is known as the "no-hair" conjecture [65]. Since Bartnik and McKinnon discovered the

first self gravitating Einstein-Yang-Mills soliton in 1988 [6], a variety of new black hole solutions which violate the no-hair conjecture (i.e. black holes not described uniquely by their mass, angular momentum and electric or magnetic charge) have been discovered.

In asymptotically flat space, EYM black holes have been found which violate the no-hair conjecture. For $\mathfrak{su}(2)$ EYM, discrete families of numerical solutions have been found, indexed by the number of zeros (or nodes) n in the gauge field function ω [16, 53, 77, 78], all of which have $n > 0$. These solutions carry no magnetic charge, and are indistinguishable from Schwarzschild black holes [30, 31]. Note that the results of [30, 31] do not extend to larger gauge groups or to asymptotically AdS space. For $\mathfrak{su}(N)$ we can have solutions that carry both electric and magnetic charge, which we return to later.

Although these asymptotically flat EYM solitons and black holes violate the no-hair conjecture, they have been shown to be unstable [23, 24, 34, 73, 72, 76, 85]. This led Bizon to make several modifications to the no-hair conjecture in [17], the most relaxed of which states that within a given matter model, a stable stationary black hole is uniquely determined by global charges (charges given by a surface integral at spatial infinity). Clearly this is satisfied by the $\mathfrak{su}(2)$ asymptotically flat black holes since the only stable posibility is the Schwarzschild solution. In de-Sitter space (which takes a positive cosmological constant) there are also EYM black hole solutions to the field equations [74], although all are found to be unstable [24], and are not considered further in this thesis.

We therefore turn to asymptotically AdS space, and investigate whether we can find stable black holes which satisfy the no-hair conjecture. Since the boundary conditions at infinity are less restrictive, it is possible to find not only continuous sets of EYM spherically symmetric black holes and solitons, but also solutions for which the gauge field function has no nodes, leading to the possibility of stable solutions (there has been much work on EYM black holes, see [79, 82] for detailed reviews). There are also non-spherically symmetric solutions (see e.g. [48, 49]), although they will not be considered in this thesis.

For spherically symmetric black holes with no electric charge, stability under spherically symmetric linear perturbations has been proved [7, 9, 10, 81, 82] for fields with $\mathfrak{su}(N)$ gauge groups, and investigating whether such black holes obey Bizon's modified no-hair conjecture will be the subject of chapter 2. Since in AdS we can have vacuum black holes with positive specific heat [41], we will consider

not only classical stability, but also thermodynamic stability. The global charges we will use are the mass (computed using the counterterm formalism of [4]), and $N-1$ $\mathfrak{su}(N)$ charges which we will construct using the approach of [27]. We will then present both numerical and analytic evidence that suggests that $\mathfrak{su}(N)$ EYM black holes in AdS do indeed obey Bizon's modified no-hair conjecture.

As mentioned previously, there are EYM black holes and solitons which carry both electric and magnetic charge, which are known as dyonic black holes. Unlike in flat space, in AdS it is possible to find dyonic black holes and solitons with an $\mathfrak{su}(2)$ gauge group [18, 19]. The subject of chapter 3 will be to extend the work of [18, 19] (which considered $\mathfrak{su}(2)$ dyonic black hole and solitons) to the $\mathfrak{su}(N)$ gauge group, for both black holes with spherical event horizons and solitons. We will present numerical results for $\mathfrak{su}(2)$ (for comparison with [18, 19]) and $\mathfrak{su}(3)$. However, the stability analysis of such black holes remains an open problem (the $\mathfrak{su}(2)$ case is currently being undertaken [63]), and because of this we do not consider dyonic black holes in the context of the modified no-hair conjecture.

Unlike in asymptotically flat space, in asymptotically AdS space the event horizon of a black hole is not constrained to be spherically symmetric [15, 22, 56, 57, 58, 75]; we can also find black holes with planar or hyperbolic event horizons, and this result can be extended to black holes with stable $\mathfrak{su}(2)$ Yang-Mills fields [64]. In particular, EYM black holes with planar event horizons and $\mathfrak{su}(N)$ gauge fields will be the subject of chapter 4. Although the stability of such black holes is currently a work in progress [11], the motivation for studying such black holes does not arise from the modified no-hair conjecture, but instead from the AdS/CFT correspondence.

The AdS/CFT correspondence [60] proposes an equivalence between type IIB string theory in $AdS_5 \times S^5$ (the product of five dimensional anti-de Sitter space and a five dimensional sphere), and maximally supersymmetric $\mathfrak{su}(N)$ Yang-Mills theory in conformally flat space [60, 84]. The boundary of AdS_5 is conformal to four dimensional flat space, and the gravitational theory in the bulk is mapped to the conformal field theory (CFT) on the boundary (see [1] for a review). This not only provides a way of investigating type IIB supergravity or string theory by studying Yang-Mills fields, but also a way of studying strongly coupled field theories (such as QCD) in the limit where the gravitational field theory can be approximated by classical gravity. In this way, the AdS/CFT correspondence provides a way of studying d-dimensional strongly coupled field theories in flat space by mapping them to a gravitational theory in $(d+1)$–dimensional asymptotically anti-de Sitter space.

There has been much recent interest applying this correspondence to condensed matter systems, in particular superconductivity (see [39, 43, 45, 47] for reviews).

Superconductivity occurs when, below a certain critical temperature T_C, the electrical resistivity of most metals drops to zero, which was first observed in mercury at 4.2K. A phenomenological description of this property was given by F. and H. London in 1935 [59]. In 1950, Ginzburg and Landau described superconductivity in terms of a phase transition with order parameter ϕ, occurring at the critical temperature T_C [35]. For temperatures above T_C, the minimum free energy occurs at $\phi = 0$, while below T_C the minimum free energy occurs at a non-zero value of ϕ. The order parameter ϕ is related to the number density of superconducting electrons n_s by $n_s = |\phi|^2$, so that above T_C the state with the minimum free energy has no superconducting electrons, while below T_C the number density of superconducting electrons is greater than zero. A mechanism for this was discovered by Bardeen, Cooper and Schrieffer in 1957, and is known as BCS theory [5]. In BCS theory, electrons with opposite spin couple together to form pairs, called Cooper pairs. These Cooper pairs are effectively spin zero particles, which allows them to condense into the ground state at low temperatures. As long as the energy gap between the ground state and first excited state is sufficiently large, the Cooper pairs remain in the ground state and do not interact with the metal ions, giving rise to superconductivity.

More recently, new types of superconductor have been discovered with much higher critical temperatures (typically around 100K). These are the layered cuprates [13, 14], and while there is evidence that in this case superconductivity is caused by condensation of electron pairs [29], the pairing mechanism is not well understood as, unlike BCS theory, the field theory is strongly coupled, and there are few methods in condensed matter physics to study strongly coupled field theories. The AdS/CFT correspondence provides an alternative way to study these systems, and due to the layered nature of cuprate superconductors, there has been much recent interest in the gravitational dual to $(2 + 1)$-dimensional strongly coupled feld theories at finite temperature.

One of the first models was proposed by Gubser in [36]. To introduce a temperature in the dual field theory, a black hole was added to the bulk, with the temperature of the field theory being equal to the Hawking temperature of the black hole. The role of the electron condensate was played by a scalar field - the critical result being that a charged black hole can support a charged scalar field at low tem-

peratures but not at high temperatures, thus the scalar field behaves like an electron condensate, forming only below a certain critical temperature. Models with a scalar field condensate have been extensively studied, for reviews see, for example, [45, 66].

There have since been models which employ dyonic $\mathfrak{su}(2)$ black holes, where the magnetic part of the gauge field acts as a dual to the condensate rather than a scalar field. Two were proposed by Gubser in [37, 38]. The ansatz presented in [37] was symmetric under rotations in the (x, y) plane, and was intended as a dual to an s-wave superconductor. The ansatz in [38] was superconducting only in the x direction and behaved as a normal metal in the y direction, as would be expected from a p-wave superconductor.

Both ansatze from [37, 38] were generalised to higher dimensions in [62]. However, in this thesis we will take a different approach and extend the ansatze to larger gauge groups, while keeping a $(3 + 1)$-dimensional bulk theory. We will be interested in three main properties of superconductors, which we expect to be shared by planar dyonic EYM black holes: that the condensate (the magnetic part of the Yang-Mills field) exists only below a critical temperature; that it is thermodynamically favourable to form a condensate below the critical temperature, and that the frequency dependent electrical conductivity behaves as one would expect from a real superconductor, especially that the D.C. conductivity is infinite.

Chapter 2

Characterization of spherically symmetric $\mathfrak{su}(N)$ EYM black holes

In this chapter we consider the case of static, four dimensional, asymptotically anti de-Sitter (AdS) black holes in the presence of an $\mathfrak{su}(N)$ Yang-Mills field, in the context of the "no-hair" conjecture. While a natural extension of the black hole uniqueness theorem [65] would be that black holes are characterized by their mass, angular momentum and electric or magnetic charge, we will see that this is not the case for $\mathfrak{su}(N)$ EYM black holes in AdS. We will instead argue, based on numerical evidence and analytic arguments, that the black holes considered in this chapter obey Bizon's modified no-hair conjecture, which states that, within a given matter model, stable stationary black holes are characterized by a set of global charges [17] (see chapter 1 for further details). In order to check whether Bizon's modified no-hair conjecture holds for $\mathfrak{su}(N)$ EYM black holes in AdS, we therefore must find black holes which are stable, construct the global charges associated with them, and then check whether these global charges do indeed characterize the stable black holes.

We begin by reviewing the ansatz, field equations and black hole solutions of the field equations of $\mathfrak{su}(N)$ EYM theory in AdS in sections 2.1 to 2.3. Existence of solutions which are stable under spherically symmetric perturbations has been proved for large $|\Lambda|$ in a neighbourhood of embedded $\mathfrak{su}(2)$ solutions, and we review the results presented in [7, 9, 10, 81, 82] in sections 2.4.1 and 2.4.2. In particular, we will present the conditions which must be satisfied in order for black holes to be stable under linear, spherically symmetric perturbations. We will then go on to discuss thermodynamics in section 2.4.3 and show that, for sufficiently large event horizon radius r_h, there are black holes which have a positive specific heat, and are

therefore thermodynamically stable.

The next step will be to find the global charges carried by $\mathfrak{su}(N)$ EYM black holes in AdS. We will review the counterterm formalism [4] used to compute a divergence-free mass for black holes in AdS in section 2.5.1, and then in section 2.5.2 use the approach of [27] to find expressions for the $N-1$ charges associated with the $\mathfrak{su}(N)$ gauge field.

Finally we will consider black holes which satisfy the (necessary but not sufficient) conditions to be stable, both thermodynamically and under spherically symmetric linear perturbations (i.e. we expect to include all black holes which are stable, as well as some that are not) in section 2.6. We will present numerical and analytic evidence that these black holes are characterized by their mass and $\mathfrak{su}(N)$ charges. We therefore conclude that stable (and possibly some unstable) $\mathfrak{su}(N)$ black holes in AdS are characterized by global charges, and therefore $\mathfrak{su}(N)$ EYM black holes in AdS do obey Bizon's modified no-hair conjecture.

§ 2.1 Gauge field, metric ansatz and field equations

We consider static, spherically symmetric black hole geometries in AdS space, with line element given by

$$ds^2 = -\sigma^2\mu\, dt^2 + r^2(d\theta^2 + \sin^2\,\theta\, d\phi^2) + \mu^{-1}dr^2, \tag{2.1}$$

where the metric function $\mu = \mu(r)$ is given by

$$\mu = 1 - \frac{2m(r)}{r} - \frac{\Lambda r^2}{3}, \tag{2.2}$$

with a negative cosmological constant Λ, and $\sigma = \sigma(r)$ is a function of r only. We study four dimensional $\mathfrak{su}(N)$ Einstein-Yang-Mills (EYM) theory described by the action

$$S_{EYM} = \int d^4x\sqrt{-g}\left[\frac{1}{16\pi G}(R - 2\Lambda) - \frac{1}{4}\mathrm{Tr}\, F^a_{\mu\nu}F^{a\mu\nu}\right] \tag{2.3}$$

where R is the Ricci scalar and the field strength tensor

$$F_{\mu\nu} = F^a_{\mu\nu}T_a = \partial_\mu A_\nu - \partial_\nu A_\mu + g[A_\mu, A_\nu], \tag{2.4}$$

with coupling constant g, and T_a denoting the generators of the Lie algebra $\mathfrak{su}(N)$ (see appendix A). Varying the action (2.3) gives the field equations

$$T_{\mu\nu} = R_{\mu\nu} - \frac{1}{2}Rg_{\mu\nu} + \Lambda g_{\mu\nu}; \tag{2.5}$$

$$D_\mu F^\mu_\nu = \nabla_\mu F^\mu_\nu + g\left[A_\mu, F^\mu_\nu\right] = 0; \tag{2.6}$$

where the stress-energy tensor is

$$T_{\mu\nu} = F^a_{\mu\alpha}F^a_{\nu\beta}g^{\alpha\beta} - \frac{1}{4}g_{\mu\nu}F^a_{\alpha\beta}F^{a\alpha\beta}. \tag{2.7}$$

The generalised ansatz for a spherically symmetric $\mathfrak{su}(N)$ gauge potential is given by [51]

$$gA = \mathcal{A}\,dt + \frac{1}{2}\left(C - C^H\right)d\theta - \frac{i}{2}\left[\left(C + C^H\right)\sin\theta + D\cos\theta\right]d\phi + \mathcal{B}\,dr \tag{2.8}$$

where $\mathcal{A}$, $\mathcal{B}$, C and D are $N \times N$ matrices which depend only on r. The matrices $\mathcal{A}$ and $\mathcal{B}$ are purely imaginary, diagonal and traceless. For a purely magnetic gauge field we set $\mathcal{A} = 0$, and we can set $\mathcal{B} = 0$ by a choice of gauge [51]. The matrix C is upper triangular, with non-zero entries

$$C_{j,j+1} = \omega_j(r)e^{i\gamma_j(r)}. \tag{2.9}$$

The constant matrix D is diagonal and traceless, and is given by

$$D = \mathrm{diag}(N-1, N-3, ..., 3-N, 1-N). \tag{2.10}$$

If $\omega_j \neq 0$ for all j then one of the Yang-Mills equations becomes $\gamma_j = 0$ for all j and (2.8) reduces to

$$gA = gA_\mu dx^\mu = \frac{1}{2}(C - C^H)d\theta - \frac{i}{2}\left[(C + C^H)\sin\theta + D\cos\theta\right]d\phi, \tag{2.11}$$

where the only non-zero entries in the matrix C are now

$$C_{j,j+1} = \omega_j(r). \tag{2.12}$$

The gauge field is then described by the $N-1$ gauge field functions ω_j, and there are $N-1$ non-trivial Yang-Mills equations for the ω_j given by [82]

$$0 = \omega_j'' + \left(\frac{\sigma'}{\sigma} + \frac{\mu'}{\mu}\right)\omega_j' + \frac{\omega_j}{2\mu r^2}\left(2 + \omega_{j-1}^2 - 2\omega_j^2 + \omega_{j+1}^2\right) \tag{2.13}$$

where $j = 1, 2, ..., N-1$, a prime denotes differentiation with respect to r, i.e. $\omega_j' = \frac{d\omega_j}{dr}$ and we take $\omega_0 = \omega_N = 0$. The corresponding Einstein equations are then

$$m' = \alpha^2 \sum_{j=1}^{N-1} \left\{ \frac{j(j+1)}{4r^2}\left(1 - \frac{\omega_j^2}{j} + \frac{\omega_{j+1}^2}{j+1}\right)^2 + \mu\omega_j'^2 \right\}, \tag{2.14}$$

$$\sigma' = \frac{2\alpha^2\sigma}{r}\sum_{j=1}^{N-1}\omega_j'^2, \tag{2.15}$$

and we set the coupling $\alpha^2 = 4\pi G/g^2 = 1$. We note that in the literature (see e.g. [82]) the equation for m' is written in terms of

$$p_\theta = \frac{1}{4r^4}\sum_{j=1}^{N}\left[\left(\omega_j^2 - \omega_{j-1}^2 - N - 1 + 2j\right)^2\right], \tag{2.16}$$

but that the expressions for m' are the same since

$$\sum_{j=1}^{N}\left[\left(\omega_j^2 - \omega_{j-1}^2 - N - 1 + 2j\right)^2\right] = \sum_{j=1}^{N-1} j(j+1)\left(1 - \frac{\omega_j^2}{j} + \frac{\omega_{j+1}^2}{j+1}\right)^2. \tag{2.17}$$

We use the form (2.14) since it is written in terms of the magnetic charges carried by the gauge field (see section 2.5.2).

§ 2.2 Boundary conditions

We wish to find black hole solutions to the EYM equations (2.13–2.15), which have an event horizon at $r = r_h$. We assume the variables $\sigma(r)$, $\omega_j(r)$ and $m(r)$ have regular Taylor expansions near $r = r_h$,

$$\begin{aligned} \omega_j(r) &= \omega_j(r_h) + \omega_j'(r_h)(r - r_h) + \dots, \\ m(r) &= m(r_h) + m'(r_h)(r - r_h) + \dots, \\ \sigma(r) &= \sigma(r_h) + \sigma'(r_h)(r - r_h) + \dots. \end{aligned} \tag{2.18}$$

At the event horizon we have

$$\mu(r_h) = 0 \Rightarrow m(r_h) = \frac{r_h}{2}\left(1 - \frac{\Lambda r_h^2}{3}\right). \tag{2.19}$$

For the black hole to be non-extremal (i.e. have a non-zero surface gravity and Hawking temperature) we require

$$\mu'(r_h) = \frac{1}{r_h} - \frac{2m'(r_h)}{r_h} - \Lambda r_h > 0. \tag{2.20}$$

To find the values of $\omega_j'(r_h)$, $m'(r_h)$ and $\sigma'(r_h)$, we multiply (2.13) through by μ, and evaluate (2.13–2.15) at the event horizon, giving

$$\begin{aligned}
\omega_j'(r_h) &= \frac{\omega_j(r_h)}{2\mu'(r_h)r_h^2}\left(2\omega_j(r_h)^2 - 2 - \omega_{j-1}(r_h)^2 - \omega_{j+1}(r_h)^2\right), \\
m'(r_h) &= \sum_{j=1}^{N-1} \frac{j(j+1)}{4r_h^2}\left(1 - \frac{\omega_j(r_h)^2}{j} + \frac{\omega_{j+1}(r_h)^2}{j+1}\right)^2, \\
\sigma'(r_h) &= \frac{2\sigma(r_h)}{r_h}\sum_{j=1}^{N-1}\omega_j'(r_h')^2.
\end{aligned} \tag{2.21}$$

We then have

$$\begin{aligned}
\omega_j(r) &= \omega_j(r_h) + \frac{\omega_j(r_h)}{2\mu'(r_h)r_h^2}\left(2\omega_j(r_h)^2 - 2 - \omega_{j-1}(r_h)^2 - \omega_{j+1}(r_h)^2\right)(r - r_h) + ... \\
m(r) &= \frac{r_h}{2}\left(1 - \frac{\Lambda r_h^2}{3}\right) + \sum_{j=1}^{N-1}\frac{j(j+1)}{4r_h^2}\left(1 - \frac{\omega_j(r_h)^2}{j} + \frac{\omega_{j+1}(r_h)^2}{j+1}\right)^2(r - r_h) + ... \\
\sigma(r) &= \sigma(r_h) + \frac{2\sigma(r_h)}{r_h}\sum_{j=1}^{N-1}\omega_j'(r_h')^2(r - r_h) + ...
\end{aligned} \tag{2.22}$$

where

$$\mu'(r_h) = \frac{1}{r_h} - \sum_{j=1}^{N-1}\frac{j(j+1)}{2r_h^3}\left(1 - \frac{\omega_j(r_h)^2}{j} + \frac{\omega_{j+1}(r_h)^2}{j+1}\right)^2 - \Lambda r_h > 0. \tag{2.23}$$

Since the space-time is asymptotically AdS we expect the following expansions in the limit $r \to \infty$:

$$\sigma(r) = 1 + O\left(\frac{1}{r}\right);$$

$$\begin{aligned} \omega_j(r) &= \omega_{j,\infty} + \frac{c_j}{r} + O\left(\frac{1}{r^2}\right); \\ m(r) &= m_0 + O\left(\frac{1}{r}\right). \end{aligned} \tag{2.24}$$

While in asymptotically flat space the values of the gauge field functions at infinity are constrained to be $\omega_{j,\infty} = \pm\sqrt{j(N-j)}$ [52], there are no such constraints in AdS space, hence we expect continuous sets of black hole solutions. Proof of local existence of solutions in the neighbourhoods of $r = 0$, $r = r_h$ and $r = \infty$ are given in [12], where it was found that at the event horizon black hole solutions are characterized by the $N+1$ parameters r_h, $\omega_j(r_h)$ and Λ. At infinity, there is a $2N$ parameter family of solutions, which are uniquely specified by Λ, c_j, $\omega_{j,\infty}$ and the mass parameter m_0. We return to this point in section 2.6, where we argue that only $N+1$ of these parameters are independent, with the c_j being single valued functions of Λ, $\omega_j(\infty)$ and m_0.

§ 2.3 Solutions of the field equations

In this section we find solutions to the field equations (2.13–2.15). While (2.13–2.15) cannot be solved analytically in general, there are some "trivial" solutions which we discuss in section 2.3.1. We will then go on to discuss numerical solutions with $\mathfrak{su}(2)$ and $\mathfrak{su}(3)$ gauge groups in sections 2.3.2–2.3.4.

2.3.1 Trivial solutions

Although the field equations (2.13–2.15) are non-linear and have to be solved numerically in general, there are some "trivial" solutions:

- *Schwarzschild-AdS*
  Setting $\omega_j(r) \equiv \pm\sqrt{j(N-j)}$ for all j gives the Schwarzschild-AdS black hole with $m(r) = m_0 = \text{constant}$.

- *Reissner-Nordström-AdS*
  Setting $\omega_j(r) \equiv 0$ for all j gives the Reissner-Nordström-AdS black hole with magnetic charge given by

$$Q^2 = \frac{1}{6}N(N+1)(N-1). \tag{2.25}$$

- *Embedded* $\mathfrak{su}(2)$ *solutions*
  Setting
  $$\omega_j(r) = \pm\sqrt{j(N-j)}\omega(r), \tag{2.26}$$
  and rescaling the variables
  $$R = \lambda_N^{-1} r; \qquad \tilde{\Lambda} = \lambda_N^2 \Lambda; \qquad \tilde{m}(R) = \lambda_N^{-1} m(r);$$
  $$\tilde{\sigma}(R) = \sigma(r); \qquad \tilde{\omega}(R) = \omega(r); \tag{2.27}$$
  where
  $$\lambda_N = \sqrt{\frac{1}{2}N(N-1)(N+1)}, \tag{2.28}$$
  gives the $\mathfrak{su}(2)$ field equations [82] with
  $$\mu = 1 - \frac{2\tilde{m}(R)}{R} - \frac{\tilde{\Lambda}R^2}{3}. \tag{2.29}$$
  Since we can always embed $\mathfrak{su}(2)$ in $\mathfrak{su}(N)$ we can check our results for general N in section 2.5 by ensuring that embedded $\mathfrak{su}(2)$ charges are proportional to the well-known $\mathfrak{su}(2)$ charges. We can also test code used to produce numerical results by checking that results for larger gauge groups reduce to the well known results for $\mathfrak{su}(2)$.

2.3.2 $\mathfrak{su}(2)$ SPHERICALLY SYMMETRIC BLACK HOLES

The $\mathfrak{su}(2)$ case has been widely studied in the literature (see e.g. [18, 19, 61, 81, 82]). In this section we reproduce the numerical results for Λ = -0.1, -3 and -10. The EYM equations for $\mathfrak{su}(2)$ are given by

$$0 = \omega'' + \left(\frac{\sigma'}{\sigma} + \frac{\mu'}{\mu}\right)\omega' + \frac{\omega}{\mu r^2}(1-\omega^2), \tag{2.30}$$

$$m' = \mu\omega'^2 + \frac{\omega^2-1}{2r^2}, \qquad \sigma' = \frac{2\sigma\omega'^2}{r}, \tag{2.31}$$

with boundary conditions at the event horizon given by

$$\begin{aligned} \omega(r) &= \omega(r_h) + \frac{\omega(r_h)}{\mu'(r_h)r_h^2}\left(\omega(r_h)^2 - 1\right)(r - r_h) + ... \\ m(r) &= \frac{r_h}{2}\left(1 - \frac{\Lambda r_h^2}{3}\right) + \frac{1}{2r_h^2}\left(1 - \omega(r_h)^2\right)^2(r - r_h) + ... \end{aligned}$$

$$\sigma(r) \;=\; \sigma(r_h) + \frac{2\sigma(r_h)\omega'(r_h)^2}{r_h}(r - r_h) + ... \tag{2.32}$$

where

$$\mu'(r_h) = \frac{1}{r_h} - \frac{1}{r_h^3}\left(1 - \omega(r_h)^2\right)^2 - \Lambda r_h > 0. \tag{2.33}$$

We will require the values of the constant c_1 in equation (2.24) in section 2.6, since at infinity $\mathfrak{su}(2)$ EYM black holes in AdS can be characterized by their mass, $\omega(\infty)$ and c_1 [12]. Differentiating (2.24) and rearranging gives

$$c_1 = -r^2\omega'(r) + O\left(\frac{1}{r}\right). \tag{2.34}$$

We then define a function $c_1(r)$ by

$$c_1(r) = -r^2\omega'(r), \tag{2.35}$$

so that the constant c_1 is given by

$$c_1 = \lim_{r\to\infty} c_1(r) = \lim_{r\to\infty}\left[-r^2\omega'(r)\right]. \tag{2.36}$$

In general we cannot solve (2.30, 2.31) analytically. Instead, we first decouple (2.30) into two first order ODEs in ω and ω', and then use a Bulirsch-Stoer algorithm [32] to solve the field equations numerically subject to the initial conditions (2.32). Since the field equations are singular at $r = r_h$, we start at $r - r_h = 10^{-7}$ and integrate outwards to large r, using a step length of 10^{-7} in r. While we are interested in the values of ω and c_1 at infinity, we cannot integrate outwards with increasing r indefinitely. However, we expect $\omega(r)$ and $c_1(r)$ to converge to constant values at large r. For this reason, we use relative convergence criteria of 10^{-7} in ω and c_1, i.e. we stop the integration at some r_f when $\omega(r_f)$ and $c_1(r_f)$ differ from $\omega(r_f - 10^{-7})$ and $c_1(r_f - 10^{-7})$ by a factor of 10^{-7} or less.

In the $\mathfrak{su}(2)$ case, solutions are characterized by r_h, $\omega(r_h)$ and Λ at the event horizon [12], so for each value of Λ we vary r_h and $\omega(r_h)$ with a step size of 10^{-3} in $\log_{10}(r_h)$ and $\omega(r_h)$. Since (2.30, 2.31) are invariant under the transformation $\omega(r) \to -\omega(r)$ we can consider only values of $\omega(r_h) > 0$ without loss of generality. We write to file data for $\omega(r)$, $m(r)$, $\sigma(r)$ and $c_1(r)$ in the large r limit, as well as the number of zeros n in the gauge field function $\omega(r)$, as we are interested in stable solutions with $n = 0$ [81].

Figures 2.1 – 2.3 show the phase spaces of $\mathfrak{su}(2)$ black holes with $\Lambda = -0.1$, -3 and -10 respectively, colour coded by the number of zeros in the gauge field function ω. The regions labeled "no solution" correspond to where the inequality (2.33) is satisfied, but we do not find black hole solutions. It is clear that the size of the region where we find $n = 0$ (potentially stable - see section 2.4) black hole solutions increases with the value of $|\Lambda|$.

While there are continuous sets of solutions for $\Lambda < 0$, this continuum of solutions becomes discrete in the $\Lambda \to 0$ limit, and remains discrete for all $\Lambda > 0$ [74, 80]. At $\Lambda = 0$, for any given value of r_h, there are discrete values of $\omega(r_h)$ for which we find solutions, with different $\omega(r_h)$ corresponding to different numbers of nodes in the gauge field function (these values of $\omega(r_h)$ can be found for $r_h = 1$ in [16]).

Black hole solutions with the $\mathfrak{su}(2)$ gauge group can be embedded to give $\mathfrak{su}(N)$ black holes for any N, and existence of $\mathfrak{su}(N)$ black hole solutions in a neighbourhood of these embedded $\mathfrak{su}(2)$ solutions has been proved in [12] for $|\Lambda| \gg 1$.

2.3.3 $\mathfrak{su}(2)$ TOPOLOGICAL BLACK HOLES

It has been shown that in the presence of a negative cosmological constant, the topology of the event horizon is no longer restricted to be spherical [3, 15, 22, 56, 57, 58, 75]. The set of black hole solutions can be extended to those with flat ($k = 0$) and hyperbolic ($k = -1$) horizons (see, e.g. [3]), and this has been extended to the $\mathfrak{su}(2)$ EYM case in [64] ($k = 1$ corresponds to spherical topology). The line element for these topological black hole solutions is given by [64]

$$ds^2 = -\sigma^2\mu\, dt^2 + \mu^{-1}dr^2 + r^2(d\theta^2 + f^2(\theta)\, d\phi^2), \tag{2.37}$$

where

$$\mu = k - \frac{2m(r)}{r} - \frac{\Lambda r^2}{3}, \tag{2.38}$$

and

$$f(\theta) = \begin{cases} \sin\theta & \text{for} \quad k = 1, \\ \theta, & \text{for} \quad k = 0, \\ \sinh\theta & \text{for} \quad k = -1. \end{cases} \tag{2.39}$$

The Einstein-Yang-Mills equations are given by [64]

$$0 = \omega'' + \left(\frac{\sigma'}{\sigma} + \frac{\mu'}{\mu}\right)\omega' + \frac{\omega}{\mu r^2}(k - \omega^2),$$

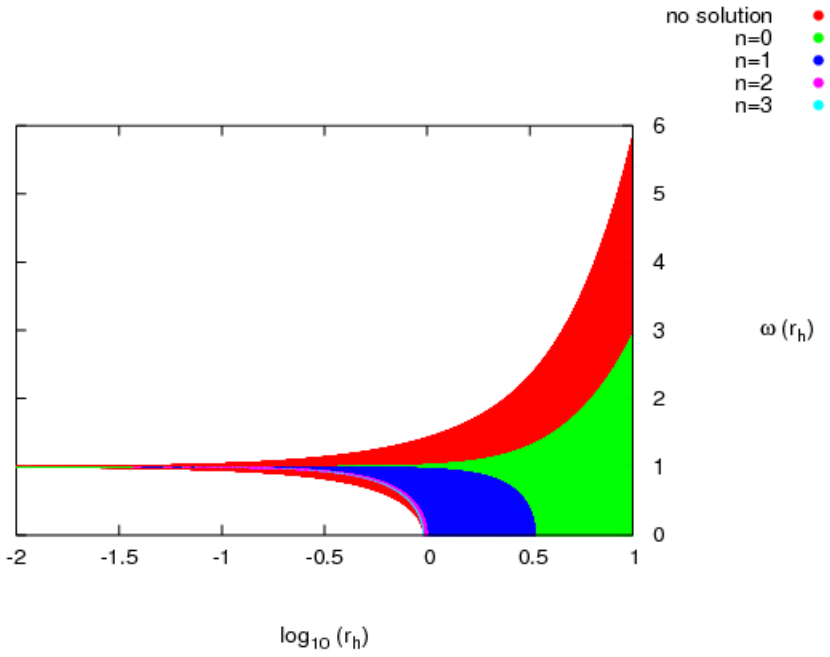

Figure 2.1: Phase space plot for $\mathfrak{su}(2)$ spherically symmetric black holes with $\Lambda = -0.1$, colour coded by the number of nodes n in the gauge field function $\omega(r)$. The red "no solution" region indicates where the inequality (2.33) is satisfied but we do not find black hole solutions. The green "$n = 0$" region indicates nodeless solutions (potentially stable, see section 2.4).

$$m' = \mu\omega'^2 + \frac{(\omega^2 - k)^2}{2r^2}, \qquad r\sigma' = 2\omega'^2\sigma, \tag{2.40}$$

while the inequality (2.33) becomes

$$\mu'(r_h) = \frac{k}{r_h} - \frac{1}{r_h^3}\left(k - \omega(r_h)^2\right)^2 - \Lambda r_h > 0 \tag{2.41}$$

for $k = 0, -1$ (for $k = 1$ we recover the spherically symmetric $\mathfrak{su}(2)$ solutions, see section 2.3.2). We note that in the $k = -1$ case there is a minimum value of r_h, since we require

$$r_h^2\left(|\Lambda| r_h^2 - 1\right) > \left(1 + \omega(r_h)^2\right)^2. \tag{2.42}$$

Using equations (2.40), along with the constraint (2.41), we find solutions in the same way as in section 2.3.2 for $\Lambda = -3$ with $k = 0, -1$. The phase space plots are

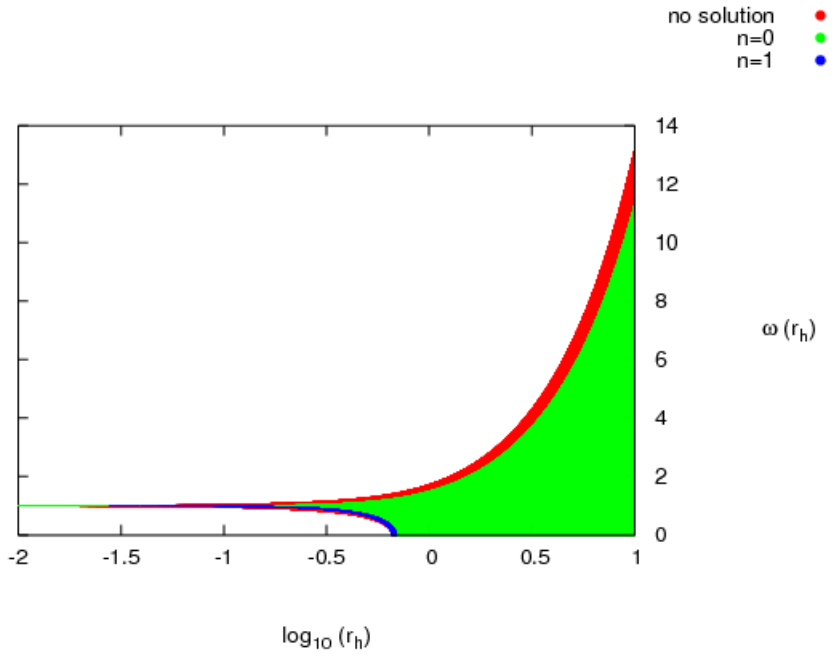

Figure 2.2: Phase space plot for $\mathfrak{su}(2)$ spherically symmetric black holes with $\Lambda = -3$, colour coded by the number of nodes n in the gauge field function $\omega(r)$. The red "no solution" region indicates where the inequality (2.33) is satisfied but we do not find black hole solutions. The green "$n = 0$" region indicates nodeless solutions (potentially stable, see section 2.4).

very similar, and for this reason we present only the $k = 0$ case (figure 2.4). We note in figure 2.4 that there are only nodeless ($n = 0$) solutions, in agreement with [64], and this is also the case when $k = -1$. Stability under linear perturbations of these black hole solutions has been proved in [64] for nodeless solutions with $\omega(\infty) > 0$ and $|\Lambda|$ sufficiently large. Thermodynamic stability has been proved in [61]. Research into the existence and stability of topological $\mathfrak{su}(N)$ black holes is currently being undertaken by J. Baxter and E. Winstanley [11].

2.3.4 $\mathfrak{su}(3)$ spherically symmetric black holes

In the $\mathfrak{su}(3)$ case we have two gauge field functions ω_1 and ω_2. Black holes are characterized by Λ, r_h, $\omega_1(r_h)$ and $\omega_2(r_h)$ at the event horizon, and as before we

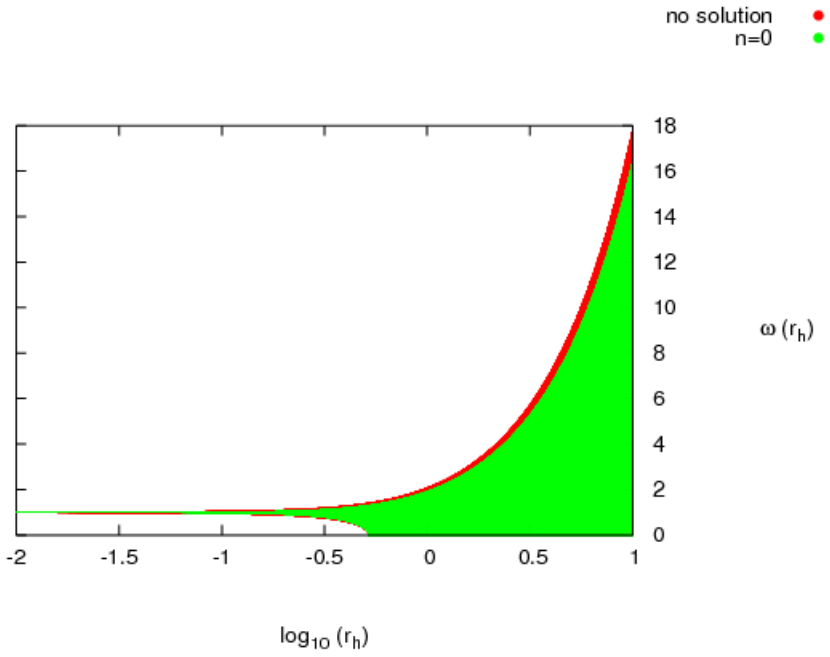

Figure 2.3: Phase space plot for $\mathfrak{su}(2)$ spherically symmetric black holes with $\Lambda = -10$, colour coded by the number of nodes n in the gauge field function $\omega(r)$. The red "no solution" region indicates where the inequality (2.33) is satisfied but we do not find black hole solutions. The green "$n = 0$" region indicates nodeless solutions (potentially stable, see section 2.4). Since $|\Lambda|$ is large, we find only nodeless solutions.

set $\omega_1(r_h), \omega_2(r_h) > 0$ using the symmetry of the field equations under the mapping $\omega_j \to -\omega_j$. At infinity $\mathfrak{su}(3)$ black holes are characterized by Λ, m_0, $\omega_1(\infty)$, $\omega_2(\infty)$, c_1 and c_2 [12]. As before we define new functions $c_j(r)$ such that

$$c_j(r) = -r^2\omega_j'(r) \tag{2.43}$$

so the constants c_j are

$$c_j = \lim_{r\to\infty}\left[-r^2\omega_j'(r)\right]. \tag{2.44}$$

We now have two Yang-Mills equations for ω_1 and ω_2 (2.13), in addition to the Einstein equations (2.14, 2.15), and we can recover the embedded $\mathfrak{su}(2)$ solutions

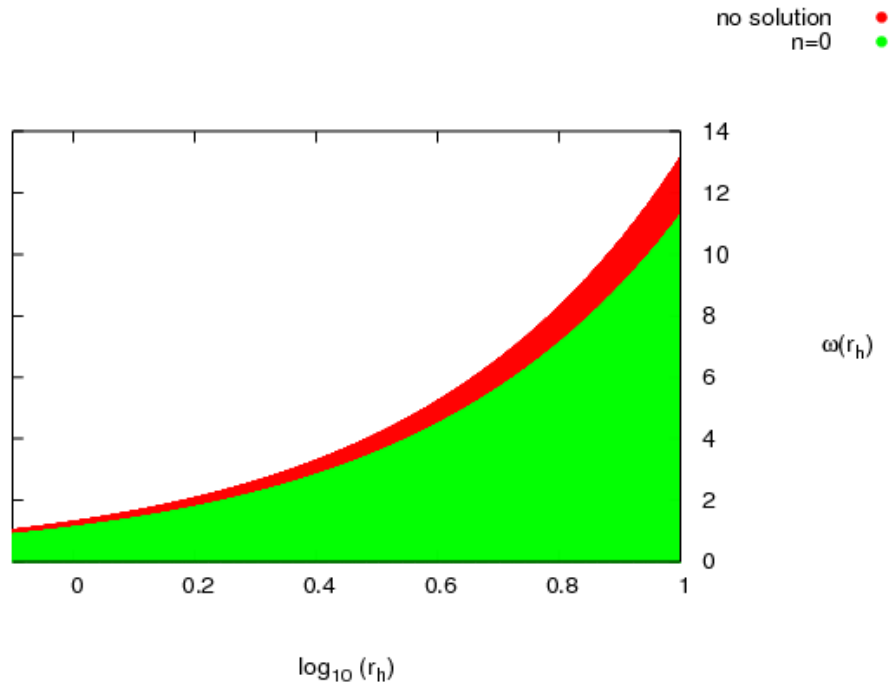

Figure 2.4: Phase space plot for topological $k = 0$ black holes with $\Lambda = -3$. The red "no solution" region indicates where the inequality (2.41) is satisfied but we do not find black hole solutions. When $k = 0$ we find solutions as r_h approaches zero. This is in constrast to the $k = -1$ case where there is a minimum value of r_h due to (2.41).

by setting

$$\omega_1(r) = \sqrt{2}\omega(r) = \omega_2(r). \tag{2.45}$$

From (2.23), for the event horizon to be non-extremal we require

$$\left[\omega_1(r_h)^2 - 2\right]^2 + \left[\omega_1(r_h)^2 - \omega_2(r_h)^2\right]^2 + \left[2 - \omega_2(r_h)^2\right]^2 < 2r_h^2\left(1 - \Lambda r_h^2\right). \tag{2.46}$$

As in previous sections, we integrate outwards from $r - r_h = 10^{-7}$, but this time we require ω_j and c_j for $j = 1, 2$. Since we must scan over all values of ω_2 for which (2.46) is satisfied for each value of ω_1, and vice versa, we used a larger step size of 10^{-2} in $\log_{10}(r_h)$, $\omega_1(r_h)$ and $\omega_2(r_h)$ to reduce the running time and output

file size, but once again used a 10^{-7} test for convergence in $\omega_1(\infty)$, $\omega_2(\infty)$, $c_1(\infty)$ and $c_2(\infty)$.

In the $\mathfrak{su}(3)$ case, black holes are characterized at the event horizon by r_h, Λ, $\omega_1(r_h)$ and $\omega_2(r_h)$ [12], so to obtain a two dimensional plot we must fix two variables. A phase space plot of our data at fixed $r_h = 1$, $\Lambda = -3$ is shown in figure 2.5, where we have scanned over $\omega_j(r_h) > 0$ for $j = 1, 2$ (similar plots for $\lambda = -0.0001, -1, -5$ can be found in [8]). The nodeless region ($n_1 = n_2 = 0$) shows where there are potentially stable black holes, and expands as we increase $|\Lambda|$ [8]. We do not expect to find stable black holes in the regions where $n_1 = 1$ or $n_2 = 1$ (see section 2.4). Again, the "no solution" region is where (2.46) is satisfied but we do not find black hole solutions.

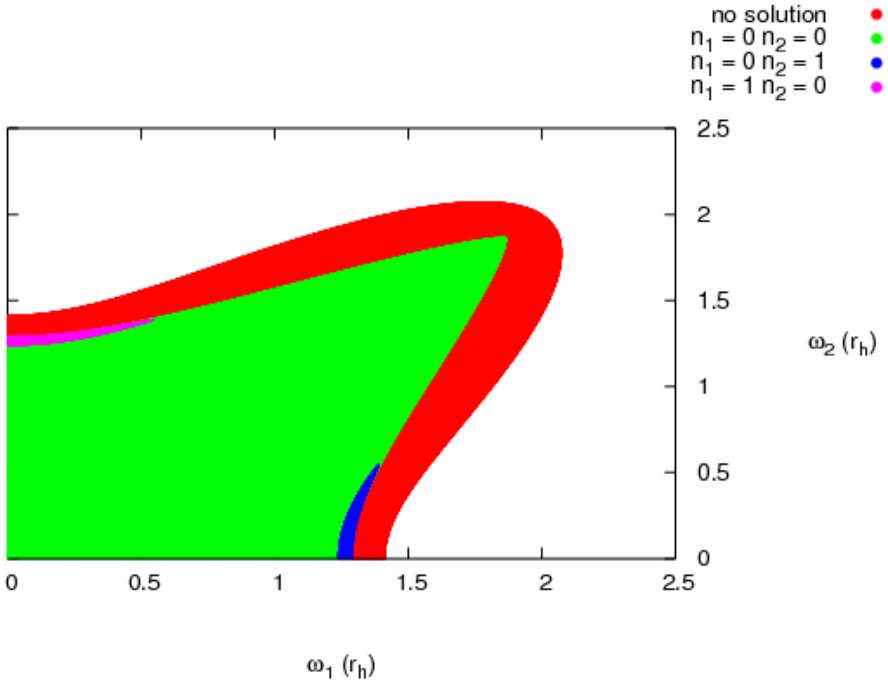

Figure 2.5: Phase space plot for spherically symmetric $\mathfrak{su}(3)$ solutions with $r_h = 1$ and $\Lambda = -3$. The red "no solution" region indicates where the inequality (2.46) is satisfied but we do not find black hole solutions. The green "$n = 0$" region indicates nodeless solutions (potentially stable, see section 2.4). If either $n_1 = 1$ (ω_1 has a node) or $n_2 = 1$ (ω_2 has a node) then we expect the black holes to be unstable.

§ 2.4 Stability

We wish to check whether Bizon's modified no hair conjecture holds for $\mathfrak{su}(N)$ EYM black holes in AdS, i.e. whether stable stationary black holes are characterized by a set of global charges. Having found solutions to the field equations, we will now look at conditions for stability, both thermodynamically and under linear perturbations.

In sections 2.4.1 and 2.4.2 we review the results given in [7, 9, 81, 82] regarding the stability of the black hole solutions under time dependent, linear, spherically symmetric perturbations. We note that the stability analysis for non-spherically symmetric perturbations with the $\mathfrak{su}(2)$ gauge group is carried out in [67, 83]. We will then go on to discuss thermodynamic stability in section 2.4.3.

We start by returning to the generalised ansatz for the gauge potential (2.8), although the matrices $\mathcal{A}$, $\mathcal{B}$ and C now depend on the time t as well as r, and set $\mathcal{A} = 0$ through a choice of gauge. We consider time dependent perturbations of the form

$$\begin{aligned} \omega_j(t,r) &= \omega_j^0(r) + \delta\omega(t,r), \\ \mu(t,r) &= \mu_0(r) + \delta\mu(t,r), \\ \sigma(t,r) &= \sigma_0(r) + \delta\sigma(t,r), \end{aligned} \tag{2.47}$$

where $\omega_j^0(r)$, $\mu_0(r)$ and $\sigma_0(r)$ are the equilibrium functions. We also have perturbations $\delta\gamma_j$ (2.9), and $\delta\beta_j$, where the matrix $\mathcal{B}$ is given by

$$\mathcal{B} = \mathrm{diag}(i\delta\beta_1, ..., i\delta\beta_N). \tag{2.48}$$

We will also use the "tortoise" co-ordinate r_* defined by

$$\frac{dr_*}{dr} = \frac{1}{\mu_0\sigma_0}. \tag{2.49}$$

The perturbations now separate into the "sphaleronic" and "gravitational" sectors [55], and we follow the analysis of [7, 9, 10, 81].

2.4.1 Sphaleronic sector

The sphaleronic sector is comprised of the perturbations $\delta\beta_j$ and $\delta\gamma_j$. We define new variables $\delta\epsilon_j$ and $\delta\Phi_j$ for $j = 1, ..., N-1$ by [7]

$$\delta\epsilon_j = r\sqrt{\mu}\delta\beta_j, \qquad \delta\Phi_j = \omega_j^0\delta\gamma_j \tag{2.50}$$

where ω_j^0 are the unperturbed gauge field functions. The perturbation equations for the sphaleronic sector arise from the Yang-Mills equations [82] and after some algebra can be cast in the form

$$-\ddot{\Psi} = \mathcal{M}_S\Psi \tag{2.51}$$

where $\Psi = (\delta\epsilon_1, ..., \delta\epsilon_N, \delta\Phi_1, ..., \delta\Phi_{N-1})$, $\mathcal{M}_S$ is a second order differential operator in r_* and a dot denotes differentiation with respect to time t (the detailed form of $\mathcal{M}_S$ can be found in [7]). The solutions are stable under the perturbations $\delta\Phi_j$ and $\delta\epsilon_j$ if the matrix $\mathcal{M}_S$ is regular and positive definite. It can be shown [7] that this is the case if the unperturbed gauge field functions ω_j^0 have no zeros and satisfy the $N-1$ inequalities

$$\omega_j^{0\,2} > 1 + \frac{1}{2}\left({\omega_{j+1}^0}^2 + {\omega_{j-1}^0}^2\right) \tag{2.52}$$

for all $r \geq r_h$ and all $j = 1, ..., N-1$. Figure 2.6 shows the region of figure 2.5 where (2.52) is satisfied at the event horizon. It has been shown [7] that for any N and sufficiently large $|\Lambda|$, black hole solutions exist for which (2.52) are satisfied for all $r \geq r_h$, i.e. for at least some of the solutions where (2.52) is satisfied at the event horizon, the gauge field functions remain in this region for all $r \geq r_h$.

2.4.2 Gravitational sector

The gravitational sector consists of the perturbations $\delta\mu$, $\delta\sigma$ and $\delta\omega_j$, although the metric perturbations can be eliminated to obtain [7]

$$\delta\ddot{\boldsymbol{\omega}} = \partial_{r_*}^2(\delta\boldsymbol{\omega}) + \mathcal{M}_G\delta\boldsymbol{\omega}, \tag{2.53}$$

where $\delta\boldsymbol{\omega} = (\delta\omega_1, ..., \delta\omega_{N-1})^T$. The $(N-1)\times(N-1)$ matrix $\mathcal{M}_G$ is a function of r and contains only equilibrium quantities and no derivatives. The system is stable under these perturbations if $\mathcal{M}_G$ is negative definite. It has been shown [81] that this is the case for $\mathfrak{su}(2)$ solutions if we have sufficiently large $|\Lambda|$, as long as $\omega^2(r) > 1/3$ for all $r \geq r_h$, and existence of these solutions has also been proved in [81]. There then exist genuinely $\mathfrak{su}(N)$ solutions a neighbourhood of the embedded $\mathfrak{su}(2)$ solutions such that (2.52) are satisfied for all $r \geq r_h$ and $\mathcal{M}_G$ remains negative definite [7]. We conclude that there are some genuinely $\mathfrak{su}(N)$ EYM solutions in

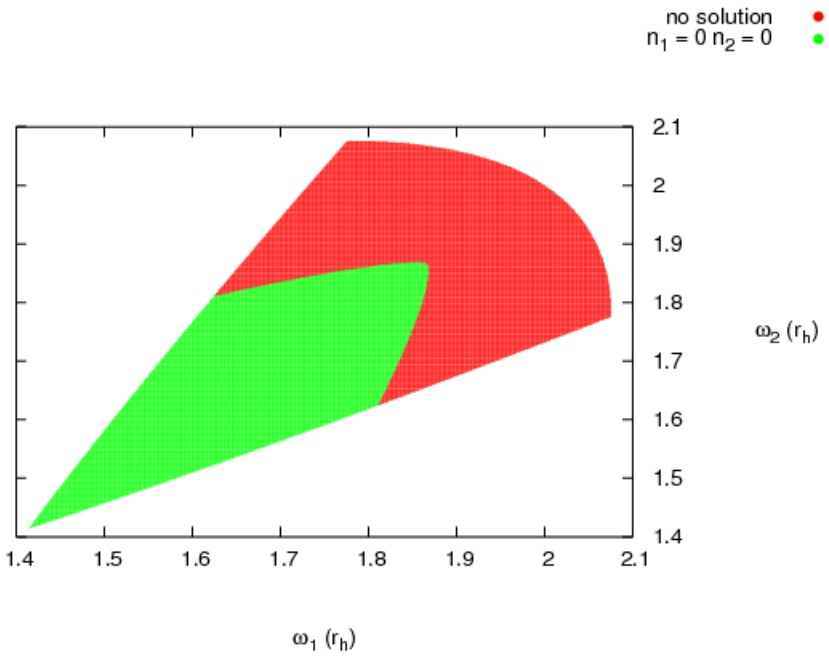

Figure 2.6: Solution space for $\mathfrak{su}(3)$ black holes with $\Lambda = -3$, $r_h = 1$ where (2.52) holds at the horizon. Potentially stable solutions are found in the "$n = 0$" region. For the black holes to be stable, we require (2.52) to be satisfied at all $r \geq r_h$.

AdS which are stable under spherically symmetric perturbations in the sphaleronic and gravitational sectors, provided that $|\Lambda|$ is sufficiently large [7].

2.4.3 Thermodynamic stability

As in flat space, black holes in AdS space have thermodynamic properties including a characteristic temperature and an intrinsic entropy, which for a gravitational action of the form (2.3) is proportional to one quarter of the area of the event horizon [46]. In asymptotically flat space, while a black hole can be in equilibrium with thermal radiation at the same temperature, this equilibrium is unstable. Any increase in mass would cause the temperature of the black hole to decrease, hence the absorption would increase and the black hole would continue to grow. However, in AdS space, black holes above a certain mass may have a positive specific heat, and therefore may be in equilibrium with thermal radiation at a fixed temperature [41], and we take this as being the condition for thermodynamic stability. In this section we extend the approach of [41] to $\mathfrak{su}(N)$ EYM black holes in AdS space, as has been done for the $\mathfrak{su}(2)$ case in [61].

The heat capacity C of a black hole is given by

$$C = T_H \left(\frac{\partial T_H}{\partial S} \right)_Q , \tag{2.54}$$

where T_H is the Hawking temperature, S is the entropy, and the derivative is taken at fixed charge Q (we note here that this statement is only relevant if we can define global charges to hold fixed, see section 2.5). The Hawking temperature is given by

$$T_H = \frac{\sigma(r_h)(1 - 2m'(r_h) - \Lambda r_h^2)}{4\pi r_h}, \tag{2.55}$$

where $\sigma(r_h)$ refers to the metric function in (2.1), $m'(r_h)$ is given by (2.21) and the entropy associated with the action (2.3) is

$$S = \frac{A}{4}, \tag{2.56}$$

where A is the area of the event horizon. Thermodynamic stability requires a positive heat capacity, i.e. $C > 0$ [41]. Figure 2.7 shows the Hawking temperature plotted as a function of entropy for $\mathfrak{su}(2)$ black holes at fixed $\omega(\infty)$ (which is equivalent to fixing the charge, see section 2.5 for details). Clearly there are two

branches of solutions, one which is thermodynamically stable, and one which is not. We note also that there is a minimum temperature for which black holes are stable (which is noted for the Schwarzschild-AdS case in [41]), and a phase transition where the plotted line tends to the vertical (similar results were found in [61]). We also find that stable solutions have higher entropy (and therefore larger r_h) than the unstable solutions.

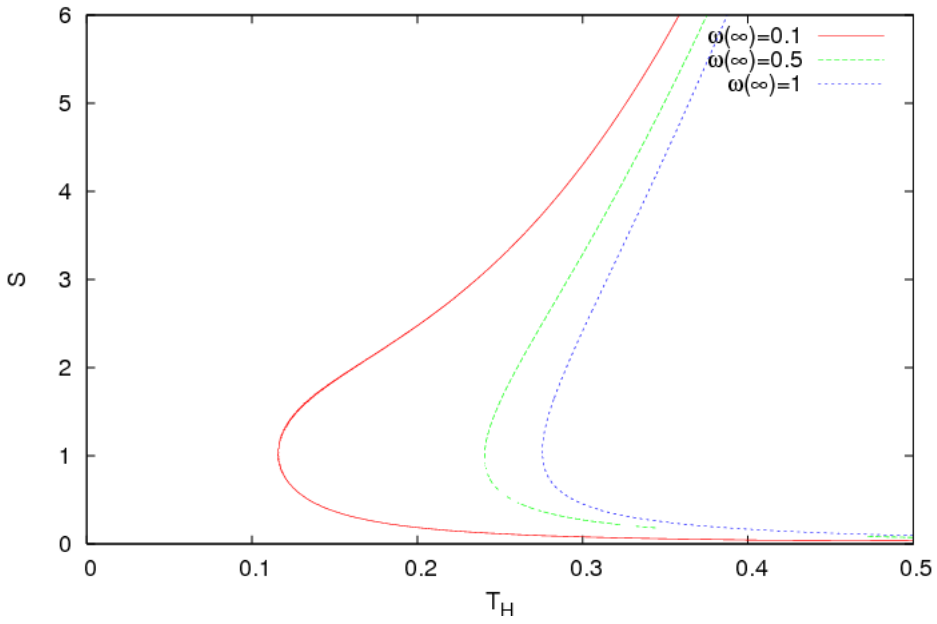

Figure 2.7: Entropy plotted as a function of Hawking temperature for $\mathfrak{su}(2)$ EYM black holes with $\Lambda = -3$. Thermodynamically stable soutions lie on the part of the line with positive slope (and therefore positive heat capacity), and have higher entropy (and therefore larger r_h) than thermodynamically unstable solutions.

Figure 2.8 shows a plot of Hawking temperature for $\mathfrak{su}(3)$ black holes with $\Lambda = -3$. Again we have fixed the values of $\omega_1(\infty)$ and $\omega_2(\infty)$, which is equivalent to fixing the charges (see section 2.5.2). We find solutions with positive heat capacity for both embedded $\mathfrak{su}(2)$ (where $\omega_1(\infty) = \omega_2(\infty)$) and genuinely $\mathfrak{su}(3)$ solutions. While there are both stable and unstable solutions for the embedded $\mathfrak{su}(2)$ solutions, numerically only thermodynamiclly stable solutions were found for genuinely $\mathfrak{su}(3)$ solutions. It is unclear whether there are no unstable solutions, or simply that none were found in our analysis. However, here we are only interested in thermodynamically stable solutions.

As mentioned in the introduction, version three of Bizon's modification of the no

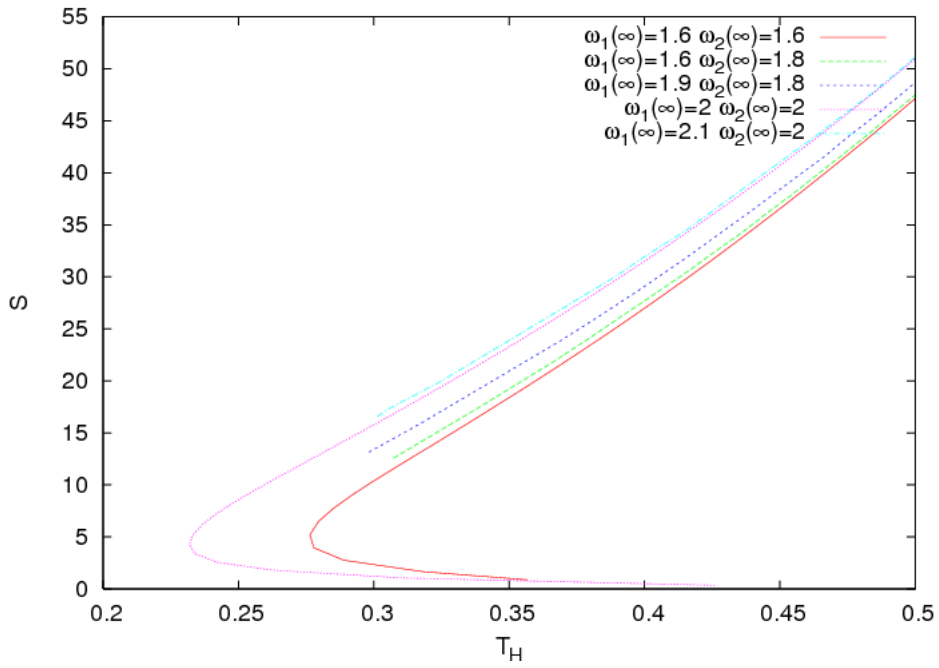

Figure 2.8: Entropy plotted as a function of Hawking temperature for $\mathfrak{su}(3)$ EYM black holes with $\Lambda = -3$. Thermodynamically stable solutions lie on the part of the line with positive slope (and therefore positive heat capacity). Thermodynamically stable solutions are found for both embedded $\mathfrak{su}(2)$ and genuinely $\mathfrak{su}(3)$ solutions.

hair conjecture [17] states that within a given model, stable stationary black hole solutions are uniquely determined by a set of global charges. For the remainder of the chapter we will therefore restrict our attention to thermodynamically stable black holes.

§ 2.5 Definition of charges for $\mathfrak{su}(N)$ EYM

In this section we define and then calculate the conserved charges measured from infinity, i.e. the mass and the $\mathfrak{su}(N)$ magnetic charges (our ansatz for the gauge potential (2.11) has no electric part) as we require these, along with the cosmological constant Λ, to characterize the stable black hole solutions uniquely from infinity. In AdS space we find divergent quantities in the mass, and we review the counterterm formalism proposed by Balasubramanian and Kraus in [4] and applied to $\mathfrak{su}(2)$ EYM black holes in [61] to remove these divergent quantities.

We find conserved charges corresponding to diagonal generators of the Lie algebra of $\mathfrak{su}(N)$. The rank of $\mathfrak{su}(N)$ is $N-1$ and we find $N-1$ conserved charges. As

noted in [61] the problem of constructing these charges has been approached in different ways by different authors. In this section we use the approach of [27] to construct these charges in a gauge invariant way. The particular case of $\mathfrak{su}(2)$ has been widely studied in the literature, and we find that our results are in agreement with [28] and [61]. We then go on to generalise these results first to $\mathfrak{su}(3)$, for which we have numerical results, and then to $\mathfrak{su}(N)$.

2.5.1 Mass

In this section we calculate the mass of black hole solutions in AdS space with line element given by (2.1), using the boundary counterterm subtraction method of Balasubramanian and Kraus [4], which was applied to the $\mathfrak{su}(2)$ case in [61]. It is unnatural, in a generally covariant theory, to assign a local energy-momentum tensor to a gravitational field. Instead, we define a "quasilocal stress tensor", defined locally on the boundary of a given space-time. The quasilocal stress tensor is given by [4]

$$T^{\mu\nu} = \frac{2}{\sqrt{-\gamma}} \frac{\delta S_{grav}}{\delta \gamma_{\mu\nu}} \tag{2.57}$$

where the gravitational action $S_{grav} = S_{grav}(\gamma_{\mu\nu})$ is viewed as being a function of the boundary metric $\gamma_{\mu\nu}$. In AdS space, the stress tensor typically diverges as the boundary is taken to infinity. However, we are free to add boundary terms S_{ct} to the action, as these do not alter the equations of motion in the bulk. We then need to vary the action with respect to the boundary metric. Since we are considering solutions to the equations of motion, only the boundary term contributes and the quasilocal stress tensor is given by [4]

$$T^{\mu\nu} = \frac{1}{2}\left(\Theta^{\mu\nu} - \Theta\gamma^{\mu\nu} + \frac{2}{\sqrt{-\gamma}} \frac{\delta S_{ct}}{\delta \gamma_{\mu\nu}}\right). \tag{2.58}$$

The extrinsic curvature $\Theta^{\mu\nu}$ is given by [4]

$$\Theta^{\mu\nu} = -\frac{1}{2}\left(\nabla^{\mu}\hat{n}^{\nu} + \nabla^{\nu}\hat{n}^{\mu}\right) \tag{2.59}$$

and $\hat{n}^{\mu}$ is the outward pointing normal to surfaces of constant r. For a line element given by (2.1) we have

$$\hat{n}^{\mu} = (0, 0, 0, \mu^{\frac{1}{2}})^{T}, \tag{2.60}$$

and

$$\Theta^{\mu\nu} = \mathrm{diag}\left(\frac{\mu\sigma(r)' + \sigma(r)\mu'}{\mu^{\frac{5}{2}}\sigma^3}, -\frac{\mu^{\frac{1}{2}}}{r^3}, -\frac{\mu^{\frac{1}{2}}}{r^3\sin^2\theta}, 0\right). \tag{2.61}$$

The counterterms in [4] and [61] are given by

$$S_{ct} = -\frac{2}{l}\int_{\partial\mathcal{M}_r}\sqrt{-\gamma}\left(1 - \frac{l^2}{4}R\right), \tag{2.62}$$

where $\partial\mathcal{M}_r$ is the large r boundary, and the boundary stress tensor becomes

$$T^{\mu\nu} = \frac{1}{2}\left(\Theta^{\mu\nu} - \Theta\gamma^{\mu\nu} - \frac{2}{l}\gamma^{\mu\nu} - lG^{\mu\nu}\right), \tag{2.63}$$

where $G^{\mu\nu}$ is the Einstein tensor of the boundary metric and is divergence free (which is a requirement of energy conservation).

We obtain the mass by integrating the quasilocal stress tensor (2.63) over a sphere of constant r in the limit $r \to \infty$, and we require $T^{\mu\nu} \sim r^k$ where $k \leq 0$ for a finite mass. In the $\mathfrak{su}(2)$ case, the asymptotic expressions at large r for $S(r)$, $\omega(r)$ and $m(r)$ (2.24) are given by [61]

$$\begin{aligned}
\sigma(r) &= \left[1 + \frac{c_1^2}{r^4} + O\left(\frac{1}{r^5}\right)\right]^{-1}, \\
\omega(r) &= \omega_\infty + \frac{c_1}{r} + O\left(\frac{1}{r^2}\right), \\
m(r) &= m_0 + \left[\frac{\Lambda c_1^2}{3} - \frac{1}{2}\left(\omega_\infty^2 - 1\right)^2\right]\frac{1}{r} + O\left(\frac{1}{r}\right),
\end{aligned} \tag{2.64}$$

and substituting into (2.63) gives

$$T_{tt} = \frac{m_0}{lr} - \frac{4c_1^2 + l^2(\omega_\infty^2 - 1)^2}{r^2 l^3} + \mathcal{O}\left(\frac{1}{r^3}\right). \tag{2.65}$$

In agreement with [61], the gauge field quantities ω_∞ and c_1 appear only in the order r^{-2} term. We do find some discrepancy with regards to the exact form of this term as compared to [61], where T_{tt} is given as

$$T_{tt} = \frac{m_0}{lr} - \frac{8c_1^2 + 4l^2(\omega_\infty^2 - 1)^2 - l^4}{4r^2} + \mathcal{O}\left(\frac{1}{r^3}\right). \tag{2.66}$$

However, this discrepancy does not affect the mass, which is given by [4]

$$M = \int lrT_{00}\, d^2x = 4\pi m_0. \tag{2.67}$$

We note here that in the $\mathfrak{su}(2)$ case the gauge field function does not contribute directly to the mass. Similarly we can also find the mass from the asymptotic value of the variable m for $\mathfrak{su}(N)$ gauge fields. However, the gauge fields do contribute indirectly to the mass since they appear in the differential equation for m (2.14).

2.5.2 $\mathfrak{su}(N)$ CHARGES

The Cartan subalgebra of a Lie algebra is defined to be the largest set of group elements which commute with themselves [42]. In the matrix representation of the Lie algebra, elements of the Cartan subalgebra are formed by taking linear combinations of the diagonal generators of the Lie algebra since diagonal matrices commute with each other.

In particle physics, the rank of the symmetry group is the number of conserved charges that each particle carries, with one charge for each diagonal generator. For example, there is an approximate $\mathfrak{su}(3) \times \mathfrak{u}(1)$ symmetry between the three lightest quarks. In total there are three diagonal generators in the group $\mathfrak{su}(3) \times \mathfrak{u}(1)$, corresponding to three conserved charges: isospin, baryon number and strangeness. The number of diagonal generators in a Lie algebra, those which make up the Cartan subalgebra, is called the rank, and $\mathfrak{su}(N)$ has rank $N-1$. We then expect our $\mathfrak{su}(N)$ EYM black holes to carry $N-1$ conserved charges.

In electromagnetism the magnetic charge is given by $Q = \int_{S_\infty} F$, where S_∞ denotes a sphere at spatial infinity, over which the integration is taken, and $F = \frac{1}{2}F_{\mu\nu}dx^\mu \wedge dx^\nu$ where $F_{\mu\nu}$ is the electromagnetic field strength tensor. Since the components of $F_{\mu\nu}$ are gauge scalars, the expression for Q is inherently gauge invariant. However, this is not the case for $\mathfrak{su}(N)$ EYM theory, as the components of $F_{\mu\nu}$ are $N \times N$ matrices (see equations (2.4) and (2.11)), which are not gauge invariant in general.

While there is agreement in the literature that the $\mathfrak{su}(N)$ charges (and any observable quantity) should be gauge invariant, constructing the charges has been approached by different authors in different ways (see e.g. [20, 27, 28, 50, 54]). Details regarding quantization of charge can be found in [20], although in this section we will consider a purely classical approach.

In [28] (a similar approach was used in [50]), the single charge associated with an $\mathfrak{su}(2)$ gauge field was found using

$$Q = \frac{1}{4\pi} \oint_{S_\infty} \sqrt{\sum_{i=1}^{3} \left(F^i_{\theta\phi}\right)^2}\, d\theta\, d\phi, \tag{2.68}$$

where

$$F_{\theta\phi} = \sum_{i=1}^{3} F^i_{\theta\phi} T_i, \tag{2.69}$$

and the sum is taken over the generators T_i of $\mathfrak{su}(2)$ (see appendix A for details). While this works when we are only interested in finding a single charge, there is no obvious way to generalise this to find the $N-1$ charges associated with an $\mathfrak{su}(N)$ gauge field (in fact it turns out that this expression gives us the effective charge, to which we will return later in this section).

An alternative definition was provided in [27] (a similar definition can be found in [54]), which we will use since it allows us to find $N-1$ charges associated with an $\mathfrak{su}(N)$ gauge field. We define

$$Q(X,\Sigma) = \frac{1}{4\pi} \sup_{g(x)} k\left(X, \int_{S_\infty} g^{-1} F g\right) \tag{2.70}$$

where X is in the Cartan subalgebra $\mathcal{X}$ of $\mathfrak{su}(N)$, g is an element of the group $SU(N)$ (see appendix A), and $k(X,Y) = \mathrm{Tr}\{\mathrm{ad}X \mathrm{ad}Y\}$ is the Killing form [68], with $\mathrm{ad}X$ denoting the adjoint representation of the Cartan subalgebra element X as defined in [68]. The integrand takes its maximal value when $g^{-1}Fg \in \mathcal{X}$ [27]. The integral is taken over a sphere of constant radius in the limit $r \to \infty$, so since $dr = 0$ and our ansatz is time-independent we need only consider

$$F = \frac{1}{2}(F_{\theta\phi}\, d\theta \wedge d\phi + F_{\phi\theta}\, d\phi \wedge d\theta) = F_{\theta\phi}\, d\theta \wedge d\phi \tag{2.71}$$

where

$$F_{\theta\phi} = \partial_\theta A_\phi - \partial_\phi A_\theta + [A_\theta, A_\phi]. \tag{2.72}$$

From (2.11) we have

$$A_\theta = \frac{1}{2}(C - C^H), \qquad A_\phi = -\frac{i}{2}\left((C + C^H)\sin\theta + D\cos\phi\right) \tag{2.73}$$

and substituting into (2.72) gives

$$F_{\theta\phi} = -\frac{i}{2}\left([C, C^H] - D\right)\sin\theta \tag{2.74}$$

with

$$[C, C^H] = \mathrm{diag}(\omega_1^2, \omega_2^2 - \omega_1^2, \omega_3^2 - \omega_2^2, ..., -\omega_{N-1}^2). \tag{2.75}$$

The charges (2.70) are then given by

$$Q_i(X, \Sigma) = \frac{1}{4\pi} k \left(X, \int_{S_\infty} g^{-1} F_{\theta\phi} g \, d\theta \, d\phi\right) \tag{2.76}$$

where the group element g is chosen such that $g^{-1}F_{\theta\phi}g$ is an element of the Cartan subalgebra $\mathcal{X}$. We will show that in fact $F_{\theta\phi}$ is already an element of $\mathcal{X}$, so we will take $g = e$. We note here that there may be other possible choices of g which transform $F_{\theta\phi}$ into a different element of $\mathcal{X}$. However, in both cases the values along the diagonal must be the eigenvalues of $F_{\theta\phi}$, so doing such a transformation corresponds to choosing a different basis for $\mathcal{X}$. This would give a different set of equally physical charges.

We define an effective charge by requiring that in the Reissner-Nordström case, the metric function $\mu(r)$ reduces to

$$\mu(r) = 1 - \frac{2m(r)}{r} - \frac{\Lambda r^2}{3} = 1 - \frac{2M}{r} + \frac{Q^2}{r^2} - \frac{\Lambda r^2}{3} \tag{2.77}$$

with constant mass M and charge Q, i.e.

$$m(r) = M - \frac{Q^2}{2r} \Rightarrow Q^2 = 2r^2 m'(r). \tag{2.78}$$

By comparison with (2.14) we take

$$Q^2 = \sum_{j=1}^{N-1} \frac{j(j+1)}{2}\left(1 - \frac{\omega_j(\infty)^2}{j} + \frac{\omega_{j+1}(\infty)^2}{j+1}\right)^2, \tag{2.79}$$

which reduces in the Reissner-Nordström case ($\omega_j \equiv 0$ for all j) to

$$Q^2 = \frac{1}{6}N(N-1)(N+1). \tag{2.80}$$

In the rest of this section we will explicitly calculate the charges for $\mathfrak{su}(2)$ and $\mathfrak{su}(3)$

gauge fields, checking that they give the appropriate effective charge (2.79), and then go on to generalise these results to $\mathfrak{su}(N)$ gauge fields with general N.

Charge carried by an $\mathfrak{su}(2)$ gauge field

For the $\mathfrak{su}(2)$ case we have only one gauge field function $\omega(r)$, and

$$[C, C^H] = \begin{pmatrix} \omega^2 & 0 \\ 0 & -\omega^2 \end{pmatrix}, \qquad D = \begin{pmatrix} 1 & 0 \\ 0 & -1 \end{pmatrix}. \tag{2.81}$$

Substituting into (2.74), and expressing $F_{\theta\phi}$ in terms of the generators T_i of the real Lie algebra of $\mathfrak{su}(2)$(see appendix A) we have

$$\begin{aligned} F_{\theta\phi} &= -\frac{i}{2}\left(\omega^2 \begin{pmatrix} 1 & 0 \\ 0 & -1 \end{pmatrix} - \begin{pmatrix} 1 & 0 \\ 0 & -1 \end{pmatrix}\right) \sin\theta \\ &= (\omega^2 - 1) T_3 \sin\theta. \end{aligned} \tag{2.82}$$

The Lie algebra $\mathfrak{su}(2)$ is of rank one and we have only one generator of the Cartan subalgebra, T_3, and one conserved charge. Since $F_{\theta\phi}$ is proportional to the diagonal generator, it is already an element of the Cartan subalgebra, so we can choose $g = e$ where e is the identity. If X is an element of the Cartan subalgebra it must be proportional to T_3, hence $X = \alpha_3 T_3$ for $X \in \mathcal{X}$ and substituting into (2.76) gives

$$Q = \frac{1}{4\pi} k\left(X, 4\pi(\omega(\infty)^2 - 1)T_3\right) = 2\alpha_3(\omega(\infty)^2 - 1) \tag{2.83}$$

since $\mathrm{Tr}\{\mathrm{ad}T_i \, \mathrm{ad}T_j\} = N\delta_{ij}$ for $\mathfrak{su}(N)$ [20]. We then have

$$Q^2 = 4\alpha_3^2(\omega(\infty)^2 - 1)^2 \tag{2.84}$$

so (2.79) is only satisfied if we take $\alpha_3 = \pm\frac{1}{2}$, i.e. $Q = \pm(1 - \omega(\infty)^2)^2$. To agree with conventions in the literature [28, 61] we take the positive root

$$Q = 1 - \omega(\infty)^2, \tag{2.85}$$

i.e. the negative of the coefficient of $\sin(\theta)T_3$ in $F_{\theta\phi}$ in equation (2.82), with the gauge field function evaluated at infinity.

Charges carried by an $\mathfrak{su}(3)$ gauge field

We now have two gauge field functions ω_1 and ω_2, and

$$[C, C^H] = \begin{pmatrix} \omega_1^2 & 0 & 0 \\ 0 & \omega_2^2 - \omega_1^2 & 0 \\ 0 & 0 & -\omega_2^2 \end{pmatrix}, \qquad D = \begin{pmatrix} 2 & 0 & 0 \\ 0 & 0 & 0 \\ 0 & 0 & -2 \end{pmatrix}. \tag{2.86}$$

Substituting into (2.74)

$$\begin{aligned} F_{\theta\phi} &= -\frac{i}{2}\left[\begin{pmatrix} \omega_1^2 & 0 & 0 \\ 0 & \omega_2^2 - \omega_1^2 & 0 \\ 0 & 0 & -\omega_2^2 \end{pmatrix} - \begin{pmatrix} 2 & 0 & 0 \\ 0 & 0 & 0 \\ 0 & 0 & -2 \end{pmatrix}\right] \sin\theta \\ &= \sin\theta\left[\left(\omega_1^2 - 1 - \frac{\omega_2^2}{2}\right) T_3 + \sqrt{3}\left(\frac{\omega_2^2}{2} - 1\right) T_8\right], \end{aligned} \tag{2.87}$$

where T_i are the generators of the $\mathfrak{su}(3)$ Lie algebra and are defined in appendix A. The Cartan subalgebra $\mathcal{X}$ of $\mathfrak{su}(3)$ is generated by T_3 and T_8, so the elements X of $\mathcal{X}$ are given by $X = \rho T_3 + \sigma T_8$ for some ρ and σ. We expect to find two charges, and therefore require two elements of the Cartan subalgebra to substitute into (2.76), which we denote $X_i = \rho_i T_3 + \sigma_i T_8$ for $i = 1, 2$. As in the $\mathfrak{su}(2)$ case, $F_{\theta\phi}$ is also a linear combination of diagonal generators, so we can choose $g = e$ in (2.76). Evaluating (2.76) using (2.87) then gives

$$Q_i = 3\rho_i\left(\omega_1(\infty)^2 - 1 - \frac{\omega_2(\infty)^2}{2}\right) + 3\sqrt{3}\sigma_i\left(\frac{\omega_2(\infty)^2}{2} - 1\right) \tag{2.88}$$

or equivalently

$$Q_i = \alpha_i\omega_1(\infty)^2 + \frac{\beta_i - \alpha_i}{2}\omega_2(\infty)^2 - (\alpha_i + \beta_i), \tag{2.89}$$

where $\alpha_i = 3\rho_i$ and $\beta_i = 3\sqrt{3}\sigma_i$. The Lie algebra $\mathfrak{su}(3)$ has rank two and we have two conserved charges. Using (2.79), the effective charge squared is

$$Q_1^2 + Q_2^2 = \omega_1(\infty)^4 + \omega_2(\infty)^4 - 2\omega_1(\infty)^2 - 2\omega_2(\infty)^2 - \omega_1(\infty)^2\omega_2(\infty)^2 + 4. \tag{2.90}$$

We now square and add (2.89) and compare coefficients with (2.90). This gives six simultaneous equations in the four unknowns, of which three are independent:

$$\begin{aligned} \alpha_1^2 + \alpha_2^2 &= 1; && (2.91)\\ \alpha_1\beta_1 + \alpha_2\beta_2 &= 0; && (2.92)\\ \beta_1^2 + \beta_2^2 &= 3. && (2.93) \end{aligned}$$

Combining (2.92) and (2.93), and then using (2.91) gives

$$\beta_1^2 + \frac{\beta_1^2\alpha_1^2}{\alpha_2^2} = \beta_1^2\left(1 + \frac{1-\alpha_2^2}{\alpha_2^2}\right) = \frac{\beta_1^2}{\alpha_2^2} = 3 \tag{2.94}$$

so $\beta_1^2 = 3\alpha_2^2$, and similarly $\beta_2^2 = 3\alpha_1^2$. Substituting for α_2 from (2.91) the charges become

$$\begin{aligned} Q_1 &= \alpha_1\omega_1(\infty)^2 + \frac{\sqrt{3-3\alpha_1^2}-\alpha_1}{2}\omega_2(\infty)^2 - \left(\alpha_1 + \sqrt{3-3\alpha_1^2}\right),\\ Q_2 &= \sqrt{1-\alpha_1^2}\,\omega_1(\infty)^2 + \frac{\sqrt{3}\alpha_1 - \sqrt{1-\alpha_1^2}}{2}\omega_2(\infty)^2 - \left(\sqrt{1-\alpha_1^2} + \sqrt{3}\alpha_1\right). \end{aligned} \tag{2.95}$$

Calculating $Q_1^2 + Q_2^2$, we obtain (2.90) plus terms proportional to $\sqrt{3-3\alpha_1^2}$, implying that $\alpha_1 = \pm 1$. We then have

$$Q_1 = \pm\left(\omega_1(\infty)^2 - 1 - \frac{\omega_2(\infty)^2}{2}\right), \qquad Q_2 = \pm\sqrt{3}\left(\frac{\omega_2(\infty)^2}{2} - 1\right). \tag{2.96}$$

We require the charges Q_1 and Q_2 to be proportional to the $\mathfrak{su}(2)$ charge (2.85) for embedded $\mathfrak{su}(2)$ solutions, when we insert equation (2.26) into (2.96). For this reason we take the negative root, i.e.

$$Q_1 = \left(1 - \omega_1(\infty)^2 + \frac{\omega_2(\infty)^2}{2}\right), \qquad Q_2 = \sqrt{3}\left(1 - \frac{\omega_2(\infty)^2}{2}\right), \tag{2.97}$$

such that the charges for the embedded $\mathfrak{su}(2)$ solutions become $Q_1 = 1 - \omega^2$, $Q_2 = \sqrt{3}\,(1-\omega^2)$. Once again the charges are the coefficients of $T_k \sin\theta$ in $F_{\theta\phi}$ multiplied by -1, where $T_k \in \mathcal{X}$, and the gauge field functions are evaluated at infinity.

Charges carried by an $\mathfrak{su}(N)$ gauge field

The Cartan subalgebra of the Lie algebra $\mathfrak{su}(N)$ has $N-1$ generators, denoted H_i for $i = 1, 2, ..., N-1$ and given in appendix A. We find we can express $F_{\theta\phi}$ (2.74) in terms of the H_i, so $F_{\theta\phi}$ is then a member of the Cartan subalgebra and we do not need to make a gauge transformation before using equation (2.76). To find $F_{\theta\phi}$ we first require

$$\begin{aligned}[C, C^H] &= \text{diag}(\omega_1^2, \omega_2^2 - \omega_1^2, \omega_3^2 - \omega_2^2, ..., -\omega_{N-1}^2) \\ &= \omega_1^2 \text{diag}(1, -1, 0, ..., 0) + \omega_2^2 \text{diag}(0, 1, -1, 0, ...0) \\ &\quad + ... + \omega_{N-1}^2 \text{diag}(0, ..., 0, 1, -1)\end{aligned}$$

$$\begin{aligned}= \; & 2i\omega_1^2 H_1 + i\omega_2^2 \left(\sqrt{3}H_2 - H_1\right) \\ & + ... + \frac{i}{N-1}\omega_{N-1}^2 \left(\sqrt{2N(N-1)}H_{N-1} - \sqrt{2(N-1)(N-2)}H_{N-2}\right).\end{aligned} \tag{2.98}$$

In (2.98) the matrix multiplying ω_k^2 is given by

$$\frac{i}{k}\left(\sqrt{2k(k+1)}H_k - \sqrt{2k(k-1)}H_{k-1}\right). \tag{2.99}$$

Hence

$$[C, C^H] = \sum_{k=1}^{N-1} \frac{i}{k}\left(\sqrt{2k(k+1)}H_k - \sqrt{2k(k-1)}H_{k-1}\right)\omega_k^2. \tag{2.100}$$

We also note that

$$\sum_{k=1}^{N-1} i\sqrt{2k(k+1)}H_k = \text{diag}(N-1, N-3, ..., 3-N, 1-N) = D \tag{2.101}$$

so we can write

$$F_{\theta\phi} = \frac{\sin(\theta)}{2}\sum_{k=1}^{N-1}\left(\sqrt{2k(k+1)}\left(\frac{\omega_k^2}{k} - 1\right)H_k - \sqrt{2k(k-1)}H_{k-1}\frac{\omega_k^2}{k}\right). \tag{2.102}$$

Since

$$\sum_{k=1}^{N-1}\sqrt{2k(k-1)}H_{k-1}\frac{\omega_k^2}{k} \;=\; \sum_{k=1}^{N-1}\sqrt{2k(k+1)}H_k\frac{\omega_{k+1}^2}{k+1} \tag{2.103}$$

(where we have used the fact that $H_0=\omega_N=0$), equation (2.102) becomes

$$F_{\theta\phi}=\frac{\sin(\theta)}{2}\sum_{k=1}^{N-1}\sqrt{2k(k+1)}\left(\frac{\omega_k^2}{k}-1-\frac{\omega_{k+1}^2}{k+1}\right)H_k. \tag{2.104}$$

We now have $F_{\theta\phi}$ in the Cartan subalgebra for $\mathfrak{su}(N)$ EYM black holes for all N. By comparison with the results of the previous sections we have

$$Q_k=\frac{\sqrt{2k(k+1)}}{2}\left(1-\frac{\omega_k(\infty)^2}{k}+\frac{\omega_{k+1}(\infty)^2}{k+1}\right), \tag{2.105}$$

with $\omega_0=\omega_N=0$. For the $\mathfrak{su}(2)$ case this gives $Q=1-\omega(\infty)^2$, while for $\mathfrak{su}(3)$ we have $Q_1=1-\omega_1(\infty)^2+\frac{\omega_2(\infty)^2}{2}$, $Q_2=\sqrt{3}\left(1-\frac{\omega_2(\infty)^2}{2}\right)$. The $\mathfrak{su}(3)$ effective charge squared is then

$$\begin{aligned} Q_1^2+Q_2^2 &= \left(1-\omega_1(\infty)^2+\frac{\omega_2(\infty)^2}{2}\right)^2+3\left(1-\frac{\omega_2(\infty)^2}{2}\right)^2 \\ &= \sum_{j=1}^{2}\frac{j(j+1)}{2}\left(1-\frac{\omega_j(\infty)^2}{j}+\frac{\omega_{j+1}(\infty)^2}{j+1}\right)^2 \end{aligned} \tag{2.106}$$

since $\omega_3=0$ for $\mathfrak{su}(3)$, which is in agreement with (2.79). Similarly, in the $\mathfrak{su}(N)$ case the effective charge squared is

$$Q^2=\sum_{j=1}^{N-1}Q_j^2=\sum_{j=1}^{N-1}\frac{j(j+1)}{2}\left(1-\frac{\omega_j(\infty)^2}{j}+\frac{\omega_{j+1}(\infty)^2}{j+1}\right)^2. \tag{2.107}$$

We wish to show that stable black hole solutions can be determined uniquely by their global charges. Since the black holes are characterized by the values of the gauge field functions at infinity (as well as the mass M, cosmological constant Λ and the constants c_j) [12], we need to be able to determine the values of the gauge field functions at infinity from the charges, i.e. we require that the expressions (2.105) are invertible. Rearranging (2.105) for $k=N-1$ gives

$$\frac{\omega_{N-1}(\infty)^2}{N-1}=1-\frac{2Q_{N-1}}{\sqrt{2N(N-1)}}. \tag{2.108}$$

Similarly

$$\begin{aligned}
\frac{\omega_{N-2}(\infty)^2}{N-2} &= 1-\frac{2Q_{N-2}}{\sqrt{2(N-1)(N-2)}}+\frac{\omega_{N-1}(\infty)^2}{N-1} \\
&= 2-2\left(\frac{Q_{N-2}}{\sqrt{2(N-1)(N-2)}}+\frac{Q_{N-1}}{\sqrt{2N(N-1)}}\right), \qquad (2.109)\\
\frac{\omega_{N-3}(\infty)^2}{N-3} &= 3-\frac{2Q_{N-3}}{\sqrt{2(N-2)(N-3)}} \\
&\quad -2\left(\frac{Q_{N-2}}{\sqrt{2(N-1)(N-2)}}+\frac{Q_{N-1}}{\sqrt{2N(N-1)}}\right), \qquad (2.110)
\end{aligned}$$

and in general

$$\omega_j(\infty)^2 = j\left((N-j)-2\sum_{k=j}^{N-1}\frac{Q_k}{\sqrt{2k(k+1)}}\right). \qquad (2.111)$$

Again we check with the expressions for $\mathfrak{su}(2)$ and $\mathfrak{su}(3)$. From (2.85) we have $\omega(\infty)^2 = 1-Q$ while substituting $N=2$ into (2.111) gives $\omega_1^2 = 1-2\frac{Q_1}{\sqrt{4}} = 1-Q_1$. For $\mathfrak{su}(3)$, equation (2.111) implies

$$\begin{aligned}
\omega_1(\infty)^2 &= 2-2\sum_{k=1}^{2}\frac{Q_k}{\sqrt{2k(k+1)}} = 2-Q_1-\frac{Q_2}{\sqrt{3}}, \\
\omega_2(\infty)^2 &= 2\left(1-2\frac{Q_2}{2\sqrt{3}}\right) = 2\left(1-\frac{Q_2}{\sqrt{3}}\right), \qquad (2.112)
\end{aligned}$$

which can be rearranged to give (2.97) as required. We note that, up to an overall sign, the values of the gauge field functions at infinity can be determined from the charges. Since the EYM equations (2.13–2.15) are invariant under the transformations $\omega_j \to -\omega_j$, the sign is irrelevant. Therefore, since we can characterize $\mathfrak{su}(N)$ EYM black holes in AdS at infinity by Λ, the mass M, the quantities c_j and the $\omega_j(\infty)$ [12], we can equivalently characterize them by Λ, M, c_j and Q_j.

§ 2.6 Characterization of stable black holes

According to the "no-hair" conjecture [65], in asymptotically flat space and in the presence of an electromagnetic field, black holes are characterized by their mass, angular momentum, and electric or magnetic charge. However, as we shall demonstrate in this section, static EYM black holes with an $\mathfrak{su}(N)$ gauge field in AdS space are not characterized uniquely by their mass and total effective charge Q given by

(2.79) if $N > 2$. With an $\mathfrak{su}(N)$ gauge field there are $N-1$ gauge field functions, or equivalently $N-1$ charges Q_i (see previous section). The aim of this section is to argue, based on numerical evidence in section 2.6.1 and analytic work in section 2.6.2, that the charges Q_i, along with the mass M and cosmological constant Λ, are sufficient to characterize stable black hole solutions uniquely. Hence the purely magnetic $\mathfrak{su}(N)$ EYM black holes, in the presence of a negative cosmological constant, obey Bizon's modified no hair conjecture [17].

2.6.1 Numerical evidence

In the $\mathfrak{su}(2)$ case, there is only one magnetic charge Q, which we plot against the mass parameter m_0 at fixed $\Lambda = -3$ with various values of the event horizon radius r_h in figure 2.9. At the event horizon, these black holes are characterized by Λ, r_h and $\omega(r_h)$ [12]. Since there are no two black holes with the same M and Q but different values of r_h, we conclude that the black holes are indeed characterized by their mass M and charge Q. However, in the $\mathfrak{su}(3)$ case there are two magnetic charges Q_1 and Q_2, and the effective charge $Q = \sqrt{Q_1^2 + Q_2^2}$. At the event horizon, these black holes are characterized by Λ, r_h, $\omega_1(r_h)$ and $\omega_2(r_h)$ [12]. If $\mathfrak{su}(3)$ black holes were characterized uniquely by M and Q, we would therefore not expect to find two black holes with the same M and Q, but different r_h. In figure 2.10 we plot M and Q for $\mathfrak{su}(3)$ black holes with $\Lambda = -3$ and various values of r_h. We note that there are solutions with the same mass parameter $m_0 = 6.1$ and effective charge $Q = 5$ for $r_h = 1$, 1.25 and 1.5. We therefore conclude that $\mathfrak{su}(3)$ black holes are not uniquely characterized by M and Q.

As shown in [12], $\mathfrak{su}(N)$ EYM black holes are characterized by $N+1$ parameters at the event horizon: the cosmological constant Λ, the event horizon radius r_h and the $N-1$ gauge field functions $\omega_j(r_h)$. At infinity, they are characterized by $2N$ parameters: Λ, the mass M as measured from infinity (or equivalently the mass parameter $m_0 = \frac{M}{4\pi}$, see section 2.5.1), the $N-1$ charges Q_j (or equivalently the gauge field functions at infinity, see section 2.5.2) and the $N-1$ quantities c_j [12]. We therefore have $N-1$ additional parameters at infinity, we will argue that the c_j are single valued functions of M, Λ and the $\omega_j(\infty)$ and that the solutions are therefore characterized uniquely by these latter $N+1$ parameters.

A plot of c as a function of m_0 and Q for $\mathfrak{su}(2)$ black holes is given in figure 2.11, where the constraint (2.52) is satisfied both at the horizon and at infinity. In figure 2.11, c appears to be single valued for $\Lambda = -3$ (similar results are obtained

for $\Lambda = -10$ and -0.1). The equivalent plots for the $\mathfrak{su}(3)$ case, with $\Lambda = -3$, for c_1 and c_2 are shown in figure 2.12 and figure 2.13 respectively. In these we have plotted $m_0 = 10 \pm 0.1, 20 \pm 0.1, 30 \pm 0.1$, which gives rise to the bands. If we were to plot the exact values, these bands would decrease to rings, although we did not have sufficient resolution in our data to do this. Once again we have added the constraint that the stability inequalities (2.52) are satisfied both on the horizon and at infinity. Figures 2.12 and 2.13 show that in the $\mathfrak{su}(3)$ case, and for the range of data plotted, the c_j appear to be single valued functions of the charges Q_j and the mass M. The numerical evidence therefore suggests that the c_j are functions of M, Λ and the Q_j.

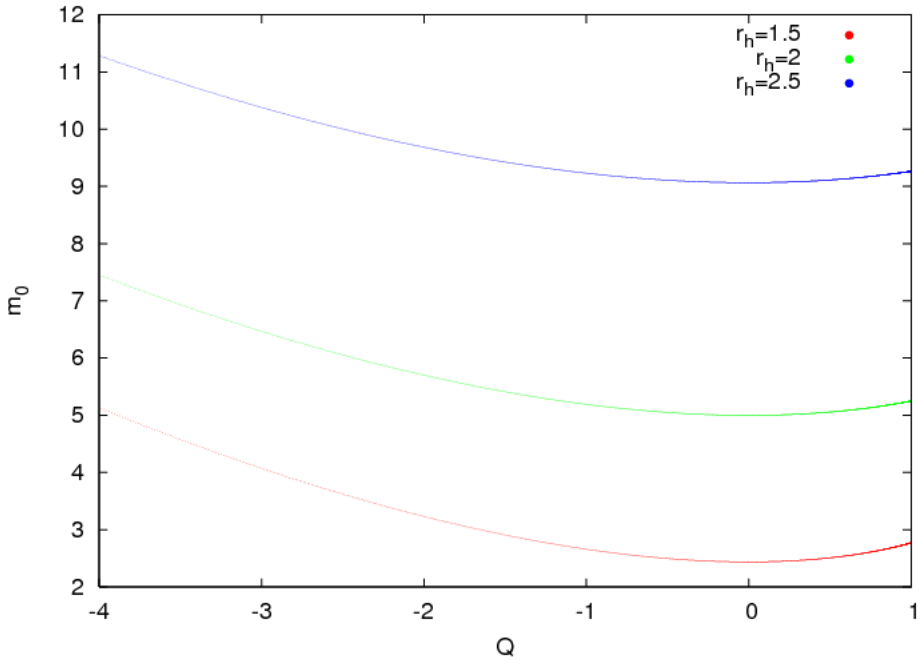

Figure 2.9: Mass parameter m_0 plotted as a function of charge Q for spherically symmetric $\mathfrak{su}(2)$ black holes with $\Lambda = -3$ and $n = 0$. Since we do not find two black holes with the same m_0 and Q but different r_h, we conclude that $\mathfrak{su}(2)$ black holes are characterized by their mass and charge.

To provide further numerical evidence, we examined the space of solutions in terms of the mass M and the charges Q_j at fixed Λ. Figures 2.9 and 2.14 show plots of M and Q_j for $\mathfrak{su}(2)$ and $\mathfrak{su}(3)$ black holes respectively. The lines in figure 2.9, and the surfaces in figure 2.14, appear to foliate the whole of the parameter space, and unlike figure 2.10 we do not see any places where two different solutions have the same mass and charges.

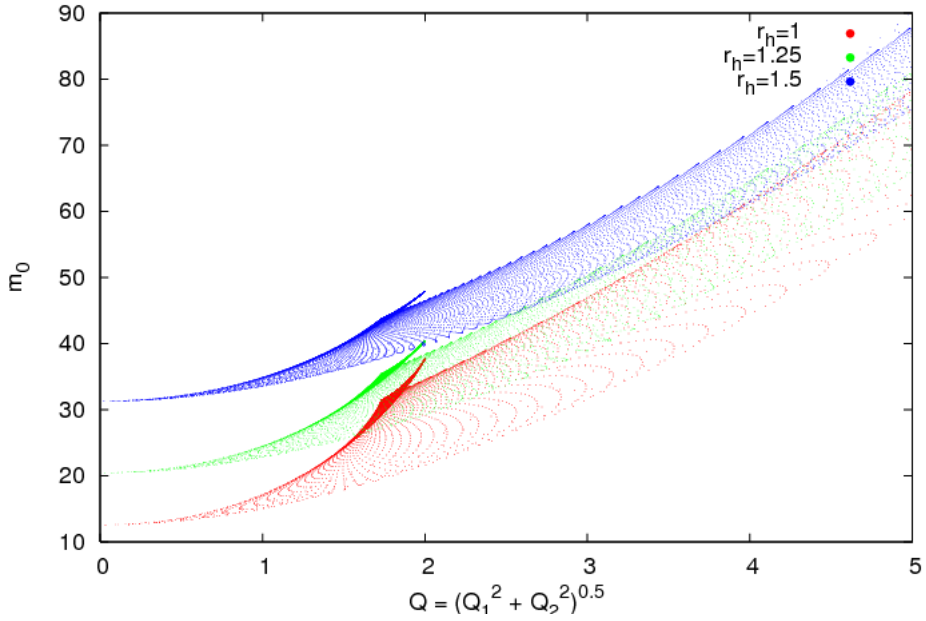

Figure 2.10: Mass parameter m_0 plotted as a function of total effective charge Q for spherically symmetric $\mathfrak{su}(3)$ black holes with $\Lambda = -3$, $n_1 = 0$, $n_2 = 0$. We find that there are black holes with the same m_0 and Q, but different r_h, hence $\mathfrak{su}(3)$ black holes are not characterized uniquely by their mass and effective charge.

Therefore the numerical evidence suggests firstly that the c_j are functions of M, Λ and Q_j, which in turn means that the $N+1$ parameters required to characterize the black holes at infinity are M, Λ and Q_j. Secondly, by looking directly at M, Λ and Q_j the numerical evidence suggests that we do not require any additional parameters to characterize the black holes at infinity.

2.6.2 Analytic work

In the previous section, we found numerical evidence suggesting that, for a given value of Λ, black holes are characterized at infinity by their mass M and charges Q_j. In this section we will prove that this is the case, at least for stable black holes with $|\Lambda|$ large but fixed. We know that the black holes are characterized at the event horizon by r_h and the $\omega_j(r_h)$ [12].

The goal of this section will be to find an approximate, invertible, analytic map $(r_h, \omega_j(r_h)) \to (M, Q_j)$, which we expect to be valid when $l = \sqrt{-3/\Lambda}$. If such a map exists, we can deduce that M and Q_j uniquely characterize the black holes.

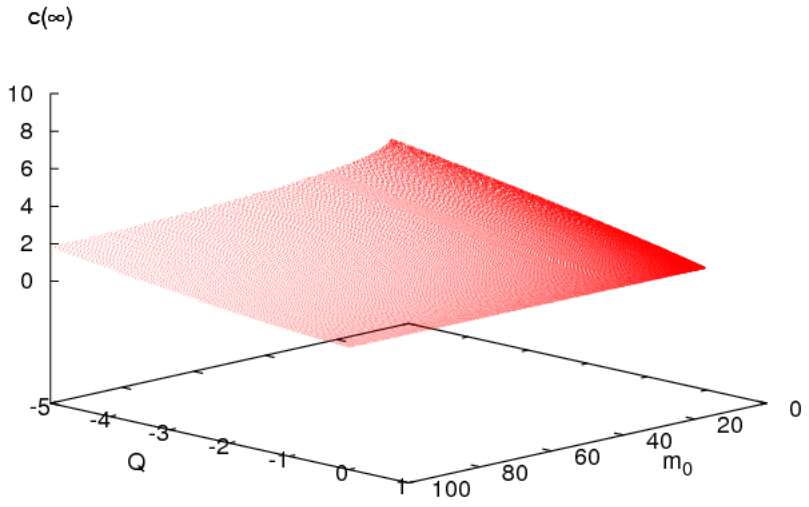

Figure 2.11: c_1 plotted as a function of the m_0 and charge for spherically symmetric $\mathfrak{su}(2)$ black holes with $\Lambda = -3$, $n = 0$. It appears that c_1 is a single valued function of the mass and charge Q, and hence not required to characterize the black holes at infinity.

We start by introducing a new dimensionless radial co-ordinate $x = r/r_h$, such that $x \in [1, \infty)$ for all values of the event horizon radius r_h. The field equations (2.13–2.15) become

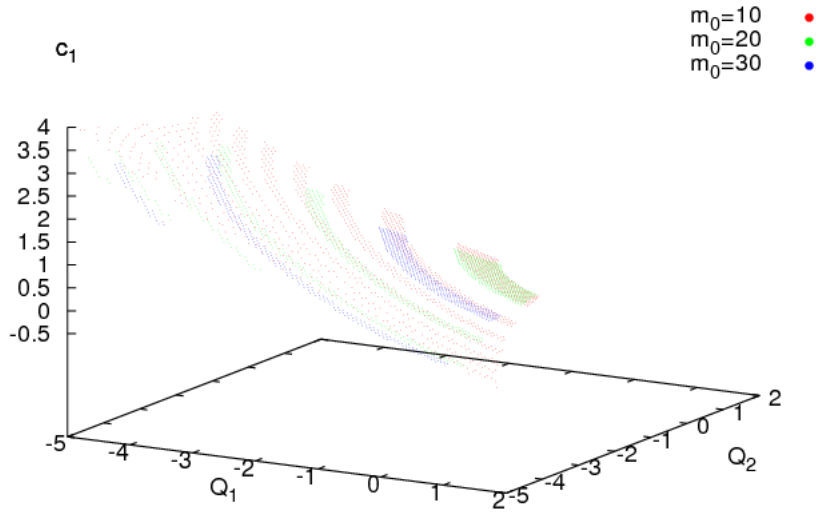

Figure 2.12: c_1 plotted as a function of the two $\mathfrak{su}(3)$ charges Q_1 and Q_2 for spherically symmetric $\mathfrak{su}(3)$ black holes with $\Lambda = -3$ and $n = 0$. It appears that c_1 is a single valued function of M, Q_1 and Q_2, and hence not required to characterize the black holes at infinity.

$$0 = x^2\mu\frac{d^2\omega_j}{dx^2} + x^2\left(\frac{\mu}{\sigma}\frac{d\sigma}{dx} + \frac{d\mu}{dx}\right)\frac{d\omega_j}{dx} + \frac{\omega_j}{2}\left(2 + \omega_{j-1}^2 - 2\omega_j^2 + \omega_{j+1}^2\right) \tag{2.113}$$

$$\frac{d\hat{m}}{dx} = \frac{\alpha^2}{r_h^2}\sum_{j=1}^{N-1}\left\{\frac{j(j+1)}{4x^2}\left(1 - \frac{\omega_j^2}{j} + \frac{\omega_{j+1}^2}{j+1}\right)^2 + \mu\left(\frac{d\omega_j}{dx}\right)^2\right\}, \tag{2.114}$$

$$\frac{d\sigma}{dx} = \frac{2\alpha^2\sigma}{r_h^2 x}\sum_{j=1}^{N-1}\left(\frac{d\omega_j}{dx}\right)^2, \tag{2.115}$$

where $\hat{m} = m/r_h$. At the event horizon, $x = 1$, we have

$$\hat{m}(1) = \frac{1}{2}\left(1 + \frac{r_h^2}{l^2}\right), \tag{2.116}$$

which becomes large as $l \to 0$ for fixed r_h. We define a further new variable $\tilde{m}(x)$ by

$$\hat{m}(x) = m_1 + \tilde{m}(x) \tag{2.117}$$

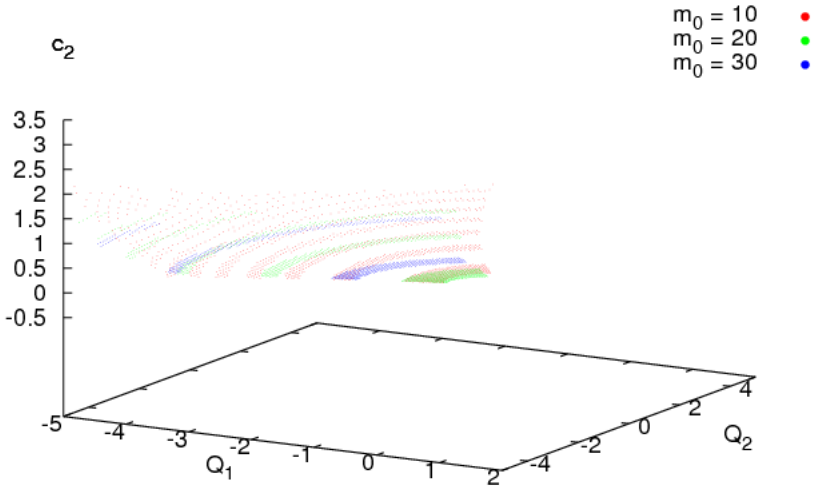

Figure 2.13: c_2 plotted as a function of the two $\mathfrak{su}(3)$ charges Q_1 and Q_2 for spherically symmetric $\mathfrak{su}(3)$ black holes with $\Lambda = -3$ and $n = 0$. It appears that c_2 is a single valued function of M, Q_1 and Q_2, and hence not required to characterize the black holes at infinity.

where $m_1 = \hat{m}(1)$ (2.116). Multiplying through by l^2, using

$$\mu = 1 - \frac{2m}{r} + \frac{r^2}{l^2} = 1 - \frac{2m_1}{x} - \frac{2\tilde{m}}{x} + \frac{r_h^2 x^2}{l^2}, \tag{2.118}$$

and substituting for $\frac{d\sigma}{dx}$ and $\frac{d\mu}{dx}$ using (2.114, 2.115, 2.118) we can write (2.113, 2.114) as

$$\begin{aligned} 0 &= x^2\left[l^2 - \frac{2m_1 l^2}{x} - \frac{2\tilde{m}l^2}{x} + r_h^2 x^2\right]\frac{d^2\omega_j}{dx^2} \\ &\quad + \left[2m_1 l^2 + 2\tilde{m}l^2 - 2r_h^2 x^3 l^2 p_\theta + 2r_h^2 x^3\right]\frac{d\omega_j}{dx} + l^2 W_j \omega_j, \qquad (2.119) \\ l^2\frac{d\tilde{m}}{dx} &= \frac{1}{r_h^2}\left[l^2 - \frac{2m_1 l^2}{x} - \frac{2\tilde{m}l^2}{x} + r_h^2 x^2\right]\sum_{j=1}^{N-1}\left(\frac{d\omega_j}{dx}\right)^2 \\ &\quad + \frac{l^2}{4x^2 r_h^2}\sum_{j=1}^{N}\left[\left(\omega_j^2 - \omega_{j-1}^2 - N - 1 + 2j\right)^2\right], \qquad (2.120) \end{aligned}$$

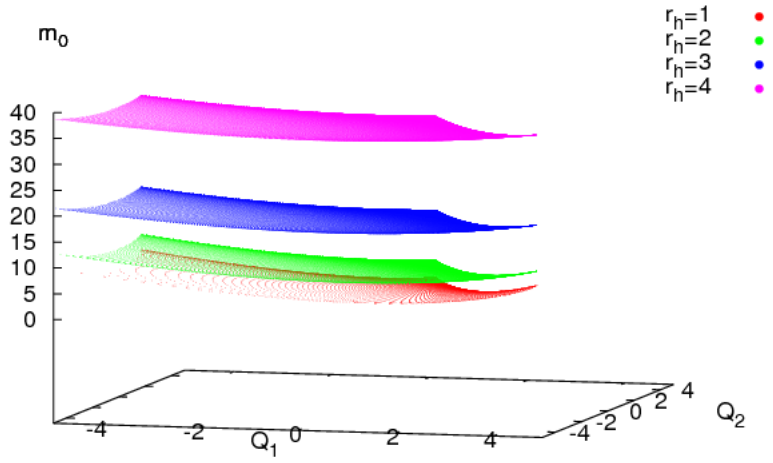

Figure 2.14: Mass parameter m_0 plotted as a function of the two $\mathfrak{su}(3)$ charges Q_1 and Q_2 as given in (2.97) for spherically symmetric black hole solutions with $\Lambda = -3$ and $n = 0$. We do not find two black holes with the same mass and charges but different event horizon radii, providing evidence that $\mathfrak{su}(3)$ black holes are characterized by m_0, Q_1 and Q_2.

where

$$p_\theta = \sum_{j=1}^{N-1} \frac{j(j+1)}{4r_h^2 x^2} \left(1 - \frac{\omega_j^2}{j} + \frac{\omega_{j+1}^2}{j+1}\right)^2, \tag{2.121}$$

$$W_j = 1 - \omega_j^2 + \frac{1}{2}\left(\omega_{j-1}^2 + \omega_{j+1}^2\right), \tag{2.122}$$

and we have used (2.17).

From the constraint (2.23) that the event horizon must be non-extremal, we have

$$l^2 \sum_{j=1}^{N} \left[\left(\omega_j^2(r_h) - \omega_{j-1}^2(r_h) - N - 1 + 2j\right)^2\right] < 2r_h^2 l^2 + 6r_h^4, \tag{2.123}$$

and therefore for each j we must have

$$l^2 \left(\omega_j^2(r_h) - \omega_{j-1}^2(r_h) - N - 1 + 2j\right)^2 < 2r_h^2 l^2 + 6r_h^4. \tag{2.124}$$

If we define

$$\begin{aligned} \varrho_j &= \omega_j^2(r_h) - \omega_{j-1}^2(r_h) - N - 1 + 2j, && (2.125) \\ \lambda_j &= \omega_j^2(r_h) - j(N-j), && (2.126) \end{aligned}$$

then we have

$$\begin{aligned} l|\varrho_1| &= l|\lambda_1| < \left(2r_h^2 l^2 + 6r_h^4\right)^{\frac{1}{2}} \\ l|\varrho_2| &= l|\lambda_2 - \lambda_1| < \left(2r_h^2 l^2 + 6r_h^4\right)^{\frac{1}{2}} \quad \Rightarrow \quad l|\lambda_2| < 2\left(2r_h^2 l^2 + 6r_h^4\right)^{\frac{1}{2}} \\ l|\varrho_j| &= l|\lambda_j - \lambda_{j-1}| < \left(2r_h^2 l^2 + 6r_h^4\right)^{\frac{1}{2}} \quad \Rightarrow \quad l|\lambda_j| < j\left(2r_h^2 l^2 + 6r_h^4\right)^{\frac{1}{2}}, \end{aligned} \tag{2.127}$$

and hence we have a bound on $(\omega_j^2(r_h) - j(N-j))$ given by

$$l|\omega_j^2(r_h) - j(N-j)| < j\left(2r_h^2 l^2 + 6r_h^4\right)^{\frac{1}{2}}. \tag{2.128}$$

The phase space plots in section 2.3 suggest that we do not find black hole solutions close to the edges of the region defined by (2.123), so we do not need to consider all $\omega_j(r_h)$ such that (2.123) is satisfied. We also note that the region where we find $n = 0$ (potentially stable) solutions grows as l decreases. We therefore consider a region of the $\omega_j(r_h)$ parameter space which, for small l, is smaller than the region defined by (2.123) but grows as l decreases. We therefore define new functions q_j by

$$l^2\left[\omega_j^2(r) - j\,(N-j)\right]^2 = l^{2\varsigma} q_j^2(x), \tag{2.129}$$

where the constant $\varsigma > 0$ is the same for all j, and $q_j(x)$ is order one for small l. Setting $\varsigma = 0$ then corresponds to considering the whole of the region of the parameter space satisfying (2.123), while $\varsigma = 1$ corresponds to an upper bound on ω_j which is independent of l. We therefore expect that $0 < \varsigma < 1$.

For $\mathfrak{su}(2)$ black holes, $l^{-1}\omega'(r) \to 0$ as $l \to 0$ [81], so we define new functions $\eta_j(x)$ by

$$l^{-1}\frac{d\omega_j}{dx} = l^{\varkappa}\eta_j(x) \tag{2.130}$$

for some $\varkappa > 0$, where η is of order one for small l. Our goal will now be to find suitable values of the constants ς and $\varkappa$ which give approximate analytic solutions to the field equations (2.119, 2.120) for small l - we view q_j and η_j as being the first terms in asymptotic series for the field variables, which is asymptotic for small l.

We start by writing (2.119, 2.120) in terms of q_j and η_j:

$$\begin{aligned} l^2\frac{d\tilde{m}}{dx} &= \frac{l^{2\varkappa+2}}{r_h^2}\left[l^2-\frac{2m_1l^2}{x}-\frac{2\tilde{m}l^2}{x}+r_h^2x^2\right]\sum_{j=1}^{N-1}\eta_j^2(x) \\ &\quad +\frac{l^{2\varsigma}}{4x^2r_h^2}\sum_{j=1}^{N}\left[q_j(x)-q_{j-1}(x)\right]^2; \qquad (2.131) \\ 0 &= x^2l^{\varkappa+1}\left[l^2-\frac{2m_1l^2}{x}-\frac{2\tilde{m}l^2}{x}+r_h^2x^2\right]\frac{d\eta_j}{dx} \\ &\quad +l^{\varkappa+1}\left[2m_1l^2+2\tilde{m}l^2-2r_h^2x^3l^2p_\theta+2r_h^2x^3\right]\eta_j(x) \\ &\quad +\frac{1}{2}l^{\varsigma+1}\left[q_{j+1}(x)-2q_j(x)+q_{j-1}(x)\right]\omega_j(x). \qquad (2.132) \end{aligned}$$

For equation (2.132) to be non-trivial, we require the first two terms on the right hand side to be of the same order in l as the last term. Since from (2.129) we have $\omega_j \sim l^{\frac{\varsigma-1}{2}}$, it must be the case that

$$\varkappa+1=\frac{3\varsigma}{2}+\frac{1}{2} \qquad \Rightarrow \qquad \varkappa=\frac{3\varsigma}{2}-\frac{1}{2}, \qquad (2.133)$$

so requiring that $\varkappa>0$ means we must have $\varsigma>1/3$. Turning to equation (2.131), it must be the case that the first line on the right hand side is small compared to the second line for small l since $2\varkappa+2=3\varsigma+3>2\varsigma$. Differentiating (2.129) and comparing with (2.130) gives

$$\frac{dq_j}{dx}\sim 2q_j\eta_j l^{1+\varsigma} \qquad (2.134)$$

for $\omega_j^4 \sim l^{2\varsigma-2}q_j^2$ and $\varkappa$ given by (2.133). Therefore the functions $q_j(x)$ are approximately constant for small l. Integrating (2.131) then gives, to leading order in l,

$$\begin{aligned} l^2\tilde{m}(x) &= \frac{l^{2\varsigma}}{4r_h^2}\left(1-\frac{1}{x}\right)\sum_{j=1}^{N}\left[q_j(1)-q_{j-1}(1)\right]^2 \\ &= \frac{l^2}{4r_h^2}\left(1-\frac{1}{x}\right)\sum_{j=1}^{N}\left[\left(\omega_j^2(r_h)-\omega_{j-1}^2(r_h)-N-1+2j\right)^2\right], \qquad (2.135) \end{aligned}$$

where we have used the initial condition $\tilde{m}=0$ at the event horizon $x=1$. We note that (2.135) implies that $\tilde{m}\sim\mathcal{O}\left(l^{2\varsigma-2}\right)$, so the $l^2\tilde{m}$ terms in (2.132) are small compared with $l^2m_1\sim\mathcal{O}(1)$ for small l and so can be ignored to leading order in l.

If we take the leading order expression $\omega_j=l^{\frac{1}{2}(\varsigma-1)}q_j^{\frac{1}{2}}$, the Yang-Mills equations

(2.132) are given by

$$\begin{aligned} 0 &= x^2\left[r_h^2x^2-\frac{2m_1l^2}{x}\right]\frac{d\eta_j}{dx}+\left[2m_1l^2+2r_h^2x^3\right]\eta_j(x) \\ &\quad +\frac{1}{2}\left[q_{j+1}(x)-2q_j(x)+q_{j-1}(x)\right]q_j(x)^{\frac{1}{2}}, \end{aligned} \tag{2.136}$$

to leading order in l, since $\tilde{m}\sim\mathcal{O}\left(l^{2\varsigma-2}\right)$ and

$$2r_h^2x^3l^2p_\theta = 2r_h^2x^3l^{2\varsigma}\sum_{j=1}^{N}\left[q_j(x)-q_{j-1}(x)\right]^2. \tag{2.137}$$

Taking the $q_j(x)$ to be approximately constant, (2.136) can be integrated directly to give

$$\eta_j(x) = -\frac{1}{2r_h^2\left(x^2+x+1\right)}\left[q_{j+1}(1) - 2q_j(1) + q_{j-1}(1)\right] q_j(1)^{\frac{1}{2}}, \tag{2.138}$$

where we have chosen the arbitrary constant of integration to be such that $\eta(x)$ is finite at the event horizon $x = 1$.

We have now obtained a consistent, approximate set of solutions of the field equations which are valid for all $r_h \gg l$ and all $\omega_j(r_h)$ such that

$$\left[\omega_j^2(r_h) - j\left(N-j\right)\right]^2 < l^{2\varsigma-2} \tag{2.139}$$

for some $\varsigma \in \left(\frac{1}{3}, 1\right)$. For these approximate solutions, the gauge field functions ω_j are approximately constant, and therefore the charges (2.105) are given by

$$Q_j = \frac{\sqrt{j(j+1)}}{\sqrt{2}}\left(1 - \frac{\omega_j(r_h)^2}{j} + \frac{\omega_{j+1}(r_h)^2}{j+1}\right), \tag{2.140}$$

while the masses of the black holes are given by

$$M = \frac{r_h}{2} - \frac{\Lambda r_h^3}{6} + \frac{1}{4r_h}\sum_{j=1}^{N}\left[\left(\omega_j^2(r_h) - \omega_{j-1}^2(r_h) - N - 1 + 2j\right)^2\right]. \tag{2.141}$$

At the event horizon, black holes are characterized by Λ, r_h and $\omega_j(r_h)$. We wish to show that these approximate analytic solutions are characterized by Λ, M and Q_j at infinity, which will be the case if we can determine the values of r_h and $\omega_j(r_h)$ from M and the Q_j, i.e. if the expressions (2.140) and (2.141) are invertible. Using the inverse function theorem, this will be the case if the Jacobian

$$\mathcal{J} = \begin{vmatrix} \dfrac{\partial M}{\partial r_h} & \dfrac{\partial M}{\partial \omega_1(r_h)} & \cdots & \dfrac{\partial M}{\partial \omega_{N-1}(r_h)} \\ \dfrac{\partial Q_1}{\partial r_h} & \dfrac{\partial Q_1}{\partial \omega_1(r_h)} & \cdots & \dfrac{\partial Q_1}{\partial \omega_{N-1}(r_h)} \\ \vdots & \vdots & \ddots & \vdots \\ \dfrac{\partial Q_{N-1}}{\partial r_h} & \dfrac{\partial Q_{N-1}}{\partial \omega_1(r_h)} & \cdots & \dfrac{\partial Q_{N-1}}{\partial \omega_{N-1}(r_h)} \end{vmatrix} \tag{2.142}$$

is non-zero.

Differentiating (2.140) and (2.141) we find

$$\begin{aligned}
\frac{\partial M}{\partial r_h} &= \frac{1}{2} - \frac{\Lambda r_h^2}{2} - \frac{1}{4r_h^2}\sum_{j=1}^{N}\left[\left(\omega_j^2(r_h) - \omega_{j-1}^2(r_h) - N - 1 + 2j\right)^2\right]; \\
\frac{\partial M}{\partial \omega_k(r_h)} &= -\frac{2}{r_h} W_k(r_h)\omega_k(r_h); \\
\frac{\partial Q_j}{\partial r_h} &= 0; \\
\frac{\partial Q_j}{\partial \omega_k(r_h)} &= \frac{\sqrt{j(j+1)}}{\sqrt{2}}\frac{2\omega_k(r_h)}{k}\left(-\delta_{j,k} + \delta_{j+1,k}\right).
\end{aligned} \tag{2.143}$$

Since the Q_j do not depend on the r_h, we have

$$\mathcal{J} = \frac{\partial M}{\partial r_h}\mathcal{J}_Q, \tag{2.144}$$

where $\mathcal{J}_Q$ is the Jacobian of the charges Q_j in terms of the $\omega_k(r_h)$. From (2.23) it can be shown that $\frac{\partial M}{\partial r_h} > 0$, while $\mathcal{J}_Q$ must be non-zero since we can determine the $\omega_j(r_h)$ from the charges (2.111). Therefore the Jacobian $\mathcal{J}$ (2.144) is non-zero and r_h and $\omega_j(r_h)$ can be uniquely determined from M and the Q_j.

Since black holes are characterized uniquely by r_h and $\omega_j(r_h)$, they are therefore also characterized uniquely by M and Q_j, at least when l is small.

Figures 2.15 – 2.17 show the accuracy of the approximations. In figures 2.15 and 2.16 we plot ω_1 and ω_2 respectively for $\mathfrak{su}(3)$ black holes with increasing values of $|\Lambda|$. We note that the gauge field functions are indeed approximately constant for large $|\Lambda|$, and that this approximation becomes increasingly accurate as $|\Lambda|$ increases.

Figure 2.17 shows the difference between the mass as a function of raduis $m(r)$ for an $\mathfrak{su}(3)$ black hole with large $|\Lambda|$, and the approximation (2.141). We note that at large r this difference is approximately zero, and that therefore the M is a good approximation to the mass measured from infinity.

2.6.3 Distinguishability of solitons from black holes

In the previous section we derived approximate analytic expressions for the mass M and charges Q_j of black hole solutions to the EYM equations for small but fixed l, and showed that these approximate analytic expressions are characterized by M

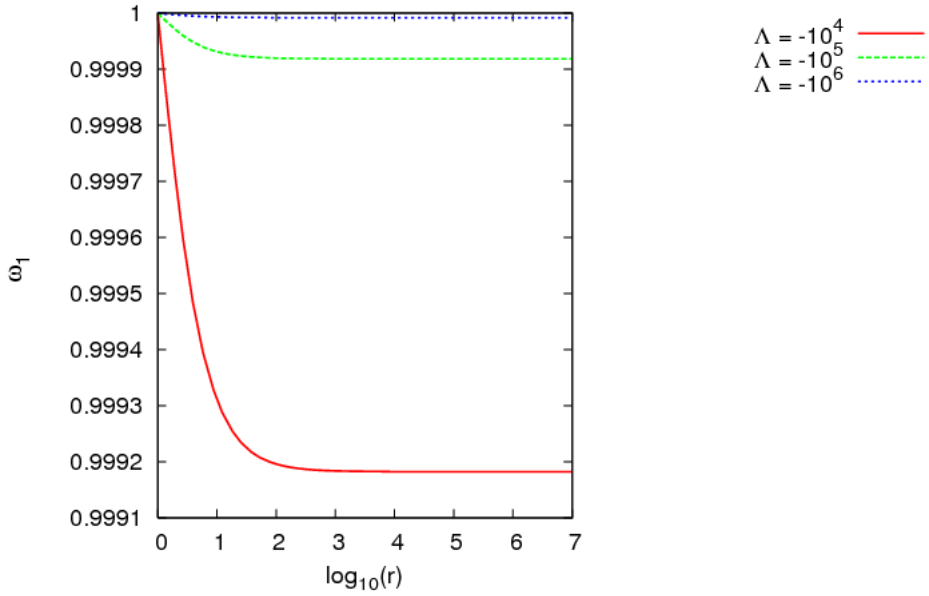

Figure 2.15: Plot of $\omega_1(r)$ for $\mathfrak{su}(3)$ black holes with $\omega_1(r_h) = 1$ and increasing values of $|\Lambda|$. We that note the accuracy of the approximation $\omega_j = const.$ increases with $|\Lambda|$.

and Q_j at infinity. In this section we will use a similar approach to find approximate analytic soliton solutions to the EYM equations, and check whether it is possible to distinguish between solitons and black holes from infinity given the mass M and charges Q_j.

Solitons are globally regular and have no event horizon. There is therefore only one length scale, the AdS length l, and we define a new radial co-ordinate by $y = r/l$. Following the analysis of [12] we consider the $(N-1) \times (N-1)$ matrix A with entries

$$A_{i,j} = [j\,(N-j)]^{\frac{1}{2}}\,[2\delta_{i,j} - \delta_{i+1,j} - \delta_{i-1,j}]\,, \tag{2.145}$$

and eigenvectors $\boldsymbol{\varphi_k}$ such that

$$A\boldsymbol{\varphi}_k = k\,(k-1)\,\boldsymbol{\varphi}_k. \tag{2.146}$$

We then write the gauge field functions ω_j as

$$\omega_j(r) = [j\,(N-j)]^{\frac{1}{2}}\,u_j(y), \tag{2.147}$$

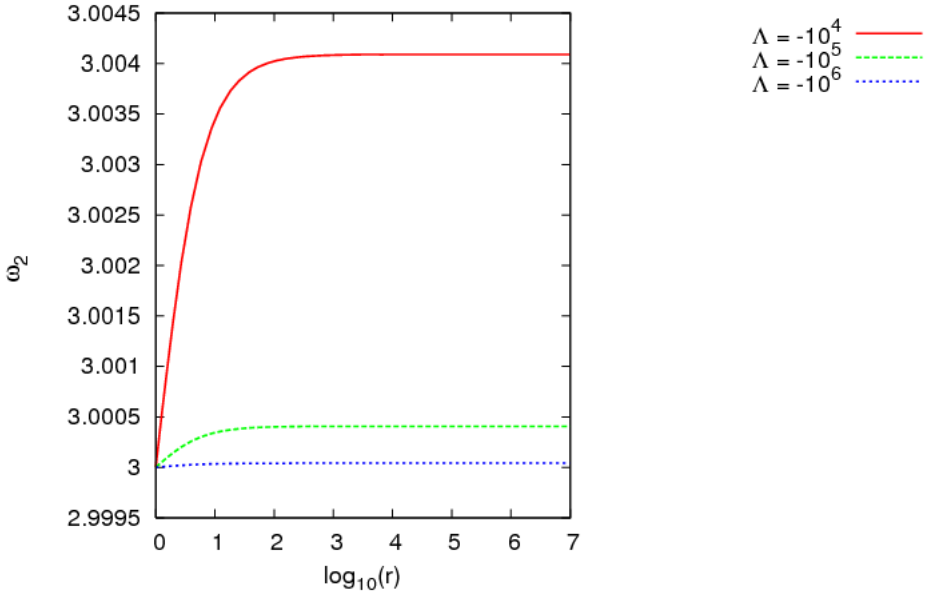

Figure 2.16: Plot of $\omega_1(r)$ for $\mathfrak{su}(3)$ black holes with $\omega_2(r_h) = 3$ and increasing values of $|\Lambda|$. We that note the accuracy of the approximation $\omega_j = const.$ increases with $|\Lambda|$.

where the vector

$$\boldsymbol{u}(y) = (u_1, \ldots, u_{N-1})^T = \boldsymbol{u}_0 + \sum_{k=2}^{N} \boldsymbol{\varphi}_k(y) y^k l^k, \tag{2.148}$$

and $\boldsymbol{u}_0 = (1, 1, \ldots, 1)^T$. Next we define scalar variables $\zeta_k(y)$ by

$$\zeta_k(y) = \boldsymbol{v}_k^T \boldsymbol{\varphi}_k(y), \tag{2.149}$$

where $\boldsymbol{v}_k^T$ is the $k-$th left eigenvector of the matrix A. In terms of these new variables, the Yang-Mills equations (2.13) can be written as [12],

$$\begin{aligned} 0 \;=\; & y^2\mu\left[y^k\frac{d^2\zeta_k}{dy^2} + 2ky^{k-1}\frac{d\zeta_k}{dy} + k\left(k-1\right)y^{k-2}\zeta_k\right] \\ & + \left[2\hat{m} + 2y^3 - \tilde{P}\right]\left[y^k\frac{d\zeta_k}{dy} + ky^{k-1}\zeta_k\right] + \frac{1}{l^k}\boldsymbol{v}_k^T\boldsymbol{W}. \end{aligned} \tag{2.150}$$

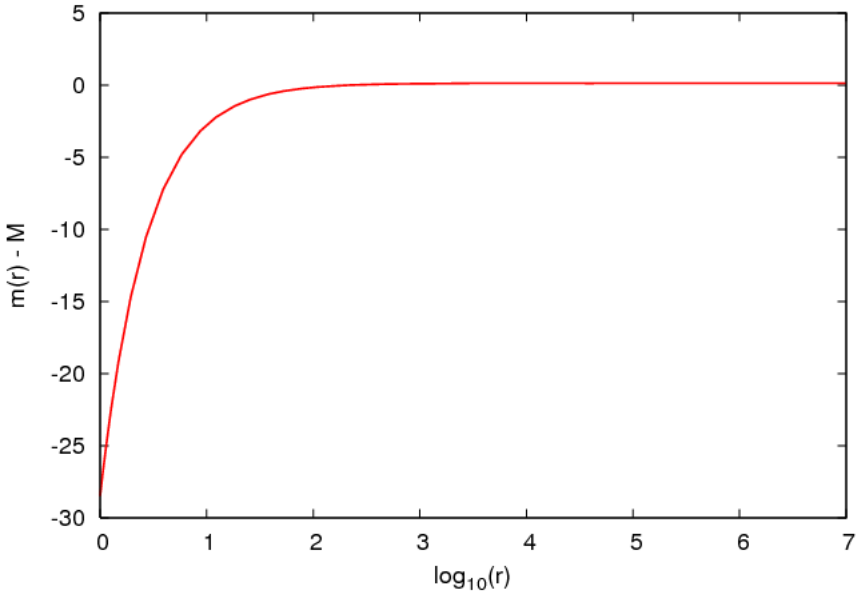

Figure 2.17: Difference between the mass function $m(r)$ and the approximate mass M given by (2.141) for $\mathfrak{su}(3)$ black holes with $\omega_1(r_h) = 1$, $\omega_2(r_h) = 3$, $\Lambda = 10^4$, showing good agreement for large r, so that M is a good approximation to the mass measured from infinity. Results become more accurate with increasing $|\Lambda|$.

The vector $\boldsymbol{W}$ is defined by $\boldsymbol{W} = (W_1, W_2, \ldots, W_{N-1})^T$, with W_j given by

$$W_j = 1 - \omega_j^2 + \frac{1}{2}\left(\omega_{j-1}^2 + \omega_{j+1}^2\right), \tag{2.151}$$

and

$$\hat{m}(y) = \frac{m(r)}{l}, \qquad \tilde{P}(y) = \frac{1}{2yl^2}\sum_{j=1}^{N}\left(\omega_j^2 - \omega_{j-1}^2 - N - 1 + 2j\right)^2. \tag{2.152}$$

Using (2.17), the Einstein equation (2.14) becomes

$$\frac{d\hat{m}}{dy} = \frac{1}{2y}\tilde{P} + \mu G, \tag{2.153}$$

where

$$G = \sum_{j=1}^{N-1}\left(\frac{d\omega_j}{dy}\right)^2. \tag{2.154}$$

In a neighbourhood of the origin, soliton solutions are determined by Λ and the

$N-1$ parameters $\zeta_j(0)$ [12]. While there are no upper bounds on the values of $\zeta_j(0)$ for the existence of regular solutions, like the black hole case the size of the region where we find $n = 0$ (potentially stable) solutions increases as l decreases [8]. It is argued in [21] that in the $\mathfrak{su}(2)$ case, the parameter space expands like l^{-1}. We therefore define new variables $\alpha_k(y)$ by

$$\zeta_k(y) = \alpha_k(y) l^{\varsigma_k - 1}, \tag{2.155}$$

where the ς_k are constants, but unlike the black hole case we allow for different values of ς_k for each k. We expect that $\varsigma_k < 1$ so that the space of solutions to be considered grows as l decreases. In the $\mathfrak{su}(2)$ case, taking $0 < \varsigma < 1$ would correspond to considering a region of the parameter space smaller than that studied in [21]. Like the black hole case we will assume that the $\alpha_k(y)$ are of order one for small l and all y.

In terms of the new variables, the Yang-Mills equation (2.150) takes the form

$$\begin{aligned} 0 &= y^2\mu\left[y^k\frac{d^2\alpha_k}{dy^2} + 2ky^{k-1}\frac{d\alpha_k}{dy} + k\left(k-1\right)y^{k-2}\alpha_k\right] \\ &\quad + \left[2\hat{m} + 2y^3 - \tilde{P}\right]\left[y^k\frac{d\alpha_k}{dy} + ky^{k-1}\alpha_k\right] + \frac{1}{l^{k+\sigma_k-1}}\boldsymbol{\sigma}_k^T\boldsymbol{W}. \end{aligned} \tag{2.156}$$

We start by considering the term $\boldsymbol{\sigma}_k^T\boldsymbol{W}$ which is given by [12]

$$\boldsymbol{\upsilon}_k^T\boldsymbol{W} = -k\left(k-1\right)y^k l^{k+\varsigma_k-1}\alpha_k + \sum_{j=k+1}^{Z}\boldsymbol{\upsilon}_k^T\boldsymbol{\tau}_j y^j l^j, \tag{2.157}$$

for some $Z \in \mathbb{N}$. The $\boldsymbol{\sigma}_k^T\boldsymbol{\tau}_j$ are involve products of up to three of the ζ_k and are therefore of order $l^{j-3+\varsigma_a+\varsigma_b+\varsigma_c}$ for some a, b, c. These will be subleading compared to the first term in (2.157) if $k+\varsigma_k-1 < j-3+\varsigma_a+\varsigma_b+\varsigma_c$, with $j \geq k+1$. This inequality is satisfied if $\varsigma_j > 2/3$ for all j, in which case we consider only the first term in (2.157). This gives, to leading order in l,

$$\begin{aligned} 0 &= \mu\left[y^2\frac{d^2\alpha_k}{dy^2} + 2ky\frac{d\alpha_k}{dy} + k\left(k-1\right)\alpha_k\right] \\ &\quad + \left[2\hat{m} + 2y^3 - \tilde{P}\right]\left[\frac{d\alpha_k}{dy} + ky^{-1}\alpha_k\right] - k\left(k-1\right)\alpha_k. \end{aligned} \tag{2.158}$$

We now turn our attention to the quantities G and $\tilde{P}$. We start by writing the

$\boldsymbol{\beta}_k$ as

$$\boldsymbol{\beta}_k(y) = \boldsymbol{v}_k \zeta_k(y) = \boldsymbol{v}_k l^{\varsigma_k - 1} \alpha_k(y), \tag{2.159}$$

where the $\boldsymbol{v}_k = (v_{k,1}, v_{k,2}, \ldots, v_{k,N-1})$ are right-eigenvectors of the matrix A. The ω_j are then given by

$$\omega_j = \left[j\,(N-j)\right]^{\frac{1}{2}} \left[1 + \sum_{k=2}^{N} v_{k,j} y^k l^{k+\varsigma_k - 1} \alpha_k(y)\right]. \tag{2.160}$$

The leading order in l clearly has $k = 2$, and therefore the leading order behaviour of G (2.154) is

$$G = l^{2\varsigma_2} \Sigma_G \left[y^2 \frac{d\alpha_2}{dy} + 2y\alpha_2\right]^2 + o\left(l^2\right), \tag{2.161}$$

where

$$\Sigma_G = \sum_{j=1}^{N-1} j\,(N-j)\,v_{2,j}^2. \tag{2.162}$$

Using the expression (2.160) we find that

$$\begin{aligned}
\omega_j^2 - \omega_{j-1}^2 - N - 1 + 2j \;=\; & 2\left[j\,(N-j)\right] \sum_{k=2}^{N} v_{k,j} y^k l^{k+\varsigma_k - 1} \alpha_k(y) \\
& + \left[j\,(N-j)\right] \left(\sum_{k=2}^{N} v_{k,j} y^k l^{k+\varsigma_k - 1} \alpha_k(y)\right)^2 \\
& - 2\left[(j-1)\,(N-j+1)\right] \sum_{k=2}^{N} v_{k,j-1} y^k l^{k+\varsigma_k - 1} \alpha_k(y) \\
& - \left[(j-1)\,(N-j+1)\right] \left(\sum_{k=2}^{N} v_{k,j-1} y^k l^{k+\varsigma_k - 1} \alpha_k(y)\right)^2,
\end{aligned} \tag{2.163}$$

which to leading order in l is given by

$$\omega_j^2 - \omega_{j-1}^2 - N - 1 + 2j = 2\Sigma_p y^2 l^{1+\varsigma_2} \alpha_2(y), \tag{2.164}$$

where

$$\Sigma_p = \sum_{j=1}^{N-1} \left[j\,(N-j)\,v_{2,j} - (j-1)\,(N-j+1)\,v_{2,j-1}\right]. \tag{2.165}$$

Substituting into (2.152), we find that the leading order behaviour of $\tilde{P}$ is

$$\tilde{P} = 2l^{2\varsigma_2}\Sigma_P^2\alpha_2^2 y^3. \tag{2.166}$$

Substituting the leading order expressions for G (2.161) and $\tilde{P}$ (2.166) into the Einstein equation (2.153), we find a consistent, non-trivial solution when

$$\hat{m} = l^{2\varsigma_2}\chi(y), \tag{2.167}$$

with $\chi(y)$ satisfying, to leading order in l, the differential equation

$$\frac{d\chi}{dy} = \left(1+y^2\right)\Sigma_G\left[y^2\frac{d\alpha_2}{dy} + 2y\alpha_2\right]^2 + \Sigma_P^2\alpha_2^2 y^2. \tag{2.168}$$

If $\varsigma_2 > 0$, the $\hat{m}$ and $\tilde{P}$ terms in (2.156) are subleading since they are both of order $l^{2\varsigma_2}$, and (2.156) becomes

$$0 = y\left(1+y^2\right)\frac{d^2\alpha_k}{dy^2} + 2\left[k + (k+1)\,y^2\right]\frac{d\alpha_k}{dy} + k\,(k+1)\,y\alpha_k. \tag{2.169}$$

The solution to (2.169) is a hypergeometric function

$$\alpha_k(y) = {}_2F_1\left(\frac{1}{2}\left[k+1\right], \frac{k}{2}; k+\frac{1}{2}; -y^2\right)\alpha_k(0), \tag{2.170}$$

which has a magnitude bounded by $|\alpha_k(0)|$ and tends monotonically to zero as $y \to \infty$ as y^{-2} for $k = 2$ and y^{4-2k} for $k > 2$. Equation (2.168) can then be integrated directly to find $\chi(y)$, which has the boundary conditions

$$\chi(y) = O(y^3), \quad y \to 0, \qquad \chi(y) = \chi_\infty + O(y^{-1}), \quad y \to \infty. \tag{2.171}$$

Hence we have a consistent, approximate set of solutions valid for small l. Returning to the original variables, we find that $m(r)$, and therefore the mass is of order $l^{2\varsigma_2+1}$, where $0 < \varsigma_2 < 1$, and

$$\omega_j(r) = \left[j\,(N-j)\right]^{\frac{1}{2}}\left[1 + \sum_{k=2}^{N} v_{k,j}r^k\alpha_k(y)l^{\varsigma_k-1}\right]. \tag{2.172}$$

We find that, unlike black holes, in the small l limit solitons with a non-negligible charge have a negligible mass. We therefore conclude that it is possible to distinguish

between solitons and black holes from infinity, by measuring the mass and non-abelian charges Q_i.

§ 2.7 Summary

The purpose of this chapter was to investigate whether EYM black holes in AdS with an $\mathfrak{su}(N)$ gauge field obey Bizon's modified no hair conjecture, that is whether stable black holes are uniquely characterized by global charges. In this case the appropriate charges are the mass and $N-1$ magnetic charges, which we have constructed. We have found both numerical and approximate analytic solutions to the field equations, and in both cases found evidence that the solutions are characterized by global charges, once we have removed some black holes which we know to be unstable.

This chapter has focussed entirely on purely magnetic gauge fields. In the next chapter we will consider spherically symmetric dyonic black holes and solitons, where the gauge field has both a magnetic part (again with $N-1$ magnetic charges), but also a non-zero electric part.

Chapter 3

Spherically symmetric dyons

In this chapter, we extend the work of chapter 2 by considering dyonic black holes with spherical event horizons as well as dyonic solitons, i.e. we will consider a gauge potential that has both an electric part and a magnetic part. Such black holes and solitons with an $\mathfrak{su}(2)$ gauge field have been considered in [18, 19], and in this chapter we consider a generalization to black holes and solitons with an $\mathfrak{su}(N)$ gauge field.

We begin in section 3.1 by extending the gauge potential considered in chapter 2 to include an electric part, and present the EYM equations, which reduce to those considered in chapter 2 in the limit of vanishing electric field. We will then find trivial solutions in section 3.2 which are the Schwarzschild-AdS, Reissner-Nordström-AdS and embedded $\mathfrak{su}(2)$ solutions.

In section 3.3 we will consider appropriate boundary conditions. For solitons, which are globally regular, we will find boundary conditions at the origin for $\mathfrak{su}(2)$ and $\mathfrak{su}(3)$. For black holes, we will be interested in boundary conditions close to the event horizon, which we will find for black holes with an $\mathfrak{su}(N)$ gauge field for general N. We will also find boundary conditions at infinity, which are relevant for both solitons and black holes with an $\mathfrak{su}(N)$ gauge field.

In section 3.4 we will describe the numerical method used to find solutions to the field equations. While for black holes this is similar to the method described in the previous chapter, for solitons we must use a different treatment to increase the accuracy of our results when using double precision in C++, which is an extension of the method developed in [8] for the purely magnetic case. Finally, in section 3.5 we will present numerical results. For comparison with [18, 19] we will present results for black holes and solitons with $\mathfrak{su}(2)$ gauge fields, as well as results with the larger

$\mathfrak{su}(3)$ gauge group.

§ 3.1 Gauge field, metric ansatz and field equations

An appropriate line element for spherically symmetric solutions is given by

$$ds^2 = -\sigma^2\mu\, dt^2 + r^2(d\theta^2 + \sin^2\,\theta\, d\phi^2) + \mu^{-1}dr^2, \tag{3.1}$$

where the function $\sigma = \sigma(r)$ must be determined from the field equations. The metric function μ is given by

$$\mu = 1 - \frac{2m(r)}{r} - \frac{\Lambda r^2}{3}, \tag{3.2}$$

where $\Lambda = -3/l^2$ is the cosmological constant, and for the space-time to be asymptotically AdS we require $\sigma = 1$ at large r.

As in the previous chapter, we take the generalised ansatz for a spherically symmetric $\mathfrak{su}(N)$ gauge potential, which is given by [51]

$$gA = \mathcal{A}\, dt + \frac{1}{2}\left(C - C^H\right) d\theta - \frac{i}{2}\left[\left(C + C^H\right)\sin\theta + D\cos\theta\right] d\phi + \mathcal{B}\, dr \tag{3.3}$$

where $\mathcal{A}$, $\mathcal{B}$, C and D are $N \times N$ matrices which depend only on r. The matrices $\mathcal{A}$ and $\mathcal{B}$ are purely imaginary, diagonal and traceless. Since we are now considering black hole solutions with non-zero electric field, the matrix $\mathcal{A}$ is non-zero, although we can once again set $\mathcal{B} = 0$ by a choice of gauge [51]. The matrix C is upper triangular, with non-zero entries

$$C_{j,j+1} = \omega_j(r)e^{i\gamma_j(r)}. \tag{3.4}$$

The constant matrix D is diagonal and traceless, and is given by

$$D = \mathrm{diag}(N-1, N-3, ..., 3-N, 1-N). \tag{3.5}$$

If $\omega_j \neq 0$ for all j then one of the Yang-Mills equations becomes $\gamma_j = 0$ for all j and (3.3) reduces to

$$gA = gA_\mu dx^\mu = \mathcal{A}\, dt + \frac{1}{2}(C - C^H)d\theta - \frac{i}{2}\left[(C + C^H)\sin\theta + D\cos\theta\right] d\phi, \tag{3.6}$$

where the only non-zero entries in the matrix C are now

$$C_{j,j+1} = \omega_j(r). \tag{3.7}$$

The electric part of the potential

$$\mathcal{A} = -\sum_{l=1}^{N-1} h_l H_l, \tag{3.8}$$

where $h_l = h_l(r)$ are also scalar functions of r only, and the H_l are members of the Cartan subalgebra of $\mathfrak{su}(N)$, and are given in Appendix A. We can decompose $\left(C + C^H\right)$ and $\left(C - C^H\right)$ into

$$C + C^H = 2i\sum_{m=1}^{N-1} \omega_m F_m^{(1)}, \qquad C - C^H = -2\sum_{m=1}^{N-1} \omega_m G_m^{(1)}, \tag{3.9}$$

where the $N \times N$ matrices $F_m^{(1)}$ and $G_m^{(1)}$ are generators of the Lie algebra $\mathfrak{su}(N)$ and are also given in Appendix A.

The Einstein-Yang-Mills equations corresponding to the potential (3.6) and line element (3.1) are derived in Appendix B and are given by

$$\begin{aligned}
m' &= \alpha^2 \sum_{k=1}^{N-1} \left\{ \frac{\omega_k^2}{\sigma^2\mu} \left(\sqrt{\frac{k+1}{2k}} h_k - \sqrt{\frac{k-1}{2k}} h_{k-1} \right)^2 + \frac{r^2 h_k'^2}{2\sigma^2} \right\} \\
&\quad + \alpha^2 \sum_{k=1}^{N-1} \left\{ \mu\omega_k'^2 + \frac{k(k+1)}{4r^2} \left(1 - \frac{\omega_k^2}{k} + \frac{\omega_{k+1}^2}{k+1} \right)^2 \right\}, \qquad (3.10) \\
\sigma' &= \alpha^2 \sum_{k=1}^{N-1} \left\{ \frac{2\omega_k^2}{\sigma\mu^2 r} \left(\sqrt{\frac{k+1}{2k}} h_k - \sqrt{\frac{k-1}{2k}} h_{k-1} \right)^2 + \frac{2\sigma\omega_k'^2}{r} \right\}, \qquad (3.11) \\
h_k'' &= h_k' \left(\frac{\sigma'}{\sigma} - \frac{2}{r} \right) + \sqrt{\frac{2(k+1)}{k}} \frac{\omega_k^2}{\mu r^2} \left(\sqrt{\frac{k+1}{2k}} h_k - \sqrt{\frac{k-1}{2k}} h_{k-1} \right) \\
&\quad + \sqrt{\frac{2k}{k+1}} \frac{\omega_{k+1}^2}{\mu r^2} \left(\sqrt{\frac{k}{2(k+1)}} h_k - \sqrt{\frac{k+2}{2(k+1)}} h_{k+1} \right), \qquad (3.12) \\
0 &= \omega_k'' + \omega_k' \left(\frac{\sigma'}{\sigma} + \frac{\mu'}{\mu} \right) + \frac{\omega_k}{\sigma^2\mu^2} \left(\sqrt{\frac{k+1}{2k}} h_k - \sqrt{\frac{k-1}{2k}} h_{k-1} \right)^2 \\
&\quad + \frac{\omega_k}{\mu r^2} \left(1 - \omega_k^2 + \frac{1}{2} \left(\omega_{k-1}^2 + \omega_{k+1}^2 \right) \right), \qquad (3.13)
\end{aligned}$$

and for the rest of the chapter we will set the coupling $\alpha^2 = 4\pi G/g^2 = 1$. As required, equations (3.10–3.13) reduce to the field equations of the previous chapter when we take $h_k = 0$ for all k. The planar black holes found in chapter 4 have similar field equations, except with 0 rather than 1 appearing in the expressions

$$\left(1 - \frac{\omega_k^2}{k} + \frac{\omega_{k+1}^2}{k+1}\right), \qquad \left(1 - \omega_k^2 + \frac{1}{2}\left(\omega_{k-1}^2 + \omega_{k+1}^2\right)\right), \qquad \mu = 1 - \frac{2m}{r} - \frac{\Lambda r^2}{3}. \tag{3.14}$$

§ 3.2 Trivial solutions

Although closed form solutions of the field equations (3.10–3.13) cannot be easily found in general, there are some "trivial" solutions. In this section we will find special cases where the line element (3.1) reduces to the Schwarzschild-AdS and Reissner-Nordström-AdS line elements, as well as finding embedded $\mathfrak{su}(2)$ solutions.

3.2.1 Schwarzschild-AdS

The line element for the Schwarzschild-AdS solution is given by

$$ds^2 = -\left(1 - \frac{2m_0}{r} - \frac{\Lambda r^2}{3}\right) dt^2 + r^2(d\theta^2 + \sin^2\theta\, d\phi^2) + \left(1 - \frac{2m_0}{r} - \frac{\Lambda r^2}{3}\right)^{-1} dr^2, \tag{3.15}$$

where the mass m_0 is a constant. To obtain this solution, we set $\sigma = 1$, remove the electric field (i.e. set $h_k = 0$ for all k), and require that $m' = 0$. Equation (3.10) then implies

$$\sum_{k=1}^{N-1} \left[\frac{k(k+1)}{4r^2}\left(1 - \frac{\omega_k^2}{k} + \frac{\omega_{k+1}^2}{k+1}\right)^2 + \mu\omega_k'^2\right] = 0. \tag{3.16}$$

If we take ω_k to be constant for all k, we are left with

$$\sum_{k=1}^{N-1} \frac{k(k+1)}{4r^2}\left(1 - \frac{\omega_k^2}{k} + \frac{\omega_{k+1}^2}{k+1}\right)^2 = 0, \tag{3.17}$$

which can be solved by taking $\omega_k = \pm\sqrt{k(N-k)}$, as in the previous chapter. This expression is consistent with equation (3.13), while equations (3.11, 3.12) vanish identically.

3.2.2 Reissner-Nordström-AdS

The line element for the Reissner-Nordström-AdS black hole is given by

$$ds^2 = -\mu_{RN} dt^2 + r^2(d\theta^2 + \sin^2\,\theta\, d\phi^2) + \mu_{RN}^{-1} dr^2, \tag{3.18}$$

where

$$\mu_{RN} = 1 - \frac{2m_0}{r} + \frac{\alpha_{RN}^2 q^2}{r^2} - \frac{\Lambda r^2}{3}, \tag{3.19}$$

and where both the mass m_0 and charge q are constant. Again we set $\sigma = 1$, but in this case we set $\omega_k = 0$ for all k. Equation (3.12) then reduces to

$$h_k'' = -\frac{2h_k'}{r} \qquad \Rightarrow \qquad h_k = b_k - \frac{a_k}{r}, \tag{3.20}$$

by direct integration, with constants of integration a_k and b_k. Equation (3.10) becomes

$$m' = \sum_{k=1}^{N-1} \left(\frac{r^2 h_k'^2}{2} + \frac{k(k+1)}{4r^2} \right) = \frac{\alpha_{RN}^2}{2r^2} \sum_{k=1}^{N-1} \left(a_k^2 + \frac{k(k+1)}{2} \right) \tag{3.21}$$

so that

$$m = m_0 - \frac{\alpha_{RN}^2}{2r} \sum_{k=1}^{N-1} \left(a_k^2 + \frac{k(k+1)}{2} \right). \tag{3.22}$$

Substituting this into the metric function (3.2) gives

$$\mu = 1 - \frac{2m_0}{r} + \frac{\alpha_{RN}^2}{r^2} \sum_{k=1}^{N-1} \left(a_k^2 + \frac{k(k+1)}{2} \right) - \frac{\Lambda r^2}{3}, \tag{3.23}$$

and by comparison with (3.19) we find

$$q^2 = \sum_{k=1}^{N-1} \left(a_k^2 + \frac{k(k+1)}{2} \right) = \sum_{k=1}^{N-1} \left(h_k'^2 r^4 + \frac{k(k+1)}{2} \right), \tag{3.24}$$

so the effective charge

$$q = \sqrt{\sum_{k=1}^{N-1} \left(h_k'^2 r^4 + \frac{k(k+1)}{2} \right)}. \tag{3.25}$$

Note that this charge carries an electric component from the h'_k term, which was absent in the Reissner-Nordström black hole of chapter 2, and that if we take $a_k = 0$ we find the Reissner-Nordströ solution from chapter 2 with the same charge.

3.2.3 Embedded $\mathfrak{su}(2)$ solutions

To obtain embedded $\mathfrak{su}(2)$ solutions we start by setting

$$\omega_k = A_k \omega, \qquad h_k = B_k h, \tag{3.26}$$

where $\omega = \omega(r)$, $h = h(r)$, and A_k and B_k are constants. Substituting into the Einstein equations (3.10, 3.11), and comparing with the $N = 2$ case, we require

$$\sum_{k=1}^{N-1} A_k^2 \left(\sqrt{\frac{k+1}{2k}} B_k - \sqrt{\frac{k-1}{2k}} B_{k-1} \right)^2 = \sum_{k=1}^{N-1} A_k^2 = \sum_{k=1}^{N-1} B_k^2 = \sum_{k=1}^{N-1} \frac{k(k+1)}{2}, \tag{3.27}$$

$$\left(\frac{A_k^2}{k} - \frac{A_{k+1}^2}{k+1} \right)^2 = 1. \tag{3.28}$$

Substituting (3.26) into the Yang-Mills equations (3.12, 3.13), we require

$$\begin{aligned} 1 &= \left(\sqrt{\frac{k+1}{2k}} B_k - \sqrt{\frac{k-1}{2k}} B_{k-1} \right)^2 = \frac{2A_k^2 - A_{k+1}^2 - A_{k-1}^2}{2} \\ &= \frac{\sqrt{2k(k+1)}}{2} \frac{A_{k+1}^2}{k+1} \left(\sqrt{\frac{k}{2(k+1)}} - \sqrt{\frac{k+2}{2(k+1)}} \frac{B_{k+1}}{B_k} \right) \\ &\quad + \frac{\sqrt{2k(k+1)}}{2} \frac{A_k^2}{k} \left(\sqrt{\frac{k+1}{2k}} - \sqrt{\frac{k-1}{2k}} \frac{B_{k-1}}{B_k} \right) \end{aligned} \tag{3.29}$$

to recover the $N = 2$ case. We can solve (3.27–3.29) by taking

$$A_k = \sqrt{k(N-k)}, \qquad B_k = \sqrt{\frac{k(k+1)}{2}}. \tag{3.30}$$

If we substitute our expressions (3.26) and (3.30) into the field equations (3.10–3.13), and then rescale the variables as follows

$$R = \lambda_N^{-1} r, \quad \tilde{m} = \lambda_N^{-1} m, \quad \tilde{h} = \lambda_N h, \quad \tilde{\Lambda} = \lambda_N^2 \Lambda, \tag{3.31}$$

where

$$\lambda_N^2 = \sum_{k=1}^{N-1} A_k^2 = \sum_{k=1}^{N-1} B_k^2 = \frac{1}{6}N(N^2-1), \tag{3.32}$$

we find that the field equations are

$$\begin{aligned}
\frac{d\tilde{m}}{dR} &= \frac{\omega^2\tilde{h}^2}{\sigma^2\mu} + \frac{R^2}{2\sigma^2}\left(\frac{d\tilde{h}}{dR}\right)^2 + \frac{1}{2R^2}\left(1-\omega^2\right)^2 + \mu\left(\frac{dw}{dR}\right)^2, \\
\frac{d\sigma}{dR} &= \frac{2\omega^2\tilde{h}^2}{R\sigma\mu^2} + \frac{2\sigma}{R}\left(\frac{d\omega}{dR}\right)^2, \\
\frac{d^2\tilde{h}}{dR^2} &= \frac{d\tilde{h}}{dR}\left(\frac{1}{\sigma}\frac{d\sigma}{dR} - \frac{2}{R}\right) + \frac{2\tilde{h}\omega^2}{\mu R^2}, \\
0 &= \frac{d^2\omega}{dR^2} + \frac{d\omega}{dR}\left(\frac{1}{\sigma}\frac{d\sigma}{dR} + \frac{1}{\mu}\frac{d\mu}{dR}\right) + \frac{\omega}{\mu}\left(\frac{\tilde{h}^2}{\sigma^2\mu} + \frac{1}{R^2}\left(1-\omega^2\right)\right),
\end{aligned} \tag{3.33}$$

which are precisely the $\mathfrak{su}(2)$ field equations in terms of the new variables. As with the full EYM equations, if we set $\tilde{h}$ to zero we recover the embedded $\mathfrak{su}(2)$ solutions from the previous chapter. We also find that these equations reduce to the embedded $\mathfrak{su}(2)$ equations found in chapter 4 for planar black holes if we replace (ω^2-1) with ω^2, albeit with a different metric function μ.

§ 3.3 Boundary conditions

In this section we will find boundary conditions for $\mathfrak{su}(2)$ and $\mathfrak{su}(3)$ solitons, and $\mathfrak{su}(N)$ black holes, which we will use to solve the field equations (3.10–3.13) numerically in section 3.5. Solitons are globally regular, and we expect the variables to have regular expansions at the origin, while for black holes we expect the variables to have regular expansions at the event horizon. We also expect both black holes and solitons to be regular at infinity.

3.3.1 At the origin

Boundary conditions for solitons are in general very complicated, and in this section we consider only gauge groups $\mathfrak{su}(2)$ and $\mathfrak{su}(3)$. The generalised $\mathfrak{su}(N)$ boundary conditions are presented in [12], although only for purely magnetic solutions, and we take a similar approach to find the dyonic boundary conditions in this section. Dyonic boundary conditions for $\mathfrak{su}(2)$ solitons are presented in [18, 19].

$\mathfrak{su}(2)$ solitons

In the $\mathfrak{su}(2)$ case, the field equations are given by

$$
\begin{aligned}
m' &= \frac{h_1^2\omega_1^2}{\sigma^2\mu} + \frac{r^2h_1'^2}{2\sigma^2} + \frac{\left(1-\omega_1^2\right)^2}{2r^2} + \mu\omega_1'^2, && (3.34)\\
\sigma' &= 2\left(\frac{\omega_1^2h_1^2}{\sigma\mu^2r} + \frac{\sigma\omega_1'^2}{r}\right), && (3.35)\\
\omega_1'' &= -\left(\frac{\sigma'}{\sigma} + \frac{\mu'}{\mu}\right)\omega_1' - \frac{\omega_1h_1^2}{\sigma^2\mu^2} - \frac{\omega_1\left(1-\omega_1^2\right)}{\mu r^2}, && (3.36)\\
h_1'' &= \left(\frac{\sigma'}{\sigma} - \frac{2}{r}\right)h_1' + 2\frac{\omega_1^2h_1}{\mu r^2}. && (3.37)
\end{aligned}
$$

We assume that the variables m, σ, ω and h have regular Taylor expansions near the origin, given by

$$
\begin{aligned}
m &= m_0 + m_1r + m_2r^2 + m_3r^3 + \mathcal{O}\left(r^4\right),\\
\sigma &= \sigma_0 + \sigma_1r + \sigma_2r^2 + \mathcal{O}\left(r^3\right),\\
\omega_1 &= \omega_{1,0} + \omega_{1,1}r + \omega_{1,2}r^2 + \mathcal{O}\left(r^3\right),\\
h_1 &= h_{1,0} + h_{1,1}r + h_{1,2}r^2 + h_{1,3}r^3 + \mathcal{O}\left(r^4\right). && (3.38)
\end{aligned}
$$

For the metric function (3.2) to be regular at the origin, we require $m_0 = 0$, which gives $\mu \sim \mathcal{O}(1)$ to leading order. The third term on the right hand side of (3.34) is given by

$$
\frac{\left(1-\omega_1^2\right)^2}{2r^2} = \frac{1}{2r^2}\left(1 - 2\omega_{1,0}^2 + \omega_{1,0}^4 + 4\omega_{1,0}\omega_{1,1}r - 4\omega_{1,0}^3\omega_{1,1}r + \mathcal{O}\left(r^2\right)\right). \qquad (3.39)
$$

For regularity of (3.34), we require

$$
1 - 2\omega_{1,0}^2 + \omega_{1,0}^4 = 0, \qquad 4\omega_{1,1}(\omega_{1,0} - \omega_{1,0}^3) = 0, \qquad (3.40)
$$

which are solved by $\omega_{1,0} = \pm 1$. We take $\omega_{1,0} = 1$ without loss of generality, since the field equations are invariant under the transformation $\omega_1 \to -\omega_1$. Turning now to equation (3.36), we have

$$
\omega_1\left(1-\omega_1^2\right) = \left[1 + \omega_{1,1}r + \mathcal{O}\left(r^2\right)\right]\left[-2\omega_{1,1}r + \mathcal{O}\left(r^2\right)\right], \qquad (3.41)
$$

which must be of order r^2 or higher to avoid divergences in (3.36), so that $\omega_{1,1} = 0$. Similarly, the leading order behaviour of the right hand side of (3.37) is

$$\frac{2h_{1,0}}{(1-2m_1)r^2} + \frac{2h_{1,1}}{r}\left(\frac{1}{1-2m_1} - 1\right) + \mathcal{O}(1), \tag{3.42}$$

so we must have $h_{1,0} = 0$ and either $h_{1,1} = 0$ or $m_1 = 0$. From (3.34, 3.35), we now have

$$m' = m_1 + 2m_2 r + 3m_3 r^2 + \mathcal{O}(r^3) = \left(\frac{3h_{1,1}^2}{2\sigma_0^2} + 6\omega_{1,2}^2\right) r^2 + \mathcal{O}(r^3), \tag{3.43}$$

and

$$\sigma' = \sigma_1 + 2\sigma_2 r + \mathcal{O}\left(r^2\right) = 2\left(\frac{h_{1,1}^2}{\sigma_0} + 4\sigma_0\omega_{1,2}^2\right) r + \mathcal{O}\left(r^2\right), \tag{3.44}$$

so that m_1, m_2 and σ_1 must all be zero and

$$m_3 = \frac{h_{1,1}^2}{2\sigma_0^2} + 2\omega_{1,2}^2, \qquad \sigma_2 = \frac{h_{1,1}^2}{\sigma_0} + 4\sigma_0\omega_{1,2}^2. \tag{3.45}$$

Returning to equation (3.37) we have

$$\begin{aligned} h_1'' &= 2h_{1,2} + 6h_{1,3}r + \mathcal{O}\left(r^2\right) \\ &= -2h_{1,2} + \left[2h_{1,1}\left(\frac{\sigma_2}{\sigma_0} + 2m_3 + \frac{\Lambda}{3} + 2\omega_{1,2}\right) - 4h_{1,3}\right] r + \mathcal{O}\left(r^2\right), \end{aligned} \tag{3.46}$$

hence $h_{1,2} = 0$, and

$$h_{1,3} = \frac{h_{1,1}}{5}\left(\frac{\sigma_2}{\sigma_0} + 2m_3 + \frac{\Lambda}{3} + 2\omega_{1,2}\right). \tag{3.47}$$

Equation (3.36) provides no further constraints on $\omega_{1,2}$, and altogether we have

$$\begin{aligned} m &= \left(\frac{h_{1,1}^2}{2\sigma_0^2} + 2\omega_{1,2}^2\right) r^3 + \mathcal{O}\left(r^4\right), \\ \sigma &= \sigma_0 + \left(\frac{h_{1,1}^2}{\sigma_0} + 4\sigma_0\omega_{1,2}^2\right) r^2 + \mathcal{O}\left(r^3\right), \\ \omega_1 &= 1 + \omega_{1,2} r^2 + \mathcal{O}\left(r^3\right), \\ h_1 &= h_{1,1} r + \frac{h_{1,1}}{5}\left(2\frac{h_{1,1}^2}{\sigma_0^2} + 8\omega_{1,2}^2 + \frac{\Lambda}{3} + 2\omega_{1,2}\right) r^3 + \mathcal{O}\left(r^4\right). \end{aligned} \tag{3.48}$$

The value of σ_0 is fixed by the requirement that σ approaches one at large r (i.e.

the space is asymptotically AdS). There are therefore two free parameters, $h_{1,1}$ and $\omega_{1,2}$, along with the cosmological constant Λ.

$\mathfrak{su}(3)$ solitons

In the $\mathfrak{su}(3)$ case we have 6 variables, m, σ, ω_1, ω_2, h_1 and h_2, with field equations given by

$$\begin{aligned}
m' &= \frac{h_1^2\omega_1^2}{\sigma^2\mu} + \left(\frac{\sqrt{3}}{2}h_2 - \frac{1}{2}h_1\right)^2 \frac{\omega_2^2}{\sigma^2\mu} + \frac{r^2}{2\sigma^2}\left(h_1'^2 + h_2'^2\right) \\
&\quad + \frac{1}{2r^2}\left(1 - \omega_1^2 + \frac{\omega_2^2}{2}\right)^2 + \frac{3}{2r^2}\left(1 - \frac{\omega_2^3}{2}\right)^2 + \mu\left(\omega_1'^2 + \omega_2'^2\right), \qquad (3.49)\\
\sigma' &= \frac{2\omega_1^2h_1^2}{\sigma\mu^2 r} + \frac{2\omega_2^2}{\sigma\mu^2 r}\left(\frac{\sqrt{3}}{2}h_2 - \frac{1}{2}h_1\right)^2 + \frac{2\sigma}{r}\left(\omega_1'^2 + \omega_2'^2\right), \qquad (3.50)\\
\omega_1'' &= -\left(\frac{\sigma'}{\sigma} + \frac{\mu'}{\mu}\right)\omega_1' - \frac{\omega_1 h_1^2}{\sigma^2\mu^2} - \frac{\omega_1}{\mu r^2}\left(1 - \omega_1^2 + \frac{\omega_2^2}{2}\right), \qquad (3.51)\\
\omega_2'' &= -\left(\frac{\sigma'}{\sigma} + \frac{\mu'}{\mu}\right)\omega_2' - \frac{\omega_2}{\sigma^2\mu^2}\left(\frac{\sqrt{3}}{2}h_2 - \frac{1}{2}h_1\right)^2 - \frac{\omega_2}{\mu r^2}\left(1 - \omega_2^2 + \frac{\omega_1^2}{2}\right), \qquad (3.52)\\
h_1'' &= \left(\frac{\sigma'}{\sigma} - \frac{2}{r}\right)h_1' + \frac{1}{\mu r^2}\left[\omega_2^2\left(\frac{1}{2}h_1 - \frac{\sqrt{3}}{2}h_2\right) + 2\omega_1^2 h_1\right], \qquad (3.53)\\
h_2'' &= \left(\frac{\sigma'}{\sigma} - \frac{2}{r}\right)h_2' + \frac{\sqrt{3}\omega_2^2}{\mu r^2}\left(\frac{\sqrt{3}}{2}h_2 - \frac{1}{2}h_1\right), \qquad (3.54)
\end{aligned}$$

and once again we assume that the variables have regular Taylor expansions at the origin:

$$\begin{aligned}
m &= m_0 + m_1 r + m_2 r^2 + m_3 r^3 + \mathcal{O}\left(r^4\right),\\
\sigma &= \sigma_0 + \sigma_1 r + \sigma_2 r^2 + \mathcal{O}\left(r^3\right),\\
\omega_1 &= \omega_{1,0} + \omega_{1,1} r + \omega_{1,2} r^2 + \omega_{1,3} r^3 + \mathcal{O}\left(r^4\right),\\
\omega_2 &= \omega_{2,0} + \omega_{2,1} r + \omega_{2,2} r^2 + \omega_{2,3} r^3 + \mathcal{O}\left(r^4\right),\\
h_1 &= h_{1,0} + h_{1,1} r + h_{1,2} r^2 + \mathcal{O}\left(r^3\right),\\
h_2 &= h_{2,0} + h_{2,1} r + h_{2,2} r^2 + \mathcal{O}\left(r^3\right). \qquad (3.55)
\end{aligned}$$

Again we start by considering the r^{-2} term in the m' equation (3.49). This time for regularity we require

$$\frac{1}{2}\left(1-\omega_{1,0}^2+\frac{\omega_{2,0}^2}{2}\right)^2+\frac{3}{2}\left(1-\frac{\omega_{2,0}^3}{2}\right)^2=0, \tag{3.56}$$

which is solved by $\omega_{1,0}^2=2=\omega_{2,0}^2$, and once again we take the positive square root without loss of generality. As in the $\mathfrak{su}(2)$ case, regularity of equations (3.51–3.54) requires that there are no terms of order r in the expansions for the ω_j, and no terms of order one in the h_j, i.e. $\omega_{1,1}$, $\omega_{2,1}$, $h_{1,0}$ and $h_{2,0}$ are all zero. By considering the leading order terms on the right hand sides of equations (3.49, 3.50) we again find that m_1, m_2 and σ_1 are all zero along with

$$\begin{aligned} 3m_3 &= \frac{\omega_{1,0}^2h_{1,1}^2}{\sigma_0^2}+\frac{\omega_{2,0}^2}{\sigma_0^2}\left(\frac{\sqrt{3}}{2}h_{2,1}-\frac{1}{2}h_{1,1}\right)^2+\frac{(h_{1,1}+h_{2,1})^2}{2\sigma_0^2} \\ &\quad +\frac{1}{2}\left(2\omega_{1,0}\omega_{1,2}-\omega_{2,0}\omega_{2,2}\right)^2+\frac{3}{2}\omega_{2,0}^2\omega_{2,2}^2+4\omega_{1,2}^2+4\omega_{2,2}^2, \qquad (3.57) \\ 2\sigma_2 &= \frac{4}{\sigma_0}\left[h_{1,1}^2+\left(\frac{\sqrt{3}}{2}h_{2,1}-\frac{1}{2}h_{1,1}\right)^2\right]+8\sigma_0\left(\omega_{1,2}^2+\omega_{2,2}^2\right). \qquad (3.58) \end{aligned}$$

Substituting the expansions (3.55) into equations (3.51–3.52) one can write the conditions in matrix form as

$$2\boldsymbol{\omega_2}=\mathcal{M}_2\boldsymbol{\omega_2}, \qquad 6\boldsymbol{\omega_3}=\mathcal{M}_2\boldsymbol{\omega_3}, \tag{3.59}$$

where $\boldsymbol{\omega_2}=(\omega_{1,2},\omega_{2,2})^T$, $\boldsymbol{\omega_3}=(\omega_{1,3},\omega_{2,3})^T$, and the matrix

$$\mathcal{M}_2=\begin{pmatrix}4 & -2\\ -2 & 4\end{pmatrix}. \tag{3.60}$$

The matrix $\mathcal{M}_2$ has normalized eigenvectors

$$\boldsymbol{v_1}=\frac{1}{\sqrt{2}}\begin{pmatrix}1\\1\end{pmatrix}, \qquad \boldsymbol{v_2}=\frac{1}{\sqrt{2}}\begin{pmatrix}1\\-1\end{pmatrix}, \tag{3.61}$$

corresponding to eigenvalues of 2 and 6 respectively (note that this is the same matrix and eigenvalues as found in [8]). Hence $\boldsymbol{\omega_2}$ must be proportional to $\boldsymbol{v_1}$ and $\boldsymbol{\omega_3}$ must be proportional to $\boldsymbol{v_2}$. We therefore define new constants b_1 and b_2 such

that $\boldsymbol{\omega_2} = b_1 \boldsymbol{v_1}$, $\boldsymbol{\omega_3} = b_2 \boldsymbol{v_2}$, and we have

$$\omega_{1,2} = \frac{1}{\sqrt{2}} b_1, \quad \omega_{2,2} = \frac{1}{\sqrt{2}} b_1, \quad \omega_{1,3} = \frac{1}{\sqrt{2}} b_2, \quad \omega_{2,3} = -\frac{1}{\sqrt{2}} b_2. \tag{3.62}$$

Similarly, from equations (3.53, 3.54) we find

$$-2\boldsymbol{h_1} = \mathcal{N}_2 \boldsymbol{h_1}, \qquad 2\boldsymbol{h_2} = \mathcal{N}_2 \boldsymbol{h_2}, \tag{3.63}$$

where $\boldsymbol{h_1} = (h_{1,1}, h_{2,1})^T$, $\boldsymbol{h_2} = (h_{1,2}, h_{2,2})^T$, and the matrix

$$\mathcal{N}_2 = \begin{pmatrix} 1 & -\sqrt{3} \\ -\sqrt{3} & -1 \end{pmatrix} \tag{3.64}$$

has eigenvalues of -2 and 2 (note that this is not the same as the matrix form for the conditions on the ω_k, although it is also symmetric). The corresponding normalized eigenvectors are given by

$$\boldsymbol{u_1} = \frac{1}{2} \begin{pmatrix} 1 \\ \sqrt{3} \end{pmatrix}, \qquad \boldsymbol{u_2} = \frac{1}{2} \begin{pmatrix} -\sqrt{3} \\ 1 \end{pmatrix}, \tag{3.65}$$

and we again define new constants g_1, g_2 such that $\boldsymbol{h_1} = g_1 \boldsymbol{u_1}$, $\boldsymbol{h_2} = g_2 \boldsymbol{u_2}$, and therefore

$$h_{1,1} = \frac{1}{2} g_1, \quad h_{2,1} = \frac{\sqrt{3}}{2} g_1, \quad h_{1,2} = -\frac{\sqrt{3}}{2} g_2, \quad h_{2,2} = \frac{1}{2} g_2. \tag{3.66}$$

Altogether, we then have

$$\begin{aligned}
m &= \left(\frac{2h_{1,1}}{\sigma_0} + 4\omega_{1,2} \right) r^3 + \mathcal{O}\left(r^4\right), \\
\sigma &= \left(4h_{1,1}^2 + 8\sigma_0 \omega_{1,2}^2\right) r^2 + \mathcal{O}\left(r^3\right), \\
\omega_1 &= \sqrt{2} + \frac{1}{\sqrt{2}} b_1 r^2 + \frac{1}{\sqrt{2}} b_2 r^3 + \mathcal{O}\left(r^4\right), \\
\omega_2 &= \sqrt{2} + \frac{1}{\sqrt{2}} b_1 r^2 - \frac{1}{\sqrt{2}} b_2 r^3 + \mathcal{O}\left(r^4\right), \\
h_1 &= \frac{1}{2} g_1 r - \frac{\sqrt{3}}{2} g_2 r^2 + \mathcal{O}\left(r^3\right), \\
h_2 &= \frac{\sqrt{3}}{2} g_1 r + \frac{1}{2} g_2 r^2 + \mathcal{O}\left(r^3\right).
\end{aligned} \tag{3.67}$$

Once again the value of σ_0 is fixed by the requirement that σ approaches one at

large r. We now have two free parameters which determine the behaviour of the ω_k, and two for the h_k. For the purely magnetic case, there are $N-1$ free parameters for general N [8], while for dyonic solitons we expect to find $2(N-1)$, and require expansions up to r^N in the ω_k, and r^{N-1} in h_k.

3.3.2 At the event horizon

We start by Taylor expanding our variables in a neighbourhood of the event horizon:

$$\begin{aligned} m(r) &= m(r_h) + m'(r_h)(r-r_h) + \mathcal{O}(r-r_h)^2, \\ \sigma(r) &= \sigma(r_h) + \sigma'(r_h)(r-r_h) + \mathcal{O}(r-r_h)^2, \\ \omega_k(r) &= \omega_k(r_h) + \omega_k'(r_h)(r-r_h) + \mathcal{O}(r-r_h)^2, \\ h_k(r) &= h_k'(r_h)(r-r_h) + \mathcal{O}(r-r_h)^2, \\ \mu(r) &= \mu'(r_h)(r-r_h) + \mathcal{O}(r-r_h)^2. \end{aligned} \tag{3.68}$$

We are looking for solutions where all quantities are regular at the event horizon, so we have set $h_k(r_h) = 0$ to avoid a singularity in equation (3.12) at $r = r_h$. Substituting $\mu(r_h) = h_k(r_h) = 0$ into equation (3.10), and noting that both μ and h_k are of order $(r-r_h)$ so that h_k^2/μ vanishes at $r = r_h$, we find that

$$m'(r_h) = \sum_{k=1}^{N-1} \left[\frac{r_h^2 h_k'(r_h)^2}{2\sigma(r_h)^2} + \frac{k(k+1)}{4r_h^2} \left(1 - \frac{\omega_k(r_h)^2}{k} + \frac{\omega_{k+1}(r_h)^2}{k+1} \right)^2 \right], \tag{3.69}$$

which reduces to the result from the previous chapter (2.21) when $h_k'(r_h) = 0$ for all k. Multiplying equation (3.13) through by μ and evaluating it at the event horizon, we find that

$$\omega_k'(r_h) = \frac{\omega_k(r_h)}{\mu'(r_h) r_h^2} \left(\omega_k(r_h)^2 - 1 - \frac{1}{2} \left(\omega_{k-1}(r_h)^2 + \omega_{k+1}(r_h)^2 \right) \right), \tag{3.70}$$

which does not contain any h_k and is therefore the same as in the previous chapter (2.21). Evaluating (3.11) at the event horizon we find

$$\begin{aligned} \sigma'(r_h) = {} & 2 \sum_{k=1}^{N-1} \left[\frac{\omega_k(r_h)^2}{\sigma(r_h)\mu'(r_h)^2 r_h} \left(\sqrt{\frac{k+1}{2k}} h_k'(r_h) - \sqrt{\frac{k-1}{2k}} h_{k-1}'(r_h) \right)^2 \right] \\ & + 2 \sum_{k=1}^{N-1} \frac{\sigma(r_h) \omega_k'(r_h)^2}{r_h}, \end{aligned} \tag{3.71}$$

which again reduces to the result from the previous chapter (2.21) if all the $h_k(r_h)$ are zero. For the black hole to be non-extremal (and therefore have non-zero surface gravity and Hawking temperature) we also require

$$\mu'(r_h) = \frac{1}{r_h} - \frac{2m'(r_h)}{r_h} - \Lambda r_h > 0. \tag{3.72}$$

To summarize, the boundary conditions of our variables at the event horizon are given by:

$$\begin{aligned} m(r) &= \frac{r_h}{2} - \frac{\Lambda r_h^3}{6} + m'(r_h)(r-r_h) + \mathcal{O}(r-r_h)^2, \\ \sigma(r) &= \sigma(r_h) + \sigma'(r_h)(r-r_h) + \mathcal{O}(r-r_h)^2, \\ \omega_k(r) &= \omega_k(r_h) + \omega_k'(r_h)(r-r_h) + \mathcal{O}(r-r_h)^2, \\ h_k(r) &= h_k'(r_h)(r-r_h) + \mathcal{O}(r-r_h)^2, \end{aligned} \tag{3.73}$$

where

$$\begin{aligned} \omega_k'(r_h) &= \frac{\omega_k(r_h)}{\mu'(r_h) r_h^2}\left(\omega_k(r_h)^2 - 1 - \frac{1}{2}\left(\omega_{k-1}(r_h)^2 + \omega_{k+1}(r_h)^2\right)\right), \\ m'(r_h) &= \sum_{k=1}^{N-1}\left[\frac{r_h^2 h_k'^2}{2\sigma(r_h)^2} + \frac{k(k+1)}{4r_h^2}\left(1 - \frac{\omega_k(r_h)^2}{k} + \frac{\omega_{k+1}(r_h)^2}{k+1}\right)^2\right], \\ \sigma'(r_h) &= 2\sum_{k=1}^{N-1}\left[\frac{\omega_k(r_h)^2}{\sigma(r_h)\mu'(r_h)^2 r_h}\left(\sqrt{\frac{k+1}{2k}}h_k'(r_h) - \sqrt{\frac{k-1}{2k}}h_{k-1}'(r_h)\right)^2\right] \\ &\quad + 2\sum_{k=1}^{N-1}\frac{\sigma(r_h)\omega_k'(r_h)^2}{r_h}, \end{aligned} \tag{3.74}$$

and

$$\mu'(r_h) = \frac{1}{r_h} - \frac{2m'(r_h)}{r_h} - \Lambda r_h > 0. \tag{3.75}$$

There are $2(N-1)$ free parameters in the theory: the $\omega_k(r_h)$ and the $h_k'(r_h)$ for $k = 1, .., N-1$. The value of $\sigma(r_h)$ is fixed by the requirement that σ approaches one at large r. When searching for numerical solutions in sections 3.5.1 and 3.5.2 we will consider only values of the parameters such that (3.72) is satisfied. In fact, we do not find solutions for all such values of the parameters, as can be seen in figures 3.2–3.9, as in the purely magnetic case.

3.3.3 At infinity

We assume that our variables have regular Taylor series expansions at large r:

$$\begin{aligned} m &= m_0 + \frac{m_1}{r} + \mathcal{O}\left(\frac{1}{r^2}\right), \\ \sigma &= \sigma_0 + \frac{\sigma_1}{r} + \frac{\sigma_2}{r^2} + \frac{\sigma_3}{r^3} + \frac{\sigma_4}{r^4} + \mathcal{O}\left(\frac{1}{r^5}\right), \\ \omega_k &= \omega_{k,\infty} + \frac{c_{k,1}}{r} + \mathcal{O}\left(\frac{1}{r^2}\right), \\ h_k &= h_{k,\infty} + \frac{h_{k,1}}{r} + \mathcal{O}\left(\frac{1}{r^2}\right). \end{aligned} \tag{3.76}$$

The expansions (3.76) are the same as in chapter 2, except that we now have an additional Taylor expansion for the h_k. We are looking for asymptotically AdS solutions, and therefore require $\sigma_0 = 1$ so that the line element (3.1) approaches the line element for anti-de Sitter space in the large r limit. Using (3.76) to evaluate (3.10) at large r gives

$$m' = \frac{1}{r^2}\sum_{k=1}^{N-1}\left[\frac{k(k+1)}{4}\left(1 - \frac{\omega_{k,\infty}^2}{k} + \frac{\omega_{k+1,\infty}^2}{k+1}\right)^2 + \frac{h_{k,1}^2}{2} + \frac{c_{k,1}^2}{l^2}\right] \tag{3.77}$$

$$+\frac{1}{r^2}\sum_{k=1}^{N-1}\left[\omega_{k,\infty}^2\left(\sqrt{\frac{k+1}{2k}}h_{k,\infty} - \sqrt{\frac{k-1}{2k}}h_{k-1,\infty}\right)\right] + \mathcal{O}\left(\frac{1}{r^3}\right). \tag{3.78}$$

Turning now to equation (3.11) we have

$$\sigma' = \frac{2}{r^5}\sum_{k=1}^{N-1}\left[l^4\omega_{k,\infty}^2\left(\sqrt{\frac{k+1}{2k}}h_{k,\infty} - \sqrt{\frac{k-1}{2k}}h_{k-1,\infty}\right)^2 + c_{k,1}^2\right] + \mathcal{O}\left(\frac{1}{r^6}\right). \tag{3.79}$$

Since the right hand side of (3.79) is of order r^{-5}, we must have $\sigma_1 = \sigma_2 = \sigma_3 = 0$. Finally, our Yang-Mills equations for ω_k and h_k give no constraints on $c_{k,1}$ or $h_{k,1}$ and we have

$$\begin{aligned}
\omega_k(r) &= \omega_{k,\infty} + \frac{c_{k,1}}{r} + \mathcal{O}\left(\frac{1}{r^2}\right), \\
h_k(r) &= h_{k,\infty} + \frac{h_{k,1}}{r} + \mathcal{O}\left(\frac{1}{r^2}\right), \\
m(r) &= m_0 - \frac{1}{r}\sum_{k=1}^{N-1}\left[\frac{k(k+1)}{4}\left(1 - \frac{\omega_{k,\infty}^2}{k} + \frac{\omega_{k+1,\infty}^2}{k+1}\right)^2 + \frac{h_{k,1}^2}{2} + \frac{c_{k,1}^2}{l^2}\right] \\
&\quad -\frac{1}{r}\sum_{k=1}^{N-1}\left[\omega_{k,\infty}^2 l^2\left(\sqrt{\frac{k+1}{2k}}h_{k,\infty} - \sqrt{\frac{k-1}{2k}}h_{k-1,\infty}\right)\right] + \mathcal{O}\left(\frac{1}{r^3}\right). \\
\sigma(r) &= 1 - \frac{1}{2r^4}\sum_{k=1}^{N-1}\left[l^4\omega_{k,\infty}^2\left(\sqrt{\frac{k+1}{2k}}h_{k,\infty} - \sqrt{\frac{k-1}{2k}}h_{k-1,\infty}\right)^2 + c_{k,1}\right],
\end{aligned} \tag{3.80}$$

where $l^2 = -3/\Lambda$. As required, the expansions (3.80) reduce to those of the purely magnetic solutions of chapter 2 when we take $h_{k,\infty} = 0 = h_{k,1}$ for all k.

§ 3.4 Numerical method

Numerical solutions to the field equations for black holes are found in the same way as in the previous chapter, except we have $N-1$ additional variables, which are the functions h_k describing the electric part of the potential. The $N-1$ second order ODEs for the h_k are broken into $2N-2$ first order ODEs in h_k and h_k' in the same way as the equations for the ω_k, giving a total of $4N-2$ first order ODEs in m, σ, h_k, h_k', ω_k and ω_k'. The field equations (3.10–3.13) are singular at the event horizon, so the boundary conditions (3.73) are implemented at $r - r_h = 10^{-7}$. We then integrate outwards to large r using a Bulirsch-Stoer algorithm in C++ [32].

However, for the solitons it is a little more complicated, particularly in the $\mathfrak{su}(3)$ case. In the $\mathfrak{su}(2)$ case, we parameterize ω_1 at the origin using the constant $\omega_{1,2}$ (3.48). Close to the origin we have $\omega_1 = 1 + \omega_{1,2}r^2 + \mathcal{O}(r^2)$, where r is small, but due to the limited precision of variables in C++, we risk large errors in terms of the form $(1-\omega_1^2)$. We therefore introduce a new variable $\psi = \omega_1^2 - 1$, along with a new first order ODE

$$\psi' = 2\omega_1\omega_1'. \tag{3.81}$$

In the $\mathfrak{su}(3)$ case, we introduce new variables $\beta_1(r)$ and $\beta_2(r)$ as in [8], such that

$$\omega_1 = \sqrt{2} + \frac{1}{\sqrt{2}}\left(\beta_1 + \beta_2\right), \qquad \omega_2 = \sqrt{2} + \frac{1}{\sqrt{2}}\left(\beta_1 + \beta_2\right), \tag{3.82}$$

and which have boundary conditions at the origin given by

$$\beta_j(r) = b_j r^{j+1} + \mathcal{O}\left(r^{j+2}\right). \tag{3.83}$$

Similarly for the h_1 and h_2 we introduce $\varsigma_1(r)$ and $\varsigma_2(r)$ such that

$$h_1 = \frac{1}{2}\varsigma_1 - \frac{\sqrt{3}}{2}\varsigma_2, \qquad h_2 = \frac{\sqrt{3}}{2}\varsigma_1 + \frac{1}{2}\varsigma_2 \tag{3.84}$$

and near the origin

$$\varsigma_j = g_j r^j + \mathcal{O}\left(r^{j+1}\right). \tag{3.85}$$

Our new variables then have equations given by

$$\begin{aligned}
\beta_1'' &= -\left(\frac{\sigma'}{\sigma} + \frac{\mu'}{\mu}\right)\beta_1' + \frac{1}{4\mu r^2}(2+\beta_1)(\beta_1^2 + 4\beta_1 + 7\beta_2^2) \\
&\quad -\frac{1}{\sqrt{2}\sigma^2\mu^2}\left[\sqrt{2}\left(\frac{9\varsigma_1^2}{16} + \frac{3\varsigma_2^2}{2}\right) + \frac{\beta_1}{\sqrt{2}}\left(\frac{9\varsigma_1^2}{16} + \frac{3\varsigma_2^2}{2}\right) - \frac{\sqrt{3}\beta_2\varsigma_1\varsigma_2}{\sqrt{2}}\right], \\
\beta_2'' &= -\left(\frac{\sigma'}{\sigma} + \frac{\mu'}{\mu}\right)\beta_2' + \frac{1}{4\mu r^2}(7\beta_1^2 + 28\beta_2 + \beta_2^2 + 24)\beta_2 \\
&\quad -\frac{1}{\sqrt{2}\sigma^2\mu^2}\left[\sqrt{6}\varsigma_1\varsigma_2 + \frac{\sqrt{3}\beta_2\varsigma_1\varsigma_2}{\sqrt{2}} - \frac{\beta_1}{\sqrt{2}}\left(\frac{9\varsigma_1^2}{16} + \frac{3\varsigma_2^2}{2}\right)\right], \\
\varsigma_1'' &= \left(\frac{\sigma'}{\sigma} - \frac{2}{r}\right)\varsigma_1' + \frac{2\varsigma_1}{\mu r^2} \\
&\quad +\frac{1}{\mu r^2}\left(\frac{1}{2}(\beta_1^2 + \beta_2^2) + 2(\beta_1 - \beta_2) - \beta_1\beta_2\right)\left(\frac{1}{2}\varsigma_1 + \frac{\sqrt{3}}{2}\varsigma_2\right) \\
&\quad +\frac{1}{\mu r^2}\left(\frac{1}{2}(\beta_1^2 + \beta_2^2) + 2(\beta_1 + \beta_2) + \beta_1\beta_2\right)\left(\frac{1}{2}\varsigma_1 - \frac{\sqrt{3}}{2}\varsigma_2\right), \\
\varsigma_2'' &= \left(\frac{\sigma'}{\sigma} - \frac{2}{r}\right)\varsigma_2' + \frac{6\varsigma_2}{\mu r^2} \\
&\quad +\frac{1}{\mu r^2}\left(\frac{1}{2}(\beta_1^2 + \beta_2^2) + 2(\beta_1 - \beta_2) - \beta_1\beta_2\right)\left(\frac{\sqrt{3}}{2}\varsigma_1 + \frac{3}{2}\varsigma_2\right) \\
&\quad +\frac{1}{\mu r^2}\left(\frac{1}{2}(\beta_1^2 + \beta_2^2) + 2(\beta_1 + \beta_2) + \beta_1\beta_2\right)\left(\frac{\sqrt{3}}{2}\varsigma_1 - \frac{3}{2}\varsigma_2\right).
\end{aligned} \tag{3.86}$$

Equations (3.86) can then be integrated as described above, along with (3.49, 3.50), and reduce to those of [8] if we take $\varsigma_1 = 0 = \varsigma_2$.

§ 3.5 Numerical results

In this section we present numerical results obtained using the method discussed in section 3.4, for $\mathfrak{su}(2)$ and $\mathfrak{su}(3)$ black holes and solitons. We note that the $\mathfrak{su}(2)$ case has already been studied in the literature [18, 19].

3.5.1 $\mathfrak{su}(2)$ BLACK HOLES

We begin with $\mathfrak{su}(2)$ black holes. The equation for h_1 is

$$h_1'' = \left(\frac{\sigma'}{\sigma} - \frac{2}{r}\right) h_1' + 2\frac{\omega_1^2 h_1}{\mu r^2}. \tag{3.87}$$

If (3.87) has a turning point at $r = r_0$, then $h'(r_0) = 0$ and

$$h_1(r_0)'' = 2\frac{\omega_1(r_0)^2 h_1(r_0)}{\mu r_0^2}. \tag{3.88}$$

Since $\mu > 0$ for $r > r_h$, if $h_1(r_0) > 0$ the turning point is a minimum, and if $h_1(r_0) > 0$ the turning point is a maximum. Hence we conclude that h_1 is monotonic for $\mathfrak{su}(2)$ (we also find this is true numerically from $\mathfrak{su}(3)$). We therefore label solutions by the number of nodes n in ω_1. Figure 3.1 shows a typical solution for an $\mathfrak{su}(2)$ black hole with $\Lambda = -0.01$. As expected, h_1 is monotonic, and for $\omega_1(r_h) = 0.95$, $h_1'(r_h) = 0.01$ we find one node in the gauge field function ω_1 ($n = 1$).

Figure 3.2 shows a phase space plot for black holes with $\Lambda = -0.01$, part of which is shown in [18]. We restrict our attention to the region of the parameter space where (3.72) is satisfied. However there are some regions of the parameter space where (3.72) is satisfied but we do not find black hole solutions, which are in the red "no solution" region. All other points on the plot represent black hole solutions with particular values of $h_1'(r_h)$ and $\omega_1(r_h)$, with $r_h = 1$, and are colour coded by the number of nodes n in the gauge field function ω_1. While the plot in [18] concentrated on the nodeless $n = 0$ region, we find that the parameter space is very rich for this value of Λ, with solutions with up to 17 nodes. For comparison with [18], figure 3.3 shows a close up of the $n = 0$ region which is in agreement with [18].

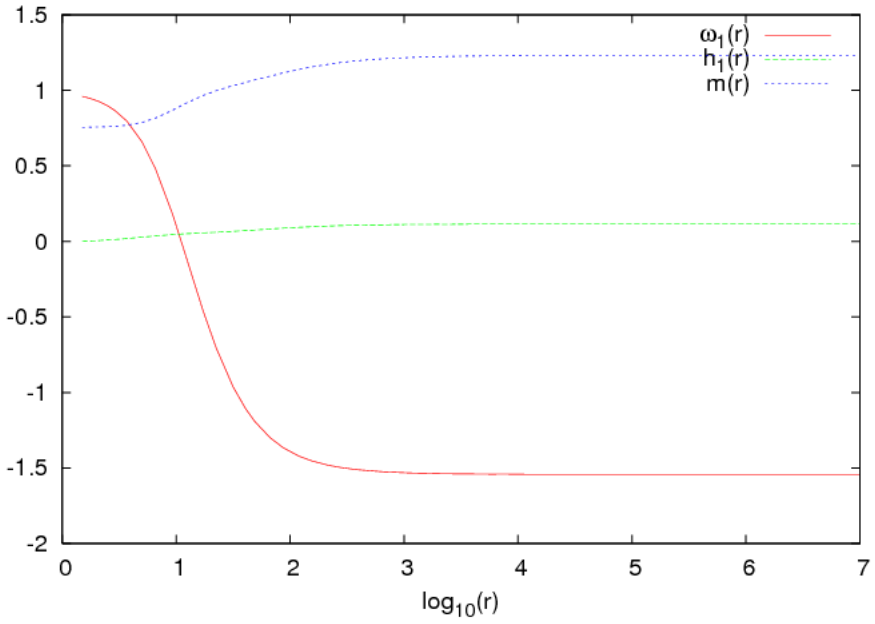

Figure 3.1: Typical $n = 1$ solution for an $\mathfrak{su}(2)$ black hole with $\Lambda = -0.01$, with $\omega_1(r_h) = 0.95$, $h_1'(r_h) = 0.01$. As expected from (3.88), the electric field function $h_1(r)$ is monotonic.

Figure 3.4 shows a similar plot for $\mathfrak{su}(2)$ black holes with $r_h = 1$ and $\Lambda = -3$. As in the previous chapter, we find that as $|\Lambda|$ increases, the size of the $n = 0$ region increases, and for these value of Λ and r_h we find no solutions with nodes. We also note a small line of "no solution" points at $\omega_1(r_h) = 1$ and small $h_1'(r_h)$, although it is possible that this is due to numerical error.

It was found in [16] that in flat space, and in the absence of an electric field, there are discrete families of solutions, which are indexed by the number of nodes in the gauge field function ω_1. It was found that there was a solution with one node for $\omega(r_h) = 0.632206952$. In figure 3.5 we plot $h_1'(r_h)$ against $\log_{10}(\Lambda)$ for black holes with $r_h = 1$ and the $n = 1$ value of $\omega_1(r_h) = 0.632206952$. We note that for this value of $\omega_1(r_h)$ we do find solutions as Λ approaches zero, although to find solutions we also require $h_1'(r_h)$ to approach zero, as expected. This is in contrast to figure 3.6, which takes $\omega_1(r_h) = 0.5$. This value of $\omega_1(r_h)$ does not correspond to a solution in flat space. In AdS we find that there is a critical value of Λ which is

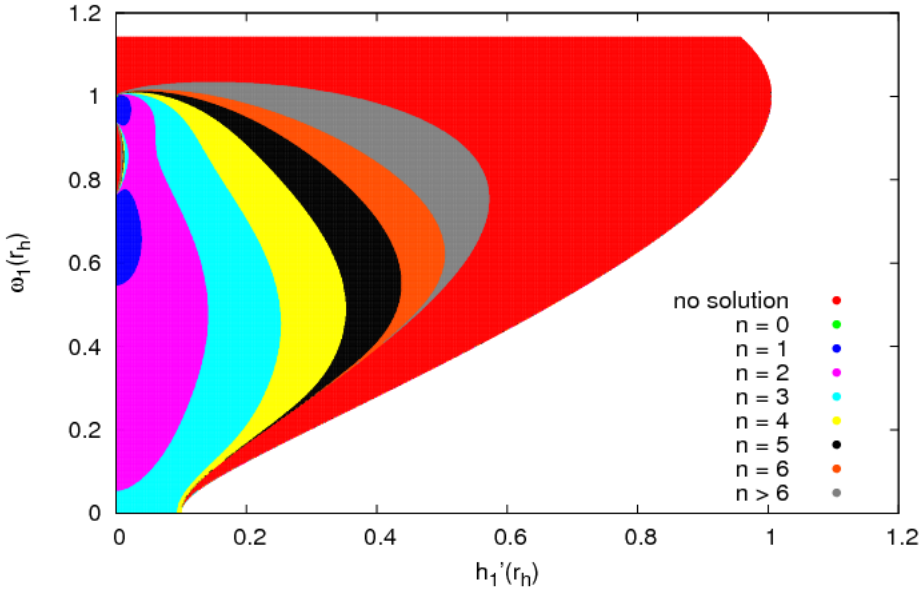

Figure 3.2: Phase space plot for $\mathfrak{su}(2)$ dyonic black holes with $\Lambda = -0.01$ and $r_h = 1$. The red "no solution" region indicates where (3.72) is satisfied but we do not find black hole solutions. We note that the $n = 0$ region where the gauge field function has no nodes makes up a small region of the parameter space, which is located around $\omega_1(r_h) = 1$, $h_1'(r_h) = 0$.

around 10^{-9}, below which we do not find any solutions for any values of $h_1'(r_h)$.

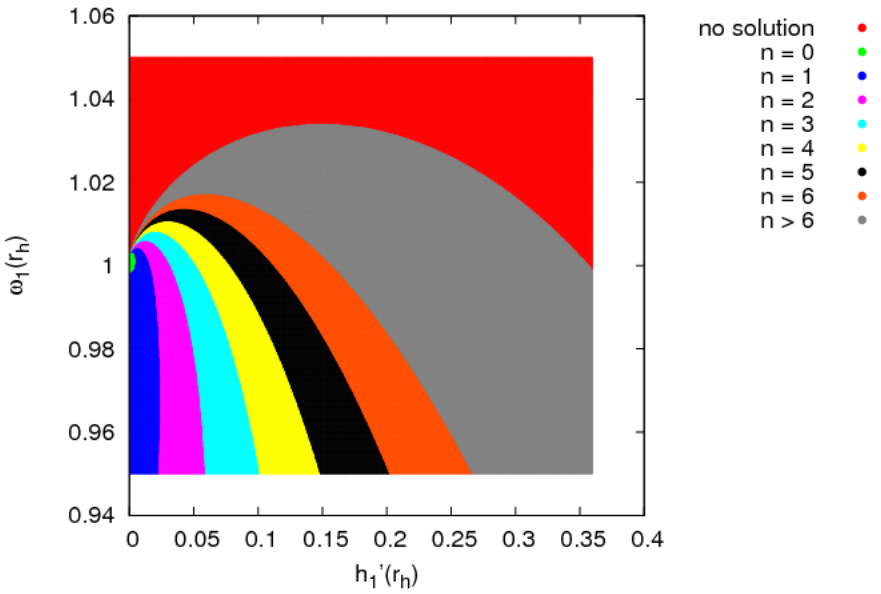

Figure 3.3: Close up view of the area surrounding the $n = 0$ region from figure 3.2. The $n = 0$ region found here is in agreement with that found in [18].

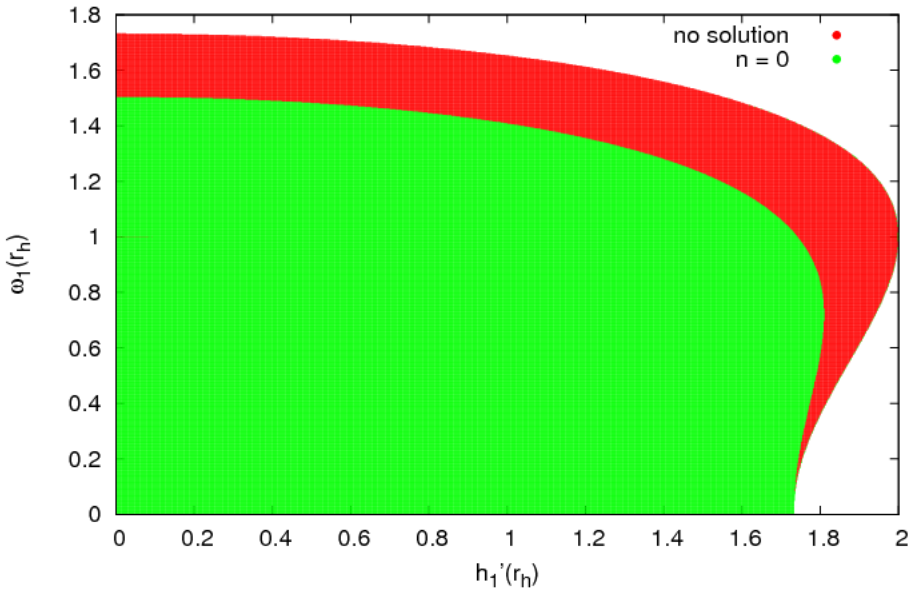

Figure 3.4: Phase space plot for $\mathfrak{su}(2)$ dyonic black holes with $\Lambda = -3$ and $r_h = 1$. The red "no solution" region indicates where (3.72) is satisfied but we do not find black hole solutions. We note that, as in the previous chapter, for $\mathfrak{su}(2)$ black holes with $\Lambda = -3$ we do not find black holes which have nodes in the gauge field function ω_1.

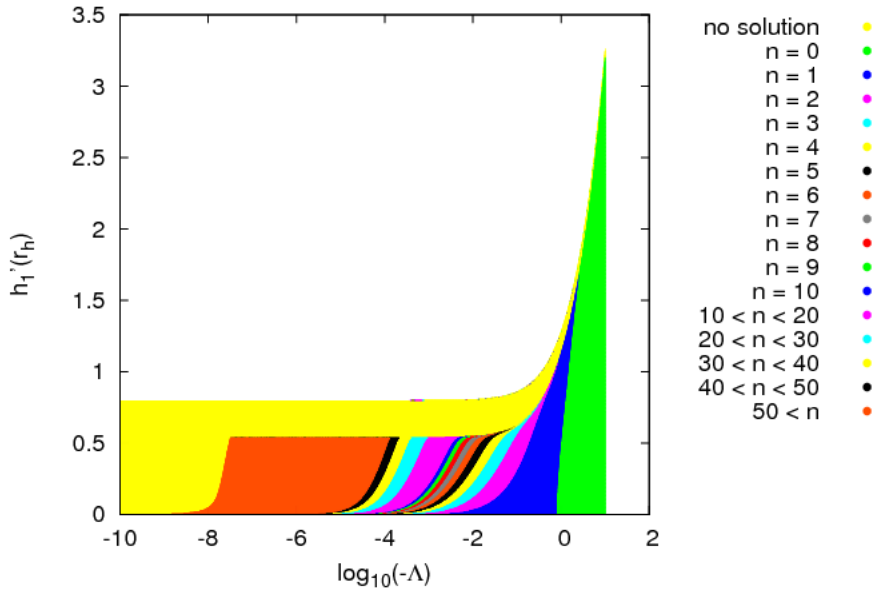

Figure 3.5: Plot of $h_1'(r_h)$ against cosmological constant Λ for the $n = 1$ asymptotically flat value of $\omega_1(r_h) = 0.632206952$ [16], colour coded by the number of nodes in the gauge field function ω_1. We note that there are $n = 1$ solutions in the limit $\Lambda \to 0$ and $h'(r_h) \to 0$. We also note a very rich structure, with potentially a very high number of nodes as $|\Lambda|$ decreases.

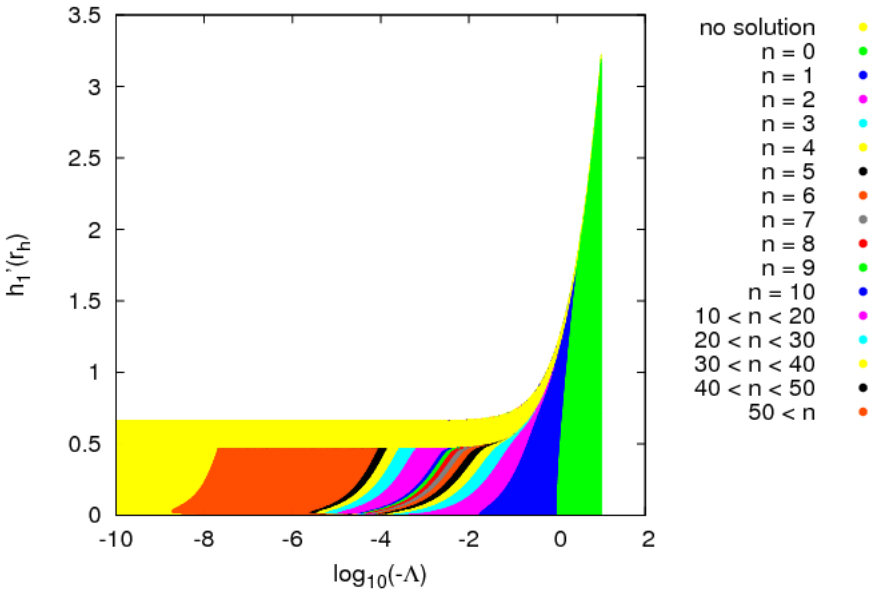

Figure 3.6: Plot of $h_1'(r_h)$ against cosmological constant Λ with $\omega_1(r_h) = 0.5$, colour coded by the number of nodes in the gauge field function ω_1. We note that there are no solutions in the limit $\Lambda \to 0$.

3.5.2 $\mathfrak{su}(3)$ BLACK HOLES

We next turn to $\mathfrak{su}(3)$ black holes. In addition to the cosmological constant Λ and event horizon radius r_h (we will take the value $r_h = 1$ for all numerical results in this section), we now have four parameters at the event hozion, $\omega_1(r_h)$, $\omega_2(r_h)$, $h_1'(r_h)$ and $h_2'(r_h)$. Figure 3.7 shows a typical solution for a black hole with $\Lambda = -0.01$. The horizon parameters are $\omega_1(r_h) = \omega_2(r_h) = 1.2$, $h_1'(r_h) = 0.01$ and $h_2'(r_h) = 0.005$. As in previous sections we label solutions by the number of nodes in the gauge field functions ω_k, noting that the electric field functions h_1 and h_2 are monotonic, with this particular solution having $n_1 = 2$, $n_2 = 3$.

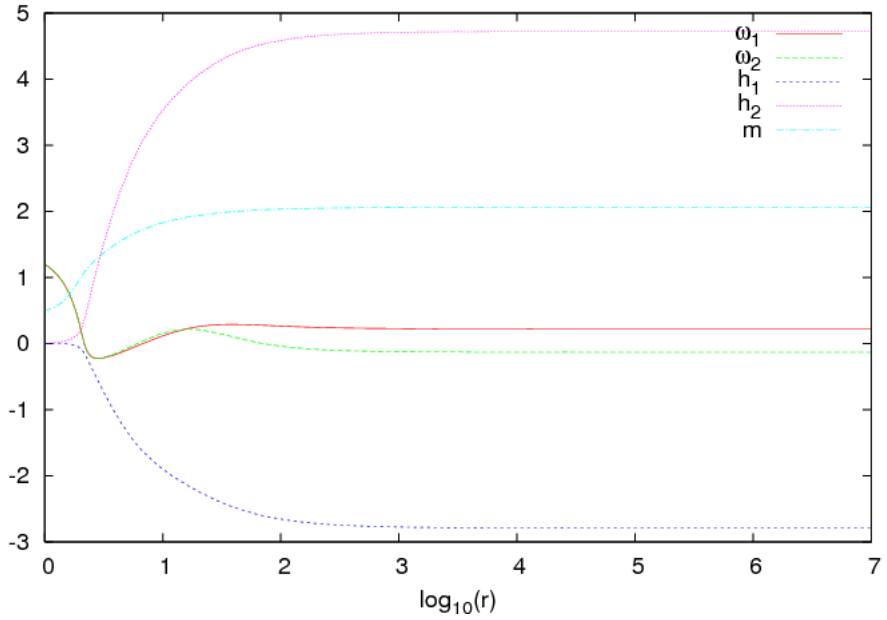

Figure 3.7: Typical solution for $\mathfrak{su}(3)$ dyonic black holes with $\Lambda = -0.01$. At the horizon $\omega_1(r_h) = \omega_2(r_h) = 1.2$, $h_1'(r_h) = 0.01$ and $h_2'(r_h) = 0.005$, giving a solution with $n_1 = 2$, $n_2 = 3$.

As before, we find a very rich solution space for small values of $|\Lambda|$. Figure 3.8 shows a phase space plot for $\mathfrak{su}(3)$ black holes with $\Lambda = -0.01$, where we have fixed the values of $\omega_1(r_h) = 1.2 = \omega_2(r_h)$ and scanned over values of $h_1'(r_h)$ and $h_2'(r_h)$. We find that there are no nodeless solutions in this case, with the smallest number of nodes being the $n_1 = 2 = n_2$ region, which is the blue region with low values of $h_1'(r_h)$ and $h_2'(r_h)$ in figure 3.8. The adjacent regions are the $n_1 = 2$, $n_2 = 3$ region in yellow, and the $n_1 = 3$, $n_2 = 2$ in green, with the number of nodes increasing with $h_1'(r_h)$ and $h_2'(r_h)$. We also note that this phase space plot is symmetric about the

line $h_2'(r_h) = \sqrt{3}h_1'(r_h)$, and that this line corresponds to embedded $\mathfrak{su}(2)$ solutions (see section 3.2.3).

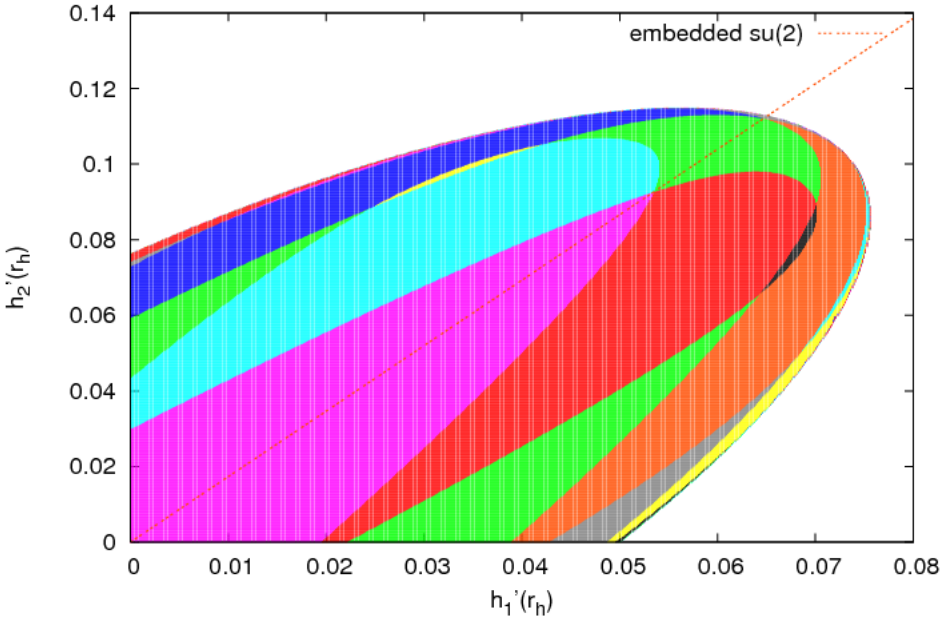

Figure 3.8: Phase space plot for $\mathfrak{su}(3)$ dyonic black holes with $\Lambda = -0.01$, $r_h = 1$ and $\omega_1(r_h) = \omega_2(r_h) = 1.2$, colour coded by the number of zeros of the gauge field functions. For these values of the parameters at the horizon, there are no nodeless solutions, with the lowest number of nodes being $n_1 = n_2 = 2$ at small $h_1'(r_h)$ and $h_2'(r_h)$. In the large red region (3.72) is satisfied but we do not find black hole solutions.

In contrast, figure 3.9 shows a similar plot for $\mathfrak{su}(3)$ black holes with $\Lambda = -3$, this time with $\omega_1(r_h) = 1.3$, $\omega_2(r_h) = 1.2$. As can be seen in figure 2.5, black holes with these horizon parameters and cosmological constant are nodeless when no electric field is present. From figure 3.9 it is clear that solutions are nodeless for all allowed values of the electric field. Note however that we do not expect this to hold for all values of $\omega_1(r_h)$ and $\omega_2(r_h)$, since it can be seen from figure 2.5 that there are some solutions with nodes.

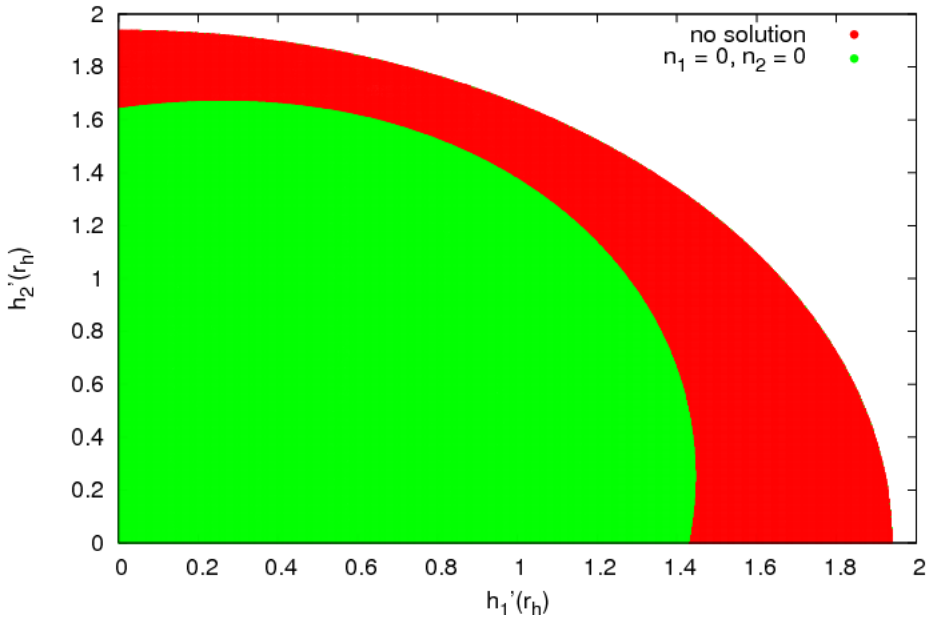

Figure 3.9: Phase space plot for $\mathfrak{su}(3)$ dyonic black holes with $\Lambda = -3$, $r_h = 1$, $\omega_1(r_h) = 1.3$, $\omega_2(r_h) = 1.2$, colour coded by the number of zeros in the gauge field function. In this case there are only nodeless solutions.

3.5.3 $\mathfrak{su}(2)$ SOLITONS

In this section we consider the case of $\mathfrak{su}(2)$ soliton solutions, which have been considered in [18, 19]. Soliton solutions have no event horizon, and are regular at the origin. In the $\mathfrak{su}(2)$ case, they are characterized by two parameters at the origin, denoted $\omega_{1,2}$ and $h_{1,1}$ (3.48), along with the cosmological constant Λ. A typical solution is shown in figure 3.10, where the gauge field function $\omega_1(r)$ has one node.

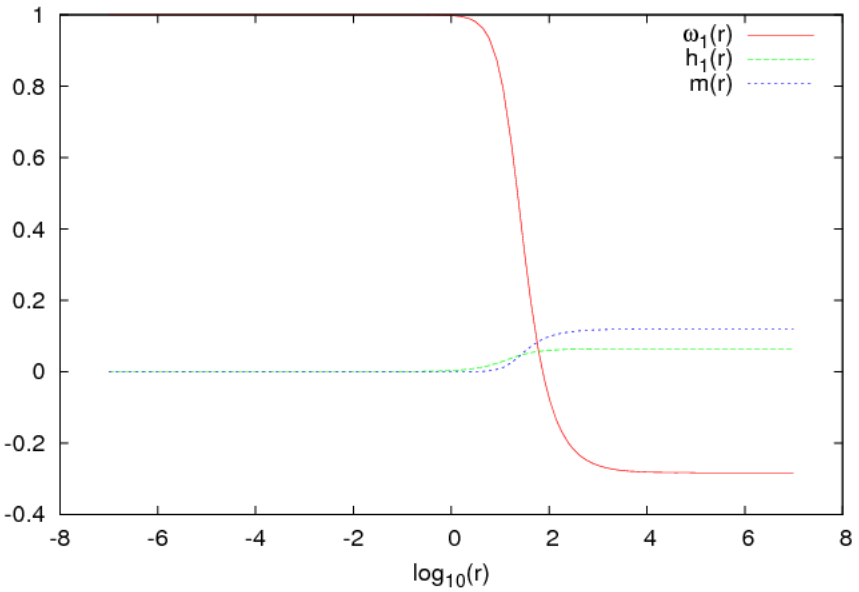

Figure 3.10: Typical $n = 1$ solution for a $\mathfrak{su}(2)$ soliton with $\Lambda = -0.01$, $\omega_{1,2} = -0.002$, $h_{1,1} = 0.003$ and $r_h = 1$.

The full solution space for solitons with $\Lambda = -0.01$ is shown in figure 3.11. As with the black holes, the $n = 0$ region is given in [18], and for comparison a similar region is shown in figure 3.12, which is in agreement with [18]. The parameter space for $\Lambda = -0.01$ is again very rich, with solutions possessing up to 17 nodes. While, as in [18], we do find nodeless solutions, we find that these make up a very small part of the parameter space.

Again this is in contrast with the $\Lambda = -3$ solutions, which have a much simpler

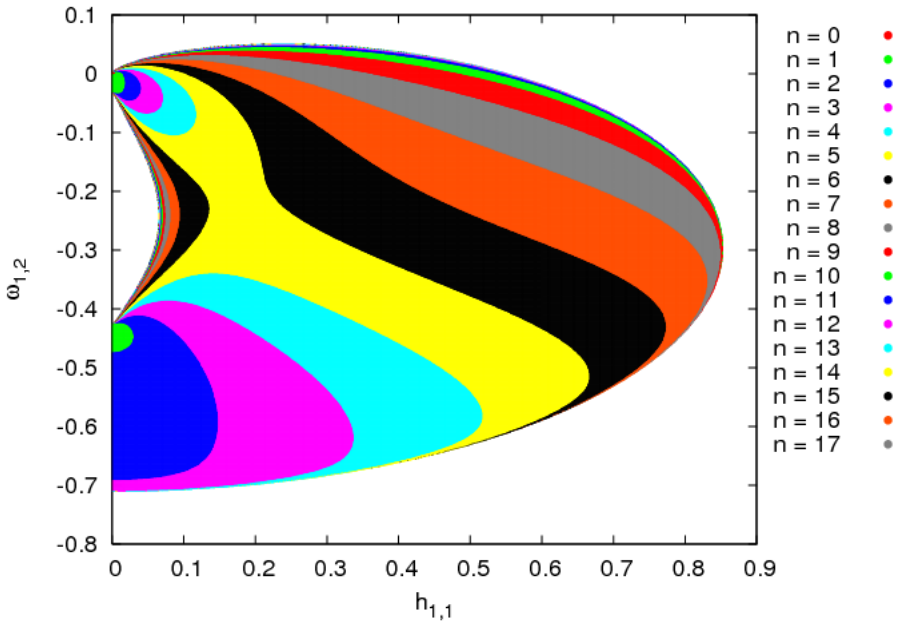

Figure 3.11: Phase space plot for $\mathfrak{su}(2)$ dyonic solitons with $\Lambda = -0.01$. We note that the green $n = 0$ region where the gauge field function has no nodes (around $\omega_{1,2} = 0,\ h_{1,1} = 0$) makes up a small region of the parameter space.

parameter space. The phase space for $\mathfrak{su}(2)$ solitons with $\Lambda = -3$ is shown in figure 3.13, and posessess only nodeless and $n = 1$ solutions, with the $n = 0$ region being much larger than in the smaller $|\Lambda|$ case.

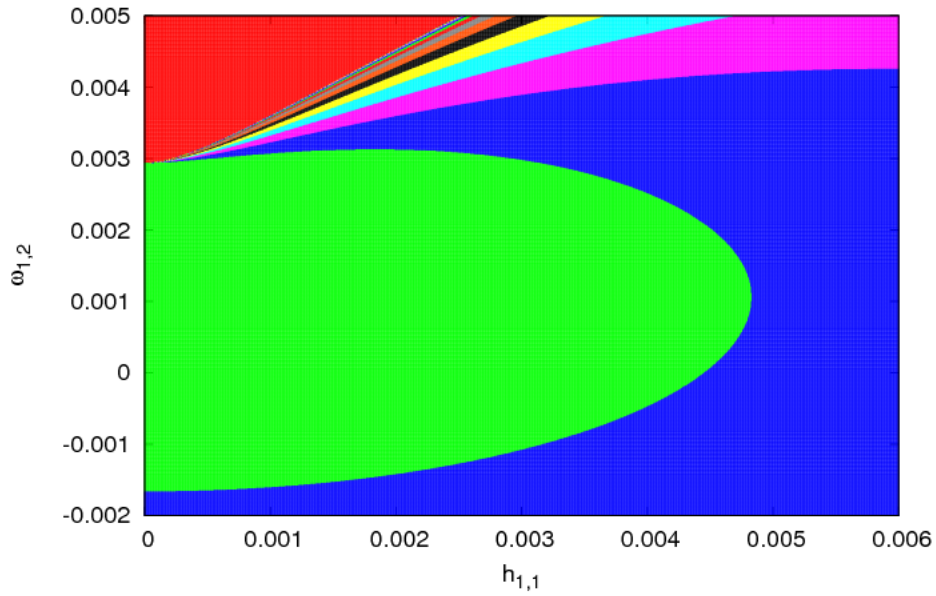

Figure 3.12: Close up view of the area surrounding the $n = 0$ region from figure 3.11. As for the black holes, the $n = 0$ region found here is in agreement with that shown in [18].

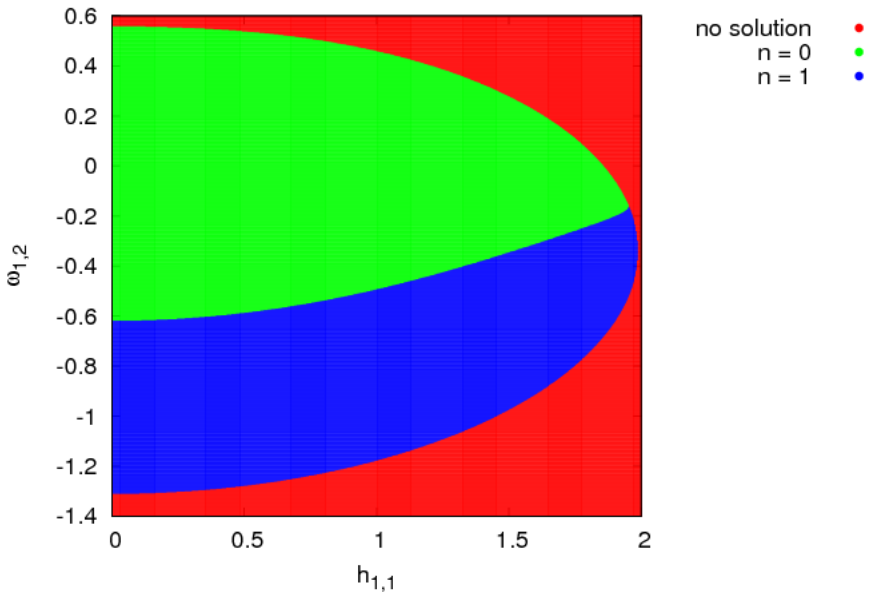

Figure 3.13: Phase space plot for $\mathfrak{su}(2)$ dyonic solitons with $\Lambda = -3$. As with the black holes, we find the solution space is much simpler with a larger value of $|\Lambda|$, and has a larger $n = 0$ region.

3.5.4 $\mathfrak{su}(3)$ SOLITONS

Finally we consider the case of $\mathfrak{su}(3)$ solitons, which are characterized at the origin by b_1, b_2, g_1 and g_2, in addition to the cosmological constant Λ (3.67). A typical solution with $\Lambda = -0.01$ is shown in figure 3.14, with parameters $b_1 = -0.002$, $b_2 = -0.00001$, $g_1 = 0.001$ and $g_2 = 0.0005$. As with the black holes, h_1 and h_2 are monotonic functions, and we label solutions by the number of nodes in the gauge field functions ω_1 and ω_2, with this particular solution taking $n_1 = 1$, $n_2 = 1$.

The full phase space plot for $\Lambda = -0.01$ is again very complicated, as in previous sections. In figure 3.15 we fix $b_1 = -0.002$, $b_2 = -0.00001$, and scan over values of g_1 and g_2. Since there is no event horizon, there is no analogue of (3.72), and therefore no obvious range of values to scan over for g_1 and g_2.

For clarity the "no solution" region is omitted, and only solutions are included. The nodeless region is the red region with small g_2, with the adjacent $n_1 = 1$, $n_2 = 0$ region in yellow, $n_1 = 0$, $n_2 = 1$ region in green, and higher numbers of nodes as g_2 increases. We note that, despite the treatment of the numerics in section 3.4, we still find some numerical errors, as can be seen in the blurred line between light blue $n_1 = 3$, $n_2 = 1$, and dark blue $n_1 = 3$, $n_2 = 3$ regions.

Again, the $\Lambda = -3$ region is much less complicated, and is plotted in figure 3.16 with fixed $b_1 = -0.2$, $b_2 = -0.1$. Once again we find that the nodeless region dominates the parameter space. However, we do find a small $n_1 = 0$, $n_2 = 1$ region, and, although it is difficult to see from figure 3.16, a very small $n_1 = 1$, $n_2 = 0$ region.

§ 3.6 Summary

To summarise, we have found black hole and soliton solutions with $\mathfrak{su}(2)$ and $\mathfrak{su}(3)$ gauge fields. In the previous chapter it was found that, for zero electric field, the size of the nodeless region of the parameter space increases with $|\Lambda|$, up to a certain value of $|\Lambda|$ above which we find only nodeless solutions. From our numerical results this appears to be the case for nonzero electric fields as well. It is likely that the nodeless region of the parameter space will play an important role in the stability analysis of the dyonic solutions, as the presence of an electric field is not expected to change the stability of the solutions [18]. However, such an analysis remains an open problem (the $\mathfrak{su}(2)$ case is currently being studied by E. Winstanley and B.

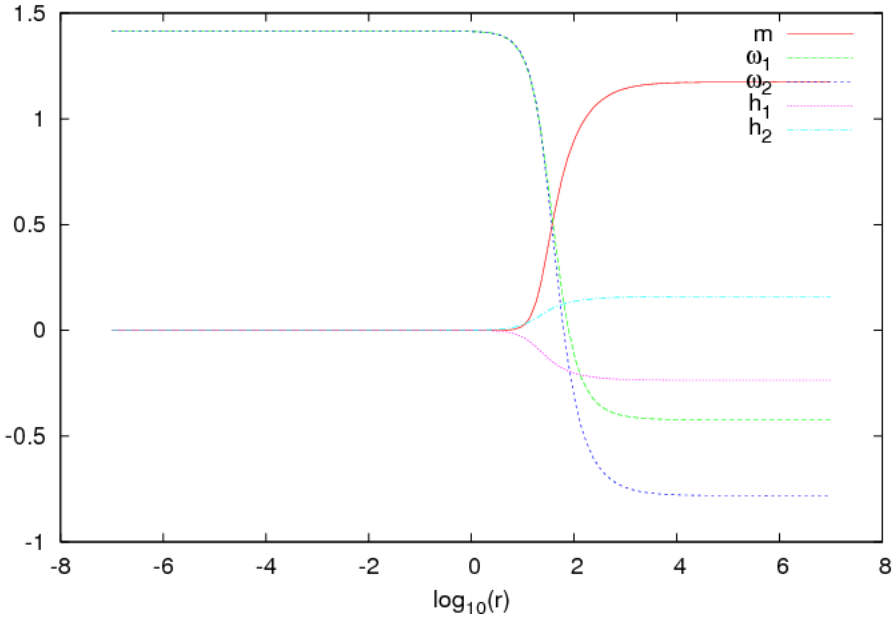

Figure 3.14: Typical $n_1 = 1$, $n_2 = 0$ solution for an $\mathfrak{su}(3)$ soliton with $\Lambda = -0.01$. Parameters at the event horizon are $b_1 = -0.002$, $b_2 = -0.00001$, $g_1 = 0.001$, $g_2 = 0.0005$.

Nolan [63]).

Much of the work on black holes in AdS space is motivated by the AdS/CFT correspondence. While dyonic black holes with spherical event horizons have no obvious application to this correspondence, dyonic black holes with planar event horizons have been considered in the context of holographic superconductivity, and are the subject of the next chapter.

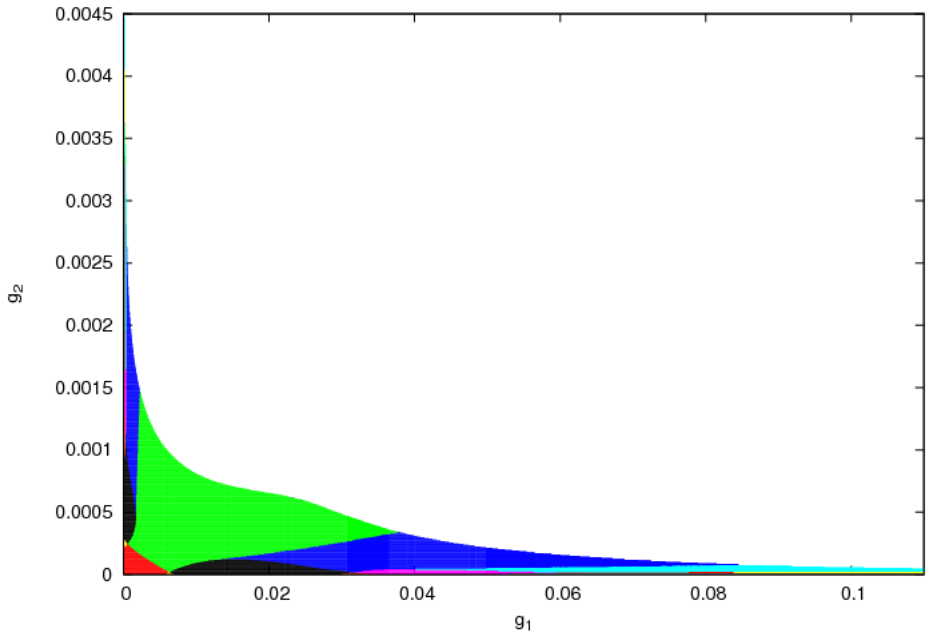

Figure 3.15: Phase space plot for $\mathfrak{su}(3)$ dyonic solitons with $\Lambda = -0.01$, $b_1 = -0.002$, $b_2 = -0.00001$. Once again, we find a very rich solution space for small $|\Lambda|$, with potentially a very large number of nodes. Again, the nodeless region makes up a small area of the parameter space, at small g_1 and g_2.

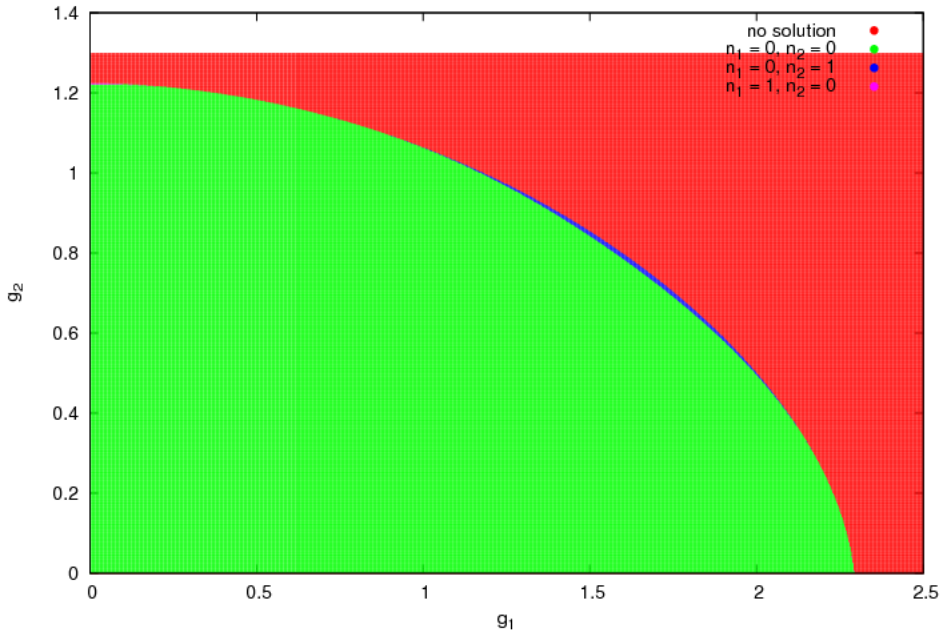

Figure 3.16: Phase space plot for $\mathfrak{su}(3)$ dyonic solitons with $\Lambda = -3$, $b_1 = -0.2$, $b_2 = -0.1$. Once again, we find the solution space is much simpler with a larger value of $|\Lambda|$, and has a larger nodeless region. For these values of the parameters, we also find solutions where either ω_1 or ω_2 has a single node.

Chapter 4

Planar black holes with superconducting horizons

Motivated by the AdS/CFT correspondence, and the work of [37, 38, 62], in this chapter we will consider Einstein-Yang-Mills black holes in $3+1$ dimensions which provide a possible gravitational dual to the $2+1$ layered cuprate superconductors as discussed in chapter 1. We will require a normal, non-superconducting state which possesses an abelian gauge symmetry, and a superconducting condensate which spontaneously breaks this symmetry at non-zero temperature. There have been a number of different gravitational analogues proposed in the literature, which are reviewed in section 4.1. As in [37, 38, 62], the role of the normal, non-superconducting state will be played by a planar Reissner-Nordström-AdS black hole, and our superconducting states will consist of black hole solutions with non-abelian gauge fields. As in previous chapters, we will generalise the well-known $\mathfrak{su}(2)$ case [37, 38, 62] to solutions with an $\mathfrak{su}(N)$ gauge group. The goal will be to find black hole solutions to the Einstein-Yang-Mills equations which have the same properties as the layered cuprates. In particular, we require that there is a critical temperature T_C below which superconducting solutions exist and are thermodynamically favoured over the Reissner-Nordström solutions. We also require that there is a mechanism by which the normal state can decay into a superconducting state, i.e. the Reissner-Nordström solution admits a static $\mathfrak{su}(N)$ EYM perturbation. Finally, we require that the frequency dependent conductivity of the $\mathfrak{su}(N)$ solutions exhibits the same behaviour as real layered cuprate superconductors, i.e. there is a gap at non-zero frequency, with lower conductivity at lower frequencies than at higher ones, and that on the boundary the conductivity becomes infinite at zero frequency. We note here that

despite being motivated by the AdS/CFT correspondence, we will not derive the gravitational theory from string theory, instead we will take a similar approach to [37, 38, 62] and simply look for a gravitational theory with the desired properties described above.

We will consider asymptotically AdS black holes, as required by the AdS/CFT correspondence. Unlike the situation in asymptotically flat space, in asymptotically AdS space we can find planar black holes [15, 22, 56, 57, 58, 75]. We can also find planar black holes with stable Yang-Mills fields [64], which are the most relevant to $(2+1)$-dimensional layered superconductors. In the planar case, we have much more freedom in our choice of gauge field ansatz, and we will not attempt to use the most general ansatz compatible with the symmetries of our space-time. We will instead propose a generalization of the ansatze in [37, 38, 62], and show that it is compatible with the space-time symmetries and the field equations. In section 4.2 we will present our ansatz and field equations, and in section 4.3 we will show that the ansatz is a solution of the symmetry equations. We will then find the appropriate boundary conditions in section 4.4, some trivial solutions in section 4.5 and the scaling symmetries of the field equations in section 4.6. In section 4.7 we will discuss the numerical method used to solve the field equations and present some numerical results.

We will then go on to study some properties of the solutions, and show that our solutions have the same properties as real layered cuprate superconductors, as discussed above. The mass, charges and thermodynamics are discussed in section 4.8. The critical temperature T_C is calculated in section 4.9, and the frequency dependent conductivity is discussed in section 4.10.

Derivations of all the Einstein-Yang-Mills equations presented in this chapter can be found in section B.2 of Appendix B.

§ 4.1 Review of known solutions

In this section we will review some previously proposed gravitational duals to superconductors. One of the first models employing a scalar field as a dual to the condensate was proposed in [36], and consists of a charged black hole and a charged scalar field with action

$$S = \int d^4x\sqrt{-g}\left(R + \frac{6}{l^2} - \frac{1}{4}F_{\mu\nu}F^{\mu\nu} - |\nabla\psi - iqA\psi|^2 - m^2|\psi|^2\right), \tag{4.1}$$

where R is the Ricci scalar, $F_{\mu\nu}$ is the field strength tensor, ψ is the scalar field and m is its mass. Black hole solutions with this action were shown to form scalar hair (playing the role of the superconducting condensate) at low temperatures, while above a critical temperature T_C the only solution has $\psi = 0$. A perturbation of the Maxwell field in the x direction A_x was added in the bulk, with time dependence $e^{-i\xi t}$ and asymptotic expansion at large r given by

$$A_x = A_x^{(0)} + \frac{A_x^{(1)}}{r} + \mathcal{O}\left(\frac{1}{r^2}\right). \tag{4.2}$$

On the boundary $r \to \infty$ this corresponds to an applied electric field with frequency ξ. The electrical conductivity on the boundary is then [40]

$$\sigma(\xi) = -\frac{iA_x^{(0)}}{\xi A_x^{(1)}}. \tag{4.3}$$

The Maxwell equation for A_x is given by

$$A_x'' + \frac{\mu'}{\mu}A_x' + \left(\frac{\xi^2}{\mu^2} - \frac{2\psi}{\mu}\right)A_x = 0, \tag{4.4}$$

where the metric function

$$\mu = -\frac{M}{r^2} - \frac{\Lambda R^2}{3}, \tag{4.5}$$

with constant mass M. The Maxwell equation (4.4) must be integrated numerically to find $A_x^{(0)}$ and $A_x^{(1)}$. It was shown in [40] that when $\psi = 0$, the conductivity σ is always finite. However, when $\psi \neq 0$, the conductivity becomes infinite at $\xi = 0$. Infinite conductivity corresponds to zero resistance, and $\xi = 0$ corresponds to an applied DC current. Hence we have zero DC resistance below the critical temperature. There has since been much interest in solutions with a scalar field (see e.g. [45, 66] for reviews), although they will not be considered further here.

It has also been shown [37, 38, 62] that a charged black hole with a non-abelian gauge field can produce similar results, with the gauge field playing the role of the superconducting condensate. Above the critical temperature T_C, the only solutions to the field equations are the planar Reissner-Nordström-AdS black holes, which play the role of the normal state. Below T_C solutions with a non-abelian gauge field are found, and these are thermodynamically favoured over the normal state. Two ansatze for models with $\mathfrak{su}(2)$ gauge fields were proposed in [37] and [38], with gauge

potentials given by

$$A = \Phi T_3 dt + \omega \left(T_1 dx + T_2 dy\right), \tag{4.6}$$

and

$$A = \Phi T_3 dt + \omega T_1 dx \tag{4.7}$$

respectively, where $\Phi = \Phi(r)$ is the electric potential, $\omega = \omega(r)$ describes the $\mathfrak{su}(2)$ gauge field, and T_i are the generators of the $\mathfrak{su}(2)$ Lie algebra (A.1), where $i = 1, 2, 3$. The gauge field (or condensate) is localized near the horizon, such that $\omega(\infty) = 0$, and the solutions carry no magnetic charge. The ansatze of [37, 38] were generalised to arbitrary space-time dimensions in [62], with (4.6) corresponding to ansatz I, and (4.7) corresponding to ansatz II in the terminology of [62]. The potential in (4.6) corresponds to an s-wave superconductor, which is isotropic in the (x, y) plane. This means that the conductivity of the superconductor does not depend on the direction in which the electric field is applied. For the ansatz (4.7) it was found in [38] that below the critical temperature, the conductivity becomes infinite when a DC current is applied.

A p-wave superconductor has different responses to electric fields applied in different directions in the (x, y) plane, which motivated the potential given in (4.7). For an electric field with time dependence $e^{i\xi t}$ applied in the x direction, it was found in [38] that the conductivity becomes infinite for small but non-zero ξ. However, in real p-wave materials, the conductivity is finite at non-zero ξ due to electron scattering, which is caused by impurities in the superconductor.

§ 4.2 Gauge field, metric ansatz and field equations

In this section we will propose an ansatz for a gauge field on a planar black hole background which generalises the $\mathfrak{su}(2)$ ansatze given in [37, 38, 62] to gauge group $\mathfrak{su}(N)$. We will decompose this ansatz into the generators of $\mathfrak{su}(N)$, and present the field equations, a detailed derivation of which can be found in Appendix B. Our metric ansatz will correspond to that of [62], but uses a different choice of co-ordinates to the metric ansatz of [37, 38].

In the spherically symmetric case, the symmetry requirements of the space-time are sufficiently restrictive that a generalised expression for the $\mathfrak{su}(N)$ gauge field ansatz can be derived [51] (see chapter 2). However, the symmetries of a planar black hole are less restrictive. In ansatz I from [62], in addition to translational

symmetry we also have an $SO(2)$ space-time symmetry corresponding to rotations in the (x, y) plane. In ansatz II there is no rotational symmetry, only translational symmetry in t, x and y. In both cases we cannot write down a completely general ansatz. Instead we propose an ansatz that generalises the potential from [62] (which has a gauge group of $\mathfrak{su}(2)$), to one with a gauge group $\mathfrak{su}(N)$, and check that it is valid by showing that it is compatible with both the symmetries of the space-time (see section 4.3), and the field equations.

An appropriate line element for a planar black hole with an electric field and a Yang-Mills gauge field is given by [62]

$$ds^2 = -\sigma^2\mu\, dt^2 + r^2 f^2 dx^2 + \frac{r^2}{f^2}dy^2 + \mu^{-1}dr^2, \tag{4.8}$$

where the function $\sigma = \sigma(r)$, $\mu = \mu(r)$ and $f = f(r)$ must be determined from the field equations in both cases. The metric function μ is given by

$$\mu = -\frac{2m(r)}{r} - \frac{\Lambda r^2}{3}, \tag{4.9}$$

which is the same as that used in chapters 2 and 3, except we have replaced the initial 1 with 0. For the space-time to be asymptotically AdS we require $f = \sigma = 1$ at large r (see section 4.4.2). The action is given by

$$S = \int d^4x\sqrt{-g}\left[\frac{1}{16\pi G}(R - 2\Lambda) - \frac{1}{4}\mathrm{Tr}\, F^a_{\mu\nu}F^{a\mu\nu}\right] \tag{4.10}$$

where R is the Ricci scalar and the field strength tensor

$$F_{\mu\nu} = F^a_{\mu\nu}T_a = \partial_\mu A_\nu - \partial_\nu A_\mu + g[A_\mu, A_\nu], \tag{4.11}$$

with coupling constant g, and T_a denoting the generators of the Lie algebra $\mathfrak{su}(N)$ (see appendix A). Varying the action (4.10) gives the field equations

$$\begin{aligned} T_{\mu\nu} &= R_{\mu\nu} - \frac{1}{2}Rg_{\mu\nu} + \Lambda g_{\mu\nu}; \\ D_\mu F^\mu_\nu &= \nabla_\mu F^\mu_\nu + g\,[A_\mu, F^\mu_\nu] = 0; \end{aligned} \tag{4.12}$$

where the stress-energy tensor is

$$T_{\mu\nu} = F^a_{\mu\alpha}F^a_{\nu\beta}g^{\alpha\beta} - \frac{1}{4}g_{\mu\nu}F^a_{\alpha\beta}F^{a\alpha\beta}. \tag{4.13}$$

We generalise the ansatz for the $\mathfrak{su}(2)$ solutions of [62] to $\mathfrak{su}(N)$ by taking

$$gA = gA_\mu dx^\mu = \mathcal{A}\,dt + \frac{i}{2}\left(C + C^H\right)dx + \frac{\zeta}{2}\left(C - C^H\right)dy, \tag{4.14}$$

where $\mathcal{A}$, C and C^H are $N \times N$ matrices, and are independent of t, x and y. The $\zeta = 1$ case is a generalization of ansatz I in [62] to larger gauge group, while $\zeta = 0$ is a generalization of ansatz II. If $\zeta = 1$ then $f = 1$ in the line element (4.8), while if $\zeta = 0$ then $f = f(r)$ must be determined from the field equations. The electric part of the potential

$$\mathcal{A} = -\sum_{l=1}^{N-1} h_l H_l, \tag{4.15}$$

where $h_l = h_l(r)$ are also scalar functions of r only, and the H_l are members of the Cartan subalgebra of $\mathfrak{su}(N)$, and are given in Appendix A (A.3). The only non-zero entries of the upper triangular matrix C are $C_{j,j+1} = \omega_j$, where $j = 1, 2, ..., N-1$ and $\omega_j = \omega_j(r)$ are $N-1$ scalar functions of the radial co-ordinate r only. We can decompose $\left(C + C^H\right)$ and $\left(C - C^H\right)$ into

$$C + C^H = 2i\sum_{m=1}^{N-1}\omega_m F_m^{(1)}, \qquad C - C^H = -2\sum_{m=1}^{N-1}\omega_m G_m^{(1)}, \tag{4.16}$$

where the $N \times N$ matrices $F_m^{(1)}$ and $G_m^{(1)}$ are generators of the Lie algebra $\mathfrak{su}(N)$ and are also given in Appendix A (A.4, A.5).

The Einstein-Yang-Mills equations corresponding to the potential (4.14) and line element (4.8) are derived in section B.2 (Appendix B) and are given by

$$\begin{aligned} m' &= \frac{\mu r^2 f'^2}{2f^2} + \alpha^2\sum_{k=1}^{N-1}\left\{\frac{\omega_k^2}{2\sigma^2\mu}\left(\sqrt{\frac{k+1}{2k}}h_k - \sqrt{\frac{k-1}{2k}}h_{k-1}\right)^2\left(\frac{1}{f^2} + \zeta^2 f^2\right)\right\} \\ &\quad + \alpha^2\sum_{k=1}^{N-1}\left\{\frac{r^2 h_k'^2}{2\sigma^2} + \frac{\mu\omega_k'^2}{2}\left(\frac{1}{f^2} + \zeta^2 f^2\right) + \frac{k(k+1)\zeta^2}{4r^2}\left(\frac{\omega_k^2}{k} - \frac{\omega_{k+1}^2}{k+1}\right)^2\right\}, \end{aligned} \tag{4.17}$$

$$\begin{aligned} \sigma' &= \frac{r\sigma f'^2}{f^2} + \alpha^2\sum_{k=1}^{N-1}\left\{\frac{\omega_k^2}{2\sigma\mu^2 r}\left(\sqrt{\frac{k+1}{2k}}h_k - \sqrt{\frac{k-1}{2k}}h_{k-1}\right)^2\left(\frac{1}{f^2} + \zeta^2 f^2\right)\right\} \\ &\quad + \alpha^2\sum_{k=1}^{N-1}\left\{\frac{\sigma\omega_k'^2}{r}\left(\frac{1}{f^2} + \zeta^2 f^2\right)\right\}, \end{aligned} \tag{4.18}$$

$$
\begin{aligned}
f'' &= \alpha^2\left(\frac{1}{f^2}-\zeta^2 f^2\right)\sum_{k=1}^{N-1}\left\{\frac{2\omega_k^2 h_k^2}{k(k+1)\sigma^2\mu^2 r^2}-\frac{\omega_k'^2}{r^2}\right\}\\
&\quad -f'\left(\frac{\sigma'}{\sigma}+\frac{\mu'}{\mu}+\frac{2}{r}-\frac{f'}{f}\right), \qquad (4.19)\\
h_k'' &= h_k'\left(\frac{\sigma'}{\sigma}-\frac{2}{r}\right)\\
&\quad +\frac{\sqrt{k(k+1)}}{2\mu r^2}\frac{\omega_k^2}{k}\left(\sqrt{\frac{k+1}{k}}h_k-\sqrt{\frac{k-1}{k}}h_{k-1}\right)\left(\frac{1}{f^2}+\zeta^2 f^2\right)\\
&\quad +\frac{\sqrt{k(k+1)}}{2\mu r^2}\frac{\omega_{k+1}^2}{k+1}\left(\sqrt{\frac{k}{k+1}}h_k-\sqrt{\frac{k+2}{k+1}}h_{k+1}\right)\left(\frac{1}{f^2}+\zeta^2 f^2\right), \qquad (4.20)\\
0 &= \omega_k''+\omega_k'\left(\frac{\sigma'}{\sigma}+\frac{\mu'}{\mu}-\frac{2f'}{f}\right)+\frac{\omega_k}{\sigma^2\mu^2}\left(\sqrt{\frac{k+1}{2k}}h_k-\sqrt{\frac{k-1}{2k}}h_{k-1}\right)^2\\
&\quad +\frac{\zeta^2 f^2\omega_k}{2\mu r^2}\left(\omega_{k-1}^2-2\omega_k^2+\omega_{k+1}^2\right), \qquad (4.21)
\end{aligned}
$$

along with a constraint equation:

$$
0 = \left(\omega_k\omega_{k+1}'-\omega_{k+1}\omega_k'\right)\left(\frac{1}{f^2}-\zeta^2 f^2\right), \qquad (4.22)
$$

where $\alpha^2=\frac{4\pi G}{g^2}$. We note that in the $N=2$ case, (4.17–4.21) reduce to the $d=4$ case in [62], with $\zeta=1$ corresponding to ansatz I, and $\zeta=0$ corresponding to ansatz II. The field equations in [38] are found in the limit where the gauge fields do not back react on the metric, and are recovered if we take $\sigma=1$, $m=1/(2l^2)$, together with $\zeta=f=1$. We note that the constraint equation (4.22) is solved automatically for the $\zeta=f=1$ case, while for $\zeta=0$ we require all ω_k to be scalar multiples of each other (assuming all ω_k are non-zero). Hence the only non-trivial solution for $\zeta=0$ is the embedded $\mathfrak{su}(2)$ solution (see section 4.5.3). We also note that there are no obvious inconsistencies in the field equations, and that we have the correct number of equations for the number of variables.

§ 4.3 Symmetry equations

In the $f=1$ case, the line element (4.8) possesses an $SO(2)$ symmetry, corresponding to rotations in the (x,y) plane. As shown in [33], the physical quantities associ-

ated with the field will be invariant under these $SO(2)$ rotations if the infinitesimal space-time symmetry transformations are equivalent to infinitesimal gauge transformations, since all physical quantities must be gauge invariant. This leads to a set of equations relating the ansatz, the space-time symmetries and the gauge group, called the symmetry equations, which must be satisfied for the ansatz to be valid. In this section we will construct the symmetry equations for planar black holes in the $\zeta = f = 1$ case and show that our ansatz does indeed satisfy the symmetry equations. Note that since the $\zeta = 0$ case breaks the $SO(2)$ symmetry, there are no further constraints on the ansatz from the space-time, since we have already assumed that $\partial_t A = \partial_x A = \partial_y A = 0$.

If $\zeta = f = 1$, the planar black hole space-times described by the line element (4.8) are invariant under rotations in the (x, y) plane. For infinitesimal rotations, these take the form

$$\begin{pmatrix} x \\ y \end{pmatrix} \to \begin{pmatrix} x' \\ y' \end{pmatrix} = \begin{pmatrix} \cos\theta & -\sin\theta \\ \sin\theta & \cos\theta \end{pmatrix} \begin{pmatrix} x \\ y \end{pmatrix} \approx \begin{pmatrix} x \\ y \end{pmatrix} + \theta \begin{pmatrix} -y \\ x \end{pmatrix}. \tag{4.23}$$

We require the physical quantities associated with our gauge field to be invariant under these transformations. Since our physical quantities must be gauge invariant, this will be the case if our co-ordinate transformation is equivalent to a gauge transformation. Under the co-ordinate transformation $x^\mu \to x^\mu + \epsilon\xi^\mu$, the gauge field transforms as [33]

$$A_\mu \to A_\mu + \epsilon \left(\partial_\mu \xi^\nu\right) A_\nu + \epsilon\xi^\nu \left(\partial_\nu A_\mu\right) + \mathcal{O}\left(\epsilon^2\right). \tag{4.24}$$

For rotations in the (x, y) plane, in co-ordinates $x^\mu = (t, x, y, r)$, we have $\xi^\mu = (0, -y, x, 0)$ from (4.23), which gives

$$A_\mu \to A_\mu + \epsilon \left[-(\partial_\mu y)A_1 + (\partial_\mu x)A_2 - y(\partial_1 A_\mu) + x(\partial_2 A_\mu)\right] + \mathcal{O}\left(\epsilon^2\right). \tag{4.25}$$

Applying an infinitesimal gauge transformation to the gauge field gives

$$A_\mu \to A_\mu + \epsilon \left(\partial_\mu W - [A_\mu, W]\right), \tag{4.26}$$

where W is an element of the Lie algebra of the gauge group, i.e. $W = W^a(x)T^a$ where the T^a are the generators of the gauge group. The requirement that the rotations in the (x, y) plane are equivalent to gauge transformations gives a set of

four symmetry equations. By comparing (4.25, 4.26) we find

$$\begin{aligned}
\partial_0 W - [A_0, W] &= x\,(\partial_2 A_0) - y\,(\partial_1 A_0)\,, && (4.27)\\
\partial_1 W - [A_1, W] &= A_2 + x\,(\partial_2 A_1) - y\,(\partial_1 A_1)\,, && (4.28)\\
\partial_2 W - [A_2, W] &= -A_1 + x\,(\partial_2 A_2) - y\,(\partial_1 A_2)\,, && (4.29)\\
\partial_3 W - [A_3, W] &= x\,(\partial_2 A_3) - y\,(\partial_1 A_3)\,. && (4.30)
\end{aligned}$$

Our proposed ansatz is valid only if we can find some W in the Lie algebra that satisfies these equations.

In the $\mathfrak{su}(2)$ case, the generators of the Lie algebra are given by $T^a = -i\sigma^a/2$, where σ^a are the Pauli matrices (A.1). Expanding $W = W^1T^1 + W^2T^2 + W^3T^3$, and substituting into equations (4.27–4.30), we can solve the symmetry equations to find

$$W = T^3 = -\frac{i}{2}\begin{pmatrix} 1 & 0 \\ 0 & -1 \end{pmatrix}. \qquad (4.31)$$

Similarly we can solve the symmetry equations for $\mathfrak{su}(3)$ explicitly by taking the Gell-Mann matrices (A.2) as the generators, in which case we find

$$W = -\frac{i}{2}\begin{pmatrix} 1 & 0 & 0 \\ 0 & -1 & 0 \\ 0 & 0 & 0 \end{pmatrix} - \frac{i}{2}\begin{pmatrix} 1 & 0 & 0 \\ 0 & 1 & 0 \\ 0 & 0 & -2 \end{pmatrix} = -i\begin{pmatrix} 1 & 0 & 0 \\ 0 & 0 & 0 \\ 0 & 0 & -1 \end{pmatrix}. \qquad (4.32)$$

For the $\mathfrak{su}(N)$ case, rather than try to solve the symmetry equations explicitly, we will take

$$W = \sum_{p=1}^{N-1} \frac{\sqrt{2p(p+1)}}{2} H_p, \qquad (4.33)$$

and verify that it is a solution to the symmetry equations. Since our gauge field $A_\mu(x)$ depends only on the radial co-ordinate r, we have $\partial_1 A_\mu = \partial_0 A_\mu = 0$ for all μ. We also have $\partial_0 W = \partial_3 W = 0$ since W does not depend on t or r, and $[A_0, W] = [A_3, W] = 0$ since $A_3 = 0$ and W is in the Cartan subalgebra. Therefore equations (4.27) and (4.30) are satisfied automatically. The two remaining equations become

$$[A_1, W] = -A_2, \qquad [A_2, W] = A_1. \qquad (4.34)$$

Using the commutation relations (A.9) we find

$$\begin{aligned}
[A_1, W] &= -\frac{1}{2g}\left[\sum_{m=1}^{N-1}\omega_m F_m^{(1)}, \sum_{p=1}^{N-1}\sqrt{2p(p+1)}H_p\right] \\
&= -\frac{1}{2g}\sum_{k=1}^{N-1}\sqrt{2k(k+1)}\left(\omega_k\left[F_k^{(1)}, H_k\right] + \omega_{k+1}\left[F_{k+1}^{(1)}, H_k\right]\right) \\
&= \frac{i}{4g}\sum_{k=1}^{N-1}\left[(k+1)\omega_k G_k^{(1)} - k\omega_{k+1}G_{k+1}^{(1)}\right], \qquad (4.35)
\end{aligned}$$

where we have used the fact that $\omega_N = 0$. Using

$$\sum_{k=1}^{N-1} k\omega_{k+1}G_{k+1}^{(1)} = \sum_{k=2}^{N}(k-1)\omega_k G_k^{(1)} = \sum_{k=2}^{N-1}(k-1)\omega_k G_k^{(1)} \qquad (4.36)$$

we have

$$\begin{aligned}
[A_1, W] &= \frac{1}{2g}\left(2\omega_1 G_1^{(1)} + \sum_{k=2}^{N-1}(k+1-k+1)\omega_k G_k^{(1)}\right) \\
&= \frac{1}{g}\sum_{k=1}^{N-1}\omega_k G_k^{(1)} \\
&= -A_2. \qquad (4.37)
\end{aligned}$$

Similarly

$$\begin{aligned}
[A_2, W] &= -\frac{1}{2g}\left[\sum_{n=1}^{N-1}\omega_n G_n^{(1)}, \sum_{p=1}^{N-1}\sqrt{2p(p+1)}H_p\right] \\
&= -\frac{1}{2g}\sum_{k=1}^{N-1}\sqrt{2k(k+1)}\left(\omega_k\left[G_k^{(1)}, H_k\right] + \omega_{k+1}\left[G_{k+1}^{(1)}, H_k\right]\right) \\
&= -\frac{1}{2g}\sum_{k=1}^{N-1}\left[(k+1)\omega_k F_k^{(1)} - k\omega_{k+1}F_{k+1}^{(1)}\right] \\
&= -\frac{1}{2g}\left(2\omega_k F_k^{(1)} + \sum_{k=2}^{N-1}(k+1-k+1)\omega_k F_k^{(1)}\right) \\
&= -\frac{1}{g}\sum_{k=1}^{N-1}\omega_k F_k^{(1)} \\
&= A_1. \qquad (4.38)
\end{aligned}$$

Hence we have shown that an infinitesimal rotation in the (x, y) plane is equivalent to an infinitesimal gauge transformation of the form (4.33). Since our physical quantities are gauge invariant, they are therefore also invariant under rotations in the (x, y) plane. Our ansatz is therefore valid, since it is compatible with both the Einstein-Yang-Mills equations and the symmetry equations.

§ 4.4 Boundary conditions

In this section we find the boundary conditions for our variables m, σ, f, h_k and ω_k at the event horizon and at infinity, keeping ζ general for completeness. We assume that our variables have regular Taylor expansions close to the event horizon and at large r, and find the leading order terms in the expansions by evaluating the field equations (4.17–4.21) in the two limits and requiring that they are regular.

4.4.1 At the event horizon

We start by Taylor expanding our variables in a neighbourhood of the event horizon:

$$\begin{aligned} m(r) &= m(r_h) + m'(r_h)(r - r_h) + \mathcal{O}(r - r_h)^2, \\ \omega_k(r) &= \omega_k(r_h) + \omega_k'(r_h)(r - r_h) + \mathcal{O}(r - r_h)^2, \\ f(r) &= f(r_h) + f'(r_h)(r - r_h) + \mathcal{O}(r - r_h)^2, \\ \sigma(r) &= \sigma(r_h) + \sigma'(r_h)(r - r_h) + \mathcal{O}(r - r_h)^2, \\ h_k(r) &= h_k'(r_h)(r - r_h) + \mathcal{O}(r - r_h)^2, \\ \mu(r) &= \mu'(r_h)(r - r_h) + \mathcal{O}(r - r_h)^2. \end{aligned} \tag{4.39}$$

At the event horizon we have $\mu(r_h) = 0$, and for the black hole to be non-extremal (and therefore have non-zero surface gravity and Hawking temperature) we also require

$$\mu'(r_h) = -\Lambda r_h - \frac{2m'(r_h)}{r_h} > 0. \tag{4.40}$$

We are looking for solutions where all quantities are regular at the event horizon, so we have set $h_k(r_h) = 0$ to avoid a singularity in equation (4.20) at $r = r_h$. Substituting $\mu(r_h) = h_k(r_h) = 0$ into equation (4.17), and noting that both μ and

h_k are of order $(r - r_h)$ so that h_k^2/μ vanishes at $r = r_h$, we find that

$$m'(r_h) = \alpha^2 \sum_{k=1}^{N-1} \left[\frac{r_h^2 h_k'^2}{2\sigma(r_h)^2} + \frac{k(k+1)\zeta^2}{4r_h^2} \left(\frac{\omega_k(r_h)^2}{k} - \frac{\omega_{k+1}(r_h)^2}{k+1} \right)^2 \right]. \tag{4.41}$$

Multiplying equation (4.21) through by μ and evaluating it at the event horizon, we find that

$$\begin{aligned} \omega_k'(r_h) &= \frac{\zeta^2 f(r_h)^2 \omega_k(r_h)}{2\mu'(r_h) r_h^2} \left(2\omega_k(r_h)^2 - \omega_{k-1}(r_h)^2 - \omega_{k+1}(r_h)^2 \right) \\ &= \frac{\zeta^2 l^2 f(r_h)^2 \omega_k(r_h) \left(2\omega_k(r_h)^2 - \omega_{k-1}(r_h)^2 - \omega_{k+1}(r_h)^2 \right)}{2r_h^2 \left(3r_h - 2m'(r_h) l^2 \right)}, \end{aligned} \tag{4.42}$$

where we have used $m(r_h) = r_h^3/2l^2$ with $l^2 = -3/\Lambda$. Multiplying equation (4.19) through by μ and evaluating at the event horizon we find that the only term that survives is $f'(r_h)\mu'(r_h)$, from which we conclude that $f'(r_h) = 0$.

Close to the event horizon we have

$$\mu = \mu'(r_h)(r - r_h) + \mathcal{O}(r - r_h)^2 = \frac{3r_h - 2m'(r_h) l^2}{r_h l^2} (r - r_h) + \mathcal{O}(r - r_h)^2, \tag{4.43}$$

so that using l'Hôpital's rule

$$\frac{h_k}{\mu} = \frac{r_h l^2 h_k'(r_h)}{3r_h - 2m'(r_h) l^2} + \mathcal{O}(r - r_h). \tag{4.44}$$

Using this to evaluate (4.18) at the event horizon we find

$$\begin{aligned} \sigma'(r_h) \;=\; & \alpha^2 \left(\frac{1}{f(r_h)} + \zeta^2 f(r_h)^2 \right) \sum_{k=1}^{N-1} \left[\frac{2\omega_k(r_h)^2 h_k'(r_h)^2 r_h l^4}{k(k+1)\sigma(r_h) \left(3r_h^2 - 2m'(r_h) l^2 \right)^2} \right] \\ & + \alpha^2 \left(\frac{1}{f(r_h)} + \zeta^2 f(r_h)^2 \right) \sum_{k=1}^{N-1} \left[\frac{\sigma(r_h) \omega_k'(r_h)^2}{r_h} \right]. \end{aligned} \tag{4.45}$$

To summarize, the boundary conditions of our variables at the event horizon are given by:

$$\begin{aligned} m(r) &= \frac{r_h^3}{2l^2} + m'(r_h)(r-r_h) + \mathcal{O}(r-r_h)^2, \\ \omega_k(r) &= \omega_k(r_h) + \omega_k'(r_h)(r-r_h) + \mathcal{O}(r-r_h)^2, \\ f(r) &= f(r_h) + \mathcal{O}(r-r_h)^2, \\ \sigma(r) &= \sigma(r_h) + \sigma'(r_h)(r-r_h) + \mathcal{O}(r-r_h)^2, \\ h_k(r) &= h_k'(r_h)(r-r_h) + \mathcal{O}(r-r_h)^2, \end{aligned} \tag{4.46}$$

where

$$\begin{aligned} \omega_k'(r_h) &= \frac{\zeta^2 l^2 f(r_h)^2 \omega_k(r_h)\left(2\omega_k(r_h)^2 - \omega_{k-1}(r_h)^2 - \omega_{k+1}(r_h)^2\right)}{2r_h^2\left(3r_h - 2m'(r_h)l^2\right)}, \\ m'(r_h) &= \alpha^2 \sum_{k=1}^{N-1} \left\{ \frac{r_h^2 h_k'^2}{2\sigma(r_h)^2} + \frac{k(k+1)\zeta^2}{4r_h^2}\left(\frac{\omega_k(r_h)^2}{k} - \frac{\omega_{k+1}(r_h)^2}{k+1}\right)^2 \right\}, \\ \sigma'(r_h) &= \alpha^2\left(\frac{1}{f(r_h)} + \zeta^2 f(r_h)^2\right) \sum_{k=1}^{N-1}\left[\frac{2\omega_k(r_h)^2 h_k'(r_h)^2 r_h l^4}{k(k+1)\sigma(r_h)\left(3r_h^2 - 2m'(r_h)l^2\right)^2}\right] \\ &\quad + \alpha^2\left(\frac{1}{f(r_h)} + \zeta^2 f(r_h)^2\right) \sum_{k=1}^{N-1}\left[\frac{\sigma(r_h)\omega_k'(r_h)^2}{r_h}\right], \end{aligned} \tag{4.47}$$

and

$$m'(r_h) < -\Lambda r_h^2. \tag{4.48}$$

4.4.2 At infinity

We assume that our variables have regular Taylor series expansions at large r:

$$\begin{aligned} m = m_0 + \frac{m_1}{r} + \mathcal{O}\left(\frac{1}{r^2}\right), \qquad f = f_0 + \frac{f_1}{r} + \frac{f_2}{r^2} + \frac{f_3}{r^3} + \mathcal{O}\left(\frac{1}{r^4}\right), \\ \sigma = \sigma_0 + \frac{\sigma_1}{r} + \frac{\sigma_2}{r^2} + \frac{\sigma_3}{r^3} + \frac{\sigma_4}{r^4} + \mathcal{O}\left(\frac{1}{r^5}\right), \\ \omega_k = \omega_{k,\infty} + \frac{c_{k,1}}{r} + \mathcal{O}\left(\frac{1}{r^2}\right), \qquad h_k = h_{k,\infty} + \frac{h_{k,1}}{r} + \mathcal{O}\left(\frac{1}{r^2}\right). \end{aligned} \tag{4.49}$$

We are looking for asymptotically anti-de Sitter solutions, so we require $f_0 = \sigma_0 = 1$ so that the line element (4.8) approaches the line element for anti-de Sitter space in

the large r limit. Using (4.49) to evaluate (4.17) at large r gives

$$\begin{aligned} m' = \frac{1}{2l^2}\left(-f_1 - \frac{2f_2}{r}\right)^2 \\ + \frac{\alpha^2}{r^2}\sum_{k=1}^{N-1}\left[\frac{k(k+1)\zeta^2}{4}\left(\frac{\omega_k^2}{k} - \frac{\omega_{k+1}^2}{k+1}\right)^2 + \frac{h_{k,1}^2}{2} + \frac{c_{k,1}^2}{2l^2}\left(1+\zeta^2\right)\right] \\ + \frac{\alpha^2}{r^2}\sum_{k=1}^{N-1}\left[\omega_{k,\infty}^2 l^2\left(\sqrt{\frac{k+1}{2k}}h_{k,\infty} - \sqrt{\frac{k-1}{2k}}h_{k-1,\infty}\right)\left(1+\zeta^2\right)\right] \\ + \mathcal{O}\left(\frac{1}{r^3}\right). \quad (4.50) \end{aligned}$$

Since terms of order r^0 in our expression for m' will lead to a divergent mass (see section 4.8.2), we must have $f_1 = 0$, so that

$$\begin{aligned} m' = -\frac{f_2^2}{l^2 r^2} + \frac{\alpha^2}{r^2}\sum_{k=1}^{N-1}\left[\frac{k(k+1)\zeta^2}{4}\left(\frac{\omega_k^2}{k} - \frac{\omega_{k+1}^2}{k+1}\right)^2 + \frac{h_{k,1}^2}{2} + \frac{c_{k,1}^2}{2l^2}\left(1+\zeta^2\right)\right] \\ + \frac{\alpha^2}{r^2}\sum_{k=1}^{N-1}\left[\frac{\omega_{k,\infty}^2 l^2}{2}\left(\sqrt{\frac{k+1}{2k}}h_{k,\infty} - \sqrt{\frac{k-1}{2k}}h_{k-1,\infty}\right)^2\left(1+\zeta^2\right)\right] \\ + \mathcal{O}\left(\frac{1}{r^3}\right). \quad (4.51) \end{aligned}$$

Turning now to equation (4.18) we have

$$\begin{aligned} \sigma' = \frac{f_2^2}{r^5} + \frac{\left(1+\zeta^2\right)\alpha^2}{r^5}\sum_{k=1}^{N-1}\left[l^4\omega_{k,\infty}^2\left(\sqrt{\frac{k+1}{2k}}h_{k,\infty} - \sqrt{\frac{k-1}{2k}}h_{k-1,\infty}\right)^2\right] \\ + \frac{\left(1+\zeta^2\right)\alpha^2}{r^5}\sum_{k=1}^{N-1} c_{k,1}^2 + \mathcal{O}\left(\frac{1}{r^6}\right). \quad (4.52) \end{aligned}$$

Since the right hand side of (4.52) is of order r^{-5}, we must have $\sigma_1 = \sigma_2 = \sigma_3 = 0$.

Inserting our asymptotic expansions into (4.19) gives

$$\begin{aligned} f'' &= \frac{1}{r^4}\left(2f_2+\frac{3f_3}{r}\right)\left(4+\frac{2f_2}{r^2}\right) \\ &\quad +\frac{(1-\zeta^2)\,\alpha^2}{r^6}\sum_{k=1}^{N-1}\left[l^4\omega_{k,\infty}^2\left(\sqrt{\frac{k+1}{2k}}h_{k,\infty}-\sqrt{\frac{k-1}{2k}}h_{k-1,\infty}\right)^2-c_{k,1}^2\right] \\ &\quad +\mathcal{O}\left(\frac{1}{r^7}\right) \\ &= \frac{8f_2}{r^4}+\frac{12f_3}{r^5}+\mathcal{O}\left(\frac{1}{r^6}\right). \end{aligned} \tag{4.53}$$

Differentiating the asymptotic expression for f in (4.49) gives

$$f'' = 6f_2r^{-4}+12f_3r^{-5}+\mathcal{O}\left(r^{-6}\right). \tag{4.54}$$

Comparing (4.53, 4.54) yields $f_2=0$, but gives no constraint on f_3.

Finally, our Yang-Mills equation for ω_k reduces to

$$\frac{2c_{k,1}}{r^3}-\frac{2c_{k,1}}{r^3}+\mathcal{O}\left(\frac{1}{r^4}\right)=0. \tag{4.55}$$

The $\mathcal{O}(r^{-4})$ term relates $c_{k,1}$ to higher order terms in the expansion of ω_k, and hence we have no constraint on $c_{k,1}$. However, we require the gauge fields to be localized around the event horizon [38, 62], and hence it must be the case that ω_k approaches zero at infinity, i.e. $\omega_{k,\infty}=0$. The equation for h_k gives

$$h_k''=\frac{2h_{k,1}}{r^3}+\mathcal{O}\left(\frac{1}{r^4}\right), \tag{4.56}$$

and again we find no constraint on $h_{k,1}$.

The boundary conditions at infinity are therefore given by:

$$\begin{aligned}
\omega_k(r) &= \frac{c_{k,1}}{r} + \mathcal{O}\left(\frac{1}{r^2}\right), \\
h_k(r) &= h_{k,\infty} + \frac{h_{k,1}}{r} + \mathcal{O}\left(\frac{1}{r^2}\right), \\
f(r) &= 1 + \frac{f_3}{r^3} + \mathcal{O}\left(\frac{1}{r^4}\right), \\
m(r) &= m_0 - \frac{\alpha^2}{r}\sum_{k=1}^{N-1}\left[\frac{\omega_{k,\infty}^2 l^2}{2}\left(\sqrt{\frac{k+1}{2k}}h_{k,\infty} - \sqrt{\frac{k-1}{2k}}h_{k-1,\infty}\right)^2\left(1+\zeta^2\right)\right] \\
&\quad -\frac{\alpha^2}{r}\sum_{k=1}^{N-1}\left[\frac{k(k+1)\zeta^2}{4}\left(\frac{\omega_k^2}{k} - \frac{\omega_{k+1}^2}{k+1}\right)^2 + \frac{h_{k,1}^2}{2} + \frac{c_{k,1}^2}{2l^2}\left(1+\zeta^2\right)\right] + \mathcal{O}\left(\frac{1}{r^2}\right). \\
\sigma(r) &= 1 - \frac{(1+\zeta^2)}{4r^4}\alpha^2\sum_{k=1}^{N-1}\left[l^4\omega_{k,\infty}^2\left(\sqrt{\frac{k+1}{2k}}h_{k,\infty} - \sqrt{\frac{k-1}{2k}}h_{k-1,\infty}\right)^2\right] \\
&\quad -\frac{(1+\zeta^2)\,\alpha^2}{4r^4}\sum_{k=1}^{N-1}c_{k,1}^2 + \mathcal{O}\left(\frac{1}{r^5}\right).
\end{aligned} \tag{4.57}$$

§ 4.5 Trivial solutions

Although closed form solutions of the field equations (4.17–4.21) cannot be easily found in general, there are some "trivial" solutions. In this section we will find constraints on our variables that will reduce our line element (4.8) to those of the planar Schwarzschild-AdS and planar Reissner-Nordström-AdS, the free energy of which will be of particular interest in section 4.8.2. We will also embed the $\mathfrak{su}(2)$ solutions of [62] into our $\mathfrak{su}(N)$ framework.

4.5.1 Planar Schwarzschild-AdS

The line element for the planar Schwarzschild-AdS solution is given by [75]

$$ds^2 = -\left(-\frac{2m_0}{r} - \frac{\Lambda r^2}{3}\right)dt^2 + r^2dx^2 + r^2dy^2 + \left(-\frac{2m_0}{r} - \frac{\Lambda r^2}{3}\right)^{-1}dr^2, \tag{4.58}$$

where the mass m_0 is a constant. To obtain this solution, we set $f = \sigma = 1$, remove the electric field (i.e. set $h_k = 0$ for all k), and require that $m' = 0$. Since the planar Schwarzschild-AdS solution is isotropic in x and y we will also take $\zeta = 1$.

Equation (4.17) then implies

$$\sum_{k=1}^{N-1}\left[\frac{k(k+1)}{4r^2}\left(\frac{\omega_k^2}{k}-\frac{\omega_{k+1}^2}{k+1}\right)^2+\mu\omega_k'^2\right]=0. \tag{4.59}$$

Therefore it must be the case that $\omega_k'=0$ and

$$\sum_{k=1}^{N-1}\frac{k(k+1)}{4r^2}\left(\frac{\omega_k^2}{k}-\frac{\omega_{k+1}^2}{k+1}\right)^2=0, \tag{4.60}$$

which can be solved by taking $\omega_k=\pm A\sqrt{k}$ for some constant A, where A is the same for all k. In the spherically symmetric case, the constant A is fixed by the field equations, although in this case we have more freedom and we find that A is arbitrary due to scaling symmetries discussed later. We note that with $h_k=0$ for all k, and with constant ω_k, f and σ, all other field equations (4.18–4.21) vanish identically.

4.5.2 Planar Reissner-Nordström-AdS

The line element for the planar Reissner-Nordström-AdS black hole is given by [22]

$$ds^2=-\mu_{RN}dt^2+r^2dx^2+r^2dy^2+\mu_{RN}^{-1}dr^2, \tag{4.61}$$

where

$$\mu_{RN}=-\frac{2m_0}{r}+\frac{\alpha_{RN}^2q^2}{r^2}-\frac{\Lambda r^2}{3}, \tag{4.62}$$

and where both the mass m_0 and charge q are constant. Again we set $f=\sigma=1$, but in this case we set $\omega_k=0$ for all k. Equation (4.20) then reduces to

$$h_k''=-\frac{2h_k'}{r}\qquad\Rightarrow\qquad h_k=b_k-\frac{a_k}{r}, \tag{4.63}$$

by direct integration, with constants of integration a_k and b_k. Equation (4.17) becomes

$$m'=\alpha_{RN}^2\sum_{k=1}^{N-1}\frac{r^2h_k'^2}{2}=\frac{\alpha_{RN}^2}{2r^2}\sum_{k=1}^{N-1}a_k^2 \tag{4.64}$$

so that

$$m=m_0-\frac{\alpha_{RN}^2}{2r}\sum_{k=1}^{N-1}a_k^2. \tag{4.65}$$

Substituting this into the metric function (4.9) gives

$$\mu = -\frac{2m_0}{r} + \frac{\alpha_{RN}^2}{r^2}\sum_{k=1}^{N-1} a_k^2 - \frac{\Lambda r^2}{3}, \tag{4.66}$$

and by comparison with (4.62)

$$q^2 = \sum_{k=1}^{N-1} a_k^2 = \sum_{k=1}^{N-1} h_k'^2 r^4 \qquad \Rightarrow \qquad q = \sqrt{\sum_{k=1}^{N-1} h_k'^2 r^4}. \tag{4.67}$$

4.5.3 Embedded $\mathfrak{su}(2)$ solutions

To obtain embedded $\mathfrak{su}(2)$ solutions we start by setting

$$\omega_k = A_k \omega, \qquad\qquad h_k = B_k h, \tag{4.68}$$

where $\omega = \omega(r)$, $h = h(r)$, and A_k and B_k are constants. Substituting into the Einstein equations (4.17–4.19), and comparing with the $N = 2$ case, we require

$$\begin{aligned}\sum_{k=1}^{N-1} A_k^2 \left(\sqrt{\frac{k+1}{2k}} B_k - \sqrt{\frac{k-1}{2k}} B_{k-1}\right)^2 &= \sum_{k=1}^{N-1} A_k^2 \\ &= \sum_{k=1}^{N-1} B_k^2 = \sum_{k=1}^{N-1} \frac{k(k+1)}{2}\left(\frac{A_k^2}{k} - \frac{A_{k+1}^2}{k+1}\right)^2.\end{aligned} \tag{4.69}$$

Substituting (4.68) into the Yang-Mills equations (4.20, 4.21), we require

$$\begin{aligned} 1 &= \left(\sqrt{\frac{k+1}{2k}} B_k - \sqrt{\frac{k-1}{2k}} B_{k-1}\right)^2 = \frac{2A_k^2 - A_{k+1}^2 - A_{k-1}^2}{2} \\ &= \frac{\sqrt{2k(k+1)}}{2}\frac{A_{k+1}^2}{k+1}\left(\sqrt{\frac{k}{2(k+1)}} - \sqrt{\frac{k+2}{2(k+1)}}\frac{B_{k+1}}{B_k}\right) \\ &\quad + \frac{\sqrt{2k(k+1)}}{2}\frac{A_k^2}{k}\left(\sqrt{\frac{k+1}{2k}} - \sqrt{\frac{k-1}{2k}}\frac{B_{k-1}}{B_k}\right) \end{aligned} \tag{4.70}$$

to recover the $N = 2$ case. We can solve both (4.69) and (4.70) by taking

$$A_k = \sqrt{k(N-k)}, \qquad B_k = \sqrt{\frac{k(k+1)}{2}}. \tag{4.71}$$

If we substitute our expressions (4.68) and (4.71) into the field equations (4.20, 4.21) and (4.17–4.19), and then rescale the variables as follows

$$R = \lambda_N^{-1} r, \quad \tilde{m} = \lambda_N^{-1} m, \quad \tilde{h} = \lambda_N h, \quad \tilde{\Lambda} = \lambda_N^2 \Lambda, \tag{4.72}$$

where

$$\lambda_N^2 = \sum_{k=1}^{N-1} A_k^2 = \sum_{k=1}^{N-1} k(N-k) = \frac{1}{6} N(N^2-1), \tag{4.73}$$

we find that the field equations are

$$\begin{aligned}
\frac{d\tilde{m}}{dR} &= \frac{\mu R^2}{2f^2}\left(\frac{df}{dR}\right)^2 + \alpha^2\left\{\frac{\omega^2\tilde{h}^2}{2\sigma^2\mu}\left(\frac{1}{f^2}+\zeta^2 f^2\right) + \frac{R^2}{2\sigma^2}\left(\frac{d\tilde{h}}{dR}\right)^2\right\} \\
&\quad +\alpha^2\left\{\frac{\zeta^2\omega^4}{2R^2} + \frac{\mu}{2}\left(\frac{dw}{dR}\right)^2\left(\frac{1}{f^2}+\zeta^2 f^2\right)\right\}, \qquad (4.74) \\
\frac{d\sigma}{dR} &= \frac{R\sigma}{f^2}\left(\frac{df}{dR}\right)^2 + \alpha^2\left\{\left(\frac{1}{f^2}+\zeta^2 f^2\right)\left(\frac{\omega^2\tilde{h}^2}{R\sigma\mu^2} + \frac{\sigma}{R}\left(\frac{d\omega}{dR}\right)^2\right)\right\}, \qquad (4.75) \\
\frac{d^2 f}{dR^2} &= \alpha^2\left(\frac{1}{f^2}-\zeta^2 f^2\right)\left\{\frac{\omega^2 h^2}{\sigma^2\mu^2 R^2} - \frac{1}{R^2}\left(\frac{d\omega}{dR}\right)^2\right\} \\
&\quad -\frac{df}{dR}\left(\frac{1}{\sigma}\frac{d\sigma}{dR} + \frac{1}{\mu}\frac{d\mu}{dR} + \frac{2}{R} - \frac{1}{f}\frac{df}{dR}\right), \qquad (4.76) \\
\frac{d^2\tilde{h}}{dR^2} &= \frac{d\tilde{h}}{dR}\left(\frac{1}{\sigma}\frac{d\sigma}{dR} - \frac{2}{R}\right) + \frac{\tilde{h}\omega^2}{\mu R^2}\left(\frac{1}{f^2}+\zeta^2 f^2\right), \qquad (4.77) \\
0 &= \frac{d^2\omega}{dR^2} + \frac{d\omega}{dR}\left(\frac{1}{\sigma}\frac{d\sigma}{dR} + \frac{1}{\mu}\frac{d\mu}{dR} - \frac{2}{f}\frac{df}{dR}\right) + \frac{\omega}{\mu}\left(\frac{\tilde{h}^2}{\sigma^2\mu} - \frac{\zeta^2\omega^2 f^2}{R^2}\right), \qquad (4.78)
\end{aligned}$$

which are precisely the $\mathfrak{su}(2)$ field equations in terms of the new variables.

§ 4.6 Scaling symmetries

The Einstein-Yang-Mills equations (4.17–4.21) possess several scaling symmetries [62], and these can be used to reduce the number of numerically relevant parameters. We first notice that the equations are invariant under the transformations;

$$r \to \lambda r, \quad m \to \lambda m, \quad l \to \lambda l, \quad h_k \to \lambda^{-1} h_k, \quad \alpha \to \lambda\alpha. \tag{4.79}$$

Hence by transforming the variables using $\lambda = \alpha^{-1}$ we can effectively set $\alpha = 1$. The second set of transformations under which the field equations remain invariant is

$$r \to \lambda r, \quad \omega_k \to \lambda\omega_k, \quad h_k \to \lambda h_k, \quad m \to \lambda^3 m, \tag{4.80}$$

in which case μ transforms to $\lambda^2\mu$. We can use this symmetry to remove r_h from the equations by setting $\lambda = r_h^{-1}$. We then have two remaining symmetries, the first of which is

$$h_k \to \lambda h_k, \qquad \sigma \to \lambda\sigma, \tag{4.81}$$

which can be used to set $\sigma(\infty) = 1$ by taking $\lambda = \sigma(\infty)^{-1}$, and $\omega_k \to -\omega_k$, which means that we can restrict our attention to $\omega(r_h) > 0$ without loss of generality.

The overall transformations are

$$\begin{gathered} r \to \bar{r} = \alpha^{-1} r_h^{-1} r, \quad l \to \bar{l} = \alpha^{-1} l, \quad \alpha \to \bar{\alpha} = 1, \\ \sigma \to \bar{\sigma} = \sigma(\infty)^{-1}\sigma, \quad \omega_k \to \bar{\omega}_k = r_h^{-1}\omega_k, \quad \mu \to \bar{\mu} = r_h^{-2}\mu, \\ m \to \bar{m} = \alpha^{-1} r_h^{-3} m, \quad h_k \to \bar{h}_k = \alpha r_h^{-1}\sigma(\infty)^{-1} h_k, \end{gathered} \tag{4.82}$$

with f unchanged. The field equations then become:

$$\begin{aligned} \bar{h}_k'' &= \bar{h}_k' \left(\frac{\bar{\sigma}'}{\bar{\sigma}} - \frac{2}{\bar{r}} \right) \\ &\quad + \frac{\sqrt{2k(k+1)}}{2\bar{\mu}\bar{r}^2} \frac{\bar{\omega}_k^2}{k} \left(\sqrt{\frac{k+1}{2k}} \bar{h}_k - \sqrt{\frac{k-1}{2k}} \bar{h}_{k-1} \right) \left(\frac{1}{f^2} + \zeta^2 f^2 \right) \\ &\quad + \frac{\sqrt{2k(k+1)}}{2\bar{\mu}\bar{r}^2} \frac{\bar{\omega}_{k+1}^2}{k+1} \left(\sqrt{\frac{k}{2(k+1)}} \bar{h}_k - \sqrt{\frac{k+2}{2(k+1)}} \bar{h}_{k+1} \right) \left(\frac{1}{f^2} + \zeta^2 f^2 \right), \end{aligned} \tag{4.83}$$

$$\begin{aligned} 0 &= \bar{\omega}_k'' + \bar{\omega}_k' \left(\frac{\bar{\sigma}'}{\bar{\sigma}} + \frac{\bar{\mu}'}{\bar{\mu}} - \frac{2f'}{f} \right) + \frac{\bar{\omega}_k}{\bar{\sigma}^2\bar{\mu}^2} \left(\sqrt{\frac{k+1}{2k}} \bar{h}_k - \sqrt{\frac{k-1}{2k}} \bar{h}_{k-1} \right)^2 \\ &\quad + \frac{\zeta^2 f^2 \bar{\omega}_k^2}{2\bar{\mu}\bar{r}^2} \left(\bar{\omega}_{k-1}^2 - 2\bar{\omega}_k^2 + \bar{\omega}_{k+1}^2 \right), \end{aligned} \tag{4.84}$$

$$\begin{aligned} \bar{m}' &= \frac{\bar{\mu}\bar{r}^2 f'^2}{2f^2} + \sum_{k=1}^{N-1} \left\{ \frac{\bar{\omega}_k^2}{2\bar{\sigma}^2\bar{\mu}} \left(\sqrt{\frac{k+1}{2k}} \bar{h}_k - \sqrt{\frac{k-1}{2k}} \bar{h}_{k-1} \right)^2 \left(\frac{1}{f^2} + \zeta^2 f^2 \right) \right\} \\ &\quad + \sum_{k=1}^{N-1} \left\{ \frac{\bar{r}^2 \bar{h}_k'^2}{2\bar{\sigma}^2} + \frac{\bar{\mu}\bar{\omega}_k'^2}{2} \left(\frac{1}{f^2} + \zeta^2 f^2 \right) + \frac{k(k+1)\zeta^2}{4\bar{r}^2} \left(\frac{\bar{\omega}_k^2}{k} - \frac{\bar{\omega}_{k+1}^2}{k+1} \right)^2 \right\}, \end{aligned} \tag{4.85}$$

$$\begin{aligned}
\bar{\sigma}' &= \frac{\bar{r}\bar{\sigma}f'^2}{f^2} + \sum_{k=1}^{N-1}\left\{\frac{\bar{\omega}_k^2}{2\bar{\sigma}\bar{\mu}^2\bar{r}}\left(\sqrt{\frac{k+1}{2k}}\bar{h}_k - \sqrt{\frac{k-1}{2k}}\bar{h}_{k-1}\right)^2\left(\frac{1}{f^2}+\zeta^2 f^2\right)\right\} \\
&\quad + \sum_{k=1}^{N-1}\left\{\frac{\bar{\sigma}\bar{\omega}_k'^2}{\bar{r}}\left(\frac{1}{f^2}+\zeta^2 f^2\right)\right\}, \qquad (4.86)\\
f'' &= \left(\frac{1}{f^2}-\zeta^2 f^2\right)\sum_{k=1}^{N-1}\left\{\frac{2\bar{\omega}_k^2\bar{h}_k^2}{k(k+1)\bar{\sigma}^2\bar{\mu}^2\bar{r}^2} - \frac{\bar{\omega}_k'^2}{\bar{r}^2}\right\} - f'\left(\frac{\bar{\sigma}'}{\bar{\sigma}} + \frac{\bar{\mu}'}{\bar{\mu}} + \frac{2}{\bar{r}} - \frac{f'}{f}\right), \qquad (4.87)
\end{aligned}$$

with boundary conditions at the event horizon:

$$\begin{aligned}
\bar{m}(\bar{r}) &= \frac{1}{2\bar{l}^2} + \bar{m}'(1)(\bar{r}-1) + \mathcal{O}(\bar{r}-1)^2,\\
\bar{\omega}_k(\bar{r}) &= \bar{\omega}_k(1) + \bar{\omega}_k'(1)(\bar{r}-1) + \mathcal{O}(\bar{r}-1)^2,\\
f(\bar{r}) &= f(1) + \mathcal{O}(\bar{r}-1)^2,\\
\bar{\sigma} &= \bar{\sigma}(1) + \bar{\sigma}'(1)(\bar{r}-1) + \mathcal{O}(\bar{r}-1)^2,\\
\bar{h}_k(\bar{r}) &= \bar{h}_k'(1)(\bar{r}-1) + \mathcal{O}(\bar{r}-1)^2, \qquad (4.88)
\end{aligned}$$

where

$$\begin{aligned}
\bar{\omega}_k'(1) &= \frac{\zeta^2\bar{l}^2 f(1)^2\bar{\omega}_k(1)\left(2\bar{\omega}_k(1)^2 - \bar{\omega}_{k-1}(1)^2 - \bar{\omega}_{k+1}(1)^2\right)}{2\left(3-2\bar{m}'(1)\bar{l}^2\right)},\\
\bar{m}'(1) &= \alpha^2\sum_{k=1}^{N-1}\left\{\frac{\bar{h}_k'^2}{2\bar{\sigma}(1)^2} + \frac{k(k+1)\zeta^2}{4}\left(\frac{\bar{\omega}_k(1)^2}{k} - \frac{\bar{\omega}_{k+1}(1)^2}{k+1}\right)^2\right\},\\
\bar{\sigma}'(1) &= \left(\frac{1}{f(1)}+\zeta^2 f(1)^2\right)\sum_{k=1}^{N-1}\left[\frac{2\bar{\omega}_k(1)^2\bar{h}_k'(1)^2\bar{l}^4}{k(k+1)\bar{\sigma}(1)\left(3-2\bar{m}'(1)\bar{l}^2\right)^2}\right]\\
&\quad + \left(\frac{1}{f(1)}+\zeta^2 f(1)^2\right)\sum_{k=1}^{N-1}\bar{\sigma}(1)\bar{\omega}_k'(1)^2. \qquad (4.89)
\end{aligned}$$

In (4.83–4.89), all quantities are functions of the new radial co-ordinate $\bar{r}$, and a prime now denotes differentiation with respect to $\bar{r}$. For the remainder of this chapter we shall assume that the variables have been rescaled in this way, i.e. so that $r_h = \alpha = \sigma(\infty) = 1$, although we will revert to the original notation, i.e. in subsequent sections we will denote $\bar{\omega}_k$ simply as ω_k etc.

§ 4.7 Solutions of the field equations

In this section, and for the rest of the chapter, we consider the $f = \zeta = 1$ case, since we do not find genuinely $\mathfrak{su}(N)$ solutions for $\zeta = 0$. The field equations are then given by

$$\begin{aligned}
m' &= \alpha^2 \sum_{k=1}^{N-1} \left\{ \frac{\omega_k^2}{\sigma^2 \mu} \left(\sqrt{\frac{k+1}{2k}} h_k - \sqrt{\frac{k-1}{2k}} h_{k-1} \right)^2 \right\} \\
&\quad + \alpha^2 \sum_{k=1}^{N-1} \left\{ \frac{r^2 h_k'^2}{2\sigma^2} + \mu \omega_k'^2 + \frac{k(k+1)}{4r^2} \left(\frac{\omega_k^2}{k} - \frac{\omega_{k+1}^2}{k+1} \right)^2 \right\}, \qquad (4.90) \\
\sigma' &= \alpha^2 \sum_{k=1}^{N-1} \left\{ \frac{2\omega_k^2}{\sigma \mu^2 r} \left(\sqrt{\frac{k+1}{2k}} h_k - \sqrt{\frac{k-1}{2k}} h_{k-1} \right)^2 + \frac{2\sigma \omega_k'^2}{r} \right\}, \qquad (4.91) \\
h_k'' &= h_k' \left(\frac{\sigma'}{\sigma} - \frac{2}{r} \right) \\
&\quad + \frac{\sqrt{2k(k+1)}}{\mu r^2} \frac{\omega_k^2}{k} \left(\sqrt{\frac{k+1}{2k}} h_k - \sqrt{\frac{k-1}{2k}} h_{k-1} \right) \\
&\quad + \frac{\sqrt{2k(k+1)}}{\mu r^2} \frac{\omega_{k+1}^2}{k+1} \left(\sqrt{\frac{k}{2(k+1)}} h_k - \sqrt{\frac{k+2}{2(k+1)}} h_{k+1} \right), \qquad (4.92) \\
0 &= \omega_k'' + \omega_k' \left(\frac{\sigma'}{\sigma} + \frac{\mu'}{\mu} \right) + \frac{\omega_k}{\sigma^2 \mu^2} \left(\sqrt{\frac{k+1}{2k}} h_k - \sqrt{\frac{k-1}{2k}} h_{k-1} \right)^2 \\
&\quad + \frac{\omega_k}{2\mu r^2} \left(\omega_{k-1}^2 - 2\omega_k^2 + \omega_{k+1}^2 \right). \qquad (4.93)
\end{aligned}$$

The field equations (4.90–4.93) cannot be solved analytically. To solve them numerically, we first decouple the second order differential equations for h_k'' (4.92) and ω_k'' (4.93) into first order ODEs in h_k, h_k', ω_k and ω_k'. We then have a set of $4N - 2$ first order ODEs. We solve these numerically using a Bulirsch-Stoer algorithm in C++ [32], and we use the scaling symmetries from section 4.6 to reduce the number of parameters. Since the field equations diverge at the event horizon where $\mu = 0$, we start at $r - 1 = 10^{-7}$, using the boundary conditions (4.88) to give our initial values, and integrate outwards using (4.90–4.93). We have $r_h = 1$ using the scaling symmetries from section 4.6, and we require $\sigma(\infty) = 1$ for the space-time to be asymptotically AdS. However, since the field equations are invariant under $\sigma \to \lambda\sigma$, $h_k \to \lambda h_k$, numerically we take $\sigma(1) = 1$, and then rescale σ and h_k by

$\sigma(\infty)^{-1}$ after we have performed the integration. The solutions are then uniquely determined by $h_k'(1)$, $\omega_k(1)$ and Λ.

Our variables have regular expansions at infinity given by (4.57), so we can stop integrating outwards when our variables have converged. In the results presented below we have used a relative convergence criterion of 10^{-7} in the quantities h_k, $h_k' r^2$, ω_k and $\omega_k' r^2$, i.e. for a step size r_{step}, our final value of r, r_f, will be such that $h_k(r_f)$ differs from $h_k(r_f - r_{step})$ by a factor of less than 10^{-7}, and similarly for the other quantities.

In the $\mathfrak{su}(2)$ case, the equation of motion for h is given by

$$h'' = h' \left(\frac{\sigma'}{\sigma} - \frac{2}{r} \right) + \frac{2h\omega^2}{\mu r^2}. \tag{4.94}$$

Since $\mu > 0$ when $r > 1$, at a stationary point $h' = 0$ it must be the case that h'' has the same sign as h. Therefore if h is positive, stationary points can only be minima, and if h is negative stationary points must be maxima. Hence we conclude that h is monotonic and zero only at the event horizon. We find numerically that this is also the case for larger gauge groups, and therefore label solutions by the number of nodes in ω_k. Note that we are interested in nodeless solutions as these have lower free energy (see section 4.8.2), and which are localized around the horizon (ω_k approaches zero at large r, see section 4.4.2).

Figures 4.1 and 4.2 show phase space plots for $\mathfrak{su}(2)$ solutions with $\Lambda = -0.6$ and $\Lambda = -0.3$ respectively, colour coded by the number of nodes n in the gauge field function ω. The red "no solution" region is where the condition for a non-extremal event horizon (4.40) is satisfied, but we do not find black hole solutions. We are interested in nodeless solutions where the gauge field function goes to zero at infinity, which is on the border between the green $n = 0$ and blue $n = 1$ regions. We also find solutions for which the gauge field function goes to zero at large r on the border between the blue $n = 1$ and purple $n = 2$ regions in figure 4.2, but these have a node and therefore higher free energy (see section 4.8.2). These solutions with a node only exist below a certain value of $|\Lambda|$, and similarly, if $|\Lambda|$ is too high we find only nodeless solutions [12], in which case we cannot find solutions for which ω goes to zero at large r.

Figure 4.3 shows a phase space plot for $\mathfrak{su}(3)$ solutions with $\Lambda = -0.1$ and $\omega_1(r_h) = \omega_2(r_h) = 0.1$. The plot is colour coded by the number of nodes in the gauge field functions, where n_1 is the number of nodes in ω_1, and n_2 is the number

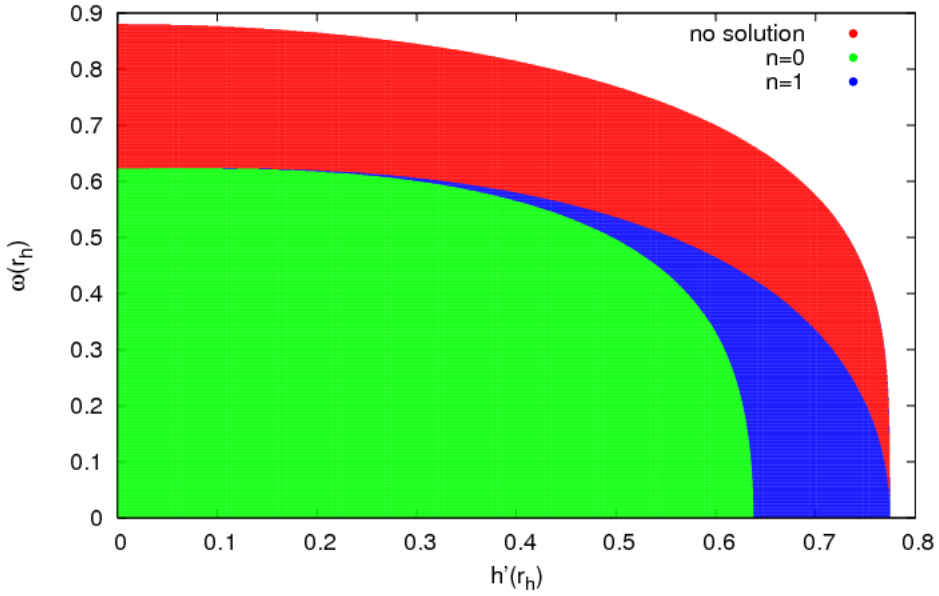

Figure 4.1: Phase space plot for $\mathfrak{su}(2)$ planar black holes with $\Lambda = -0.6$, colour coded by the number of nodes in the gauge field function. The red "no solution" region is where the condition (4.40) is satisfied but we do not find black hole solutions. We are interested in solutions which are nodeless, but where ω tends to zero at large r, which lie on the border between the green $n = 0$ and blue $n = 1$ regions.

of nodes in ω_2. The point where both ω_1 and ω_2 go to zero, and where ω_1 and ω_2 have no nodes, is where the green $(n_1 = n_2 = 0)$, blue $(n_1 = 0,\ n_2 = 1)$, yellow $(n_1 = 0,\ n_2 = 1)$ and black $(n_1 = n_2 = 1)$ regions meet, which is marked with a red cross. Again we find continuous ranges of $\omega_1(r_h)$ and $\omega_2(r_h)$ that give these solutions, with a unique value of $(h_1'(r_h), h_2'(r_h))$ associated with each $(\omega_1(r_h), \omega_2(r_h))$. Figure 4.4 shows a similar plot, but this time with $\Lambda = -0.03$. Again the solution where ω_1 and ω_2 go to zero at infinity and are nodeless is marked with a red cross, which is where the green $(n_1 = n_2 = 0)$, blue $(n_1 = 0,\ n_2 = 1)$, orange $(n_1 = 0,\ n_2 = 1)$ and grey $(n_1 = n_2 = 1)$ regions meet. As in the $\mathfrak{su}(2)$ case we note that there are more solutions with nodes at lower $|\Lambda|$.

Since the relevant solutions are those in which ω_k goes to zero at large r for all k [62], we use the GSL multidimensional root finder [2] to find these solutions. At fixed cosmological constant Λ, this involves a Newton iterative procedure, using a numerical estimate of the Jacobian, over values of $h_k'(r_h)$ to ensure $\omega_k(\infty) = 0$ for all k. We find solutions in which the gauge field functions ω_k have no nodes, as well

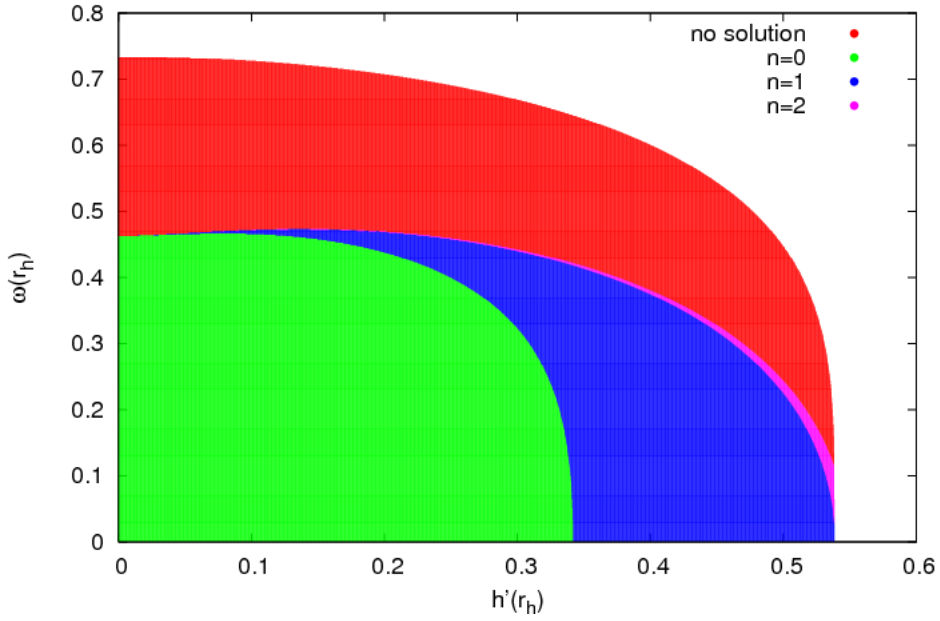

Figure 4.2: Phase space plot for $\mathfrak{su}(2)$ planar black holes with $\Lambda = -0.3$, colour coded by the number of nodes in the gauge field function. The red "no solution" region is where the condition (4.40) is satisfied but we do not find black hole solutions. We are interested in solutions which are nodeless, but where ω tends to zero at large r, which lie on the border between the green $n = 0$ and blue $n = 1$ regions.

as solutions that have nodes, and that those with nodes have higher free energy and are ignored here. However, since the root finder does not find solutions for which the gauge field functions go exactly to zero at large r, rather to small (positive or negative) values due to numerical error, we are looking not only for gauge field functions ω_k with no nodes, but also those with one node, a small negative value at infinity and a negative gradient at infinity (since we are considering only positive $\omega_k(r_h)$).

We note that, for a given value of Λ, there is a continuous range of values of $\omega_k(r_h)$ for which ω_k approach zero at large r, and that for each $\omega_k(r_h)$ there is a unique value of $h'_k(r_h)$ for each k that gives $\omega_k(\infty) = 0$. Figure 4.5 shows such a solution for $\mathfrak{su}(2)$ black holes with $\Lambda = -0.03$, $\omega(r_h) = 0.1$, where $h'(r_h)$ has been chosen such that ω goes to zero at large r. Figure 4.6 shows a solution for $\mathfrak{su}(3)$ black holes with $\omega_1(r_h) = 0.15$, $\omega_2(r_h) = 0.1$, where ω_1 and ω_2 approach zero at large r. As noted above, h_1 and h_2 are monotonically increasing functions of r.

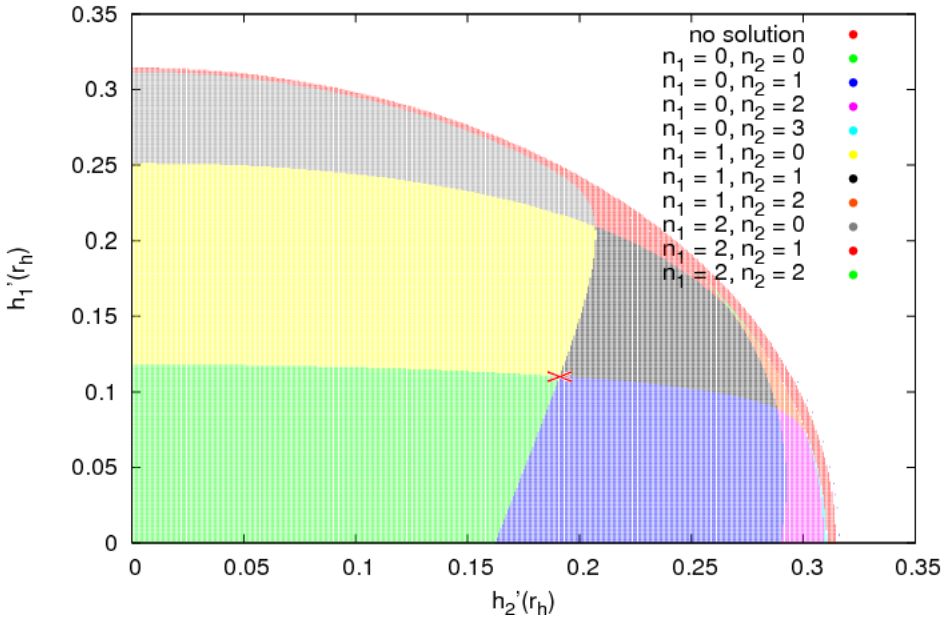

Figure 4.3: Phase space plot for $\mathfrak{su}(3)$ planar black holes with $\Lambda = -0.1$ and $\omega_1(r_h) = \omega_2(r_h) = 0.1$, colour coded by the number of nodes in the gauge field functions ω_1 and ω_2. In the red "no solution" region the constraint (4.40) is satisfied but we do not find black hole solutions. The nodeless solution where ω_1 and ω_2 go to zero at large r is marked with a red cross.

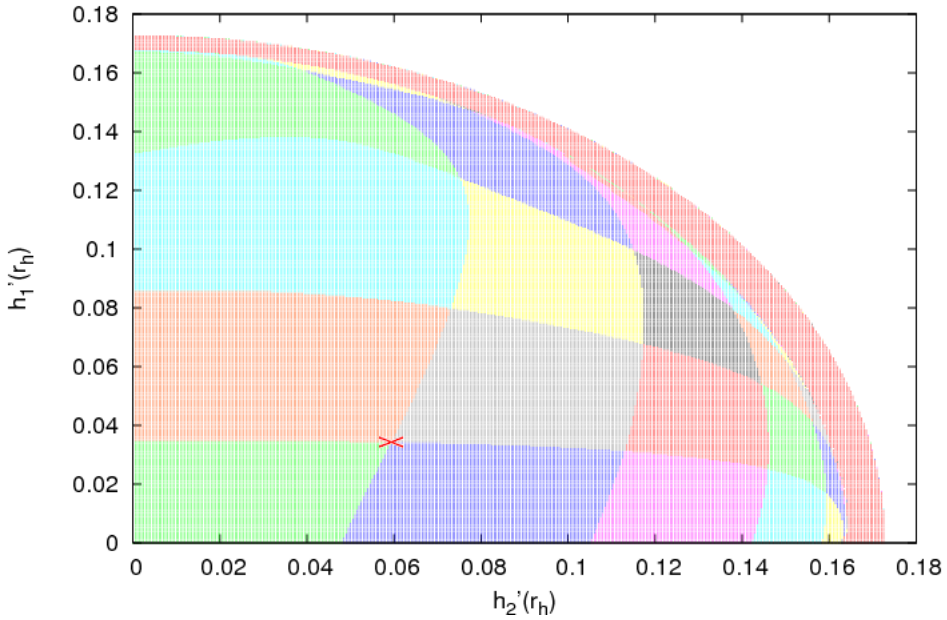

Figure 4.4: Phase space plot for $\mathfrak{su}(3)$ planar black holes with $\Lambda = -0.03$ and $\omega_1(r_h) = \omega_2(r_h) = 0.1$, colour coded by the number of nodes in the gauge field functions ω_1 and ω_2. In the red "no solution" region the constraint (4.40) is satisfied but we do not find black hole solutions. The nodeless solution where ω_1 and ω_2 go to zero at large r is marked with a red cross.

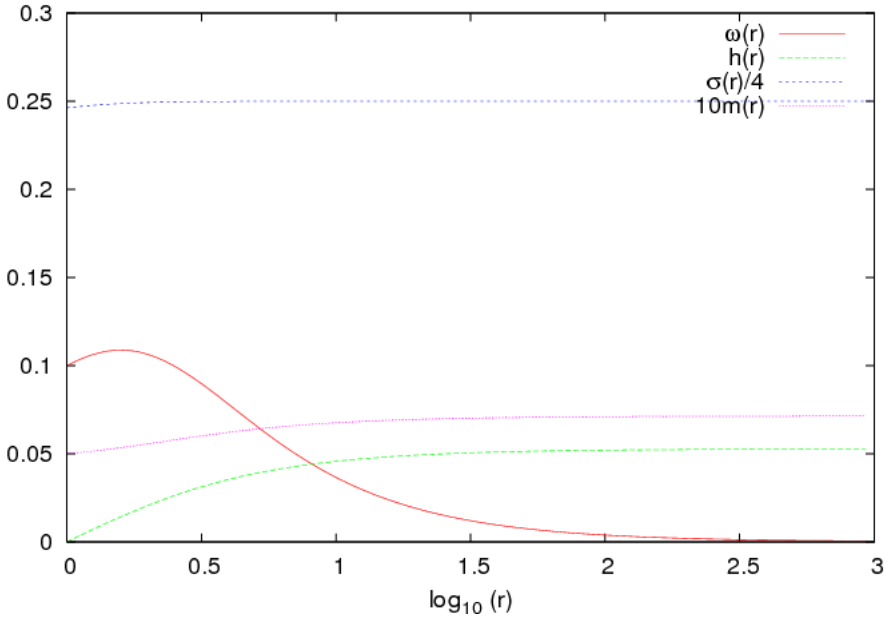

Figure 4.5: Plot of $\mathfrak{su}(2)$ solution with $\Lambda = -0.03$, $\omega(r_h) = 0.1$. The value of $h'(r_h)$ is such that ω goes to zero at large r. As expected, $h(r)$ is monotonically increasing.

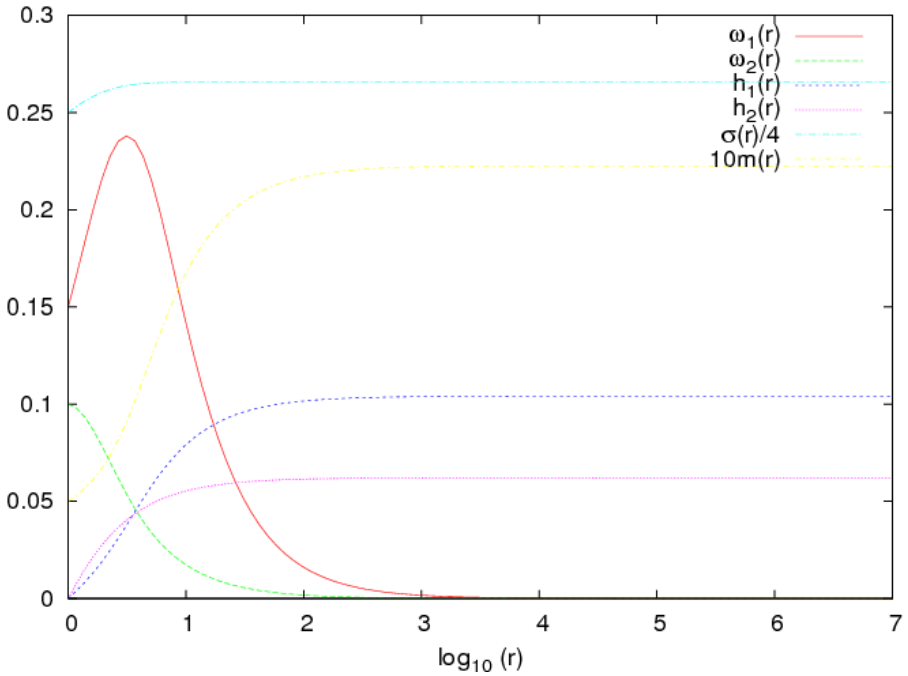

Figure 4.6: Plot of $\mathfrak{su}(3)$ solution with $\Lambda = -0.03$. the values of $h_1'(r_h)$ and $h_2'(r_h)$ are such that ω_1 and ω_2 go to zero at large r. We note that, as in the $\mathfrak{su}(2)$ case, $h_1(r)$ and $h_2(r)$ are monotonically increasing.

§ 4.8 Physical quantities

In this section we calculate the physical quantities associated with our gauge field. Our $\mathfrak{su}(N)$ gauge field carries $N-1$ conserved electric charges, and we find expressions for them in section 4.8.1. We then go on to calculate the thermodynamic quantities associated with our black hole in section 4.8.2, in particular the Hawking temperature, which plays the role of the temperature in our superconducting field theory, and the free energy, which tells us whether the superconducting state is thermodynamically favoured over the normal state.

4.8.1 Electric charges

In chapter 2 we found magnetic charges associated with an $\mathfrak{su}(N)$ gauge field using the field strength tensor $F_{\mu\nu}$. In this section we use the same method to find electric charges, using the Hodge dual of the field strength tensor $*F_{\mu\nu}$. Since the Lie algebra $\mathfrak{su}(N)$ has rank $N-1$ we have $N-1$ gauge invariant electric charges Q_j associated with the gauge potential (4.14) (see chapter 2), which we define by [27, 69]

$$Q_j = \frac{1}{4\pi} \sup_{g(x)} k \left(X, \int_{\Sigma_\infty} g^{-1} * F g \right), \tag{4.95}$$

where the supremum is taken over all possible gauge transformations $g(x)$. As in chapter 2, X is an element of the Cartan subalgebra of $\mathfrak{su}(N)$, the integral is taken over a surface at spatial infinity denoted Σ_∞, and the dual field strength is given by

$$* F = *F_{\mu\nu} dx^\mu \wedge dx^\nu = \frac{r^2 \sigma}{2} \epsilon_{\mu\nu\alpha\beta} F^{\alpha\beta} dx^\mu \wedge dx^\nu = -r^2 \sigma \sum_{k=1}^{N-1} h_k' H_k \, dx \wedge dy, \tag{4.96}$$

on Σ_∞ (at $r = \infty$), since our field strength is time independent and $dr = 0$ on Σ_∞.

The integrand in (4.95) takes its maximal value when $g^{-1} * F g$ is a member of the Cartan subalgebra [27], but since $*F$ is already in the Cartan subalgebra there is no need to perform a gauge transformation to find the supremum. Although we can choose any elements of the Cartan subalgebra to substitute for X, corresponding to a choice of basis, a natural choice is to take the $N-1$ diagonal generators of the Cartan subalgebra H_k, in which case we find

$$Q_j \propto A_0 \lim_{r \to \infty} \sigma(r) r^2 h_j'(r), \tag{4.97}$$

where A_0 is the unit area of Σ_∞, and we are free to choose the normalization. We will use the convention of [62] and define

$$Q_j = \frac{q_j}{g} = \frac{1}{g}\lim_{r\to\infty} r^2 h_j'(r). \tag{4.98}$$

We will also define a total effective charge by analogy with (4.67) as

$$Q^2 = \frac{q^2}{g} = \frac{1}{g}\sum_{j=1}^{N-1} q_j^2. \tag{4.99}$$

In general the magnetic part of the gauge field also carries $N-1$ conserved charges. For planar black holes the expressions for these charges are given by

$$Q_k = \frac{\sqrt{2k(k+1)}}{2}\left(\frac{\omega_{k+1}(\infty)^2}{k+1} - \frac{\omega_k(\infty)^2}{k}\right), \tag{4.100}$$

which is the same as chapter 2, but again replacing 1 with 0. However, since we are considering solutions in which the ω_k go to zero at large r for all k, we find that all the magnetic charges are zero.

4.8.2 Thermodynamic quantities

We use the counterterm formalism of Balasubramanian and Kraus [4] to define a "quasilocal stress tensor" on the boundary, given by

$$T_B^{\mu\nu} = \frac{2}{\sqrt{-\gamma}}\frac{\delta S_{grav}}{\delta \gamma_{\mu\nu}}, \tag{4.101}$$

where the gravitational action $S_{grav} = S_{grav}(\gamma_{\mu\nu})$ is viewed as being a function of the boundary metric $\gamma_{\mu\nu}$. In AdS space the stress tensor typically diverges as the boundary is taken to infinity. However, we are free to add boundary terms S_{ct} to the action, as these do not alter the equations of motion in the bulk. We then need to vary the action with respect to the boundary metric. Since we are considering solutions to the equations of motion, only the boundary term contributes and the quasilocal stress tensor is given by [4]

$$T_B^{\mu\nu} = \frac{1}{2}\left(\Theta^{\mu\nu} - \Theta\gamma^{\mu\nu} - \frac{2}{l}\gamma^{\mu\nu} - lG^{\mu\nu}\right), \tag{4.102}$$

where $\gamma^{\mu\nu}$ is the boundary metric, $G^{\mu\nu}$ is the Einstein tensor on the boundary, and the extrinsic curvature $\Theta^{\mu\nu}$ is given by [4]

$$\Theta^{\mu\nu} = -\frac{1}{2}\left(\nabla^{\mu}\hat{n}^{\nu} + \nabla^{\nu}\hat{n}^{\mu}\right), \tag{4.103}$$

where $\hat{n}^{\mu}$ is the outward pointing normal to surfaces of constant r.

The boundary surface Σ_{∞} is a surface of constant r, in the limit where r is taken to infinity. We can then define a divergence free-mass by

$$\begin{aligned} M &= \int_{\Sigma_{\infty}} lrT_{tt}\, dx\, dy \qquad (4.104)\\ &= \frac{1}{4\pi G}\int_{\Sigma_{\infty}} dx\, dy \left[m_0 + \frac{1}{r}\left(2m_1 - \frac{4\sigma_4}{l^2}\right) + \mathcal{O}\left(\frac{1}{r^4}\right)\right] \\ &= \frac{A_0 m_0}{4\pi G} \qquad (4.105) \end{aligned}$$

at large r, where A_0 is the unit area of the surface Σ_{∞} and is arbitrary [22].

The entropy S is given by $S = A/4G$, where A is the area of the event horizon, so for our planar black holes we have

$$S = \frac{A_0}{4G}. \tag{4.106}$$

The Hawking temperature T_H is given by

$$T_H = \frac{\mu'(1)\sigma(1)}{4\pi}, \tag{4.107}$$

so that we can define the free energy by

$$F = M - TS = \frac{A_0}{4\pi G}\left(m_0 - \frac{\mu'(1)\sigma(1)}{4}\right). \tag{4.108}$$

We wish to check whether a non-abelian $\mathfrak{su}(N)$ black hole is thermodynamically favoured over a Reissner-Nordström black hole. If we consider a Reissner-Nordström black hole with the same Hawking temperature and effective charge as our $\mathfrak{su}(N)$ black hole, and denote its free energy as F_{RN}, the $\mathfrak{su}(N)$ black hole will be thermodynamically favoured when

$$\Delta F = F - F_{RN} < 0. \tag{4.109}$$

We can determine the event horizon radius of the relevant Reissner-Nordström black hole, which we denote r_h^{RN}, using the requirement that the effective charges and Hawking temperatures are the same as those of the non-abelian solution. Using the Reissner-Nordström metric function (4.62), and (4.107) with $\sigma = 1$, the Hawking temperature of an embedded Reissner-Nordström black hole with effective charge q is given by

$$T_H^{RN} = -\frac{1}{4\pi}\left(\frac{\alpha^2 q^2}{r_h^{RN\,3}} - \frac{3r_h^{RN}}{l^2}\right). \tag{4.110}$$

We can then determine r_h^{RN} by solving (4.110) for r_h^{RN}, where q^2 is given by (4.99).

Since the metric function $\mu(r)$ goes to zero at the event horizon, we have

$$m_0^{RN} = \frac{q^2}{2r_h^{RN}} + \frac{r_h^{RN\,3}}{2l^2}, \tag{4.111}$$

so we can write the free energy of the embedded Reissner-Nordström black hole as

$$F_{RN} = \frac{A_0}{4\pi G}\left(\frac{3\alpha^2 q^2}{4r_h^{RN}} - \frac{r_h^{RN\,3}}{4l^2}\right), \tag{4.112}$$

and hence

$$\Delta F = \frac{A_0}{4\pi G}\left(m_0 - \frac{\mu(1)\sigma(1)}{4} - \frac{3\alpha^2 q^2}{4r_h^{RN}} + \frac{r_h^{RN\,3}}{4l^2}\right). \tag{4.113}$$

We will be interested in the range of temperatures for which we find non-abelian solutions, which we expect to exist only below a critical temperature T_C (see section 4.9). After finding a solution to the field equations (see section 4.7), we then use the GSL root finding algorithm [2] to solve equation (4.110), and hence find the difference in free energy between our non-abelian solution and a Reissner-Nordström black hole with the same temperature and charge using (4.113). We can then check whether our solutions with a gauge field (playing the role of a superconducting condensate) are thermodynamically favoured over the Reissner-Nordström black hole.

Figure 4.7 shows a plot of ΔF against $\omega(r_h)$ for $\mathfrak{su}(2)$ black holes at various values of $l = \sqrt{-3/\Lambda}$. We note that the $\mathfrak{su}(2)$ solutions approach the Reissner-Nordström solutions in the limit of $\omega(r_h)$ going to zero, since if this is the case, the field equations ensure that $\omega(r)$ remains zero for all r. We also note that, as expected, ΔF is negative for all solutions with non-zero $\omega(r_h)$, and therefore all genuinely $\mathfrak{su}(2)$ solutions are thermodynamically favoured over Reissner-Nordström

solutions with the same temperature and charge (as was found in [62]).

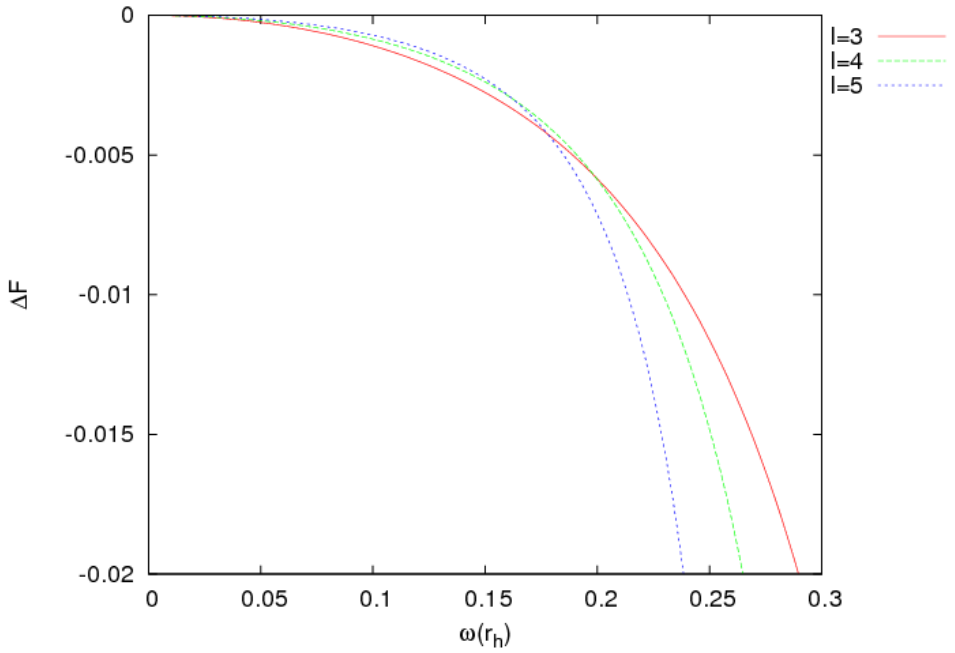

Figure 4.7: Difference in free energy between $\mathfrak{su}(2)$ solutions and Reissner-Nordström solutions with the same Hawking temperature and charge, against values of the gauge field function at the event horizon $\omega(r_h)$, for $l = \sqrt{-3/\Lambda} = 3, 4, 5$. We note that ΔF is always negative for non-zero $\omega(r_h)$, and hence an $\mathfrak{su}(2)$ black hole is always thermodynamically favoured over the equivalent Reissner-Nordström black hole.

Figure 4.8 shows a plot of ΔF against $\omega_1(r_h)$ and $\omega_2(r_h)$ for $\mathfrak{su}(3)$ solutions with $l = 5$. Again the $\mathfrak{su}(3)$ solutions approach the Reissner-Nordström solutions in the limit of $\omega_1(r_h)$ and $\omega_2(r_h)$ going to zero, and ΔF is negative for all solutions with non-zero $\omega_1(r_h)$ and $\omega_2(r_h)$. Therefore all genuinely $\mathfrak{su}(3)$ solutions are also thermodynamically favourable over Reissner-Nordström solutions with the same temperature and charge.

Figure 4.9 shows a plot of the electric charges Q_1 and Q_2 for $\mathfrak{su}(3)$ black holes, with the embedded $\mathfrak{su}(2)$ solutions overlaid. Figure 4.10 again shows Q_1 and Q_2 for $\mathfrak{su}(3)$ black holes, but this time against ΔF. The dotted embedded $\mathfrak{su}(2)$ line in figure 4.9 corresponds to the apexes of the surfaces in figure 4.10, and as such $|\Delta F|$ is smaller for the embedded $\mathfrak{su}(2)$ solutions than for genuinely $\mathfrak{su}(3)$ solutions. This means that the genuinely $\mathfrak{su}(3)$ solutions are thermodynamically favoured over the embedded $\mathfrak{su}(2)$ solutions. The interpretation of this is that for $\mathfrak{su}(3)$ solutions there

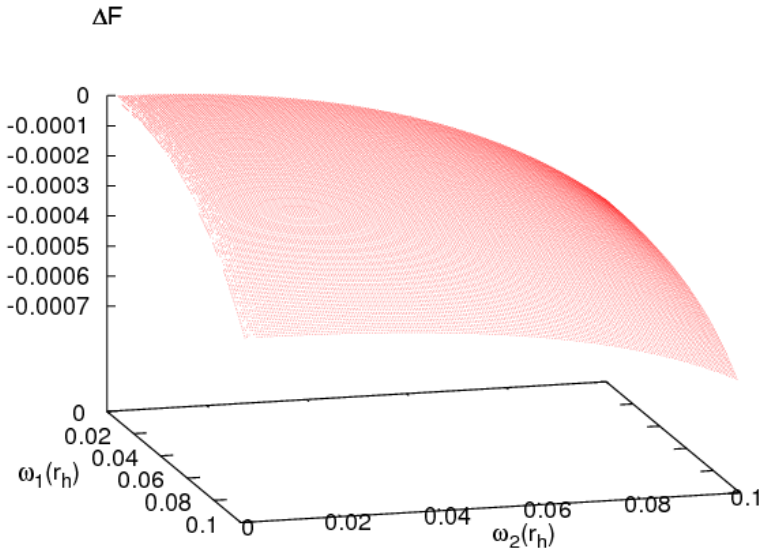

Figure 4.8: Difference in free energy between $\mathfrak{su}(3)$ solutions and Reissner-Nordström solutions with the same Hawking temperature and charge, against values of the gauge field functions at the event horizon, with $l = 5$.

are more possible field configurations that give us any particular effective charge, and hence more chance of finding a configuration with a lower free energy.

In the $\mathfrak{su}(2)$ case, there is a current on the boundary [62], given by

$$J = -\lim_{r\to\infty} \omega' r^2. \tag{4.114}$$

In the $\mathfrak{su}(N)$ case we have $N-1$ gauge field functions ω_k, and $N-1$ currents associated with our gauge field functions, which are

$$J_k = -\lim_{r\to\infty} \omega_k' r^2. \tag{4.115}$$

We expect to find a phase transition at some critical temperature T_C, above which only the Reissner-Nordström solutions exist, and below which the $\mathfrak{su}(N)$ solutions exist and have $\Delta F < 0$. The holographic interpretation for the single current in [37] is that this is an order parameter, which is zero at temperatures at and above the phase transition $T \geq T_C$. This is expected since $\omega \equiv 0$ for the Reissner-Nordström solution. Since our embedded Reissner-Nordström has $\omega_k \equiv 0$ for all k, we expect

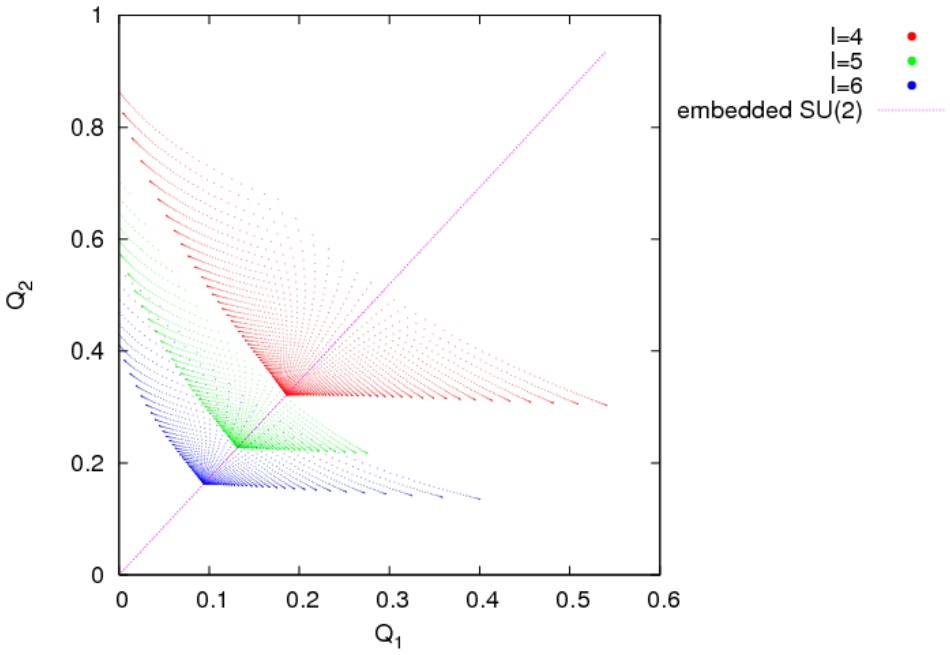

Figure 4.9: Electric charges of $\mathfrak{su}(3)$ black holes at various values of l, with embedded $\mathfrak{su}(2)$ solutions ($Q_2 = \sqrt{3}Q_1$) overlaid. Points which lie on the embedded $\mathfrak{su}(2)$ line correspond to those with the lowest $|\Delta F|$ in figure 4.10.

$J_k = 0$ for all k at the phase transition. We will therefore consider the J_k to be components of a vector order parameter, the length of which is zero at the phase transition, i.e. we expect

$$J^2 = \sum_{k=1}^{N-1} J_k^2 = 0 \tag{4.116}$$

for $T \geq T_C$, and

$$J^2 = \sum_{k=1}^{N-1} J_k^2 \neq 0 \tag{4.117}$$

for $T < T_C$. In figure 4.11 we have plotted the quantity $T/Q^{0.5}$ (which is invariant under the rescaling in section 4.6), where Q is the effective charge (4.99), against the components of our vector order parameter J_1 and J_2 for $\mathfrak{su}(3)$ black holes. We find that the maximum temperature is approached as the length of our vector order parameter $J = \sqrt{J_1^2 + J_2^2}$ goes to zero, i.e. as we approach the Reissner-Nordström solution. As expected, we find non-zero values of J_1 and J_2 at temperatures below the transition from the Reissner-Nordström solution. In the following section we will verify that this is indeed the critical temperature T_C.

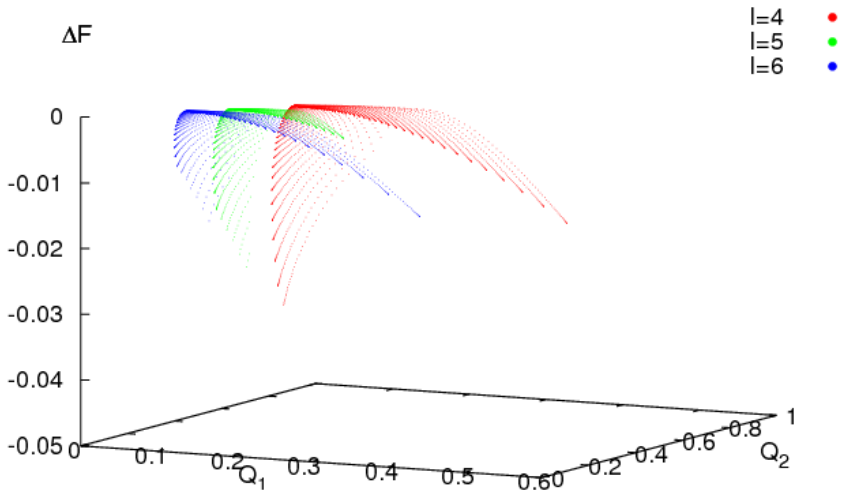

Figure 4.10: Difference in free energy between $\mathfrak{su}(3)$ solutions and Reissner-Nordström solutions with the same temperature and effective charge, plotted against electric charges Q_1 and Q_2.

§ 4.9 Perturbations of the Reissner-Nordström solution

We expect to find a phase transition between the Reissner-Nordström (RN) solution and the $\mathfrak{su}(N)$ solution when the temperature decreases below the critical temperature T_C. In addition to the $\mathfrak{su}(N)$ solution having lower free energy than the RN solution, we require that the RN solution admits a static $\mathfrak{su}(N)$ perturbation at T_C. If this is the case, then the RN solution can decay into the $\mathfrak{su}(N)$ solution when it becomes thermodynamically favourable to do so.

We consider a RN solution, with $\mathfrak{su}(N)$ gauge field perturbations δh_k and $\delta\omega_k$, and a gauge potential given by

$$A = -\frac{1}{g}\sum_l \left[h_{l,0} + \delta h_l(r)\right] H_l\, dt - \frac{1}{g}\sum_m \delta\omega_m(r) F_m^{(1)} dx - \frac{1}{g}\sum_n \delta\omega_n(r) G_n^{(1)} dy \quad (4.118)$$

where $h_{l,0}$ are the equilibrium values of h_l from section 4.5.2. Since the gauge field

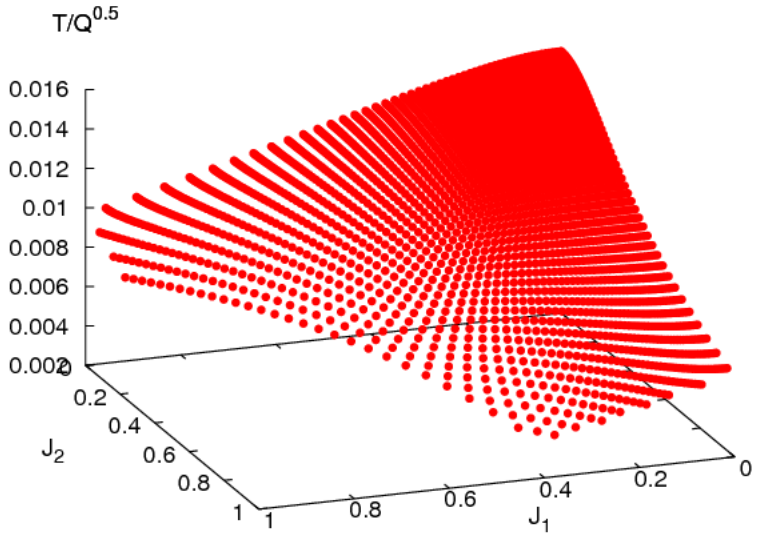

Figure 4.11: Hawking temperature divided by effective charge plotted against components of vector order parameter J_1 and J_2 for $\mathfrak{su}(3)$ black holes with $l = 4$.

perturbations give contributions to the mass, the line element is given by

$$\begin{aligned} ds^2 &= -\left[1+\delta\sigma(r)\right]^2\left[\mu_0(r)+\delta\mu(r)\right]dt^2 \\ &\quad +r^2dx^2+r^2dy^2+\left[\mu_0(r)+\delta\mu(r)\right]^{-1}dr^2, \\ &\approx -\left[\mu_0(r)+\delta\mu(r)+2\mu_0(r)\delta\sigma(r)\right]dt^2 \\ &\quad +r^2dx^2+r^2dy^2+\frac{\mu_0(r)-\delta\mu(r)}{\mu_0(r)^2}dr^2, \end{aligned} \tag{4.119}$$

where

$$\mu_0(r) = -\frac{2m_0(r)}{r} - \frac{\Lambda r^2}{r}, \qquad \delta\mu(r) = -\frac{2\delta m(r)}{r}. \tag{4.120}$$

The equilibrium mass function $m_0(r)$ is given by

$$m_0(r) = m_0^{RN} - \frac{\alpha_{RN}^2 q^2}{2r}, \tag{4.121}$$

so that the RN solution is recovered when all perturbations go to zero (see sec-

tion 4.5.2). The linearized Einstein-Yang-Mills equations for the perturbations are derived in Appendix B, and are given by

$$\delta m' = \alpha^2 r^2 \sum_{k=1}^{N-1} \left(2h'_{k,0}\delta h'_k - 2h'^2_{k,0}\delta\sigma\right), \tag{4.122}$$

$$\delta\sigma' = 0, \tag{4.123}$$

$$0 = \delta\omega''_k + \frac{\mu'_0\delta\omega'_k}{\mu_0} + \frac{\delta\omega_k}{\mu}\left(\sqrt{\frac{k+1}{2k}}h_{k,0} - \sqrt{\frac{k-1}{2k}}h_{k-1,0}\right), \tag{4.124}$$

$$\delta h''_k = h'_{k,0}\delta\sigma' - \frac{2}{r}\delta h'_k. \tag{4.125}$$

From section 4.5.2 the equilibrium values of h_k are

$$h_{k,0} = b_k - \frac{a_k}{r} \Rightarrow h'_k = \frac{a_k}{r^2} \tag{4.126}$$

and since $h_k(1) = 0$, we have $b_k = a_k = h'_k(1)$, giving

$$0 = \delta\omega''_k + \frac{\mu'_0\delta\omega'_k}{\mu_0} + \frac{\delta\omega_k}{\mu}\left(\sqrt{\frac{k+1}{2k}}h'_k(1) - \sqrt{\frac{k-1}{2k}}h'_{k-1}(1)\right)\left(1 - \frac{1}{r}\right). \tag{4.127}$$

We use the GSL root finding algorithm [2] to find solutions to (4.127) where the perturbations $\delta\omega_k$ go to zero at large r. This determines the values of $h'_k(1)$, and we find the charge using (4.67). The temperature is then determined from (4.110). Since we expect the temperature at which the RN solution admits this perturbation to be the critical temperature T_C, it should be the case that the non-abelian $\mathfrak{su}(N)$ solutions exist only at temperatures less that the critical temperature T_C.

Figure 4.12 shows a plot of the scale invariant quantity $T/Q^{0.5}$ against the length scale l for $\omega(r_h) = 0.1$ and $\omega(r_h) = 0.01$, together with the critical temperature T_C for $\mathfrak{su}(2)$. The $\omega(r_h) = 0.01$ curve lies slightly below the critical temperature curve. As expected, we find that $\mathfrak{su}(2)$ solutions exist only for temperatures less than the critical temperature, and that the critical temperature is approached as $\omega(r_h)$ goes to zero, i.e. as the RN solution is approached. Figure 4.13 is a similar plot for $\mathfrak{su}(3)$, except at discrete values of l and scanning over a range of values of $\omega_1(r_h)$ and $\omega_2(r_h)$. Again we find that the $\mathfrak{su}(3)$ solutions exist only at temperatures less than T_C, and that T_C is approached as $\omega_1(r_h)$ and $\omega_2(r_h)$ approach zero. However, since it becomes increasingly difficult to distinguish between nodeless solutions and those with nodes as $\omega_1(r_h)$ and $\omega_2(r_h)$ decrease, we were unable to find solutions

very close to the phase transition.

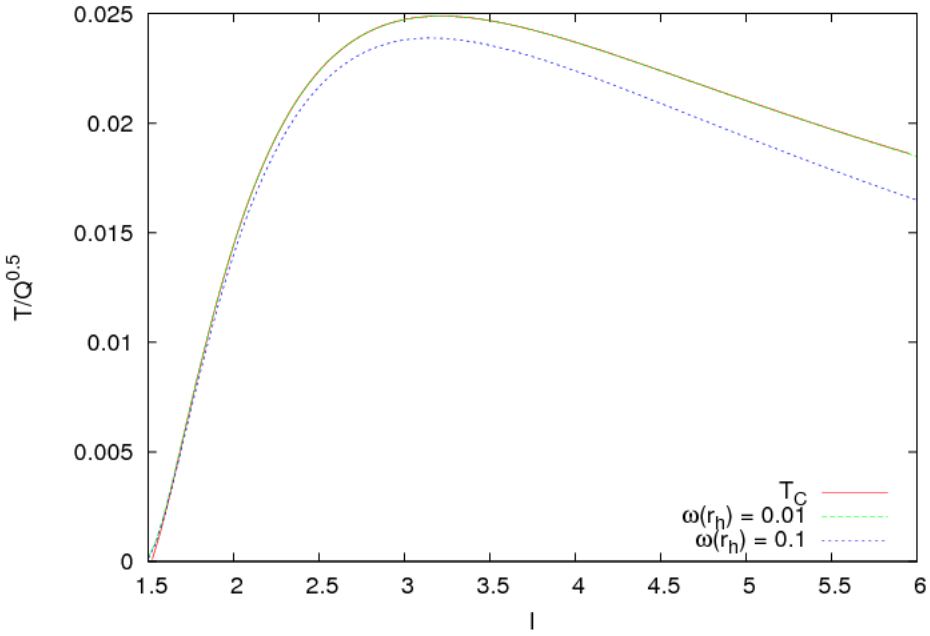

Figure 4.12: Plot of temperature divided by the square root of the electric charge against $l = \sqrt{-3/\Lambda}$ for $\mathfrak{su}(2)$ planar black holes with various values of $\omega(r_h)$, together with the critical temperature T_C. The $\omega(r_h) = 0.01$ curve lies slightly below the critical temperature curve.

In this section we have shown that there is a phase transition at a critical temperature T_C at which the RN solution can decay into $\mathfrak{su}(2)$ or $\mathfrak{su}(3)$ solutions, and that these solutions exist at temperatures below T_C. We approach the critical temperature as our non-abelian solutions approach the RN solution, so our order parameter J approaches zero as we approach the phase transition from below, and is equal to zero above the critical temperature as expected. It was also shown in the previous section that $\mathfrak{su}(2)$ and $\mathfrak{su}(3)$ solutions are thermodynamically favourable over RN solutions with the same mass and charge. Since the $\mathfrak{su}(3)$ solution is thermodynamically favoured over $\mathfrak{su}(2)$, we expect larger gauge groups to have lower free energies, and that a RN solution will decay into the most complicated solution possible.

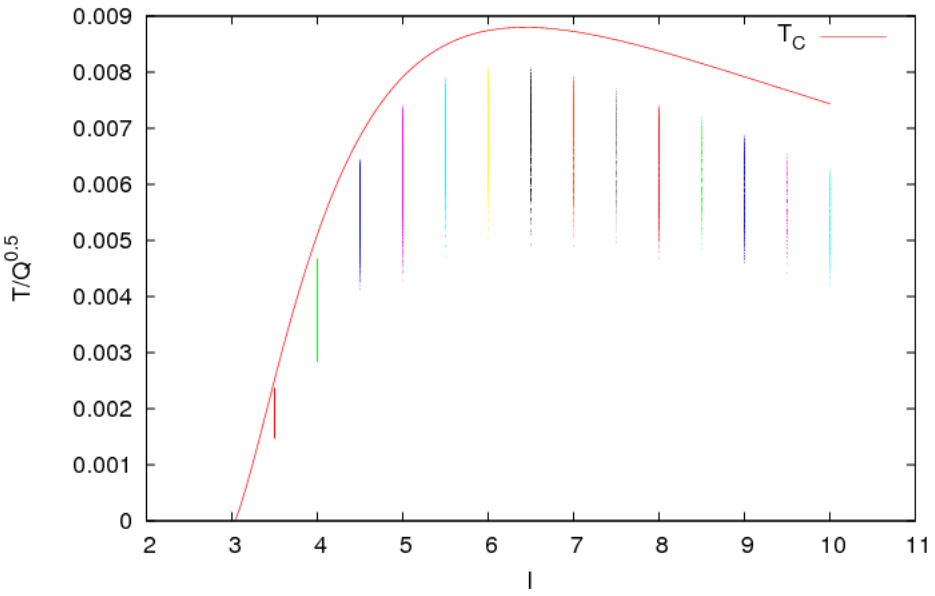

Figure 4.13: Plot of temperature divided by the square root of the electric charge against $l = \sqrt{-3/\Lambda}$ for $\mathfrak{su}(3)$ planar black holes over a range of values of $\omega_1(r_h)$ and $\omega_2(r_h)$ for which ω_1 and ω_2 go to zero at large r and are nodeless, together with the critical temperature T_C. Each dot on the vertical lines corresponds to an $\mathfrak{su}(3)$ black hole solution.

§ 4.10 Electromagnetic perturbations

In this section we will follow the prodcedure of [38] to compute the frequency dependent conductivity of the $\mathfrak{su}(N)$ solutions on a fixed background. We will apply a time dependent perturbation to the gauge field which is analogous to applying an oscillating electric field to our superconductor. We start by generalising the $\mathfrak{su}(2)$ perturbation of [38] to $\mathfrak{su}(N)$. As in [36], which is reviewed in section 4.1, the conductivity is determined from the asymptotic behaviour of the perturbations. Although we keep the field equations general, we will find numerical solutions for $\mathfrak{su}(2)$ and $\mathfrak{su}(3)$ only, as the number of equations to be solved increases rapidly with the size of the gauge group.

4.10.1 Ansatz and field equations

We will now apply an oscillating perturbation to the gauge field with frequency ξ. We generalise the ansatz of [38] by taking

$$\begin{aligned} gA &= -\sum_{l=1}^{N-1}\left(h_l H_l + e^{-i\xi t}\delta u_l F_l^{(1)} + e^{-i\xi t}\delta v_l G_l^{(1)}\right) dt \\ &\quad -\sum_{m=1}^{N-1}\left(\omega_m F_m^{(1)} + e^{-i\xi t}\delta h_{1,m} H_m\right) dx \\ &\quad -\sum_{n=1}^{N-1}\left(\omega_n G_n^{(1)} + e^{-i\xi t}\delta h_{2,n} H_n\right) dy, \end{aligned} \tag{4.128}$$

which reduces to that of [38] in the $\mathfrak{su}(2)$ case. As in [38], we will neglect the back-reaction of the fields on to the background planar Schwarzschild-AdS metric, such that the equations for h_k and ω_k are given by (4.92) and (4.93), with $m = -\Lambda/6$ and $\sigma = 1$. In terms of new complex variables

$$\begin{aligned} A_k &= \delta u_k + i\delta v_k, \qquad B_k = \delta u_k - i\delta v_k, \\ C_k &= \delta h_{1,k} + i\delta h_{2,k}, \qquad D_k = \delta h_{1,k} - i\delta h_{2,k}, \end{aligned} \tag{4.129}$$

the $4(N-1)$ Yang-Mills equations, which are derived in Appendix B, are given by

$$
\begin{aligned}
A_k'' &= -\frac{2}{r}A_k' + \frac{1}{\mu r^2}\left[\frac{\omega_{k+1}}{2}(A_k\omega_{k+1} - A_{k+1}\omega_k) + \frac{\omega_{k-1}}{2}(A_k\omega_{k-1} - A_{k-1}\omega_k)\right] \\
&+\frac{\omega_k}{\mu r^2}\left(\sqrt{\frac{k-1}{2k}}h_{k-1} - \sqrt{\frac{k+1}{2k}}h_k\right)\left(\sqrt{\frac{k+1}{2k}}C_k - \sqrt{\frac{k-1}{2k}}C_{k-1}\right) \\
&+\frac{(k+1)\omega_k}{2\mu r^2}\left(\frac{A_k\omega_k}{k} - \frac{A_{k+1}\omega_{k+1}}{k+1}\right) + \frac{(k-1)\omega_{k-1}}{2\mu r^2}\left(\frac{A_k\omega_k}{k} - \frac{A_{k-1}\omega_{k-1}}{k-1}\right) \\
&-\frac{\xi\omega_k}{\mu r^2}\left(\sqrt{\frac{k-1}{2k}}C_{k-1} - \sqrt{\frac{k+1}{2k}}C_k\right), \qquad (4.130)
\end{aligned}
$$

$$
\begin{aligned}
B_k'' &= -\frac{2}{r}A_k' + \frac{1}{\mu r^2}\left[\frac{\omega_{k+1}}{2}(B_k\omega_{k+1} - B_{k+1}\omega_k) + \frac{\omega_{k-1}}{2}(B_k\omega_{k-1} - B_{k-1}\omega_k)\right] \\
&+\frac{\omega_k}{\mu r^2}\left(\sqrt{\frac{k-1}{2k}}h_{k-1} - \sqrt{\frac{k+1}{2k}}h_k\right)\left(\sqrt{\frac{k+1}{2k}}D_k - \sqrt{\frac{k-1}{2k}}D_{k-1}\right) \\
&+\frac{(k+1)\omega_k}{2\mu r^2}\left(\frac{B_k\omega_k}{k} - \frac{B_{k+1}\omega_{k+1}}{k+1}\right) + \frac{(k-1)\omega_{k-1}}{2\mu r^2}\left(\frac{B_k\omega_k}{k} - \frac{B_{k-1}\omega_{k-1}}{k-1}\right) \\
&+\frac{\xi\omega_k}{\mu r^2}\left(\sqrt{\frac{k-1}{2k}}D_{k-1} - \sqrt{\frac{k+1}{2k}}D_k\right), \qquad (4.131)
\end{aligned}
$$

$$
\begin{aligned}
0 &= C_k'' + \frac{\mu'}{\mu}C_k' + \sqrt{\frac{k+1}{2k}}\frac{A_k\omega_k}{\mu^2}\left(\sqrt{\frac{k-1}{2k}}h_{k-1} - \sqrt{\frac{k+1}{2k}}h_k\right) \\
&+\sqrt{\frac{k}{2(k+1)}}\frac{A_{k+1}\omega_{k+1}}{\mu^2}\left(\sqrt{\frac{k+2}{2(k+1)}}h_{k+1} - \sqrt{\frac{k}{2(k+1)}}h_k\right) \\
&+\sqrt{\frac{k+1}{2k}}\frac{\omega_k^2}{\mu r^2}\left(\sqrt{\frac{k-1}{2k}}C_{k-1} - \sqrt{\frac{k+1}{2k}}C_k\right) \\
&+\sqrt{\frac{k}{2(k+1)}}\frac{\omega_{k+1}^2}{\mu r^2}\left(\sqrt{\frac{k+2}{2(k+1)}}C_{k+1} - \sqrt{\frac{k}{2(k+1)}}C_k\right) \\
&+\frac{\xi}{\mu^2}\left(\sqrt{\frac{k+1}{2k}}A_k\omega_k - \sqrt{\frac{k}{2(k+1)}}A_{k+1}\omega_{k+1} + \xi C_k\right), \qquad (4.132)
\end{aligned}
$$

$$
\begin{aligned}
0 &= D_k'' + \frac{\mu'}{\mu} D_k' + \sqrt{\frac{k+1}{2k}} \frac{B_k \omega_k}{\mu^2} \left(\sqrt{\frac{k-1}{2k}} h_{k-1} - \sqrt{\frac{k+1}{2k}} h_k \right) \\
&+ \sqrt{\frac{k}{2(k+1)}} \frac{B_{k+1} \omega_{k+1}}{\mu^2} \left(\sqrt{\frac{k+2}{2(k+1)}} h_{k+1} - \sqrt{\frac{k}{2(k+1)}} h_k \right) \\
&+ \sqrt{\frac{k+1}{2k}} \frac{\omega_k^2}{\mu r^2} \left(\sqrt{\frac{k-1}{2k}} D_{k-1} - \sqrt{\frac{k+1}{2k}} D_k \right) \\
&+ \sqrt{\frac{k}{2(k+1)}} \frac{\omega_{k+1}^2}{\mu r^2} \left(\sqrt{\frac{k+2}{2(k+1)}} D_{k+1} - \sqrt{\frac{k}{2(k+1)}} D_k \right) \\
&- \frac{\xi}{\mu^2} \left(\sqrt{\frac{k+1}{2k}} B_k \omega_k - \sqrt{\frac{k}{2(k+1)}} B_{k+1} \omega_{k+1} - \xi D_k \right), \qquad (4.133)
\end{aligned}
$$

where $k = 1, 2, ..., N-1$. We also have $2(N-2)$ zeroth order constraint equations, which are given by

$$
\begin{aligned}
0 &= \frac{h_k}{\sqrt{2k(k+1)}} \left(A_k \omega_{k+1} - A_{k+1} \omega_k \right) + \sqrt{\frac{k+2}{2(k+1)}} h_{k+1} \left(A_k \omega_{k+1} - A_{k+1} \omega_k \right) \\
&+ \sqrt{\frac{k-1}{2k}} h_{k-1} \left(A_{k+1} \omega_k - A_k \omega_{k+1} \right) + \xi \left(A_k \omega_{k+1} - A_{k+1} \omega_k \right) \\
&+ A_k \omega_{k+1} \left(\sqrt{\frac{k+2}{2(k+1)}} h_{k+1} - \sqrt{\frac{k}{2(k+1)}} h_k \right) \\
&+ A_{k+1} \omega_k \left(\sqrt{\frac{k-1}{2k}} h_{k-1} - \sqrt{\frac{k+1}{2k}} h_k \right) \\
&+ \frac{\mu \omega_k \omega_{k+1}}{r^2} \left(\sqrt{\frac{k}{2(k+1)}} C_k - \sqrt{\frac{k+2}{2(k+1)}} C_{k+1} \right) \\
&+ \frac{\mu \omega_k \omega_{k+1}}{r^2} \left(\sqrt{\frac{k+1}{2k}} C_k - \sqrt{\frac{k-1}{2k}} C_{k-1} \right), \qquad (4.134)
\end{aligned}
$$

$$
\begin{aligned}
0 \;=\; & \frac{h_k}{\sqrt{2k(k+1)}}\left(B_k\omega_{k+1}-B_{k+1}\omega_k\right)+\sqrt{\frac{k+2}{2(k+1)}}h_{k+1}\left(B_k\omega_{k+1}-B_{k+1}\omega_k\right)\\
& +\sqrt{\frac{k-1}{2k}}h_{k-1}\left(B_{k+1}\omega_k-B_k\omega_{k+1}\right)-\xi\left(B_k\omega_{k+1}-B_{k+1}\omega_k\right)\\
& +B_k\omega_{k+1}\left(\sqrt{\frac{k+2}{2(k+1)}}h_{k+1}-\sqrt{\frac{k}{2(k+1)}}h_k\right)\\
& +B_{k+1}\omega_k\left(\sqrt{\frac{k-1}{2k}}h_{k-1}-\sqrt{\frac{k+1}{2k}}h_k\right)\\
& +\frac{\mu\omega_k\omega_{k+1}}{r^2}\left(\sqrt{\frac{k}{2(k+1)}}D_k-\sqrt{\frac{k+2}{2(k+1)}}D_{k+1}\right)\\
& +\frac{\mu\omega_k\omega_{k+1}}{r^2}\left(\sqrt{\frac{k+1}{2k}}D_k-\sqrt{\frac{k-1}{2k}}D_{k-1}\right),
\end{aligned}
\tag{4.135}
$$

where $k=1,2,...,N-1$, but where the $k=N-1$ equations vanish since $\omega_N=A_N=0$, and $2(N-1)$ first order constraint equations,

$$
\begin{aligned}
0 \;=\; & \sqrt{\frac{k+1}{2k}}\left(h_kA_k'-A_kh_k'\right)+\sqrt{\frac{k-1}{2k}}\left(A_kh_{k-1}'-h_{k-1}A_k'\right)\\
& +\frac{\mu}{r^2}\left(\sqrt{\frac{k+1}{2k}}\left(\omega_kC_k'-C_k\omega_k'\right)+\sqrt{\frac{k-1}{2k}}\left(C_{k-1}\omega_k'-\omega_kC_{k-1}'\right)\right)\\
& +\xi A_k',
\end{aligned}
\tag{4.136}
$$

$$
\begin{aligned}
0 \;=\; & \sqrt{\frac{k+1}{2k}}\left(h_kB_k'-B_kh_k'\right)+\sqrt{\frac{k-1}{2k}}\left(B_kh_{k-1}'-h_{k-1}B_k'\right)\\
& +\frac{\mu}{r^2}\left(\sqrt{\frac{k+1}{2k}}\left(\omega_kD_k'-D_k\omega_k'\right)+\sqrt{\frac{k-1}{2k}}\left(D_{k-1}\omega_k'-\omega_kD_{k-1}'\right)\right)\\
& -\xi B_k',
\end{aligned}
\tag{4.137}
$$

where $k=1,2,...,N-1$. The equations for A and C are coupled, as are the equations for B and D, although the two sets of equations are independent of each other. We note that the two sets of equations differ only by the sign of the ξ terms.

If we differentiate the first order constraints (4.136) and (4.137), we find that they are consistent with the field equations (4.130–4.133) and the zeroth order constraints (4.134) and (4.135). Therefore, if the field equations and zeroth order constraints are satisfied, the first order constraints must also be satisfied. We conclude that the

first order constraints propagate, i.e. that if they are satisfied at one point in space, they will be satisfied everywhere as long as (4.130–4.135) are satisfied everywhere. However, this is not the case for the zeroth order constraints, so equations (4.134) and (4.135) must be implemented directly. This is achieved by using the zeroth order constraints to write $2(N-2)$ variables in terms of the other $2N$ variables, and hence we have $2N$ independent variables.

4.10.2 Boundary conditions at the event horizon for the $\mathfrak{su}(2)$ case

In the $\mathfrak{su}(2)$ case, the zeroth order constraints (4.134) and (4.135) vanish, since $A_N = B_N = \omega_N = 0$, and we consider only the field equations and the first order constriaints. We have four variables A, B, C and D, and two first order constraints. We start by considering the variables A and C, which have equations of motion given by

$$\begin{aligned} A'' &= -\frac{2}{r}A' + \frac{1}{\mu r^2}\left(A\omega^2 - h\omega C + \xi\omega C\right), \\ C'' &= -\frac{\mu'}{\mu}C' + \frac{Ah\omega}{\mu^2} + \frac{\omega^2 C}{\mu r^2} - \frac{\xi}{\mu^2}\left(A\omega + \xi C\right), \end{aligned} \tag{4.138}$$

and a single first order constraint given by

$$hA' - Ah' + \frac{\mu}{r^2}\left(\omega C' - C\omega'\right) + \xi A' = 0. \tag{4.139}$$

Following [38] we take the expansions of A and C near the horizon to be

$$\begin{aligned} A &= (r-1)^{i\xi\rho+\lambda_A}\left(x^{(0)} + x^{(1)}(r-1) + x^{(2)}(r-1)^2 + ...\right), \\ C &= (r-1)^{i\xi\rho+\lambda_C}\left(y^{(0)} + y^{(1)}(r-1) + y^{(2)}(r-1)^2 + ...\right), \end{aligned} \tag{4.140}$$

where ρ, λ_A, λ_C and all $x^{(a)}$ and $y^{(a)}$ are real constants. Substituting into (4.138) yields

$$\begin{aligned} 0 &= \frac{3}{l^2}(r-1)^{i\xi\rho+\lambda_A-1}(i\xi\rho+\lambda_A)(i\xi\rho+\lambda_A-1)x^{(0)} \\ &\quad +(r-1)^{i\xi\rho+\lambda_A}\left(\frac{6}{l^2}(i\xi\rho+\lambda_A) - \omega(1)^2 x^{(0)}\right) \\ &\quad +(r-1)^{i\xi\rho+\lambda_A}\left(\frac{3}{l^2}(i\xi\rho+\lambda_A)(i\xi\rho+\lambda_A+1)x^{(1)} + \mathcal{O}(r-1)\right) \\ &\quad -(r-1)^{i\xi\rho+\lambda_C}\left(\xi\omega(1)y^{(0)} + \mathcal{O}(r-1)\right), \end{aligned} \tag{4.141}$$

where we have Taylor expanded h, ω and μ at the event horizon as in section 4.4.1. For this equation to be non-trivial, we require either $x^{(0)} = 0$ and $\lambda_A = \lambda_C$, or $\lambda_A = \lambda_C + 1$. In fact, these two are equivalent, since in both cases we require $A \sim (r-1)^{i\xi\rho+\lambda_C+1}$ to leading order. We will take $\lambda_A = \lambda_C$ with $x^{(0)} = 0$. Turning now to equation (4.138) we have

$$0 = (r-1)^{i\xi\rho+\lambda_C}\left[\xi^2 + \frac{9}{l^4}\left(i\xi\rho + \lambda_C\right)^2\right] y^{(0)} + \mathcal{O}\left((r-1)^{i\xi\rho+\lambda_C+1}\right), \tag{4.142}$$

to leading order, so that

$$\xi^2 + \frac{9}{l^2}\left(\lambda_C^2 + 2i\xi\rho\lambda_C - \xi^2\rho^2\right) = 0. \tag{4.143}$$

Since we wish to consider solutions with real and non-zero ξ, we must take $\lambda_C = 0$ We then have

$$\rho^2 = \frac{l^4}{9} \quad \Rightarrow \quad \rho = \pm\frac{l^2}{3} = \pm\frac{1}{4\pi T_H}. \tag{4.144}$$

Following [38] we will consider the infalling solution and take the negative root of (4.144). Since our field equations (4.138) and constraint (4.139) are invariant under the rescaling $A \to \gamma A$, $C \to \gamma C$, we can rescale our variables by $\gamma = 1/y^{(0)}$. We then have

$$\begin{aligned} A &= (r-1)^{-\frac{i\xi l^2}{3}}\left(x^{(1)}(r-1) + x^{(2)}(r-1)^2 + ...\right), \\ C &= (r-1)^{-\frac{i\xi l^2}{3}}\left(1 + y^{(1)}(r-1) + y^{(2)}(r-1)^2 + ...\right). \end{aligned} \tag{4.145}$$

To leading order, the first order constraint (4.139) is given by

$$0 = -i\omega(1) + \left(1 - \frac{i\xi l^2}{3}\right) x^{(1)}, \tag{4.146}$$

so that

$$x^{(1)} = \frac{i\omega(1)}{1 - \frac{i\xi l^2}{3}}. \tag{4.147}$$

We then have

$$\begin{aligned} A &= (r-1)^{1-\frac{i\xi l^2}{3}}\left(\frac{i\omega(1)}{1-\frac{i\xi l^2}{3}}+\mathcal{O}(r-1)\right), \\ C &= (r-1)^{-\frac{i\xi l^2}{3}}\left(1+\mathcal{O}(r-1)\right). \end{aligned} \tag{4.148}$$

The equations of motion and constraint for B and D are the same as for A and C, except with $\xi \to -\xi$. The leading order dependence of B and D on $(r-1)$ is therefore the same, as is the symmetry $B \to \gamma B$, $D \to \gamma D$. We can therefore expand B and D near the horizon as

$$\begin{aligned} B &= (r-1)^{1-\frac{i\xi l^2}{3}}\left(z^{(1)}+\mathcal{O}(r-1)\right), \\ D &= (r-1)^{-\frac{i\xi l^2}{3}}\left(1+\mathcal{O}(r-1)\right). \end{aligned} \tag{4.149}$$

From the first order constraint (4.139) we have

$$z^{(1)} = \frac{i\omega(1)}{\frac{i\xi l^2}{3}-1}, \tag{4.150}$$

and therefore

$$\begin{aligned} B &= (r-1)^{1-\frac{i\xi l^2}{3}}\left(\frac{i\omega(1)}{\frac{i\xi l^2}{3}-1}+\mathcal{O}(r-1)\right), \\ D &= (r-1)^{-\frac{i\xi l^2}{3}}\left(1+\mathcal{O}(r-1)\right). \end{aligned} \tag{4.151}$$

4.10.3 Boundary conditions at the event horizon for the $\mathfrak{su}(3)$ case

In the $\mathfrak{su}(3)$ case we now have eight variables: A_k, B_k, C_k and D_k, for $k = 1, 2$, and we begin by considering the A_k and C_k. We then have four equations of motion given by (4.130, 4.132), one zeroth order constraint (4.134), and two first order constraints (4.134). The near horizon expansions for the A_k and C_k, are given by

$$\begin{aligned} A_k &= (r-1)^{i\xi\rho+\lambda_A}\left(x_k^{(0)}+x_k^{(1)}(r-1)+x_k^{(2)}(r-1)^2+...\right), \\ C_k &= (r-1)^{i\xi\rho+\lambda_C}\left(y_k^{(0)}+y_k^{(1)}(r-1)+y_k^{(2)}(r-1)^2+...\right). \end{aligned} \tag{4.152}$$

Substituting into (4.130) for $k = 1$ yields

$$\begin{aligned}
0 &= \frac{3}{l^2}(r-1)^{i\xi\rho+\lambda_A-1}\left(i\xi\rho+\lambda_A\right)\left(i\xi\rho+\lambda_A-1\right)x_1^{(0)} \\
&\quad +(r-1)^{i\xi\rho+\lambda_A}\left(-x_1^{(0)}\omega_1(1)^2-\frac{1}{2}x_1^{(0)}\omega_2(1)^2+x_2^{(0)}\omega_1(1)\omega_2(1)\right) \\
&\quad +(r-1)^{i\xi\rho+\lambda_A}\frac{3}{l^2}\left(i\xi\rho+\lambda_A\right)\left(i\xi\rho+\lambda_A+1\right)x_1^{(1)} \\
&\quad +(r-1)^{i\xi\rho+\lambda_A}\left(\frac{3}{l^2}\left(i\xi\rho+\lambda_A\right)x_1^{(0)}+\mathcal{O}(r-1)\right) \\
&\quad -(r-1)^{i\xi\rho+\lambda_C}\left(\xi\omega_1(1)y_1^{(0)}+\mathcal{O}(r-1)\right), \qquad (4.153)
\end{aligned}$$

while for $k = 2$ we have

$$\begin{aligned}
0 &= \frac{3}{l^2}(r-1)^{i\xi\rho+\lambda_A-1}\left(i\xi\rho+\lambda_A\right)\left(i\xi\rho+\lambda_A-1\right)x_2^{(0)} \\
&\quad +(r-1)^{i\xi\rho+\lambda_A}\left(-x_2^{(0)}\omega_2(1)^2-\frac{1}{2}x_2^{(0)}\omega_1(1)^2+x_1^{(0)}\omega_1(1)\omega_2(1)\right) \\
&\quad +(r-1)^{i\xi\rho+\lambda_A}\frac{3}{l^2}\left(i\xi\rho+\lambda_A\right)\left(i\xi\rho+\lambda_A+1\right)x_2^{(1)} \\
&\quad +(r-1)^{i\xi\rho+\lambda_A}\left(\frac{3}{l^2}\left(i\xi\rho+\lambda_A\right)x_2^{(0)}+\mathcal{O}(r-1)\right) \\
&\quad -(r-1)^{i\xi\rho+\lambda_C}\left(\frac{\sqrt{3}}{2}\xi\omega_2(1)y_2^{(0)}-\frac{1}{2}\xi\omega_2(1)y_1^{(0)}+\mathcal{O}(r-1)\right). \qquad (4.154)
\end{aligned}$$

As in the $\mathfrak{su}(2)$ case, we require either $\lambda_A = \lambda_C$ with $x_1^{(0)} = x_2^{(0)} = 0$, or $\lambda_A = \lambda_C+1$. As before the two are equivalent and we take $\lambda_A = \lambda_C$, and set $x_1^{(0)} = x_2^{(0)} = 0$. Substituting (4.152) into equation (4.132) we find

$$\begin{aligned}
0 &= (r-1)^{i\xi\rho+\lambda_A}\left(\xi x_1^{(0)}-\frac{1}{2}\xi x_2^{(0)}\omega_2(1)+\mathcal{O}(r-1)\right) \\
&\quad +(r-1)^{i\xi\rho+\lambda_C}\left(\frac{9}{l^4}\left(i\xi\rho+\lambda_C\right)^2 y_1^{(0)}+\xi^2 y_1^{(0)}+\mathcal{O}(r-1)\right), \qquad (4.155)
\end{aligned}$$

for $k = 1$, and

$$\begin{aligned}
0 &= (r-1)^{i\xi\rho+\lambda_A}\left(\frac{\sqrt{3}}{2}\xi x_2^{(0)}\omega_2(1)+\mathcal{O}(r-1)\right) \\
&\quad +(r-1)^{i\xi\rho+\lambda_C}\left(\frac{9}{l^4}\left(i\xi\rho+\lambda_C\right)^2 y_2^{(0)}+\xi^2 y_2^{(0)}+\mathcal{O}(r-1)\right), \qquad (4.156)
\end{aligned}$$

for $k = 2$. Both (4.155) and (4.156) yield

$$\frac{9}{l^4}\left(i\xi\rho + \lambda_C\right)^2 + \xi^2 = 0. \tag{4.157}$$

As in the $\mathfrak{su}(2)$ case we take $\lambda_C = \lambda_A = 0$ and find

$$\rho^2 = \frac{l^4}{9} \quad \Rightarrow \quad \rho = \pm\frac{l^2}{3} = \pm\frac{1}{4\pi T_H}, \tag{4.158}$$

and as before take the negative root. Again our equations are invariant under the transformation $A_k \to \gamma A_k$, $C_k \to \gamma C_k$, and we set $\gamma = 1/y_1^{(0)}$ so that our expansions become

$$\begin{aligned}
A_1 &= (r-1)^{-\frac{i\xi l^2}{3}}\left(x_1^{(1)}(r-1) + x_2^{(2)}(r-1)^2 + ...\right), \\
A_2 &= (r-1)^{-\frac{i\xi l^2}{3}}\left(x_2^{(1)}(r-1) + x_2^{(2)}(r-1)^2 + ...\right), \\
C_1 &= (r-1)^{-\frac{i\xi l^2}{3}}\left(1 + y_1^{(1)}(r-1) + y_2^{(2)}(r-1)^2 + ...\right), \\
C_2 &= (r-1)^{-\frac{i\xi l^2}{3}}\left(y_2^{(0)} + y_2^{(1)}(r-1) + y_2^{(2)}(r-1)^2 + ...\right).
\end{aligned} \tag{4.159}$$

In the $\mathfrak{su}(3)$ case we have two first order constraints. Substituting (4.159) into (4.136) and taking $k = 1$ we find

$$0 = -i\omega(1) + \left(1 - \frac{i\xi l^2}{3}\right)x_1^{(1)} \tag{4.160}$$

to leading order, so that

$$x_1^{(1)} = \frac{i\omega_1(1)}{1 - \frac{i\xi l^2}{3}}. \tag{4.161}$$

Similarly for $k = 2$ we find

$$x_2^{(1)} = \frac{i\omega_2(1)}{(1 - \frac{i\xi l^2}{3})}\left(\frac{\sqrt{3}}{2}y_2^{(0)} - \frac{1}{2}\right). \tag{4.162}$$

We also have a single zeroth order constraint (4.134), which to leading order is given by

$$(r-1)^{1-\frac{i\xi l^2}{3}}\left[\frac{3}{l^2}\omega_1(1)\omega_2(1)\left(\frac{3}{2} - \frac{\sqrt{3}}{2}y_2^{(0)}\right) + \xi\left(x_1^{(1)}\omega_2(1) - x_2^{(1)}\omega_1(1)\right)\right] = 0. \tag{4.163}$$

Substituting for $x_1^{(1)}$ and $x_2^{(1)}$ from (4.161) and (4.162) we find that $y_2^{(0)} = \sqrt{3}$, so that all together we have

$$\begin{aligned}
A_1 &= (r-1)^{1-\frac{i\xi l^2}{3}} \left(\frac{i\omega_1(1)}{1-\frac{i\xi l^2}{3}}(r-1) + \mathcal{O}(r-1)^2 \right), \\
A_2 &= (r-1)^{1-\frac{i\xi l^2}{3}} \left(\frac{i\omega_2(1)}{(1-\frac{i\xi l^2}{3})}(r-1) + \mathcal{O}(r-1)^2 \right), \\
C_1 &= (r-1)^{-\frac{i\xi l^2}{3}} \left(1 + \mathcal{O}(r-1)\right), \\
C_2 &= (r-1)^{-\frac{i\xi l^2}{3}} \left(\sqrt{3} + \mathcal{O}(r-1)\right).
\end{aligned} \tag{4.164}$$

Following the same procedure for the B_k and D_k equations of motion (4.131) and (4.133), and constraints (4.135) and (4.137), we find

$$\begin{aligned}
B_1 &= (r-1)^{1-\frac{i\xi l^2}{3}} \left(\frac{i\omega_1(1)}{\frac{i\xi l^2}{3}-1}(r-1) + \mathcal{O}(r-1) \right), \\
B_2 &= (r-1)^{1-\frac{i\xi l^2}{3}} \left(\frac{i\omega_2(1)}{\frac{i\xi l^2}{3}-1}(r-1) + \mathcal{O}(r-1) \right), \\
D_1 &= (r-1)^{-\frac{i\xi l^2}{3}} \left(1 + \mathcal{O}(r-1)\right), \\
D_2 &= (r-1)^{-\frac{i\xi l^2}{3}} \left(\sqrt{3} + \mathcal{O}(r-1)\right).
\end{aligned} \tag{4.165}$$

4.10.4 Conductivity of $\mathfrak{su}(2)$ solutions

In this section we compute the conductivity of $\mathfrak{su}(2)$ solutions with $\zeta = 1$, the $\zeta = 0$ case having been studied in [38]. The conductivity is computed using the boundary values of the perturbations. If we wish to compute the conductivity with respect to electric fields applied in the x direction, we therefore consider the behaviour of δh_1 at large r. Since the conductivity is an observable quantity, it must be gauge invariant.

In the $\mathfrak{su}(2)$ case, there is a set of gauge transformations which leave the matrix structure of the gauge potential (4.128) invariant. We consider an infinitesimal gauge transformation of the form

$$W = e^{-i\xi t}(W_1 F_1^{(1)} + W_2 G_1^{(1)} + W_3 H_1), \tag{4.166}$$

where F, G and H are the generators of $\mathfrak{su}(2)$. The potential (4.128) transforms

as

$$A_\mu \to A_\mu + \epsilon\left(\partial_\mu W - [A_\mu, W]\right), \tag{4.167}$$

so that, once terms of the form ϵ multiplied by a perturbation are neglected due to being quadratically small, we have

$$\begin{aligned}
A_0 &\to -e^{-i\xi t}(\delta u + \epsilon h W_2 + i\xi\epsilon W_1)F_1^{(1)} - e^{-i\xi t}(\delta v + i\xi\epsilon W_2 - hW_1)G_1^{(1)} \\
&\quad -(h + i\xi\epsilon e^{-i\xi t}W_3)H_1 \\
A_1 &\to (\epsilon e^{-i\xi t}\partial_1 W_1 - \omega)F_1^{(1)} + \epsilon e^{-i\xi t}(\partial_1 W_2 - \omega W_3)G_1^{(1)} \\
&\quad -e^{-i\xi t}(\delta h_1 - \epsilon\partial_1 W_3 - \epsilon\omega W_2)H_1 \\
A_2 &\to \epsilon e^{-i\xi t}(\partial_2 W_1 + \omega W_3)F_1^{(1)} + (\epsilon e^{-i\xi t}\partial_2 W_2 - \omega)G_1^{(1)} \\
&\quad -e^{-i\xi t}(\delta h_2 - \epsilon\partial_2 W_3 - \epsilon\omega W_1)H_1 \\
A_3 &\to \epsilon e^{-i\xi t}\left[\partial_3 W_1 F_1^{(1)} + \partial_3 W_1 G_1^{(1)} + \partial_3 W_3 H_1\right].
\end{aligned} \tag{4.168}$$

For $A_3 = 0$, we require

$$\partial_1 W_2 - \omega W_3 = \partial_2 W_1 + \omega W_3 = 0, \tag{4.169}$$

which satisfied if W is constant and $W_3 = 0$. If this is case, the transformation (4.168) is equivalent to

$$\begin{gathered}
\delta u \to \delta u + \epsilon(hW_2 + i\xi W_1), \qquad \delta v \to \delta v + \epsilon(i\xi W_2 - hW_1), \\
\delta h_1 \to \delta h_1 - \epsilon\omega W_2, \qquad \delta h_2 \to \delta h_2 - \epsilon\omega W_1.
\end{gathered} \tag{4.170}$$

However, since our conductivity (and all observable quantities) must be gauge invariant, we consider the quantities

$$\delta\hat{h}_1 = \delta h_1 + \frac{\omega(i\xi\delta v + h\delta u)}{h^2 - \xi^2}, \qquad \delta\hat{h}_2 = \delta h_2 + \frac{\omega(i\xi\delta u - h\delta v)}{h^2 - \xi^2}, \tag{4.171}$$

which are invariant under (4.170).

The conductivity in the x direction can be computed following [38], by expanding $\delta\hat{h}_1$ near the boundary at large r.

If we have

$$\begin{aligned}\delta\hat{h}_1 &= \delta h_1 + \frac{\omega(i\xi\delta v + h\delta u)}{h^2-\xi^2} \\ &= \frac{1}{2}(C+D) + \frac{\omega}{h^2-\xi^2}\left(\frac{\xi}{2}(A-B) + \frac{h}{2}(A+B)\right) \\ &= \mathcal{H}_1^{(0)} + \frac{\mathcal{H}_1^{(1)}}{r} + ... \end{aligned} \tag{4.172}$$

at large r, then the conductivity in the x direction is given by

$$\sigma_{xx} = -\frac{i}{\xi l^2}\frac{\mathcal{H}_1^{(1)}}{\mathcal{H}_1^{(0)}}. \tag{4.173}$$

Similarly, if

$$\delta\hat{h}_2 = \delta h_2 + \frac{\omega(i\xi\delta u - h\delta v)}{h^2-\xi^2} = \mathcal{H}_2^{(0)} + \frac{\mathcal{H}_2^{(1)}}{r} + ... \tag{4.174}$$

then the conductivity in the y-direction is

$$\sigma_{yy} = -\frac{i}{\xi l^2}\frac{\mathcal{H}_2^{(1)}}{\mathcal{H}_2^{(0)}}. \tag{4.175}$$

When looking for solutions to (4.130–4.133), the first step is to numerically find solutions to the background equations as described in section 4.7, i.e. to find solutions to the equations (4.83–4.86), subject to the boundary conditions (4.88), and where $\omega(r)$ approaches zero at large r. We then use the same method, the Bulirsch-Stoer algorithm in C++ [32] using a 10^{-7} convergence criteria to solve the equations for A, B, C and D (4.130–4.133) subject to the boundary conditions (4.148, 4.151), integrating outwards from $r-1 = 10^{-7}$.

The conductivities are then computed from the asymptotic values of A, B, C, D and their derivatives using (4.173) and (4.175), with

$$\begin{aligned}\mathcal{H}_1^{(0)} &= \lim_{r\to\infty}\delta\hat{h}_1 \\ &= \lim_{r\to\infty}\frac{1}{2}(C+D) + \frac{\omega}{h^2-\xi^2}\left(\frac{\xi}{2}(A-B) + \frac{h}{2}(A+B)\right), \end{aligned} \tag{4.176}$$

$$\begin{aligned}
\mathcal{H}_1^{(1)} &= \lim_{r\to\infty} -r^2\delta\hat{h}_1' \\
&= \lim_{r\to\infty}\left\{-\frac{r^2}{2}(C'+D')\right\} \\
&\quad - \lim_{r\to\infty}\left\{\frac{\omega}{h^2-\xi^2}\left(\frac{\xi}{2}(A'-B')+\frac{h}{2}(A'+B')+\frac{h'}{2}(A+B)\right)r^2\right\} \\
&\quad - \lim_{r\to\infty}\left\{\frac{(h^2-\xi^2)\omega'-2\omega hh'}{(h^2-\xi^2)^2}\left(\frac{\xi}{2}(A-B)+\frac{h}{2}(A+B)\right)r^2\right\}, \quad (4.177)
\end{aligned}$$

and similarly

$$\mathcal{H}_2^{(0)} = \lim_{r\to\infty}\frac{i}{2}(D-C)+\frac{\omega}{h^2-\xi^2}\left(\frac{i\xi}{2}(A+B)+\frac{ih}{2}(A-B)\right), \quad (4.178)$$

$$\begin{aligned}
\mathcal{H}_2^{(1)} &= \lim_{r\to\infty}\left\{\frac{ir^2}{2}(C'-D')\right\} \\
&\quad - \lim_{r\to\infty}\left\{\frac{\omega}{h^2-\xi^2}\left(\frac{i\xi}{2}(A'+B')+\frac{ih}{2}(A'-B')+\frac{ih'}{2}(A-B)\right)r^2\right\} \\
&\quad - \lim_{r\to\infty}\left\{\frac{(h^2-\xi^2)\omega'-2\omega hh'}{(h^2-\xi^2)^2}\left(\frac{i\xi}{2}(A+B)+\frac{ih}{2}(A-B)\right)r^2\right\}. \quad (4.179)
\end{aligned}$$

Figure 4.14 shows the real parts of the conductivities in the x and y directions plotted as a function of frequency ξ. We note that, as expected, there is a gap at low frequencies in both directions, i.e. the low frequency conducitvity is lower than the higher frequency conductivity, with a larger gap in σ_{yy} than σ_{xx}. As in [38], we also note that there is a pole in the imaginary part of the conductivity, plotted in figure 4.15. The same result was found in [38], from which it was deduced that there was a delta function at zero frequency in the real part of the conductivity, and we infer that the same must be true here. Both of these properties are what we would expect from a real superconductor [14, 13].

However, we also note that the conductivity diverges at non-zero frequency. Since $\mathcal{H}_1^{(0)}$ includes a $(h^2-\xi^2)^{-1}$ term, and $\mathcal{H}_1^{(1)}$ includes a $(h^2-\xi^2)^{-2}$ term, as the frequency ξ approaches the asymptotic value of h, the conductivity $\sigma_{xx}\sim\mathcal{H}_1^{(1)}/\mathcal{H}_1^{(0)}$ diverges, which is not a feature of real superconducting materials [13]. This feature was not found in [38] with the $\zeta=0$ ansatz. The conductivity of the $\zeta=1$ ansatz was not computed in [37, 62].

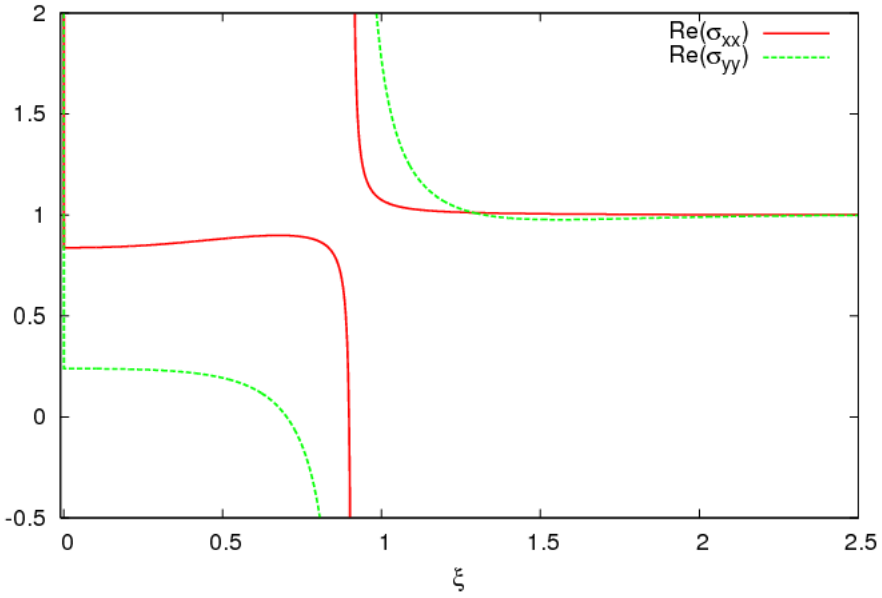

Figure 4.14: Plot of the real part of the frequency dependent conductivity for an $\mathfrak{su}(2)$ black hole with $\Lambda = -0.65$, $\omega(r_h) = 0.1$. As expected, we find a gap in the frequency dependent conductivity between low and high frequencies, and infinite D.C. conductivity. However, the divergence around $\xi = 0.9$ is not a feature of real superconducting materials.

4.10.5 Conductivity of $\mathfrak{su}(3)$ solutions

In the $\mathfrak{su}(3)$ case there are no gauge tranformations which preserve the matrix structure of (4.128), and hence it is sufficient to consider the asymptotic values of the quantities $\delta h_{1,1}$, $\delta h_{1,2}$, $\delta h_{2,1}$ and $\delta h_{2,2}$. However, the situation is made more complicated by the presence of two perturbations in both the x and y directions. The conductivity is determined from [38]

$$\mathcal{J}|_{bdy} = i\xi \begin{pmatrix} \delta h^*_{1,1} & \delta h^*_{1,1} & \dots & \delta v^*_2 \end{pmatrix} \boldsymbol{\sigma} \begin{pmatrix} \delta h_{1,1} \\ \delta h_{1,1} \\ \dots \\ \delta v_2 \end{pmatrix} \tag{4.180}$$

where $\boldsymbol{\sigma}$ is the conductivity matrix and $\mathcal{J}|_{bdy}$ is the large r limit of

$$\begin{aligned} \mathcal{J} \;=\; & r\left(\delta u^*_1 \partial_r \delta u_1 + \delta u^*_2 \partial_r \delta u_2 + \delta v^*_1 \partial_r \delta v_1 + \delta v^*_2 \partial_r \delta v_2\right) \\ & -\mu\left(\delta h^*_{1,1}\partial_r \delta h_{1,1} + \delta h^*_{1,2}\partial_r \delta h_{1,2} + \delta h^*_{2,1}\partial_r \delta h_{2,1} + \delta h^*_{2,2}\partial_r \delta h_{2,2}\right). \end{aligned} \tag{4.181}$$

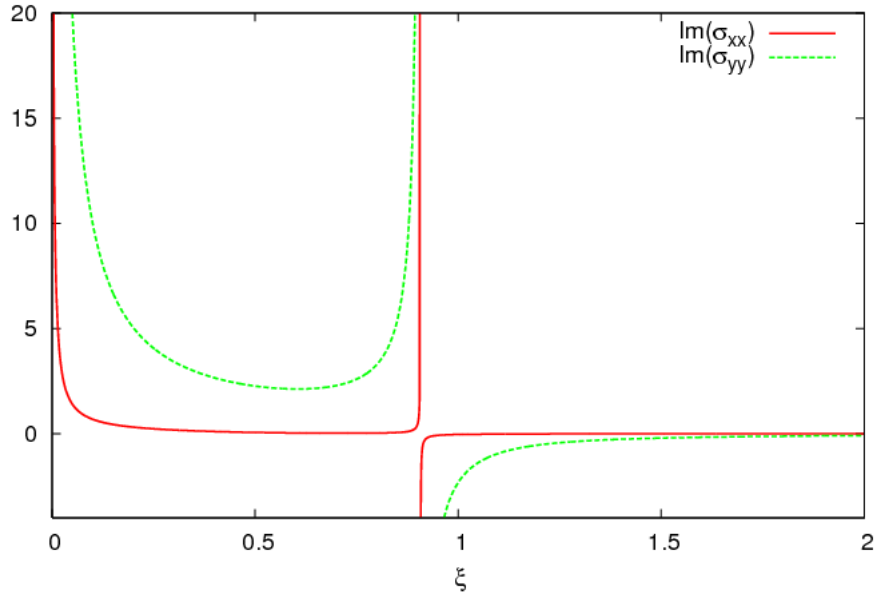

Figure 4.15: Plot of the imaginary part of the frequency dependent conductivity for an $\mathfrak{su}(2)$ black hole with $\Lambda = -0.65$, $\omega(r_h) = 0.1$. Results found here are similar to those of [38], although as with the real part we find a divergence around $\xi = 0.9$ which was not present in [38].

Considering only perterbations in the x direction $\delta h_{1,1}$ and $\delta h_{1,2}$, the appropriate part of (4.181) is

$$\mathcal{J} = \frac{1-r^3}{l^2 r}\left(\delta h^*_{1,1}\partial_r \delta h_{1,1} + \delta h^*_{1,2}\partial_r \delta h_{1,2}\right). \tag{4.182}$$

Using the zeroth order constraints (4.134, 4.135) we can write $\delta h_{1,2}$ in terms of $\delta h_{1,1}$ as

$$\delta h_{1,2} = \sqrt{3}\delta h_{1,1} + ... \tag{4.183}$$

We have omitted terms involving δu_i and δv_i, since these lead to off diagonal terms in the conductivity matrix. We are interested in the behaviour of $\delta h_{1,1}$ at large r, which is given by

$$\delta h_{1,1} = \mathcal{H}^{(0)}_{1,1} + \frac{\mathcal{H}^{(1)}_{1,1}}{r} + ... \tag{4.184}$$

The large r behaviour of (4.182) is then given by

$$\begin{aligned} i\xi\mathcal{H}^{(0)*}_{1,1}\left(\sigma_{1,1}+\sqrt{3}\sigma_{1,2}+\sqrt{3}\sigma_{2,1}+3\sigma_{2,2}\right)\mathcal{H}^{(0)}_{1,1} &= \frac{4r^2}{l^2}\mathcal{H}^{(0)*}_{1,1}\frac{\mathcal{H}^{(0)}_{1,1}}{r^2}+... \\ &= \frac{4}{l^2}\mathcal{H}^{(0)*}_{1,1}\frac{\mathcal{H}^{(1)}_{1,1}}{\mathcal{H}^{(0)}_{1,1}}\mathcal{H}^{0}_{1,1}+... \end{aligned} \tag{4.185}$$

so that using (4.182) we have

$$\sigma_{xx}=-\frac{4i}{\xi l^2}\frac{\mathcal{H}^{(1)}_{1,1}}{\mathcal{H}^{(0)}_{1,1}}, \tag{4.186}$$

where σ_{xx} is the part of $\boldsymbol{\sigma}$ depending only on $\delta h_{1,1}$ and $\delta h_{2,2}$. Similarly

$$\sigma_{yy}=-\frac{4i}{\xi l^2}\frac{\mathcal{H}^{(1)}_{2,1}}{\mathcal{H}^{(0)}_{2,1}}, \tag{4.187}$$

The first step in computing the conductivity will be to solve the field equations (4.130–4.133), subject to the constraints (4.134–4.137). The four first order constraints, given by (4.136, 4.137) are satisfied at the event horizon by our choice of boundary conditions, and are therefore satisfied everywhere since they propagate (we can therefore determine the accuracy of the numerical results from the size of the left hand sides of (4.136, 4.137)). However, we also have two zeroth order constraints which must be implemented directly. We use the zeroth order constraints to write

$$\begin{aligned} A_2 &= \frac{1}{\frac{3}{2}h_1\omega_2+\frac{\sqrt{3}}{2}h_2\omega_1+\xi\omega_1}\left\{A_1\omega_2\left(\sqrt{3}h_2+\xi\omega_2\right)+\frac{\mu\omega_1\omega_2}{2r^2}\left(C_1-\sqrt{3}C_2\right)\right\}, \\ B_2 &= \frac{1}{\frac{3}{2}h_1\omega_2+\frac{\sqrt{3}}{2}h_2\omega_1-\xi\omega_1}\left\{B_1\omega_2\left(\sqrt{3}h_2-\xi\omega_2\right)+\frac{\mu\omega_1\omega_2}{2r^2}\left(D_1-\sqrt{3}D_2\right)\right\}. \end{aligned} \tag{4.188}$$

We then have six independendent complex second order ODEs for A_1, B_1, C_1, C_2, D_1 and D_2, which we separate into real and imaginary parts, and then separate again into first order equations in A_1, A_1' etc. to give twenty four first order ODEs. Again we solve these, together with the background equations in ω_1, ω_2, h_1 and h_2, using the same Bulirsch-Stoer algorithm in C++ [32] using a 10^{-7} convergence

criteria, subject to the boundary conditions (4.164–4.165). We use the GSL root finding algorithm [2] to ensure the background gauge fields have ω_2 and ω_2 going to zero at large r, and we are interested in solutions where ω_1 and ω_2 have no nodes, since these have lower free energy, and are therefore thermodynamically favoured over solutions with nodes in ω_1 and ω_2 (see section 4.8.2).

Once solutions are obtained, we determine the conductivity in the x direction using the large r behaviour of C_1 and D_1 and (4.186) by noting that

$$\delta h_{1,1} = \frac{1}{2}\left(C_1 + D_1\right), \tag{4.189}$$

so that

$$\mathcal{H}^{(0)}_{1,1} = \lim_{r\to\infty} \frac{1}{2}\left(C_1 + D_1\right), \qquad \mathcal{H}^{(1)}_{1,1} = -\lim_{r\to\infty} \frac{r^2}{2}\left(C_1' + D_1'\right), \tag{4.190}$$

and therefore

$$\sigma_{xx} = \lim_{r\to\infty} \frac{4ir^2}{\xi l^2}\frac{C_1' + D_1'}{C_1 + D_1}. \tag{4.191}$$

Similarly

$$\sigma_{yy} = \lim_{r\to\infty} \frac{4ir^2}{\xi l^2}\frac{C_1' + D_1'}{C_1 + D_1}. \tag{4.192}$$

Figure 4.16 shows a plot of the real part of the conductivity in the x direction σ_{xx} as a function of frequency ξ for $\mathfrak{su}(3)$ black holes at various temperatures. As expected, we notice a gapped dependence in the conductivity at non-zero frequency, with a higher conductivity at higher frequencies. We also note that, as is the case in real superconducting materials, the gap decreases with increasing temperature. Unlike the $\mathfrak{su}(2)$ case, we do not find a divergence at a particular non-zero frequency, since we did not requre an additional term to make $\delta h_{1,1}$ gauge invariant (4.171). We also find that the conductivity becomes infinite in the zero frequency D.C. limit. However, unlike the $\mathfrak{su}(2)$ case, this does not need to be inferred from the imaginary part of the conductivity. Instead the real part of the frequency rises very sharply at small but non-zero frequencies and becomes large as ξ approaches zero.

Figure 4.17 shows the imaginary part of σ_{xx} As with the real part, we find the same features as we would expect from a real superconductor, without the unphysical divergence. In particular, we find that the imaginary part is large at small ξ, and tends to zero at large ξ, as was found in [38].

Figures 4.18 and 4.19 show the real and imaginary parts of the conductivity in

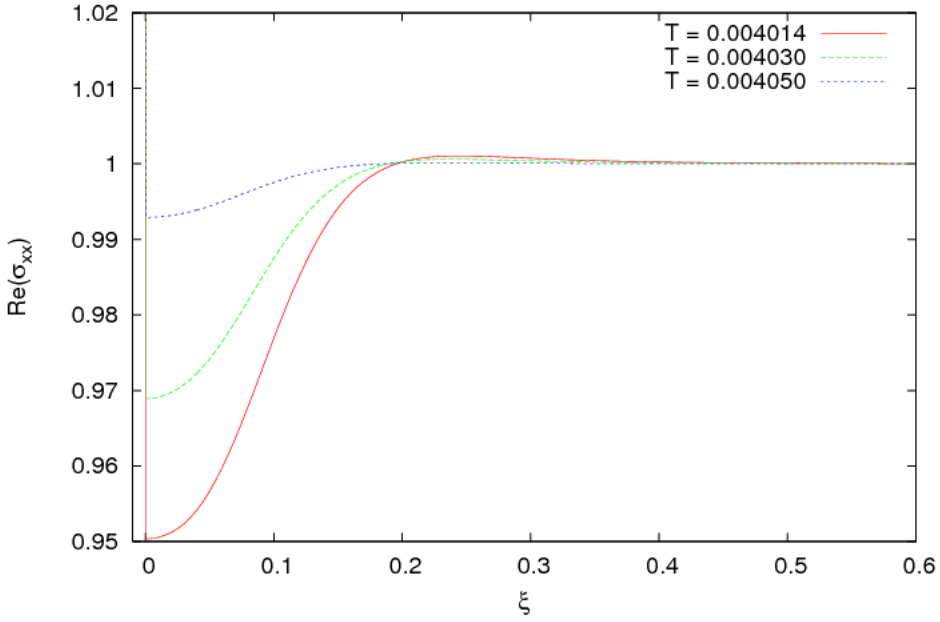

Figure 4.16: Plot of the real part of the frequency dependent conductivity in the x direction for an $\mathfrak{su}(3)$ black hole with $l = 5$ at various temperatures. As expected, there is a gap in the frequency dependent conductivity between low and high frequencies which, as expected, grows as the temperature decreases. Unlike the $\mathfrak{su}(2)$ case, there is no unphysical divergence at non-zero frequency.

the y direction, σ_{yy}. We find the same qualitative features as with σ_{xx}, which we expect from a real superconductor, without the unphysical divergences. However, the exact form is not the same as σ_{xx} in particular, we find a much larger gap in the conductivity at non-zero frequency at the same temperature, as we did in the $\mathfrak{su}(2)$ case. We also note that, while the gap does increase as temperature decreases, unlike in the x direction this difference is too small to be seen on a graph.

§ 4.11 Summary

In this chapter we have investigated planar dyonic black holes in the context of the AdS/CFT correspondence and superconductivity. We have found a gravitational analogue to superconductors which displays some of the main properties of

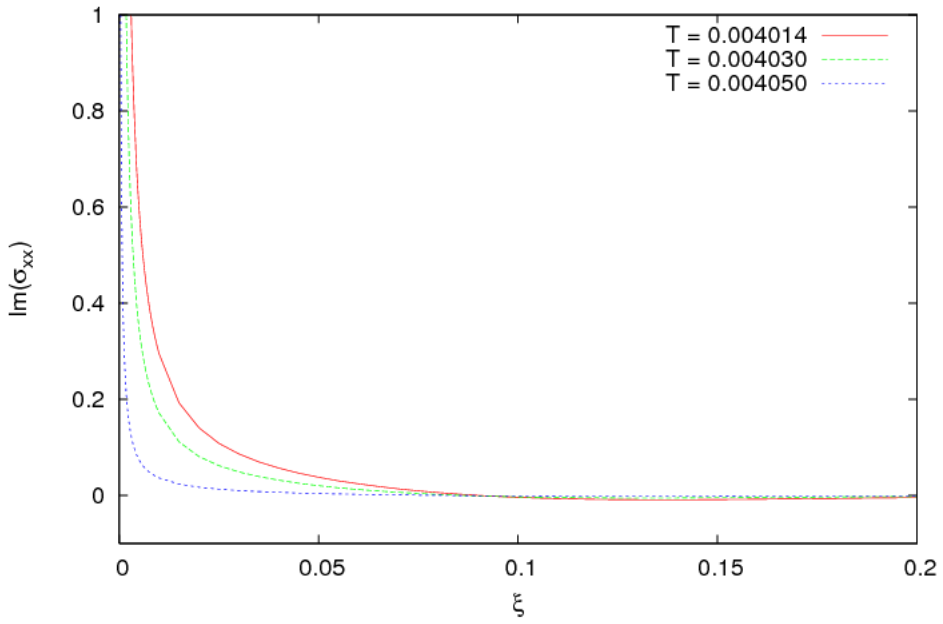

Figure 4.17: Plot of the imaginary part of the frequency dependent conductivity in the x direction for an $\mathfrak{su}(3)$ black hole with $l = 5$ at various temperatures. We find a divergence as $\xi \to 0$, and that the imaginary part of the conductivity approaches zero at large ξ, as we expect from a real superconductor.

superconductors. Our solutions can have a condensate, whose role is played by the $\mathfrak{su}(N)$ gauge field, below a certain critical temperature but not above. At the critical temperature, the "normal state" Reissner-Nordström solution admits an $\mathfrak{su}(N)$ perturbation. It is also the case that the superconducting solution (with a gauge field) is thermodynamically favourable over the Reissner-Nordström solution.

Furthermore, we have calculated the frequency dependent conductivity. In both the $\mathfrak{su}(2)$ and $\mathfrak{su}(3)$ cases, we find infinite D.C. conductivity, as well as a gap at non-zero frequency. Although there is an unphysical divergence in the conductivity at non-zero frequency for the $\mathfrak{su}(2)$ case, this is not the case for $\mathfrak{su}(3)$.

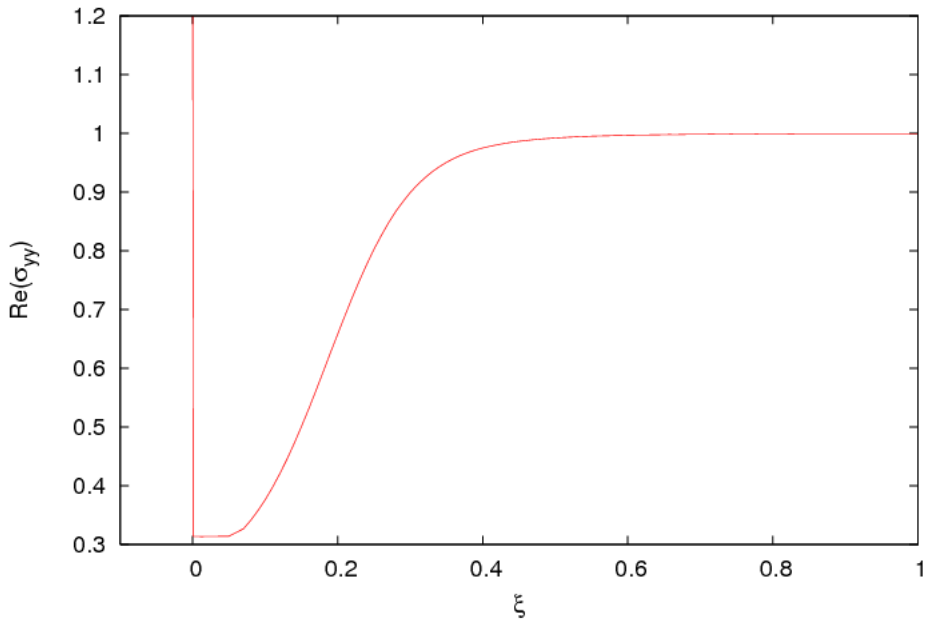

Figure 4.18: Plot of the real part of the frequency dependent conductivity in the y direction for an $\mathfrak{su}(3)$ black hole with $l = 5$ and $T = 0.004050$. The from is the same as in the x direction (and what we expect from a real superconductor), although as in the $\mathfrak{su}(2)$ case we find a larger gap at non-zero frequency than in the x direction.

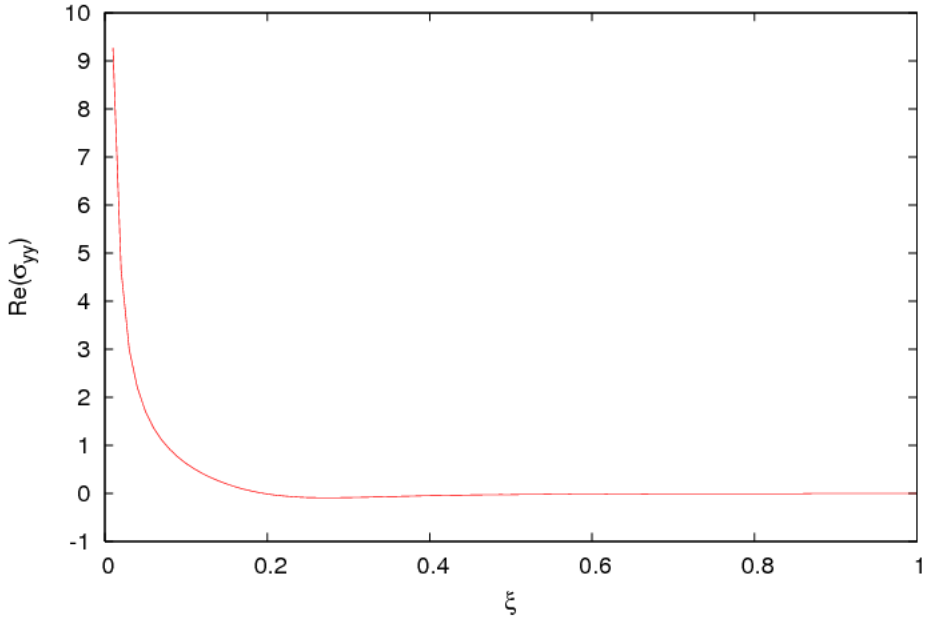

Figure 4.19: Plot of the imaginary part of the frequency dependent conductivity in the x direction for an $\mathfrak{su}(3)$ black hole with $l = 5$ and $T = 0.004050$. As in the x direction, we find a divergence as $\xi \to 0$, and that $Im(\sigma_{yy})$ approaches zero at large ξ.

Chapter 5

Conclusions

This thesis is concerned with static EYM black holes in AdS space, in the presence of an $\mathfrak{su}(N)$ gauge field. We studied black holes with purely magnetic gauge fields as well as dyonic black holes which carry both electric and magnetic charges. We considered both spherically symmetric and topological event horizons. There were two main motivations for this: firstly to check whether we can find stable black holes which satisfy the no-hair conjecture, and secondly to find gravitational analogues to superconductors in the context of the AdS/CFT correspondence.

In chapter 2 we studied spherically symmetric black holes with a purely magnetic gauge field in the context of the no-hair conjecture. After summarizing previous work on stability under linear perturbations, we looked at thermodynamic stability. We then went on to define the global charges carried by the black holes, and found both a non-divergent mass (which is non-trivial in asymptotically AdS space), and also expressions for the $N-1$ gauge invariant magnetic charges Q_j associated with the Yang-Mills field.

Although we found numerically that the black holes were not characterized by their mass and a single (effective) charge, we found evidence that they obey Bizon's modified no-hair conjecture, i.e. that stable black holes are characterized by their mass and global charges. We provided numerical evidence that the independent parameters required to characterize the black holes at infinity were the mass M and charges Q_j. Analytically, we argued that if $|\Lambda|$ is large, there is an approximate map between the parameters required to characterize the black holes at the event horizon and (M, Q_i).

Then, in chapter 3, we turned to spherically symmetric dyons, with both soliton

and black hole boundary conditions. We found the field equations and boundary conditions which generalised the $\mathfrak{su}(2)$ solutions of [18, 19] to $\mathfrak{su}(N)$, and found a method extending that of [8] to find numerical $\mathfrak{su}(3)$ solitons. We then presented numerical results for black holes and solitons with $\mathfrak{su}(2)$ and $\mathfrak{su}(3)$ gauge groups. Since a stability analysis is a work in progress [63], we did not investigate the dyons in the context of the no-hair conjecture. However, we did find that the nodeless region of the parameter space grows as $|\Lambda|$ increases, which is likely to be important for the stability analysis.

Finally, in chapter 4, we studied planar dyonic black holes as a candidate for an analogue to high temperature superconductors under the AdS/CFT correspondence. We generalised the $\mathfrak{su}(2)$ ansatze from [37, 38, 62] to $\mathfrak{su}(N)$. From the field equations we deduced that only the ansatz which is symmetric under rotations in the (x, y) plane gave a genuinely $\mathfrak{su}(N)$ field, rather than embedded $\mathfrak{su}(2)$.

We took the Reissner-Nordström solution as the normal phase, with the $\mathfrak{su}(N)$ gauge field acting as a superconducting condensate, and investigated some of the main properties of real superconducting materials. We found that, as expected, there is a critical temperature T_C at which the Reissner-Nordström solution admits an $\mathfrak{su}(N)$ perturbation. Solutions with a Yang-Mills field were found to exist below this critical temperature, and where they exist they are thermodynamically favourable over the Reissner-Nordström solutions.

We then computed the frequency dependent conductivity of the $\mathfrak{su}(2)$ and $\mathfrak{su}(3)$ solutions. In both cases we found the D.C. conductivity to be infinite, and at non-zero frequency we found a pseudogap in the conductivity between low and high frequencies. However, unlike in [38], for the rotationally symmetric ansatz we found an unphysical divergence in the conductivity at non-zero frequency in the $\mathfrak{su}(2)$ case. This arose from additional terms required to make the conductivity gauge invariant, as is required for observable quantities. No such terms were required in the $\mathfrak{su}(3)$ case, and we found an agreement in the form of the frequency and temperature dependent conductivity with real superconducting materials found experimentally in [13].

While we found that a certain subset of purely magnetic EYM black holes obey the modified no-hair conjecture, whether all do remains an open question, i.e. whether all stable EYM black holes are uniquely characterized by their global charges. It would also be interesting to investigate whether dyonic black holes also obey the modified no-hair conjecture, although this would require a stability analysis

to be carried out first.

With regard to the planar black holes with superconducting horizons, one would guess that larger gauge groups are thermodynamically favoured over smaller ones, i.e. that $\mathfrak{su}(4)$ solutions have lower free energy than those with an $\mathfrak{su}(3)$ gauge group. It may be possible to prove this in general. If this is the case, it may also be the case that solutions with larger gauge groups are better analogues to superconductors than those with smaller gauge groups. In addition, for the correspondence between $\mathfrak{su}(N)$ black holes and condensed matter systems to hold, it would be necessary to use the full string theory approach, rather than the classical approximation to the gravitational side which is taken here. We leave these questions for future work.

Appendix A

The Lie group SU(N) and Lie algebra $\mathfrak{su}(N)$

stuff

In this appendix we present a matrix representation of the generators of the Lie algebra $\mathfrak{su}(N)$, which generalises the Pauli matrices for $\mathfrak{su}(2)$ and Gell-Mann matrices for $\mathfrak{su}(3)$. The group $SU(N)$ has dimension N^2-1 (which is equal to the number of generators) and rank $N-1$ (which is equal to the number of diagonal traceless generators which make up the Cartan subalgebra).

The generators of the real Lie algebra of $\mathfrak{su}(2)$ given by $T_i = -\frac{i}{2}\sigma_i$, where σ_i are the Pauli matrices (we note here that other authors may take $\frac{1}{2}\sigma_i$ to be the generators of $\mathfrak{su}(2)$ as these are Hermitian, although in this case the coefficients are purely imaginary [68] - the important thing is that the charges are real). Explicitly they are

$$T_1 = -\frac{i}{2}\begin{pmatrix} 0 & 1 \\ 1 & 0 \end{pmatrix}, \qquad T_2 = -\frac{i}{2}\begin{pmatrix} 0 & -i \\ i & 0 \end{pmatrix}, \qquad T_3 = -\frac{i}{2}\begin{pmatrix} 1 & 0 \\ 0 & 1 \end{pmatrix}. \tag{A.1}$$

The Cartan subalgebra $\mathcal{X}$ of $\mathfrak{su}(2)$ is generated by T_3, so the elements X of $\mathcal{X}$ are given by $X = \rho T_3$ for some ρ.

The generators of $\mathfrak{su}(3)$ are similarly defined by $T_j = -\frac{i}{2}\lambda_j$, where λ_i are the

Gell-Mann matrices [68], so that

$$T_1 = -\frac{i}{2}\begin{pmatrix} 0 & 1 & 0 \\ 1 & 0 & 0 \\ 0 & 0 & 0 \end{pmatrix}, \qquad T_2 = -\frac{i}{2}\begin{pmatrix} 0 & -i & 0 \\ i & 0 & 0 \\ 0 & 0 & 0 \end{pmatrix},$$

$$T_3 = -\frac{i}{2}\begin{pmatrix} 1 & 0 & 0 \\ 0 & -1 & 0 \\ 0 & 0 & 0 \end{pmatrix}, \qquad T_4 = -\frac{i}{2}\begin{pmatrix} 0 & 0 & 1 \\ 0 & 1 & 0 \\ 1 & 0 & 0 \end{pmatrix},$$

$$T_5 = -\frac{i}{2}\begin{pmatrix} 0 & 0 & -i \\ 0 & 0 & 0 \\ i & 0 & 0 \end{pmatrix}, \qquad T_6 = -\frac{i}{2}\begin{pmatrix} 0 & 0 & 0 \\ 0 & 0 & 1 \\ 0 & 1 & 0 \end{pmatrix},$$

$$T_7 = -\frac{i}{2}\begin{pmatrix} 0 & 0 & 0 \\ 0 & 0 & -i \\ 0 & i & 0 \end{pmatrix}, \qquad T_8 = -\frac{i}{2\sqrt{3}}\begin{pmatrix} 1 & 0 & 0 \\ 0 & 1 & 0 \\ 0 & 0 & -2 \end{pmatrix}. \tag{A.2}$$

The Cartan subalgebra $\mathcal{X}$ of $\mathfrak{su}(3)$ is generated by T_3 and T_8, so the elements X of $\mathcal{X}$ are given by $X = \rho T_3 + \sigma T_8$ for some ρ and σ.

For $\mathfrak{su}(N)$, we note that there are three families of generators. Firstly there are the $N-1$ diagonal generators of the Cartan subalgebra, which we denote H_l, and define in a smiliar way to [20], using a slightly different normalisation:

$$[H_l]_{j,k} = -\frac{i}{\sqrt{2l(l+1)}}\left(\sum_{p=1}^{l}[\delta_{j,p}\delta_{k,p}] - l\delta_{j,l+1}\delta_{k,l+1}\right), \tag{A.3}$$

for $l = 1, .., N-1$. In the $\mathfrak{su}(2)$ case we have only H_1, which is equal to T_3 from (A.1), while in the $\mathfrak{su}(3)$ case we have H_1 and H_2, which are equal to T_3 and T_8 from (A.2) respectively. We split the remaining $N(N-1)$ generators into two groups. The first are complex and are of the form T_1, T_4 and T_6 from (A.2) for $\mathfrak{su}(3)$, which we denote $F_m^{(n)}$ and are

$$\left[F_m^{(n)}\right]_{j,k} = -\frac{i}{2}\left(\delta_{j,m}\delta_{k,m+n} + \delta_{j,m+n}\delta_{k,m}\right), \tag{A.4}$$

and the second, which are real, and are of the form T_2, T_5 and T_7 from (A.2) for

$\mathfrak{su}(3)$, which we denote $G_m^{(n)}$ and are

$$\left[G_m^{(n)}\right]_{j,k} = \frac{1}{2}\left(\delta_{j,m+n}\delta_{k,m} - \delta_{j,m}\delta_{k,m+n}\right). \tag{A.5}$$

The indices take the values $n = 1, 2, ..., N-1$, $m = 1, 2, ..., N-n$ to give the correct number of generators. Comparison with (A.2) yields, for $\mathfrak{su}(3)$,

$$\begin{aligned} &F_1^{(1)} = T_1, \qquad G_1^{(1)} = T_2, \qquad H_1 = T_3, \qquad F_1^{(2)} = T_4, \\ &G_1^{(2)} = T_5, \qquad F_2^{(1)} = T_6, \qquad G_2^{(1)} = T_7, \qquad H_2 = T_8, \end{aligned} \tag{A.6}$$

For the spherically symmetric black holes considered in chapters 2 and 3, we will consider the matrix

$$D = \mathrm{diag}(N-1, N-3, ..., 3-N, 1-N), \tag{A.7}$$

which can be written in terms of the generators of $\mathfrak{su}(N)$ as

$$D = \sum_{k=1}^{N-1} i\sqrt{2k(k+1)}H_k. \tag{A.8}$$

The non-zero commutation relations between the $F_m^{(n)}$, $G_m^{(n)}$, H_m and D which are used in this thesis are then:

$$[F_{k-1}, F_k] = \frac{1}{2}G_{k-1}^{(2)}, \quad [F_k, H_k] = -\sqrt{\frac{k+1}{2k}}G_k, \quad [F_k, H_{k-1}] = \sqrt{\frac{k-1}{2k}}G_k,$$

$$[F_k, G_k] = -\frac{1}{2k}\left(\sqrt{2k(k+1)}H_k - \sqrt{2k(k-1)}H_{k-1}\right),$$

$$[F_{k-1}, G_k] = -\frac{1}{2}F_{k-1}^{(2)}, \qquad [F_k, G_{k-1}] = \frac{1}{2}G_{k-1}^{(2)},$$

$$[G_{k-1}, G_k] = -\frac{1}{2}G_{k-1}^{(2)}, \quad [G_k, H_k] = \sqrt{\frac{k+1}{2k}}F_k, \quad [G_k, H_{k-1}] = -\sqrt{\frac{k-1}{2k}}F_k,$$

$$\left[F_k^{(2)}, H_k\right] = -\frac{1}{\sqrt{2k(k+1)}}G_k^{(2)}, \quad \left[F_{k+1}^{(2)}, H_k\right] = \sqrt{\frac{k}{2(k+1)}}G_{k+1}^{(2)},$$

$$\left[G_k^{(2)}, H_k\right] = \frac{1}{\sqrt{2k(k+1)}}F_k^{(2)}, \quad \left[G_{k+1}^{(2)}, H_k\right] = -\sqrt{\frac{k}{2(k+1)}}F_{k+1}^{(2)},$$

$$\left[F_k^{(2)}, H_{k+1}\right] = -\sqrt{\frac{k+2}{2(k+1)}}G_k^{(2)} \quad \left[G_k^{(2)}, H_{k+1}\right] = \sqrt{\frac{k+2}{2(k+1)}}F_k^{(2)},$$

$$\left[F_k, G_k^{(2)}\right] = -\frac{1}{2}F_{k+1}, \quad \left[F_{k+1}, G_k^{(2)}\right] = \frac{1}{2}F_k, \quad \left[F_k, G_{k+1}^{(2)}\right] = -\frac{1}{2}F_k^{(3)},$$

$$\left[F_{k+2}, G_k^{(2)}\right] = \frac{1}{2}F_k^{(3)}, \quad \left[F_k, F_k^{(2)}\right] = \frac{1}{2}G_{k+1}, \quad \left[F_{k+1}, F_k^{(2)}\right] = -\frac{1}{2}G_k,$$

$$\left[F_k, F_{k+1}^{(2)}\right] = \frac{1}{2}G_k^{(3)}, \quad \left[F_{k+2}, F_k^{(2)}\right] = -\frac{1}{2}G_k^{(3)}, \quad \left[G_k, F_k^{(2)}\right] = \frac{1}{2}F_{k+1},$$

$$\left[G_{k+1}, F_k^{(2)}\right] = -\frac{1}{2}F_k, \quad \left[G_k, F_{k+1}^{(2)}\right] = -\frac{1}{2}F_k^{(3)}, \quad \left[G_{k+1}, F_k^{(2)}\right] = \frac{1}{2}F_k^{(3)},$$

$$\left[G_k, G_k^{(2)}\right] = \frac{1}{2}G_{k+1}, \quad \left[G_{k+1}, G_k^{(2)}\right] = -\frac{1}{2}G_k, \quad \left[G_k, G_{k+1}^{(2)}\right] = -\frac{1}{2}G_k^{(3)},$$

$$\left[G_{k+2}, G_k^{(2)}\right] = \frac{1}{2}G_k^{(3)}, \quad [D, F_k] = 2iG_k, \quad [D, G_k] = -2iF_k \tag{A.9}$$

where $k = 1, 2, ..., N-1$.

Appendix B

The Einstein-Yang-Mills equations

[] In this appendix we derive the Einstein-Yang-Mills equations used in chapters 3 and 4. In each case, the first stage will be to find the components of the field strength tensor

$$F_{\mu\nu} = \partial_\mu A_\nu - \partial_\nu A_\mu + g\left[A_\mu, A_\nu\right], \tag{B.1}$$

for the gauge potential $A = A_\mu dx^\mu$, with coupling constant g. The components of (B.1), along with the Christoffel symbols

$$\Gamma^\alpha_{\beta\gamma} = \frac{1}{2} g^{\alpha\mu}\left(g_{\mu\beta,\gamma} + g_{\mu\gamma,\beta} - g_{\beta\gamma,\mu}\right), \tag{B.2}$$

where $g_{\mu\nu}$ is the metric tensor, then give the Yang-Mills equations

$$D_\mu F^{\mu\nu} = \partial_\mu F^{\mu\nu} + \Gamma^\mu_{\mu\alpha} F^{\alpha\nu} + \Gamma^\nu_{\mu\alpha} F^{\mu\alpha} + g\left[A_\mu, F^{\mu\nu}\right] = 0. \tag{B.3}$$

We can also find the components of the stress tensor using (B.1), which are given by

$$T_{\mu\nu} = F^a_{\mu\alpha} F^a_{\nu\beta} g^{\alpha\beta} - \frac{1}{4} g_{\mu\nu} F^a_{\alpha\beta} F^{a\alpha\beta}. \tag{B.4}$$

These in turn determine the Einstein equations, which are

$$R_{\mu\nu} - \frac{1}{2} g_{\mu\nu} R + \Lambda g_{\mu\nu} = 8\pi G T_{\mu\nu}. \tag{B.5}$$

§ B.1 Dyonic solutions

The spherically symmetric line element (3.1) is

$$ds^2 = -\sigma^2\mu\, dt^2 + r^2(d\theta^2 + \sin^2\,\theta d\phi^2) + \mu^{-1}dr^2, \tag{B.6}$$

with metric function (3.2)

$$\mu = 1 - \frac{2m(r)}{r} - \frac{\Lambda r^2}{3}. \tag{B.7}$$

In terms of the generators (A.3–A.5), the gauge potential (3.6) is

$$gA = \sum_{k=1}^{N-1}\left\{-h_k H_k\, dt - \omega_k G_k^{(1)} d\theta + \left[\omega_k F_k^{(1)}\sin\theta + \sqrt{\frac{k(k+1)}{2}}H_k\cos\theta\right]d\phi\right\}, \tag{B.8}$$

where h_k and ω_k depend on r only. Using (B.1) and the commutation relations (A.9), the components of the field strength tensor are

$$\begin{aligned}
F_{01} &= \frac{1}{g}\sum_{k=1}^{N-1}\left(\sqrt{\frac{k-1}{2k}}h_{k-1} - \sqrt{\frac{k+1}{2k}}h_{k+1}\right)\omega_k G_k^{(1)}, \quad F_{03} = \frac{1}{g}\sum_{k=1}^{N-1} h_k' H_k,\\
F_{02} &= \frac{\sin\theta}{g}\sum_{k=1}^{N-1}\left(\sqrt{\frac{k-1}{2k}}h_{k-1} - \sqrt{\frac{k+1}{2k}}h_{k}\right)\omega_k G_k^{(1)}, \quad F_{13} = \frac{1}{g}\sum_{k=1}^{N-1}\omega_k' G_k^{(1)},\\
F_{12} &= \frac{\sin\theta}{g}\sum_{k=1}^{N-1}\sqrt{2k(k+1)}\left(\frac{\omega_k^2}{k} - \frac{\omega_{k+1}^2}{k+1} - 1\right)H_k, \quad F_{23} = -\frac{\sin\theta}{g}\sum_{k=1}^{N-1}\omega_k' F_k^{(1)}.
\end{aligned} \tag{B.9}$$

Substituting (B.9) into equation (B.3) we obtain three Yang-Mills equations;

$$\begin{aligned}
0 \;=\; & \sum_{k=1}^{N-1}\left\{\frac{-2h_k'}{\sigma^2 r} + \frac{\sigma' h_k'}{\sigma^3} - \frac{h_k''}{\sigma^2}\right\}H_k\\
& + \sum_{k=1}^{N-1}\left\{\frac{\sqrt{2k(k+1)}}{\sigma^2\mu r^2}\frac{\omega_{k+1}^2}{k+1}\left(\sqrt{\frac{k}{2(k+1)}}h_k - \sqrt{\frac{k+2}{2(k+1)}}h_{k+1}\right)\right\}H_k\\
& + \sum_{k=1}^{N-1}\left\{\frac{\sqrt{2k(k+1)}}{\sigma^2\mu r^2}\frac{\omega_k^2}{k}\left(\sqrt{\frac{k+1}{2k}}h_k - \sqrt{\frac{k-1}{2k}}h_{k-1}\right)\right\}H_k,
\end{aligned} \tag{B.10}$$

$$
\begin{aligned}
0 &= \sum_{k=1}^{N-1}\left\{\frac{\mu\omega_k'}{r^2}\left(\frac{\sigma'}{\sigma}+\frac{\mu'}{\mu}\right)+\frac{\omega_k}{2r^4}\left(2+\omega_{k-1}^2-2\omega_k^2+\omega_{k+1}^2\right)\right\}G_k^{(1)} \\
&\quad+\sum_{k=1}^{N-1}\left\{\frac{\mu\omega_k''}{r^2}+\frac{\omega_k}{\sigma^2\mu r^2}\left(\sqrt{\frac{k+1}{2k}}h_k-\sqrt{\frac{k-1}{2k}}h_{k-1}\right)^2\right\}G_k^{(1)}, \quad \text{(B.11)}
\end{aligned}
$$

$$
\begin{aligned}
0 &= \sum_{k=1}^{N-1}\left\{\frac{\mu\omega_k'}{r^2}\left(\frac{\sigma'}{\sigma}+\frac{\mu'}{\mu}\right)+\frac{\omega_k}{2r^4}\left(2+\omega_{k-1}^2-2\omega_k^2+\omega_{k+1}^2\right)\right\}F_k^{(1)} \\
&\quad+\sum_{k=1}^{N-1}\left\{\frac{\mu\omega_k''}{r^2}+\frac{\omega_k}{\sigma^2\mu r^2}\left(\sqrt{\frac{k+1}{2k}}h_k-\sqrt{\frac{k-1}{2k}}h_{k-1}\right)^2\right\}F_k^{(1)}, \quad \text{(B.12)}
\end{aligned}
$$

while the fourth vanishes identically. Equations (B.11) and (B.12) are equivalent, giving two Yang-Mills equations:

$$
\begin{aligned}
h_k'' &= h_k'\left(\frac{\sigma'}{\sigma}-\frac{2}{r}\right)+\sqrt{\frac{2(k+1)}{k}}\frac{\omega_k^2}{\mu r^2}\left(\sqrt{\frac{k+1}{2k}}h_k-\sqrt{\frac{k-1}{2k}}h_{k-1}\right) \\
&\quad+\sqrt{\frac{2k}{k+1}}\frac{\omega_{k+1}^2}{\mu r^2}\left(\sqrt{\frac{k}{2(k+1)}}h_k-\sqrt{\frac{k+2}{2(k+1)}}h_{k+1}\right), \quad \text{(B.13)} \\
0 &= \omega_k''+\omega_k'\left(\frac{\sigma'}{\sigma}+\frac{\mu'}{\mu}\right)+\frac{\omega_k}{\sigma^2\mu^2}\left(\sqrt{\frac{k+1}{2k}}h_k-\sqrt{\frac{k-1}{2k}}h_{k-1}\right)^2 \\
&\quad+\frac{\omega_k}{\mu r^2}\left(1-\omega_k^2+\frac{1}{2}\left(\omega_{k-1}^2+\omega_{k+1}^2\right)\right). \quad \text{(B.14)}
\end{aligned}
$$

Substituting (B.9) into (B.4) gives the components of the field strength tensor

$$\begin{aligned}
T_{00} &= \frac{1}{g^2}\sum_{k=1}^{N-1}\left[\frac{\omega_k^2}{r^2}\left(\sqrt{\frac{k+1}{2k}}h_k - \sqrt{\frac{k-1}{2k}}h_{k-1}\right)^2 + \frac{\mu h_k'^2}{2}\right] \\
&\quad + \frac{1}{g^2}\sum_{k=1}^{N-1}\left[\frac{\sigma^2\mu^2\omega_k'^2}{r^2} + \frac{k(k+1)\sigma^2\mu}{4r^4}\left(1 - \frac{\omega_k^2}{k} + \frac{\omega_{k+1}^2}{k+1}\right)^2\right], \\
T_{11} &= \frac{1}{g^2}\sum_{k=1}^{N-1}\left[\frac{k(k+1)}{4r^2}\left(1 - \frac{\omega_k^2}{k} + \frac{\omega_{k+1}^2}{k+1}\right)^2 + \frac{r^2 h_k'^2}{2\sigma^2}\right], \\
T_{22} &= \frac{\sin^2\theta}{g^2}\sum_{k=1}^{N-1}\left[\frac{k(k+1)}{4r^2}\left(1 - \frac{\omega_k^2}{k} + \frac{\omega_{k+1}^2}{k+1}\right)^2 + \frac{r^2 h_k'^2}{2\sigma^2}\right], \\
T_{33} &= \frac{1}{g^2}\sum_{k=1}^{N-1}\left[\frac{\omega_k^2}{\sigma^2\mu^2 r^2}\left(\sqrt{\frac{k+1}{2k}}h_k - \sqrt{\frac{k-1}{2k}}h_{k-1}\right)^2 - \frac{h_k'^2}{2\sigma^2\mu}\right] \\
&\quad + \frac{1}{g^2}\sum_{k=1}^{N-1}\left[\frac{\omega_k'^2}{r^2} + \frac{k(k+1)}{4\mu r^4}\left(1 - \frac{\omega_k^2}{k} + \frac{\omega_{k+1}^2}{k+1}\right)^2\right],
\end{aligned} \tag{B.15}$$

with the corresponding Einstein tensor

$$G_{00} = \frac{2\sigma^2\mu m'}{r^2} - \frac{\Lambda\sigma^2\mu}{3} - \frac{2\sigma^2\mu m}{r^3} - \frac{\sigma^2\mu^2}{r^2}, \tag{B.16}$$

$$G_{11} = \frac{\mu r\sigma'}{\sigma} + \mu' r + \frac{3}{2}\frac{\mu' r^2\sigma'}{\sigma} + \frac{\mu r^2\sigma''}{\sigma} + \Lambda r^2 + \frac{\mu'' r^2}{2}, \tag{B.17}$$

$$G_{22} = \sin^2\theta\left(\frac{\mu r\sigma'}{\sigma} + \mu' r + \frac{3}{2}\frac{\mu' r^2\sigma'}{\sigma} + \frac{\mu r^2\sigma''}{\sigma} + \Lambda r^2 + \frac{\mu'' r^2}{2}\right), \tag{B.18}$$

$$G_{33} = \frac{\mu'}{\mu r} + \frac{2\sigma'}{r\sigma} + \frac{1}{r^2} + \frac{\Lambda}{\mu} - \frac{1}{\mu r^2}. \tag{B.19}$$

Rearranging (B.16), substituting for μ (B.7) and using (B.5) we find

$$\begin{aligned}
m' &= \frac{4\pi G r^2 T_{00}}{\sigma^2\mu} \\
&= \alpha^2\sum_{k=1}^{N-1}\left\{\frac{\omega_k^2}{\sigma^2\mu}\left(\sqrt{\frac{k+1}{2k}}h_k - \sqrt{\frac{k-1}{2k}}h_{k-1}\right)^2 + \frac{r^2 h_k'^2}{2\sigma^2}\right\} \\
&\quad + \alpha^2\sum_{k=1}^{N-1}\left\{\mu\omega_k'^2 + \frac{k(k+1)}{4r^2}\left(1 - \frac{\omega_k^2}{k} + \frac{\omega_{k+1}^2}{k+1}\right)^2\right\},
\end{aligned} \tag{B.20}$$

where $\alpha^2 = 4\pi G/g^2$. Similarly (B.19) yields

$$\begin{aligned}\sigma' &= \frac{4\pi G r T_{00}}{\sigma\mu^2} + 4\pi G r \sigma T_{33} \\ &\quad +\alpha^2 \sum_{k=1}^{N-1} \left\{ \frac{2\omega_k^2}{\sigma\mu^2 r} \left(\sqrt{\frac{k+1}{2k}} h_k - \sqrt{\frac{k-1}{2k}} h_{k-1} \right)^2 + \frac{2\sigma\omega_k'^2}{r} \right\}. \end{aligned} \tag{B.21}$$

The remaining Einstein equations are $G_{11} = 8\pi G T_{11}$ and $G_{22} = 8\pi G T_{22}$, which are equivalent and vanish identically using (B.20, B.21). Altogether the EYM equations are

$$\begin{aligned} m' &= \alpha^2 \sum_{k=1}^{N-1} \left\{ \frac{\omega_k^2}{\sigma^2\mu} \left(\sqrt{\frac{k+1}{2k}} h_k - \sqrt{\frac{k-1}{2k}} h_{k-1} \right)^2 + \frac{r^2 h_k'^2}{2\sigma^2} \right\} \\ &\quad +\alpha^2 \sum_{k=1}^{N-1} \left\{ \mu\omega_k'^2 + \frac{k(k+1)}{4r^2} \left(1 - \frac{\omega_k^2}{k} + \frac{\omega_{k+1}^2}{k+1} \right)^2 \right\}, \\ \sigma' &= \alpha^2 \sum_{k=1}^{N-1} \left\{ \frac{2\omega_k^2}{\sigma\mu^2 r} \left(\sqrt{\frac{k+1}{2k}} h_k - \sqrt{\frac{k-1}{2k}} h_{k-1} \right)^2 + \frac{2\sigma\omega_k'^2}{r} \right\}, \\ h_k'' &= h_k' \left(\frac{\sigma'}{\sigma} - \frac{2}{r} \right) + \sqrt{\frac{2(k+1)}{k}} \frac{\omega_k^2}{\mu r^2} \left(\sqrt{\frac{k+1}{2k}} h_k - \sqrt{\frac{k-1}{2k}} h_{k-1} \right) \\ &\quad +\sqrt{\frac{2k}{k+1}} \frac{\omega_{k+1}^2}{\mu r^2} \left(\sqrt{\frac{k}{2(k+1)}} h_k - \sqrt{\frac{k+2}{2(k+1)}} h_{k+1} \right) \\ 0 &= \omega_k'' + \omega_k' \left(\frac{\sigma'}{\sigma} + \frac{\mu'}{\mu} \right) + \frac{\omega_k}{\sigma^2\mu^2} \left(\sqrt{\frac{k+1}{2k}} h_k - \sqrt{\frac{k-1}{2k}} h_{k-1} \right)^2 \\ &\quad + \frac{\omega_k}{\mu r^2} \left(1 - \omega_k^2 + \frac{1}{2} \left(\omega_{k-1}^2 + \omega_{k+1}^2 \right) \right). \end{aligned} \tag{B.22}$$

§ B.2 Planar dyonic black holes

We begin with the gauge potential

$$gA = gA_\mu dx^\mu = -\sum_{l=1}^{N-1} h_l H_l \, dt - \sum_{m=1}^{N-1} \omega_m F_m^{(1)} dx - \zeta \sum_{m=1}^{N-1} \omega_m G_m^{(1)} dy, \tag{B.23}$$

and planar line element

$$ds^2 = -\sigma^2\mu\, dt^2 + r^2 f^2 dx^2 + \frac{r^2}{f^2}dy^2 + \mu^{-1}dr^2, \tag{B.24}$$

where

$$\mu = -\frac{2m(r)}{r} - \frac{\Lambda r^2}{3}. \tag{B.25}$$

Using (B.1), and the commutation relations (A.9), the components of the field strength tensor are

$$\begin{aligned}
F_{01} &= \frac{1}{g}\sum_{k=1}^{N-1}\left(\sqrt{\frac{k+1}{2k}}h_k - \sqrt{\frac{k-1}{2k}}h_{k-1}\right)\omega_k G_k^{(1)}, \quad F_{03} = \frac{1}{g}\sum_{k=1}^{N-1} h_k' H_k, \\
F_{02} &= \frac{\zeta}{g}\sum_{k=1}^{N-1}\left(\sqrt{\frac{k-1}{2k}}h_{k-1} - \sqrt{\frac{k+1}{2k}}h_k\right)\omega_k F_k^{(1)}, \quad F_{13} = \frac{i}{2g}\sum_{k=1}^{N-1}\omega_k' F_k^{(1)}, \\
F_{12} &= \frac{\zeta}{g}\sum_{k=1}^{N-1}\sqrt{2k(k+1)}\left(\frac{\omega_k^2}{k} - \frac{\omega_{k+1}^2}{k+1}\right)H_k, \quad F_{23} = \frac{i\zeta}{2g}\sum_{k=1}^{N-1}\omega_k' G_k^{(1)}.
\end{aligned} \tag{B.26}$$

Substituting (B.26) into equation (B.3) we obtain four Yang-Mills equations;

$$\begin{aligned}
0 &= \sum_{k=1}^{N-1}\left\{\frac{-2h_k(r)'}{\sigma^2 r} + \frac{\sigma' h_k'}{\sigma^3} - \frac{h_k''}{\sigma^2}\right\}H_k \\
&\quad + \sum_{k=1}^{N-1}\left\{\frac{\sqrt{2k(k+1)}}{2\sigma^2\mu r^2}\frac{\omega_{k+1}^2}{k+1}\left(\sqrt{\frac{k}{2(k+1)}}h_k - \sqrt{\frac{k+2}{2(k+1)}}h_{k+1}\right)\left(\frac{1}{f^2} + \zeta^2 f^2\right)\right\}H_k \\
&\quad + \sum_{k=1}^{N-1}\left\{\frac{\sqrt{2k(k+1)}}{2\sigma^2\mu r^2}\frac{\omega_k^2}{k}\left(\sqrt{\frac{k+1}{2k}}h_k - \sqrt{\frac{k-1}{2k}}h_{k-1}\right)\left(\frac{1}{f^2} + \zeta^2 f^2\right)\right\}H_k, \quad \text{(B.27)} \\
0 &= \sum_{k=1}^{N-1}\left\{\frac{\mu\omega_k'}{f^2 r^2}\left(\frac{\sigma'}{\sigma} + \frac{\mu'}{\mu} - \frac{2f'}{f}\right) + \frac{\omega_k}{2r^4}\left(\omega_{k-1}^2 - 2\omega_k^2 + \omega_{k+1}^2\right)\right\}F_k^{(1)} \\
&\quad + \sum_{k=1}^{N-1}\left\{\frac{\mu\omega_k''}{r^2 f^2} + \frac{\omega_k}{\sigma^2\mu f^2 r^2}\left(\sqrt{\frac{k+1}{2k}}h_k - \sqrt{\frac{k-1}{2k}}h_{k-1}\right)^2\right\}F_k^{(1)}, \quad \text{(B.28)}
\end{aligned}$$

$$
\begin{aligned}
0 &= \zeta \sum_{k=1}^{N-1} \left\{ \frac{\omega_k' \mu f^2}{r^2} \left(\frac{\sigma'}{\sigma} + \frac{\mu'}{\mu} + \frac{2f'}{f} \right) + \frac{\zeta^2 \omega_k}{2r^4} \left(\omega_{k-1}^2 - 2\omega_k^2 + \omega_{k+1}^2 \right) \right\} F_k^{(1)} \\
&\quad + \zeta \sum_{k=1}^{N-1} \left\{ \frac{f^2 \mu \omega_k''}{r^2} + \frac{f^2 \omega_k}{\sigma^2 \mu r^2} \left(\sqrt{\frac{k+1}{2k}} h_k - \sqrt{\frac{k-1}{2k}} h_{k-1} \right)^2 \right\} F_k^{(1)}, \quad \text{(B.29)} \\
0 &= \frac{\mu}{4r^2} \sum_{k=1}^{N-1} \left(\omega_k \omega_{k+1}' - \omega_{k+1} \omega_k' \right) \left(\frac{1}{f^2} - \zeta^2 f^2 \right) i G_k^{(2)}. \quad \text{(B.30)}
\end{aligned}
$$

We note that equation (B.29) is non-trivial only if $\zeta = 1$, in which case we have $f = 1$, and (B.29) reduces to (B.28) in the $\zeta = f = 1$ case. By considering the components of the matrices $F_k^{(1)}$, $G_k^{(2)}$ and H_k we can split these four equations into two Yang-Mills equations which govern ω_k and h_k;

$$
\begin{aligned}
h_k'' &= h_k' \left(\frac{\sigma'}{\sigma} - \frac{2}{r} \right) \\
&\quad + \frac{\sqrt{2k(k+1)}}{2\mu r^2} \frac{\omega_k^2}{k} \left(\sqrt{\frac{k+1}{2k}} h_k - \sqrt{\frac{k-1}{2k}} h_{k-1} \right) \left(\frac{1}{f^2} + \zeta^2 f^2 \right) \\
&\quad + \frac{\sqrt{2k(k+1)}}{2\mu r^2} \frac{\omega_{k+1}^2}{k+1} \left(\sqrt{\frac{k}{2(k+1)}} h_k - \sqrt{\frac{k+2}{2(k+1)}} h_{k+1} \right) \left(\frac{1}{f^2} + \zeta^2 f^2 \right), \quad \text{(B.31)} \\
0 &= \omega_k'' + \omega_k' \left(\frac{\sigma'}{\sigma} + \frac{\mu'}{\mu} - \frac{2f'}{f} \right) + \frac{\omega_k}{\sigma^2 \mu^2} \left(\sqrt{\frac{k+1}{2k}} h_k - \sqrt{\frac{k-1}{2k}} h_{k-1} \right)^2 \\
&\quad + \frac{\zeta^2 f^2 \omega_k^2}{2\mu r^2} \left(\omega_{k-1}^2 - 2\omega_k^2 + \omega_{k+1}^2 \right), \quad \text{(B.32)}
\end{aligned}
$$

and a constraint equation;

$$
0 = \left(\omega_k \omega_{k+1}' - \omega_{k+1} \omega_k' \right) \left(\frac{1}{f^2} - \zeta^2 f^2 \right), \quad \text{(B.33)}
$$

where $k = 1, 2, ..., N-1$ and $\omega_0 = \omega_N = 0$. The constraint equation is satisfied automatically for $\zeta = 1$, while for $\zeta = 0$, we have

$$
\omega_k \omega_{k+1}' - \omega_{k+1} \omega_k' = 0, \quad \text{(B.34)}
$$

which is solved by

$$
\frac{\omega_k}{\omega_{k+1}} = \frac{\omega_k'}{\omega_{k+1}'}. \quad \text{(B.35)}
$$

This means that all ω_k must be scalar multiples of each other (assuming all ω_k are non-zero). In the $N = 2$ case, equations (B.31) and (B.32) reduce to the $d = 4$ Yang-Mills equations in [62], where taking $\zeta = 1$ corresponds to ansatz I, and $\zeta = 0$ corresponds to ansatz II. The constraint equation (B.33) vanishes in the $N = 2$ case since we have $h_2 = \omega_2 = 0$.

The components of the stress tensor (B.4) are

$$T_{00} = \frac{1}{g^2}\sum_{k=1}^{N-1}\left[\frac{\omega_k^2}{2r^2}\left(\sqrt{\frac{k+1}{2k}}h_k - \sqrt{\frac{k-1}{2k}}h_{k-1}\right)^2\left(\frac{1}{f^2}+\zeta^2 f^2\right) + \frac{\mu h_k'^2}{2}\right] + \frac{1}{g^2}\sum_{k=1}^{N-1}\left[\frac{\sigma^2\mu^2\omega_k'^2}{2r^2}\left(\frac{1}{f^2}+\zeta^2 f^2\right) + \frac{\zeta^2 k(k+1)\sigma^2\mu}{4r^4}\left(\frac{\omega_k^2}{k} - \frac{\omega_{k+1}^2}{k+1}\right)^2\right], \quad \text{(B.36)}$$

$$T_{11} = \frac{1}{g^2}\sum_{k=1}^{N-1}\left[\frac{\omega_k^2}{2\sigma^2\mu}\left(\sqrt{\frac{k+1}{2k}}h_k - \sqrt{\frac{k-1}{2k}}h_{k-1}\right)^2\left(\zeta^2 f^4 - 1\right) + \frac{f^2 r^2 h_k'^2}{2\sigma^2}\right] + \frac{1}{g^2}\sum_{k=1}^{N-1}\left[\frac{\mu\omega_k'^2}{2}\left(1-\zeta^2 f^2\right) + \frac{\zeta^2 f^2 k(k+1)}{4r^2}\left(\frac{\omega_k^2}{k} - \frac{\omega_{k+1}^2}{k+1}\right)^2\right], \quad \text{(B.37)}$$

$$T_{22} = \frac{1}{g^2}\sum_{k=1}^{N-1}\left[\frac{\omega_k^2}{2\sigma^2\mu}\left(\sqrt{\frac{k+1}{2k}}h_k - \sqrt{\frac{k-1}{2k}}h_{k-1}\right)^2\left(\frac{1}{f^4} - \zeta^2\right) + \frac{r^2 h_k'^2}{2\sigma^2 f^2}\right] + \frac{1}{g^2}\sum_{k=1}^{N-1}\left[\frac{\mu\omega_k'^2}{2}\left(\zeta^2 - \frac{1}{f^4}\right) + \frac{\zeta^2 k(k+1)}{4f^2 r^2}\left(\frac{\omega_k^2}{k} - \frac{\omega_{k+1}^2}{k+1}\right)^2\right], \quad \text{(B.38)}$$

$$T_{33} = \frac{1}{g^2}\sum_{k=1}^{N-1}\left[\frac{\omega_k^2}{2\sigma^2\mu^2 r^2}\left(\sqrt{\frac{k+1}{2k}}h_k - \sqrt{\frac{k-1}{2k}}h_{k-1}\right)^2\left(\frac{1}{f^2}+\zeta^2 f^2\right) - \frac{h_k'^2}{2\sigma^2\mu}\right] + \frac{1}{g^2}\sum_{k=1}^{N-1}\left[\frac{\omega_k'^2}{2r^2}\left(\frac{1}{f^2}+\zeta^2 f^2\right) + \frac{\zeta^2 k(k+1)}{4\mu r^4}\left(\frac{\omega_k^2}{k} - \frac{\omega_{k+1}^2}{k+1}\right)^2\right], \quad \text{(B.39)}$$

while the corresponding components of the Einstein tensor are

$$G_{00} = \frac{2\sigma^2\mu m'}{r^2} - \frac{\Lambda\sigma^2\mu}{3} - \frac{2\sigma^2\mu m}{r^3} - \frac{\sigma^2\mu^2}{r^2} - \frac{\sigma^2\mu^2 f'^2}{f^2}, \tag{B.40}$$

$$G_{11} = \frac{f^2\mu r\sigma'}{\sigma} - \frac{ff'\mu r^2\sigma'}{\sigma} + f^2\mu' r - ff'\mu' r^2 + 2f'\mu r^2 - 2ff'\mu r - ff''\mu r^2 + \frac{3}{2}\frac{f^2\mu' r^2\sigma'}{\sigma} + \frac{f^2\mu r^2\sigma''}{\sigma} + \Lambda f^2 r^2 + \frac{f^2\mu'' r^2}{2} + \frac{f^2\mu r^2\sigma''}{\sigma}, \tag{B.41}$$

$$G_{22} = \frac{\mu r\sigma'}{f^2\sigma} + \frac{f'\mu r^2\sigma'}{f^3\sigma} + \frac{\mu' r}{f^2} + \frac{f'\mu' r^2}{f^3} + \frac{2f'\mu r}{f^3} + \frac{f''\mu r^2}{f^3} + \frac{3}{2}\frac{\mu' r^2\sigma'}{f^2\sigma} + \frac{\Lambda r^2}{f^2} + \frac{\mu'' r^2}{2f^2} + \frac{\mu r^2\sigma''}{f^2\sigma}, \tag{B.42}$$

$$G_{33} = \frac{\mu'}{\mu r} - \frac{f'^2}{f^2} + \frac{2\sigma'}{r\sigma} + \frac{1}{r^2} + \frac{\Lambda}{\mu}. \tag{B.43}$$

Using (B.25) we can cancel three of the terms in (B.40), and rearranging gives

$$m' = \frac{\mu r^2 f'^2}{2f^2} + \frac{r^2 G_{00}}{2\sigma^2\mu}, \tag{B.44}$$

which implies that

$$\mu' = \frac{2m}{r^2} - \frac{2\Lambda r}{3} - \frac{\mu r f'^2}{f^2} + \frac{rG_{00}}{\sigma^2\mu}. \tag{B.45}$$

Rearranging (B.43) and substituting for μ' using (B.45) gives

$$\sigma' = \frac{r\sigma f'^2}{f^2} + \frac{rG_{00}}{2\sigma\mu^2} + \frac{r\sigma G_{33}}{2}. \tag{B.46}$$

Finally, by looking at the last two terms in equations (B.41) and (B.42) we can see that by taking $G_{11} - f^4 G_{22}$ we can eliminate both the σ'' and μ'' terms. After some cancellations we then obtain

$$f'' = \frac{f^3}{2\mu r^2}\left(G_{22} - \frac{G_{11}}{f^4}\right) - f'\left(\frac{\sigma'}{\sigma} + \frac{\mu'}{\mu} + \frac{2}{r} - \frac{f'}{f}\right), \tag{B.47}$$

giving Einstein equations for m', σ' and f''. We are now in a position to substitute for $G_{\mu\nu}$ using our expressions (B.36–B.39) and $G_{\mu\nu} = 8\pi G T_{\mu\nu}$, which gives the field

equations

$$\begin{aligned} m' &= \frac{\mu r^2 f'^2}{2f^2} + \alpha^2 \sum_{k=1}^{N-1} \left\{ \frac{\omega_k^2}{2\sigma^2 \mu} \left(\sqrt{\frac{k+1}{2k}} h_k - \sqrt{\frac{k-1}{2k}} h_{k-1} \right)^2 \left(\frac{1}{f^2} + \zeta^2 f^2 \right) \right\} \\ &\quad + \alpha^2 \sum_{k=1}^{N-1} \left\{ \frac{r^2 h_k'^2}{2\sigma^2} + \frac{\mu \omega_k'^2}{2} \left(\frac{1}{f^2} + \zeta^2 f^2 \right) + \frac{k(k+1)\zeta^2}{4r^2} \left(\frac{\omega_k^2}{k} - \frac{\omega_{k+1}^2}{k+1} \right)^2 \right\}, \quad \text{(B.48)} \\ \sigma' &= \frac{r\sigma f'^2}{f^2} + \alpha^2 \sum_{k=1}^{N-1} \left\{ \frac{\omega_k^2}{2\sigma \mu^2 r} \left(\sqrt{\frac{k+1}{2k}} h_k - \sqrt{\frac{k-1}{2k}} h_{k-1} \right)^2 \left(\frac{1}{f^2} + \zeta^2 f^2 \right) \right\}, \\ &\quad + \alpha^2 \sum_{k=1}^{N-1} \left\{ \frac{\sigma \omega_k'^2}{r} \left(\frac{1}{f^2} + \zeta^2 f^2 \right) \right\}, \quad \text{(B.49)} \\ f'' &= \alpha^2 \left(\frac{1}{f^2} - \zeta^2 f^2 \right) \sum_{k=1}^{N-1} \left\{ \frac{2\omega_k^2 h_k^2}{k(k+1)\sigma^2 \mu^2 r^2} - \frac{\omega_k'^2}{r^2} \right\} \\ &\quad - f' \left(\frac{\sigma'}{\sigma} + \frac{\mu'}{\mu} + \frac{2}{r} - \frac{f'}{f} \right), \quad \text{(B.50)} \end{aligned}$$

where $\alpha^2 = \frac{4\pi G}{g^2}$. We note that in the $N = 2$ case, these equations reduce to the $d = 4$ case in [62], with $\zeta = 1$ corresponding to ansatz I, and $\zeta = 0$ corresponding to ansatz II. Our ansatz also satisfies the symmetry equations in the $\zeta = 1$ case, and there are no inconsistencies in the field equations.

B.2.1 Perturbations of the Reissner-Nordström solution

The gauge potential is

$$A = -\frac{1}{g} \sum_l \left[h_{l,0} + \delta h_l(r) \right] H_l dt - \frac{1}{g} \sum_m \delta \omega_m(r) F_m^{(1)} dx - \frac{1}{g} \sum_n \delta \omega_n(r) G_n^{(1)} dy \quad \text{(B.51)}$$

where $h_{l,0}$ are the equilibrium values of h_l from section 4.5.2. The line element is given by

$$\begin{aligned} ds^2 &= -\left[1 + \delta\sigma(r) \right]^2 \left[\mu_0(r) + \delta\mu(r) \right] dt^2 \\ &\quad + r^2 dx^2 + r^2 dy^2 + \left[\mu_0(r) + \delta\mu(r) \right]^{-1} dr^2, \\ &\approx -\left[\mu_0(r) + \delta\mu(r) + 2\mu_0(r)\delta\sigma(r) \right] dt^2 \\ &\quad + r^2 dx^2 + r^2 dy^2 + \frac{\mu_0(r) - \delta\mu(r)}{\mu_0(r)^2} dr^2, \quad \text{(B.52)} \end{aligned}$$

where

$$\mu_0(r) = -\frac{2m_0(r)}{r} - \frac{\Lambda r^2}{r}, \qquad \delta\mu(r) = -\frac{2\delta m(r)}{r}. \tag{B.53}$$

The equilibrium mass function $m_0(r)$ is given by

$$m_0(r) = m_0^{RN} - \frac{\alpha_{RN}^2 q^2}{2r}. \tag{B.54}$$

To leading order in the perturbations, the components of the field strength tensor are then given by

$$F_{01} = \frac{1}{g}\sum_{k=1}^{N-1}\left(\sqrt{\frac{k+1}{2k}}h_{k,0} - \sqrt{\frac{k-1}{2k}}h_{k-1,0}\right)\delta\omega_k\, G_k^{(1)}, \tag{B.55}$$

$$F_{02} = \frac{a}{g}\sum_{k=1}^{N-1}\left(\sqrt{\frac{k-1}{2k}}h_{k-1,0} - \sqrt{\frac{k+1}{2k}}h_{k,0}\right)\delta\omega_k\, F_k^{(1)}, \tag{B.56}$$

$$F_{03} = \frac{1}{g}\sum_{k=1}^{N-1}\left(h'_{k,0} + \delta h'_k\right) H_k, \tag{B.57}$$

$$F_{12} = 0, \tag{B.58}$$

$$F_{13} = \frac{1}{g}\sum_{k=1}^{N-1}\delta\omega'_k F_k^{(1)}, \tag{B.59}$$

$$F_{23} = \frac{a}{g}\sum_{k=1}^{N-1}\delta\omega'_k G_k^{(1)}, \tag{B.60}$$

where a prime denotes differentiation with respect to r. Since we are considering only terms which are first order in $\delta\omega_k$ and δh_k, only the F_{03} component contributes

to the stress tensor, which then has components

$$\begin{aligned}
T_{00} &\approx \frac{(\mu_0+\delta\mu)}{2g^2}\sum_{k=1}^{N-1}\left(h'_{k,0}+\delta h'_k\right)^2 \\
&\approx \frac{1}{2g^2}\sum_{k=1}^{N-1}\left[h'^2_{k,0}\left(\mu_0+\delta\mu\right)+2\mu_0 h_{k,0}\delta h_k\right], \qquad \text{(B.61)}\\
T_{11} &\approx \frac{r^2(1+\delta f)^2}{2g^2(1+\delta\sigma)^2}\sum_{k=1}^{N-1}\left(h'_{k,0}+\delta h'_k\right)^2 \\
&\approx \frac{r^2}{g^2\left(1+\delta\sigma\right)^2}\sum_{k=1}^{N-2}\left[h'^2_{k,0}\left(1+2\delta f\right)+2h_{k,0}\delta f\right], \qquad \text{(B.62)}\\
T_{22} &\approx \frac{r^2}{2g^2(1+\delta\sigma)^2}\sum_{k=1}^{N-1}\left(h'_{k,0}+\delta h'_k\right)^2 \\
&\approx \frac{r^2}{g^2\left(1+2\delta f+2\delta\sigma\right)}\sum_{k=1}^{N-2}\left(h'^2_{k,0}+2h'_{k,0}\delta h'_k\right), \qquad \text{(B.63)}\\
T_{33} &\approx -\frac{1}{2g^2(1+\delta\sigma)^2(\mu_0+\delta\mu)}\sum_{k=1}^{N-1}\left(h'_{k,0}+\delta h'_k\right)^2 \\
&\approx -\frac{1}{2g^2\left(\mu_0+\delta\mu+2\mu_0\delta\sigma\right)}\sum_{k=1}^{N-2}\left(h'^2_{k,0}+2h'_{k,0}\delta h'_k\right). \qquad \text{(B.64)}
\end{aligned}$$

The corresponding components of the Einstein tensor are

$$\begin{aligned}
G_{00} &= -(\mu_0+\delta\mu)(1+\delta\sigma)^2\left(\frac{\mu'_0+\delta\mu'}{r}+\frac{\mu_0+\delta\mu}{r^2}+\Lambda\right) \\
&= -\frac{1}{r^2}\left(r\mu_0\mu'_0+r\mu_0\delta\mu'+\mu_0^2+\mu_0\delta\mu+2r\mu_0\mu'_0\delta\sigma+2\mu_0^2\delta\sigma\right) \\
&\quad -\frac{1}{r^2}\left(r\mu'_0\delta\mu+\mu_0\delta\mu\right)-\Lambda\left(\mu_0+\delta\mu+2\mu_0\delta\sigma\right), \qquad \text{(B.65)}\\
G_{03} &= -\frac{\dot{\delta\mu}}{(\mu_0+\delta\mu)r}, \qquad \text{(B.66)}\\
G_{11} &= \frac{r\mu_0\delta\sigma'}{1+\delta\sigma}+\mu_0\mu'_0+\mu_0\delta\mu'+\frac{3}{2}\frac{r^2\mu'_0\delta\sigma'}{1+\delta\sigma}+\frac{r^2\mu_0\delta\sigma''}{1+\delta\sigma}+\frac{r^2\mu''_0}{2} \\
&\quad +\frac{\Lambda r^2}{\left(1+\delta f(r,t)\right)^2}, \qquad \text{(B.67)}
\end{aligned}$$

$$
\begin{aligned}
G_{22} &= \frac{r\mu_0\delta\sigma'}{1+\delta\sigma} + \mu_0\mu_0' + \mu_0\delta\mu' + \frac{3}{2}\frac{r^2\mu_0'\delta\sigma'}{1+\delta\sigma} + \frac{r^2\mu_0\delta\sigma''}{1+\delta\sigma} + \frac{r^2\mu_0''}{2} \\
&\quad + \frac{r^2\ddot{\delta\mu}}{2(\mu_0^2 + 2\mu_0\delta\mu + 2\mu_0^2\delta\sigma)} + \Lambda r^2\left(1+\delta f(r,t)\right)^2, \qquad \text{(B.68)} \\
G_{33} &= \frac{1}{r^2}\left(\frac{r(\mu_0'+\delta\mu')}{\mu_0+\delta\mu} + \frac{2r\delta\sigma'}{1+\delta\sigma} + 1\right) + \Lambda\left(\mu_0(r) + \delta\mu(r,t)\right)^{-1}, \qquad \text{(B.69)}
\end{aligned}
$$

to leading order, and are related to the components of the stress tensor by the Einstein equation

$$G_{\mu\nu} = 8\pi G T_{\mu\nu}. \qquad \text{(B.70)}$$

Since the stress tensor has no off diagonal components, it is clear from (B.66) that $\dot{\delta\mu} = 0$, i.e. $\delta\mu$ and therefore δm are functions of r only. Substituting for μ_0 and $\delta\mu$ from (B.53) into (B.65) and rearranging gives

$$
\begin{aligned}
\delta m' &= \frac{r^2 G_{00}}{2(\mu + \delta\mu + 2\mu\delta\sigma)} - m_0' \\
&= \frac{\alpha^2 r^2}{1+2\delta\sigma}\sum_{k=1}^{N-1}\left(h_{k,0}'^2 + 2h_{k,0}'\delta h_k'\right) - m_0'. \qquad \text{(B.71)}
\end{aligned}
$$

Combining equations (B.65) and (B.69) and rearranging gives

$$
\begin{aligned}
\delta\sigma' &= \frac{r(1+\delta\sigma)}{2}G_{33} + \frac{r}{2(\mu_0+\delta\mu)^2(1+\delta\sigma)}G_{00} \\
&= 4\pi G r(1+\delta\sigma)T_{33} + \frac{4\pi G r T_{00}}{(\mu_0+\delta\mu)^2(1+\delta\sigma)} \\
&= 0. \qquad \text{(B.72)}
\end{aligned}
$$

Using the ansatz (B.51), the line element (B.52) and the components of the field strength tensor (B.55 – B.60), we can construct the Yang-Mills equations, which are approximately given by:

$$
\begin{aligned}
0 &= \frac{1}{g}\sum_{k=1}^{N-1}\left[\frac{2(h_{k,0}' - \delta h_k')}{r} - \frac{h_{k,0}'}{1+\delta\sigma} + h_{k,0}'' + \delta h_k''\right]H_k, \qquad \text{(B.73)} \\
0 &= \frac{1}{g}\sum_{k=1}^{N-1}\left[\frac{\mu\delta\omega''}{r^2} - \frac{\ddot{\delta\omega}}{\mu_0+\delta\mu+2\mu_0\delta\sigma} + \frac{\mu_0'\delta\omega_k'}{r^2}\right]F_k^{(1)} \\
&\quad + \frac{1}{g}\sum_{k=1}^{N-1}\left[\frac{\delta\omega_k}{r^2(\mu+\delta\mu+\mu\delta\sigma)}\left(\sqrt{\frac{k+1}{2k}}h_k - \sqrt{\frac{k-1}{2k}}h_{k-1}\right)\right]F_k^{(1)}. \qquad \text{(B.74)}
\end{aligned}
$$

By considering the components of the matrices $F_k^{(1)}$ and H_k we then have

$$\begin{aligned} 0 &= \delta\omega_k'' + \left(\frac{\delta\sigma'}{1+\delta\sigma} + \frac{\mu'+\delta\mu'}{\mu+\delta\mu}\right)\delta\omega_k' \\ &\quad + \frac{\delta\omega_k}{\mu+\delta\mu+\mu\delta\sigma}\left(\sqrt{\frac{k+1}{2k}}h_k - \sqrt{\frac{k-1}{2k}}h_{k-1}\right), \qquad \text{(B.75)} \\ \delta h_k'' &= h_{k,0}'\left(\frac{\delta\sigma'}{1+\delta\sigma} - \frac{2}{r}\right) - \frac{2}{r}\delta h_k' - h_{k,0}''. \qquad \text{(B.76)} \end{aligned}$$

B.2.2 The conductivity

The gauge potential (4.128) is

$$\begin{aligned} gA &= -\sum_{l=1}^{N-1}\left(h_l H_l + e^{-i\xi t}\delta u_l F_l^{(1)} + e^{-i\xi t}\delta v_l G_l^{(1)}\right)dt \\ &\quad -\sum_{m=1}^{N-1}\left(\omega_m F_m^{(1)} + e^{-i\xi t}\delta h_{1,m} H_m\right)dx \\ &\quad -\sum_{n=1}^{N-1}\left(\omega_n G_n^{(1)} + e^{-i\xi t}\delta h_{2,n} H_n\right)dy, \qquad \text{(B.77)} \end{aligned}$$

and we take a fixed background with $\zeta = f = 1$

$$ds^2 = -\sigma^2\mu\, dt^2 + r^2dx^2 + r^2dy^2 + \mu^{-1}dr^2, \qquad \text{(B.78)}$$

where

$$\mu = -\frac{2m_0}{r} - \frac{\Lambda r^2}{3} \qquad \text{(B.79)}$$

with constant mass m_0. The components of the field strength tensor are

$$\begin{aligned} F_{01} &= \frac{1}{g}\sum_{k=1}^{N-1}\left[\left(\sqrt{\frac{k+1}{2k}}h_k - \sqrt{\frac{k-1}{2k}}h_{k-1}\right)\omega_k G_k^{(1)} - i\xi e^{-i\xi t}\delta h_{1,k} H_k\right] \\ &\quad + \frac{e^{-i\xi t}}{g}\sum_{k=1}^{N-1}\left[\frac{1}{2}\left(\delta v_{k+1}\omega_k - \delta v_k\omega_{k+1}\right)F_k^{(2)} + \frac{1}{2}\left(\delta u_k\omega_{k+1} - \delta u_{k+1}\omega_k\right)G_k^{(2)}\right] \\ &\quad + \frac{e^{-i\xi t}}{g}\sum_{k=1}^{N-1}\left[\frac{\sqrt{2k(k+1)}}{2}\left(\frac{\delta v_{k+1}\omega_{k+1}}{k+1} - \frac{\delta v_k\omega_k}{k}\right)H_k\right], \end{aligned}$$

$$
\begin{aligned}
F_{02} &= \frac{1}{g}\sum_{k=1}^{N-1}\left[\left(\sqrt{\frac{k-1}{2k}}h_{k-1}-\sqrt{\frac{k+1}{2k}}h_k\right)\omega_k F_k^{(1)} - i\xi e^{-i\xi t}\delta h_{2,k}H_k\right] \\
&\quad +\frac{e^{-i\xi t}}{g}\sum_{k=1}^{N-1}\left[\frac{1}{2}\left(\delta u_{k+1}\omega_k-\delta u_k\omega_{k+1}\right)F_k^{(2)}+\frac{1}{2}\left(\delta v_{k+1}\omega_k-\delta v_k\omega_{k+1}\right)G_k^{(2)}\right] \\
&\quad +\frac{e^{-i\xi t}}{g}\sum_{k=1}^{N-1}\left[\frac{\sqrt{2k(k+1)}}{2}\left(\frac{\delta u_k\omega_k}{k}-\frac{\delta u_{k+1}\omega_{k+1}}{k+1}\right)H_k\right], \\
F_{03} &= \frac{1}{g}\sum_{k=1}^{N-1}\left[h_k'H_k+e^{-i\xi t}\delta u_k'F_k^{(1)}+e^{-i\xi t}\delta v_k'G_k^{(1)}\right], \\
F_{12} &= \frac{1}{g}\sum_{k=1}^{N-1}\left[\sqrt{2k(k+1)}\left(\frac{\omega_k^2}{k}-\frac{\omega_{k+1}^2}{k+1}\right)H_k\right] \\
&\quad +\frac{e^{-i\xi t}}{g}\sum_{k=1}^{N-1}\left[\omega_k\left(\sqrt{\frac{k+1}{2k}}\delta h_{2,k}-\sqrt{\frac{k-1}{2k}}\delta h_{2,k-1}\right)G_k^{(1)}\right] \\
&\quad +\frac{e^{-i\xi t}}{g}\sum_{k=1}^{N-1}\left[\omega_k\left(\sqrt{\frac{k+1}{2k}}\delta h_{1,k}-\sqrt{\frac{k-1}{2k}}\delta h_{1,k-1}\right)F_k^{(1)}\right], \\
F_{13} &= \sum_{k=1}^{N-1}\left(\omega_k'F_k+e^{-i\xi t}\delta h_{1,k}'H_k\right), \\
F_{23} &= \sum_{k=1}^{N-1}\left(\omega_k G_k+e^{-i\xi t}\delta h_{2,k}H_k\right).
\end{aligned}
\tag{B.80}
$$

We then substitute (B.80) into (B.3) to find the Yang-Mills equations. For $\nu = 0$ we recover an equilibrium equation for h_k'', together with

$$
\begin{aligned}
\delta u_k'' &= -\frac{2}{r}\delta u_k' + \frac{1}{\mu r^2}\left[\frac{\omega_{k+1}}{2}(\delta u_k\omega_{k+1}-\delta u_{k+1}\omega_k)+\frac{\omega_{k-1}}{2}(\delta u_k\omega_{k-1}-\delta u_{k-1}\omega_k)\right] \\
&\quad +\frac{\omega_k}{\mu r^2}\left(\sqrt{\frac{k-1}{2k}}h_{k-1}-\sqrt{\frac{k+1}{2k}}h_k\right)\left(\sqrt{\frac{k+1}{2k}}\delta h_{1,k}-\sqrt{\frac{k-1}{2k}}\delta h_{1,k-1}\right) \\
&\quad +\frac{(k+1)\omega_k}{2\mu r^2}\left(\frac{\delta u_k\omega_k}{k}-\frac{\delta u_{k+1}\omega_{k+1}}{k+1}\right) \\
&\quad +\frac{(k-1)\omega_{k-1}}{2\mu r^2}\left(\frac{\delta u_k\omega_k}{k}-\frac{\delta u_{k-1}\omega_{k-1}}{k-1}\right) \\
&\quad -\frac{i\xi\omega_k}{\mu r^2}\left(\sqrt{\frac{k-1}{2k}}\delta h_{2,k-1}-\sqrt{\frac{k+1}{2k}}\delta h_{2,k}\right),
\end{aligned}
\tag{B.81}
$$

$$\begin{aligned}
\delta v_k'' &= -\frac{2}{r}\delta v_k' + \frac{1}{\mu r^2}\left[\frac{\omega_{k+1}}{2}(\delta v_k\omega_{k+1} - \delta v_{k+1}\omega_k) + \frac{\omega_{k-1}}{2}(\delta v_k\omega_{k-1} - \delta v_{k-1}\omega_k)\right] \\
&\quad + \frac{\omega_k}{\mu r^2}\left(\sqrt{\frac{k-1}{2k}}h_{k-1} - \sqrt{\frac{k+1}{2k}}h_k\right)\left(\sqrt{\frac{k+1}{2k}}\delta h_{2,k} - \sqrt{\frac{k-1}{2k}}\delta h_{2,k-1}\right) \\
&\quad + \frac{(k+1)\omega_k}{2\mu r^2}\left(\frac{\delta v_k\omega_k}{k} - \frac{\delta v_{k+1}\omega_{k+1}}{k+1}\right) \\
&\quad + \frac{(k-1)\omega_{k-1}}{2\mu r^2}\left(\frac{\delta v_k\omega_k}{k} - \frac{\delta v_{k-1}\omega_{k-1}}{k-1}\right) \\
&\quad + \frac{i\xi\omega_k}{\mu r^2}\left(\sqrt{\frac{k-1}{2k}}\delta h_{1,k-1} - \sqrt{\frac{k+1}{2k}}\delta h_{1,k}\right). \qquad \text{(B.82)}
\end{aligned}$$

From the $\nu = 1$ equation we find

$$\begin{aligned}
0 &= \delta h_{1,k}'' + \frac{\mu'}{\mu}\delta h_{1,k}' + \sqrt{\frac{k+1}{2k}}\frac{\delta u_k\omega_k}{\mu^2}\left(\sqrt{\frac{k-1}{2k}}h_{k-1} - \sqrt{\frac{k+1}{2k}}h_k\right) \\
&\quad + \sqrt{\frac{k}{2(k+1)}}\frac{\delta u_{k+1}\omega_{k+1}}{\mu^2}\left(\sqrt{\frac{k+2}{2(k+1)}}h_{k+1} - \sqrt{\frac{k}{2(k+1)}}h_k\right) \\
&\quad + \sqrt{\frac{k+1}{2k}}\frac{\omega_k^2}{\mu r^2}\left(\sqrt{\frac{k-1}{2k}}\delta h_{1,k-1} - \sqrt{\frac{k+1}{2k}}\delta h_{1,k}\right) \\
&\quad + \sqrt{\frac{k}{2(k+1)}}\frac{\omega_{k+1}^2}{\mu r^2}\left(\sqrt{\frac{k+2}{2(k+1)}}\delta h_{1,k+1} - \sqrt{\frac{k}{2(k+1)}}\delta h_{1,k}\right) \\
&\quad + \frac{i\xi}{\mu^2}\left(\sqrt{\frac{k+1}{2k}}\delta v_k\omega_k - \sqrt{\frac{k}{2(k+1)}}\delta v_{k+1}\omega_{k+1} - i\xi\delta h_{1,k}\right), \qquad \text{(B.83)}
\end{aligned}$$

while from $\nu = 2$ we have

$$\begin{aligned}
0 &= \delta h_{2,k}'' + \frac{\mu'}{\mu}\delta h_{2,k}' + \sqrt{\frac{k+1}{2k}}\frac{\delta v_k\omega_k}{\mu^2}\left(\sqrt{\frac{k-1}{2k}}h_{k-1} - \sqrt{\frac{k+1}{2k}}h_k\right) \\
&\quad + \sqrt{\frac{k}{2(k+1)}}\frac{\delta v_{k+1}\omega_{k+1}}{\mu^2}\left(\sqrt{\frac{k+2}{2(k+1)}}h_{k+1} - \sqrt{\frac{k}{2(k+1)}}h_k\right) \\
&\quad + \sqrt{\frac{k+1}{2k}}\frac{\omega_k^2}{\mu r^2}\left(\sqrt{\frac{k-1}{2k}}\delta h_{2,k-1} - \sqrt{\frac{k+1}{2k}}\delta h_{2,k}\right) \\
&\quad + \sqrt{\frac{k}{2(k+1)}}\frac{\omega_{k+1}^2}{\mu r^2}\left(\sqrt{\frac{k+2}{2(k+1)}}\delta h_{2,k+1} - \sqrt{\frac{k}{2(k+1)}}\delta h_{2,k}\right) \\
&\quad - \frac{i\xi}{\mu^2}\left(\sqrt{\frac{k+1}{2k}}\delta u_k\omega_k - \sqrt{\frac{k}{2(k+1)}}\delta u_{k+1}\omega_{k+1} + i\xi\delta h_{2,k}\right), \qquad \text{(B.84)}
\end{aligned}$$

with both the $\nu = 1$ and $\nu = 2$ equations also yielding

$$\begin{aligned}
0 \;=\; & \frac{h_k}{\sqrt{2k(k+1)}}\left(\delta u_k \omega_{k+1} - \delta u_{k+1}\omega_k\right) \\
& + \sqrt{\frac{k+2}{2(k+1)}} h_{k+1}\left(\delta u_k \omega_{k+1} - \delta u_{k+1}\omega_k\right) \\
& + \sqrt{\frac{k-1}{2k}} h_{k-1}\left(\delta u_{k+1}\omega_k - \delta u_k \omega_{k+1}\right) \\
& + \delta u_k \omega_{k+1}\left(\sqrt{\frac{k+2}{2(k+1)}} h_{k+1} - \sqrt{\frac{k}{2(k+1)}} h_k\right) \\
& + \delta u_{k+1}\omega_k\left(\sqrt{\frac{k-1}{2k}} h_{k-1} - \sqrt{\frac{k+1}{2k}} h_k\right) \\
& + \frac{\mu \omega_k \omega_{k+1}}{r^2}\left(\sqrt{\frac{k}{2(k+1)}}\delta h_{1,k} - \sqrt{\frac{k+2}{2(k+1)}}\delta h_{1,k+1}\right) \\
& + \frac{\mu \omega_k \omega_{k+1}}{r^2}\left(\sqrt{\frac{k+1}{2k}}\delta h_{1,k} - \sqrt{\frac{k-1}{2k}}\delta h_{1,k-1}\right) \\
& - i\xi\left(\delta v_k \omega_{k+1} - \delta v_{k+1}\omega_k\right), \qquad \text{(B.85)}
\end{aligned}$$

$$\begin{aligned}
0 \;=\; & \frac{h_k}{\sqrt{2k(k+1)}}\left(\delta v_k \omega_{k+1} - \delta v_{k+1}\omega_k\right) \\
& + \sqrt{\frac{k+2}{2(k+1)}} h_{k+1}\left(\delta v_k \omega_{k+1} - \delta v_{k+1}\omega_k\right) \\
& + \sqrt{\frac{k-1}{2k}} h_{k-1}\left(\delta v_{k+1}\omega_k - \delta v_k \omega_{k+1}\right) \\
& + \delta v_k \omega_{k+1}\left(\sqrt{\frac{k+2}{2(k+1)}} h_{k+1} - \sqrt{\frac{k}{2(k+1)}} h_k\right) \\
& + \delta v_{k+1}\omega_k\left(\sqrt{\frac{k-1}{2k}} h_{k-1} - \sqrt{\frac{k+1}{2k}} h_k\right) \\
& + \frac{\omega_k \omega_{k+1}}{\mu r^2}\left(\sqrt{\frac{k}{2(k+1)}}\delta h_{2,k} - \sqrt{\frac{k+2}{2(k+1)}}\delta h_{2,k+1}\right) \\
& + \frac{\omega_k \omega_{k+1}}{\mu r^2}\left(\sqrt{\frac{k+1}{2k}}\delta h_{2,k} - \sqrt{\frac{k-1}{2k}}\delta h_{2,k-1}\right) \\
& + i\xi\left(\delta u_k \omega_{k+1} - \delta u_{k+1}\omega_k\right). \qquad \text{(B.86)}
\end{aligned}$$

The $\nu = 3$ equation yields two further constraints

$$\begin{aligned} 0 &= \sqrt{\frac{k+1}{2k}}\left(h_k\delta v_k' - \delta v_k h_k'\right) + \sqrt{\frac{k-1}{2k}}\left(\delta v_k h_{k-1}' - h_{k-1}\delta v_k'\right) \\ &\quad + \frac{\mu}{r^2}\left(\sqrt{\frac{k+1}{2k}}\left(\omega_k\delta h_{2,k}' - \delta h_{2,k}\omega_k'\right) + \sqrt{\frac{k-1}{2k}}\left(\delta h_{2,k-1}\omega_k' - \omega_k\delta h_{2,k-1}'\right)\right) \\ &\quad - i\xi\delta u_k' \end{aligned} \tag{B.87}$$

$$\begin{aligned} 0 &= \sqrt{\frac{k+1}{2k}}\left(h_k\delta u_k' - \delta u_k h_k'\right) + \sqrt{\frac{k-1}{2k}}\left(\delta u_k h_{k-1}' - h_{k-1}\delta u_k'\right) \\ &\quad + \frac{\mu}{r^2}\left(\sqrt{\frac{k+1}{2k}}\left(\omega_k\delta h_{1,k}' - \delta h_{1,k}\omega_k'\right) + \sqrt{\frac{k-1}{2k}}\left(\delta h_{1,k-1}\omega_k' - \omega_k\delta h_{1,k-1}'\right)\right) \\ &\quad + i\xi\delta u_k'. \end{aligned} \tag{B.88}$$

Altogether, we have second order differential equations for δu_k, δv_k, $\delta h_{1,k}$ and $\delta h_{2,k}$ (B.81–B.84), along with two zeroth order constraints (B.85, B.86), and two first order constraints (B.87, B.88). If we introduce new complex variables

$$\begin{aligned} A_k &= \delta u_k + i\delta v_k, \qquad B_k = \delta u_k - i\delta v_k, \\ C_k &= \delta h_{1,k} + i\delta h_{2,k}, \qquad D_k = \delta h_{1,k} - i\delta h_{2,k}, \end{aligned} \tag{B.89}$$

we find that the equations in A_k and C_k decouple from those in B_k and D_k, and that the two sets of equations differ only by the sign of ξ to give

$$\begin{aligned} A_k'' &= -\frac{2}{r}A_k' + \frac{1}{\mu r^2}\left[\frac{\omega_{k+1}}{2}(A_k\omega_{k+1} - A_{k+1}\omega_k) + \frac{\omega_{k-1}}{2}(A_k\omega_{k-1} - A_{k-1}\omega_k)\right] \\ &\quad + \frac{\omega_k}{\mu r^2}\left(\sqrt{\frac{k-1}{2k}}h_{k-1} - \sqrt{\frac{k+1}{2k}}h_k\right)\left(\sqrt{\frac{k+1}{2k}}C_k - \sqrt{\frac{k-1}{2k}}C_{k-1}\right) \\ &\quad + \frac{(k+1)\omega_k}{2\mu r^2}\left(\frac{A_k\omega_k}{k} - \frac{A_{k+1}\omega_{k+1}}{k+1}\right) \\ &\quad + \frac{(k-1)\omega_{k-1}}{2\mu r^2}\left(\frac{A_k\omega_k}{k} - \frac{A_{k-1}\omega_{k-1}}{k-1}\right) \\ &\quad - \frac{\xi\omega_k}{\mu r^2}\left(\sqrt{\frac{k-1}{2k}}C_{k-1} - \sqrt{\frac{k+1}{2k}}C_k\right), \end{aligned} \tag{B.90}$$

$$
\begin{aligned}
B_k'' &= -\frac{2}{r}A_k' + \frac{1}{\mu r^2}\left[\frac{\omega_{k+1}}{2}(B_k\omega_{k+1} - B_{k+1}\omega_k) + \frac{\omega_{k-1}}{2}(B_k\omega_{k-1} - B_{k-1}\omega_k)\right] \\
&\quad + \frac{\omega_k}{\mu r^2}\left(\sqrt{\frac{k-1}{2k}}h_{k-1} - \sqrt{\frac{k+1}{2k}}h_k\right)\left(\sqrt{\frac{k+1}{2k}}D_k - \sqrt{\frac{k-1}{2k}}D_{k-1}\right) \\
&\quad + \frac{(k+1)\omega_k}{2\mu r^2}\left(\frac{B_k\omega_k}{k} - \frac{B_{k+1}\omega_{k+1}}{k+1}\right) \\
&\quad + \frac{(k-1)\omega_{k-1}}{2\mu r^2}\left(\frac{B_k\omega_k}{k} - \frac{B_{k-1}\omega_{k-1}}{k-1}\right) \\
&\quad + \frac{\xi\omega_k}{\mu r^2}\left(\sqrt{\frac{k-1}{2k}}D_{k-1} - \sqrt{\frac{k+1}{2k}}D_k\right), \qquad \text{(B.91)}
\end{aligned}
$$

$$
\begin{aligned}
0 &= C_k'' + \frac{\mu'}{\mu}C_k' + \sqrt{\frac{k+1}{2k}}\frac{A_k\omega_k}{\mu^2}\left(\sqrt{\frac{k-1}{2k}}h_{k-1} - \sqrt{\frac{k+1}{2k}}h_k\right) \\
&\quad + \sqrt{\frac{k}{2(k+1)}}\frac{A_{k+1}\omega_{k+1}}{\mu^2}\left(\sqrt{\frac{k+2}{2(k+1)}}h_{k+1} - \sqrt{\frac{k}{2(k+1)}}h_k\right) \\
&\quad + \sqrt{\frac{k+1}{2k}}\frac{\omega_k^2}{\mu r^2}\left(\sqrt{\frac{k-1}{2k}}C_{k-1} - \sqrt{\frac{k+1}{2k}}C_k\right) \\
&\quad + \sqrt{\frac{k}{2(k+1)}}\frac{\omega_{k+1}^2}{\mu r^2}\left(\sqrt{\frac{k+2}{2(k+1)}}C_{k+1} - \sqrt{\frac{k}{2(k+1)}}C_k\right) \\
&\quad + \frac{\xi}{\mu^2}\left(\sqrt{\frac{k+1}{2k}}A_k\omega_k - \sqrt{\frac{k}{2(k+1)}}A_{k+1}\omega_{k+1} + \xi C_k\right), \qquad \text{(B.92)}
\end{aligned}
$$

$$
\begin{aligned}
0 &= D_k'' + \frac{\mu'}{\mu} D_k' + \sqrt{\frac{k+1}{2k}} \frac{B_k \omega_k}{\mu^2} \left(\sqrt{\frac{k-1}{2k}} h_{k-1} - \sqrt{\frac{k+1}{2k}} h_k \right) \\
&+ \sqrt{\frac{k}{2(k+1)}} \frac{B_{k+1} \omega_{k+1}}{\mu^2} \left(\sqrt{\frac{k+2}{2(k+1)}} h_{k+1} - \sqrt{\frac{k}{2(k+1)}} h_k \right) \\
&+ \sqrt{\frac{k+1}{2k}} \frac{\omega_k^2}{\mu r^2} \left(\sqrt{\frac{k-1}{2k}} D_{k-1} - \sqrt{\frac{k+1}{2k}} D_k \right) \\
&+ \sqrt{\frac{k}{2(k+1)}} \frac{\omega_{k+1}^2}{\mu r^2} \left(\sqrt{\frac{k+2}{2(k+1)}} D_{k+1} - \sqrt{\frac{k}{2(k+1)}} D_k \right) \\
&- \frac{\xi}{\mu^2} \left(\sqrt{\frac{k+1}{2k}} B_k \omega_k - \sqrt{\frac{k}{2(k+1)}} B_{k+1} \omega_{k+1} - \xi D_k \right), \qquad \text{(B.93)}
\end{aligned}
$$

with constraints

$$
\begin{aligned}
0 &= \frac{h_k}{\sqrt{2k(k+1)}} \left(A_k \omega_{k+1} - A_{k+1} \omega_k \right) \\
&+ \sqrt{\frac{k+2}{2(k+1)}} h_{k+1} \left(A_k \omega_{k+1} - A_{k+1} \omega_k \right) \\
&+ \sqrt{\frac{k-1}{2k}} h_{k-1} \left(A_{k+1} \omega_k - A_k \omega_{k+1} \right) \\
&+ A_k \omega_{k+1} \left(\sqrt{\frac{k+2}{2(k+1)}} h_{k+1} - \sqrt{\frac{k}{2(k+1)}} h_k \right) \\
&+ A_{k+1} \omega_k \left(\sqrt{\frac{k-1}{2k}} h_{k-1} - \sqrt{\frac{k+1}{2k}} h_k \right) \\
&+ \frac{\mu \omega_k \omega_{k+1}}{r^2} \left(\sqrt{\frac{k}{2(k+1)}} C_k - \sqrt{\frac{k+2}{2(k+1)}} C_{k+1} \right) \\
&+ \frac{\mu \omega_k \omega_{k+1}}{r^2} \left(\sqrt{\frac{k+1}{2k}} C_k - \sqrt{\frac{k-1}{2k}} C_{k-1} \right) \\
&+ \xi \left(A_k \omega_{k+1} - A_{k+1} \omega_k \right), \qquad \text{(B.94)}
\end{aligned}
$$

$$
\begin{aligned}
0 \;=\; & \frac{h_k}{\sqrt{2k(k+1)}}\left(B_k\omega_{k+1}-B_{k+1}\omega_k\right) \\
& +\sqrt{\frac{k+2}{2(k+1)}}h_{k+1}\left(B_k\omega_{k+1}-B_{k+1}\omega_k\right) \\
& +\sqrt{\frac{k-1}{2k}}h_{k-1}\left(B_{k+1}\omega_k-B_k\omega_{k+1}\right) \\
& +B_k\omega_{k+1}\left(\sqrt{\frac{k+2}{2(k+1)}}h_{k+1}-\sqrt{\frac{k}{2(k+1)}}h_k\right) \\
& +B_{k+1}\omega_k\left(\sqrt{\frac{k-1}{2k}}h_{k-1}-\sqrt{\frac{k+1}{2k}}h_k\right) \\
& +\frac{\mu\omega_k\omega_{k+1}}{r^2}\left(\sqrt{\frac{k}{2(k+1)}}D_k-\sqrt{\frac{k+2}{2(k+1)}}D_{k+1}\right) \\
& +\frac{\mu\omega_k\omega_{k+1}}{r^2}\left(\sqrt{\frac{k+1}{2k}}D_k-\sqrt{\frac{k-1}{2k}}D_{k-1}\right) \\
& -\xi\left(B_k\omega_{k+1}-B_{k+1}\omega_k\right), \qquad \text{(B.95)}
\end{aligned}
$$

$$
\begin{aligned}
0 \;=\; & \sqrt{\frac{k+1}{2k}}\left(h_kA_k'-A_kh_k'\right)+\sqrt{\frac{k-1}{2k}}\left(A_kh_{k-1}'-h_{k-1}A_k'\right) \\
& +\frac{\mu}{r^2}\left(\sqrt{\frac{k+1}{2k}}\left(\omega_kC_k'-C_k\omega_k'\right)+\sqrt{\frac{k-1}{2k}}\left(C_{k-1}\omega_k'-\omega_kC_{k-1}'\right)\right) \\
& +\xi A_k', \qquad \text{(B.96)}
\end{aligned}
$$

$$
\begin{aligned}
0 \;=\; & \sqrt{\frac{k+1}{2k}}\left(h_kB_k'-B_kh_k'\right)+\sqrt{\frac{k-1}{2k}}\left(B_kh_{k-1}'-h_{k-1}B_k'\right) \\
& +\frac{\mu}{r^2}\left(\sqrt{\frac{k+1}{2k}}\left(\omega_kD_k'-D_k\omega_k'\right)+\sqrt{\frac{k-1}{2k}}\left(D_{k-1}\omega_k'-\omega_kD_{k-1}'\right)\right) \\
& +\xi B_k'. \qquad \text{(B.97)}
\end{aligned}
$$

Bibliography

[1] O. Aharony, S. S. Gubser, J. M. Maldacena, H. Ooguri, and Y. Oz. Large N field theories, string theory and gravity. *Phys. Rept.*, 323:183–386, 2000.

[2] P. Alken, M. Booth, J. Davies, M. Galassi, B. Gough, G. Jungman, F. Rossi, and J. Theiler. *GNU scientific library reference manual - 3rd edition*. Network theory ltd., 2009.

[3] S. Aminneborg, I. Bengtsson, S. Holst, and P. Peldán. Making anti-de Sitter black holes. *Class. Quant. Grav.*, 13:2707–2714, 1996.

[4] V. Balasubramanian and P. Kraus. A stress tensor for anti-de Sitter gravity. *Commun. Math. Phys.*, 208:413–428, 1999.

[5] L. N. Bardeen, L. N. Cooper, and J. R. Schreiffer. Theory of superconductivity. *Phys. Rev.*, 108:1175, 1957.

[6] R. Bartnik and J. McKinnon. Particle-like solutions of the Einstein-Yang-Mills equations. *Phys. Rev. Lett.*, 61:141–144, 1988.

[7] J. E. Baxter. *Existence and stability of solitons and black holes in SU(N) Einstein-Yang-Mills theory with a negative cosmological constant*. PhD thesis, Department of Applied Mathematics, University of Sheffield, 2006.

[8] J. E. Baxter, M. Helbling, and E. Winstanley. Soliton and black hole solutions of $\mathfrak{su}(n)$ Einstein-Yang-Mills theory in anti-de Sitter space. *Phys. Rev. D.*, 76:104017, 2007.

[9] J. E. Baxter, M. Helbling, and E. Winstanley. Abundant stable gauge field hair in anti-de Sitter space. *Phys. Rev. Lett.*, 100:011301, 2008.

[10] J. E. Baxter and E. Winstanley. On the stability of soliton and hairy black hole solutions of $\mathfrak{su}(n)$ Einstein-Yang-Mills theory with a negative cosmological constant. Paper in preparation.

[11] J. E. Baxter and E. Winstanley. Topological hairy black hole solutions of $\mathfrak{su}(n)$ Einstein-Yang-Mills theory with a negative cosmological constant. Paper in preparation.

[12] J. E. Baxter and E. Winstanley. On the existence of soliton and hairy black hole solutions of $\mathfrak{su}(n)$ Einstein-Yang-Mills theory with a negative cosmological constant. *Class. Quant. Grav.*, 25:245014, 2008.

[13] J. G. Bednorz and K. A. Muller. Possible high T_c superconductivity in the Ba-La-Cu-O system. *Z. Phys. B.*, 64:249, 1986.

[14] J. G. Bednorz and K. A. Muller. Perovskite-type oxides-The new approach to high T_c superconductivity. *Rev. Mod. Phys.*, 60:585–600, 1988.

[15] D. Birmingham. Topological black holes in anti-de Sitter space. *Class. Quant. Grav.*, 16:1197, 1997.

[16] P. Bizon. Colored black holes. *Phys. Rev. Lett.*, 64:2844–2847, 1990.

[17] P. Bizon. Gravitating solitons and hairy black holes. *Acta Phys. Polon. B.*, 25:877–898, 1994.

[18] J. Bjoraker and Y. Hosotani. Monopoles, dyons and black holes in the four-dimensional Einstein-Yang-Mills theory. *Phys. Rev. D.*, 62:043513, 2000.

[19] J. Bjoraker and Y. Hosotani. Stable monopole and dyon solutions in the Einstein-Yang-Mills theory in asymptotically anti-de Sitter space. *Phys. Rev. Lett.*, 84:1853–1856, 2000.

[20] R. A. Brandt and F. Neri. Magnetic monopoles in SU(N) gauge theories. *Nucl. Phys. B.*, 186:84–108, 1981.

[21] P. Breitenlohner, D. Maison, and G. V. Lavrelashvili. Non-Abelian gravitating solitons with negative cosmological constant. *Class. Quant. Grav.*, 21:1667–1684, 2004.

[22] D. R. Brill, J. Louko, and P. Peldán. Thermodynamics of $(3+1)$-dimensional black holes with toroidal or higher genus horizons. *Phys. Rev. D.*, 56:3600–3610, 1997.

[23] O. Brodbeck and N. Straumann. Instability of Einstein Yang-Mills solitons for arbitrary gauge groups. *Phys. Lett. B.*, 324:309–314, 1994.

[24] O. Brodbeck and N. Straumann. Instability proof for Einstein-Yang-Mills solitons and black holes with arbitrary gauge groups. *J. Math. Phys.*, 37:1414–1433, 1996.

[25] P. T. Chruściel. 'No hair' theorems: Folklore, conjectures, results. *Contemp. Math.*, 170:23–49, 1994.

[26] P. T. Chruściel. Uniqueness of stationary, electrovacuum black holes revisited. *Helv. Phys. Acta*, 69:529–552, 1996.

[27] P. T. Chruściel and W. Kondracki. Some global charges in classical Yang-Mills theory. *Phys. Rev. D.*, 36:1874–1881, 1987.

[28] A. Corichi and D. Sudarsky. Mass of colored black holes. *Phys. Rev. D.*, 61:101501, 2000.

[29] V. J. Emery. Theory of high-T_c superconductivity in oxides. *Phys. Rev. Lett.*, 58:2794–2797, 1987.

[30] A. A. Ershov and D. V. Gal'tsov. Non-abelian baldness of colored black holes. *Phys. Lett. A.*, 138:160–164, 1989.

[31] A. A. Ershov and D. V. Gal'tsov. Non-existence of regular monopoles and dyons in the SU(2) Einstein-Yang-Mills theory. *Phys. Lett. A.*, 150:159–162, 1990.

[32] B. P. Flannery, W. H. Press, S. A. Teukolsky, and W. T. Vetterling. *Numerical recipes 3rd edition: The art of scientific computing*. Cambridge University Press, 2007.

[33] P. Forgács and N. S. Manton. Space-time symmetries in gauge theories. *Commun. Math. Phys.*, 72:15–35, 1980.

[34] D. V. Gal'tsov and M. S. Volkov. Instability of Einstein Yang-Mills black holes. *Phys. Lett. A.*, 162:144–148, 1992.

[35] V. L. Ginzburg and L. D. Landau. On the theory of superconductivity. *Zh. Eksp. Teor. Fiz.*, 20:2064, 1950.

[36] S. S. Gubser. Breaking an abelian gauge symmetry near a black hole horizon. *Phys. Rev. D.*, 78:065034, 2008.

[37] S. S. Gubser. Colorful horizons with charge in anti-de Sitter space. *Phys. Rev. Lett.*, 101:191601, 2008.

[38] S. S. Gubser and S. S. Pufu. The gravity dual of a p-wave superconductor. *JHEP*, 11:033, 2008.

[39] S. A. Hartnoll. Lectures on holographic methods for condensed matter physics. *Class. Quant. Grav.*, 26:224002, 2009.

[40] S. A. Hartnoll, C. P. Herzog, and G. T. Horowitz. Building a holographic superconductor. *Phys. Rev. Lett.*, 101:031601, 2008.

[41] S. W. Hawking and D. N. Page. Thermodynamics of black holes in anti-de Sitter space. *Comm. Math. Phys.*, 87:577–588, 1983.

[42] R. Herman. *Lie groups for physicists*, volume 2 of *The mathematical physics monograph series*. W. A. Benjamin, 1966.

[43] C. P. Herzog. Lectures on holographic superfluidity and superconductivity. *J. Phys. A.*, A42:343001, 2009.

[44] M. Heusler. *Black hole uniqueness theorems*. Cambridge University Press, 1996.

[45] G. Horowitz. Introduction to holographic superconductors. *Lect. Notes Phys.*, 828:313–347, 2011.

[46] V. Iyer and R. M. Wald. Some properties of the Noether charge and a proposal for dynamical black hole entropy. *Phys. Rev. D.*, 50:846–864, 1994.

[47] M. Kaminski. Flavor superconductivity and superfluidity. *Lect. Notes Phys.*, 828:349–393, 2011.

[48] B. Kleihaus and J. Kunz. Static black hole solutions with axial symmetry. *Phys. Rev. Lett.*, 79:1595–1598, 1997.

[49] B. Kleihaus and J. Kunz. Rotating hairy black holes. *Phys. Rev. Lett.*, 86:3704–3707, 2001.

[50] B. Kleihaus, J. Kunz, and F. Navarro-Lerida. Rotating Einstein-Yang-Mills black holes. *Phys. Rev. D.*, 66:104001, 2002.

[51] H. P. Kunzle. SU(n)-Einstein-Yang-Mills fields with spherical symmetry. *Class. Quant. Grav.*, 8:2283–2297, 1991.

[52] H. P. Kunzle. Analysis of the static spherically symmetric Einstein-Yang-Mills equations. *Comm. Math. Phys.*, 162:371–397, 1994.

[53] H. P. Kunzle and A. K. M. Masood-ul Alam. Spherically symmetric static SU(2) Einstein-Yang-Mills fields. *J. Math. Phys*, 31:928–935, 1990.

[54] C. H. Lai, C. H. Oh, and C. P. Soo. Global gauge transformations and conserved, gauge-invariant electric and magnetic charges in Yang-Mills gauge theories. *Phys. Rev. D.*, 36:2532–2538, 1987.

[55] G. V. Lavrelashvili and D. Maison. A remark on the instability of the Bartnik-McKinnon solutions. *Phys. Lett. B.*, 343:214–217, 1995.

[56] J. P. S. Lemos. Three dimensional black holes and cylindrical general relativity. *Phys. Lett. B.*, 353:46–51, 1995.

[57] J. P. S. Lemos. Two-dimensional black holes and planar general relativity. *Class. Quant. Grav.*, 12:1081–1086, 1995.

[58] J. P. S. Lemos and V. T. Zanchin. Rotating charged black strings and three-dimensional black holes. *Phys. Rev. D.*, 54:3840–3853, 1996.

[59] F. London and H. London. The electromagnetic equations of the supraconductor. *Proc. Roy. Soc.*, A149:71, 1935.

[60] J. M. Maldacena. The large N limit of superconformal field theories and supergravity. *Adv. Theor. Math. Phys.*, 2:231–252, 1998.

[61] R. B. Mann, E. Radu, and D. H. Tchrakian. Non-Abelian solutions in AdS_4 and $d = 11$ supergravity. *Phys. Rev. D.*, 74:064015, 2006.

[62] R. Manvelyan, E. Radu, and D. H. Tchrakian. New AdS non-abelian black holes with superconducting horizons. *Phys. Lett. B.*, 677:79–87, 2009.

[63] B. Nolan and E. Winstanley. Stability of Dyons in SU(2) Einstein-Yang-Mills theory. Paper in preparation.

[64] E. Radu and J. J. van der Bij. New hairy black holes with negative cosmological constant. *Phys. Lett. B.*, 536:1477–1490, 2002.

[65] R. Ruffini and J. A. Wheeler. Introducing the black hole. *Phys. Today*, 24:30–41, 1971.

[66] S. Sachdev. Condensed matter and AdS/CFT. *Lect. Notes Phys.*, 828:273–311, 2011.

[67] O. Sarbach and E. Winstanley. On the linear stability of solitons and hairy black holes with a negative cosmological constant: The odd-parity sector. *Class. Quant. Grav.*, 18:2125–2146, 2001.

[68] D. H. Sattinger and O. L. Weaver. *Lie groups and algebras with applications to physics, geometry and mechanics*, volume 61 of *Applied mathematical sciences*. Springer-Verlag, 1986.

[69] B. L. Shepherd and E. Winstanley. Characterizing asymptotically anti-de Sitter black holes with abundant gauge field hair. http://arxiv.org/abs/1202.1438.

[70] B. L. Shepherd and E. Winstanley. Dyons in SU(N) Einstein-Yang-Mills theory. Paper in preparation.

[71] B. L. Shepherd and E. Winstanley. Einstein-Yang-Mills black holes with superconducting horizons. Paper in preparation.

[72] N. Straumann and Z. Zhou. Instability of a colored black hole solution. *Phys. Lett. B.*, 243:33–35, 1990.

[73] N. Straumann and Z. Zhou. Instability of the Bartnik-McKinnon solution of the Einstein-Yang-Mills equations. *Phys. Lett. B.*, 237:353–356, 1990.

[74] T. Torii, K. Maeda, and T. Tachizawa. Cosmic colored black holes. *Phys. Rev. D.*, 52:R4272–R4276, 1995.

[75] L. Vanzo. Black holes with unusual topology. *Phys. Rev. D.*, 56:6475–6483, 1997.

[76] M. S. Volkov, O. Brodbeck, G. V. Lavrelashvili, and N. Straumann. The number of sphaleron instabilities of the Bartnik-McKinnon solitons and non-Abelian black holes. *Phys. Lett. B.*, 349:438–442, 1995.

[77] M. S. Volkov and D. V. Gal'tsov. Non-Abelian Einstein-Yang-Mills black holes. *JETP Lett. B.*, 349:346–350, 1989.

[78] M. S. Volkov and D. V. Gal'tsov. Black holes in Einstein-Yang-Mills theory. *Sov. J. Nucl. Phys.*, 51:747–753, 1990.

[79] M. S. Volkov and D. V. Gal'tsov. Gravitating non-Abelian solitons and black holes with Yang-Mills fields. *Phys. Rept.*, 319:1–83, 1999.

[80] M. S. Volkov, N. Straumann, G. V. Lavrelashvili, M. Heusler, and O. Brodbeck. Cosmological analogs of the Bartnik-McKinnon solutions. *Phys. Rev. D.*, 54:7243–7251, 1996.

[81] E. Winstanley. Existence of stable hairy black holes in su(2) Einstein-Yang-Mills theory with a negative cosmological constant. *Class. Quant. Grav.*, 16:1963–1978, 1999.

[82] E. Winstanley. Classical Yang-Mills black hole hair in anti-de Sitter space. *Lect. Notes Phys.*, 769:49–87, 2009.

[83] E. Winstanley and O. Sarbach. On the linear stability of solitons and hairy black holes with a negative cosmological constant: The even-parity sector. *Class. Quant. Grav.*, 19:689–724, 2002.

[84] E. Witten. Anti-de Sitter space and holography. *Adv. Theor. Math. Phys.*, 2:253–291, 1998.

[85] Z. Zhou. Instability of SU(2) Einstein Yang-Mills solitons and non-Abelian black holes. *Helv. Phys. Acta*, 65:767–819, 1992.